Synthetic and Mechanistic Studies on the Cross-Coupling Reactions Catalyzed by Ruthenium Complexes

Ruili Gao
Marquette University

SYNTHETIC AND MECHANISTIC STUDIES ON THE
CROSS-COUPLING REACTIONS CATALYZED BY
RUTHENIUM COMPLEXES

by

Ruili Gao, B.S.

A Dissertation submitted to the Faculty of the Graduate School,
Marquette University,
in Partial Fulfillment of the Requirements for
the Degree of Doctor of Philosophy

Milwaukee, Wisconsin

May, 2011

ABSTACT
SYNTHETIC AND MECHANISTIC STUDIES ON THE
CROSS-COUPLING REACTIONS CATALYZED BY
RUTHENIUM COMPLEXES

Ruili Gao, B.A.
Marquette University, 2011

Transition metal catalyzed C-H bond activation reaction is a powerful synthetic method for forming functionalized products directly from unreactive hydrocarbons, and has enormous synthetic potentials for developing chemical processes ranging from petroleum products to pharmaceutical agents. In an attempt to mimic the high stereo selectivity and region selectivity of catalytic reactions by transition metal catalysts, recent research has focused on design and synthesis of transition metal complex and the application on the coupling reactions involving C-H bond activation.

Herein, we wish to report the highly effective coupling reactions involving C-H bond activation by using well-defined ruthenium catalysts. Ruthenium hydride complex was to found to have high activity and selectivity for hydrosilylation, silyl enol ethers formation and enol esters formation reactions. Throughout the course of the mechanistic investigation of the reactions, we found compelling evidence for mechanism of reactions by spectroscopic, structural techniques and computational (DFT) analysis.

ACKNOWLEDGMENTS

Ruili Gao, B.A.

Herein, I would like to thank the people who have contributed to this thesis. I would like to first thank my advisor, Dr. Yi for his guidance. Through these four years in the lab, you have taught me how to think and act like a chemist and to demand more from myself. I would like to thank my committee members, Dr. Donaldson, and Dr. Steinmetz, for their time, patience and suggestions. I would like to thank Dr. Timerghazin for the helps on the computational studies. I would like to thank Dr.Cai, who was always willing to share his expertise in NMR with me. Thank you for the help with the advanced NMR experiments. I would like to thank Dr. Sergey for the X-ray crystal structures of the organometallic complexes. Moreover, I would thank Chemistry Department of Marquette University for financial support. I would like to thank the Graduate School and all of the Marquette University administration.

I would like to thank my friends and family for understanding and help me. I would like to dedicate this thesis to my husband. Thank you for standing behind me and fully understanding me all the time. Without you, I would not have gotten this far.

Table of Contents

List of Figure

List of Table

Chapter 1. Introduction

Over the past decades, the quest for the most economic ways to form C-C bonds

has become a matter of increasing importance among both industrial and academic

research units. Catalytically efficient activation of unreactive C-H bonds leading to

synthetically useful C-C bond formation is of considerable interest for the chemical and

pharmaceutical industries and remains a long term challenge for chemists. It would

provide a simple, clean and economic method for making functionalized molecules.

Although there are many studies on the reaction of arenes C-H bonds with the transition

metal compounds, transition metal mediated catalytic C-H bond activation reactions have

emerged as an attractive method for forming carbon-carbon bonds. In particular,

transition metal-catalyzed C-H bond activation and functionalization reactions of

nitrogen heterocyclic compounds have attracted considerable attention, in part due to

their prominent role in the synthesis of natural products and pharmaceutical agents.

Highly regioselective catalytic C-H bond insertion reactions of nitrogen- containing

aromatic compounds, such as pyridines, pyrroles, and indoles, have been reported in

recent years. In this chapter, the literature survey of transition metal catalyzed C-H bond

activation, the formation of enol ester and the silylation reactions will be discussed.

1.1 Arene C-H Bond Activation Reactions

1.1.1 Photo-initiated C-H Bond Activation Reactions

In 1983, Eisenberg reported the preparation of the complex $IrH_3(CO)(dppe)$ (dppe

= 1,2-bis(diphenylphosphino)ethane),[1] and its photochemical behavior. Irradiation of a

benzene solution of $IrH_3(CO)(dppe)$ under CO produced a small amount of

benezaldehyde. Despite the fact that the reaction was not catalytic, the authors had

stumbled on a system that not only activated arene C-H bonds but also inserted CO to

give a functionalized product. These results were followed by studies among which only

complexes of Rh(I) and Ir(I) containing the ligand PPh_3 can promote catalytic arene

carbonylation photochemistry (Eq 1).

M: $RhCl(CO)(PPh_3)_3$, $RhH(CO)(PPh_3)_3$ and
$IrCl(CO)(PPh_3)_2$

(1)
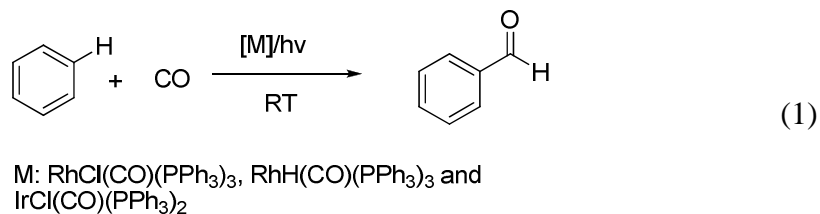
However, the use of a loosely related rhodium complex bearing a stronger

electron donating ligand, such as the PMe_3, gave better yields.[2] In addition to the

expected benezaldehyde, small amounts of biphenyl, benzyl alcohol and benzophenone

also formed. These compounds are presumably secondary products formed from

benezaldehyde. Only biphenyl seems to be a primary product because it is formed

catalytically even under nitrogen (Eq 2).

$$(2)$$
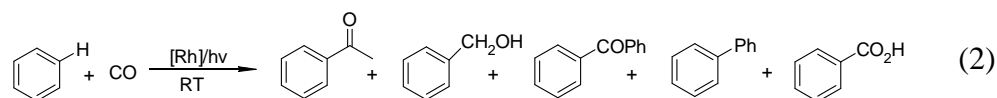
According to Tanaka et al., the restricted yield of benezaldehyde is not due simply

to thermodynamic limitations,[3] but to two other factors. The first arises from secondary

photoreactions of benezaldehyde and the second arises from the decomposition of the

catalyst.

Other transition-metal complexes, including some ruthenium complexes are less

efficient than Rh complexes.[4] The application of $RhCl(CO)(PR_3)_3$ /hv system to

substituted benzene such as toluene, anisole or chlorobenzene gave meta- and

para-subsituted products in a 2/1 statistical ratio.[5]

The mechanism for the full catalytic cycle of the Rh-catalyzed photochemical

carbonylation of benzene is shown in Scheme 1.

The most unusual aspect of this cycle is that the primary photo process does not

involve ligand loss. Therefore, the C-H addition step proceeds predominantly via an

associative process. Another striking aspect of the proposed mechanism is that a

secondary photo process, favored by short wavelengths. In addition to the primary

photoprocess which lead to a reactive state of the starting complex.
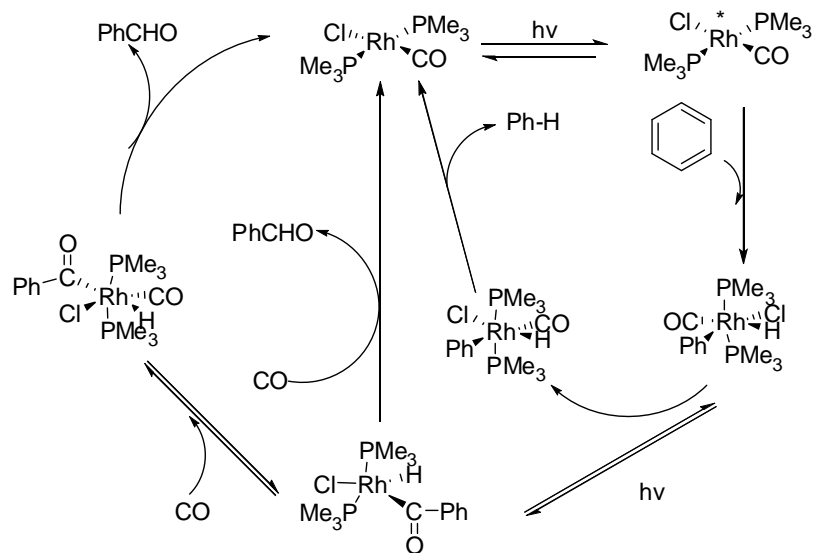
Scheme 1. Mechanism for Arene Carbonylation

1.1.2 Non-Chelation-Assisted Arene C-H Bond Activation

Examples of the non-chelation-assisted C-H bond activation are relatively rare.

Fujiwara reported the efficient metalation of aromatic C-H bonds at room temperature

using a highly electrophilic in situ generated Pd(II) and Pt(II) cationic species in

trifluoroacetic to C-C multiple bonds (Eq 3).[6]

(3)
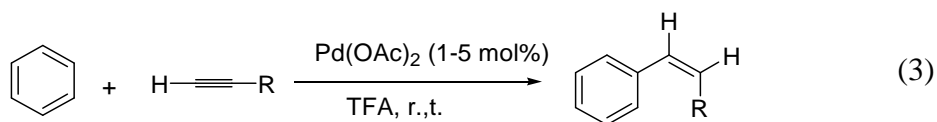
In most cases, the addition of alkynes excursively afforded the

thermodynamically less stable *cis*-aryl alkene. The intramolecular hydroarylation of C-C

triplet bonds is facile and regiospecific because of the electrophilic metalation of

aromatic C-H bonds by the Pd(II) cationic species which is assisted by the ethyl

coordination. In fact, this intramolecular reaction combines both chelation assisted and

electrophilic metalation. A possible mechanism has been outline in Scheme 2.
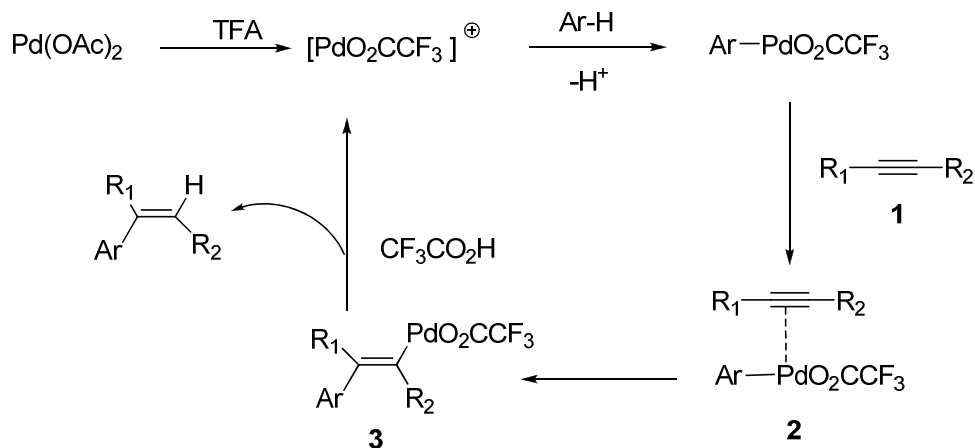
Scheme 2. Mechanism for the Addition of Alkynes to Alkenes

The proposed mechanism indicates the electrophilic attack of the aromatic C-H

bond by the cationic Pd (II) species to form complex **1** followed by coordination of

alkyne to give complex **2**. A *trans* insertion of the C-C triple bond to the σ-aryl Pd bond

results in complex **3**, and the 1 to 1 coupling product would be released from Pd (II) upon

protonation of complex **3**.

1.1.3 Chelation-Assisted Arene C-H Bond Activation

Murai discovered the first example of a chelation-assisted, regioselective,

catalytic C-H bond activation of arene and olefin coupling reactions.[7] For example,

acetophenone is added to vinyl silane to yield a regioselective alkylated product at the

ortho position (Eq 4).

$$(4)$$
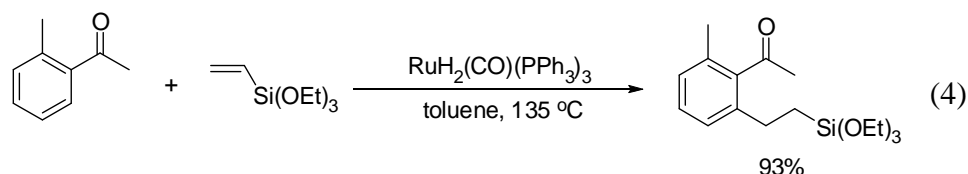
The ruthenium $RuH_2(CO)(PPh_3)_3$ was found to be an effective catalyst for this

reaction. This coupling reaction is easy to carry out, and in many cases, the reaction gives

a nearly quantitative yield.

The reaction was extended to various arenes and olefins coupling reactions.

Mechanism studies indicate that the C-H bond cleavage step is not rate-determining.

Instead a rapid equilibrium exists prior to the reductive elimination step that leads to the

C-C bond formation. Murai established that reductive elimination of alkylated products is

the turnover-limiting step (Eq 5).

$$(5)$$
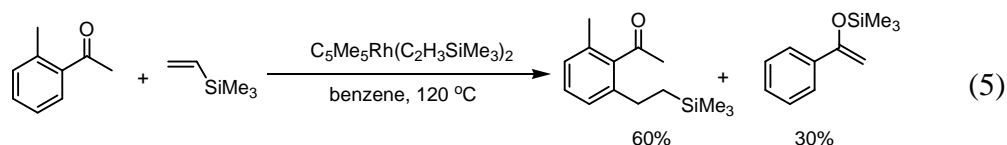
The rhodium bis-olefin complexes $[C_5Me_5Rh (C_2H_3SiMe_3)_2]$ have been shown to

be effective catalysts for the selective addition of olefin to the *ortho* position of aromatic

ketone.[8] The reactions of ketones and vinylsilane take place in benzene at 120 $^{\circ}$C to

generate the addition of the olefin and the silyl enol ether, and the ratio of these products

is around 2 to 1. For these catalytic reactions, a key difference in the mechanism from the

ruthenium-catalyzed processes is that the carbonyl coordination is presumed to be the

first step which directs the C-H bond activation to the *ortho* position of the aromatic

substrate.

From the isotope effects studies, the H/D exchange experiments establish that the

para and *meta* C-H bonds are not activated in the ruthenium system (Eq 6).

(6)
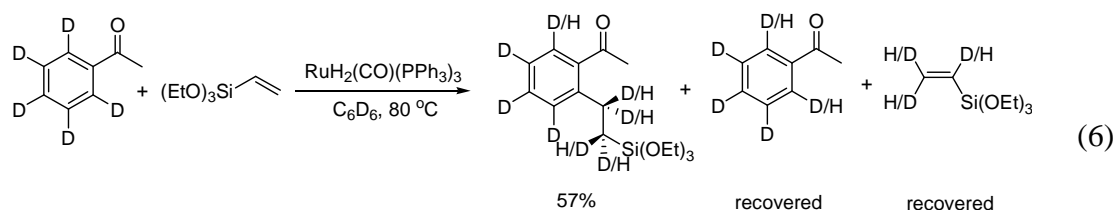
These rhodium complexes, on the other hand, are not discriminating in the C-H

bond activation step and activation of all sites (*ortho*, *meta*, *para*) of the substrate is

observed (Eq 7).

(7)
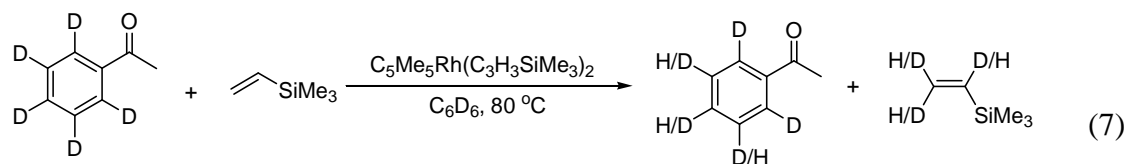
Murai has established that the C-H bond activation is fast and reversible in the

ruthenium system and the reductive elimination of the alkylated products is the

turnover-limiting step. It is believed that the same feature applies to the rhodium system

as well, but no conclusive evidence is available concerning this point. In both system,

chelation of the carbonyl group to the metal center lower in the energy barrier for reductive elimination leads to form the products.

1.2 C-H Bond Activation of Nitrogen-Containing Compounds

Transition metal-catalyzed C-H bond activation and functionalization reactions of nitrogen heterocyclic compounds have attracted considerable attention, in part due to their prominent role in the synthesis of natural products and pharmaceutical agents. Highly regioselective catalytic C-H bond insertion reactions of nitrogen- containing aromatic compounds, such as pyridines, pyrroles, and indoles, have been reported in recent years.

1.2.1 C-H Bond Activation of Pyrroles

Pyrrole moieties are important structural elements of many natural compounds of biological interest and they are important building blocks for forming biologically active family of porphyrins and related nitrogen macrocycles as well as for serving as precursors for electroactive polymeric materials. Therefore, the development of an efficient pathway for the functionalization of these compounds will be important to

pharmaceutical science, and the development of direct C-H bond functionalization

strategies for the facile generation of compounds with useful molecular architecture

remains high interest to academic and industrial chemists. People are particularly

interested in the development of new methods for direct metal catalyzed oxidative C-H

transformation of organic molecular under mild and operationally simple conditions.[9]

Filippini reported an interesting palladium-catalyzed direct arylation of N-metalated

pyrrole with bromobenzene in which the nature of the cation had varying effects on

product distribution (Eq 8).[10]

M=Na,	0%	0%	100%
M=ZnBr	40%	10%	50%
M=ZnCl	75%	5%	15%

(8)
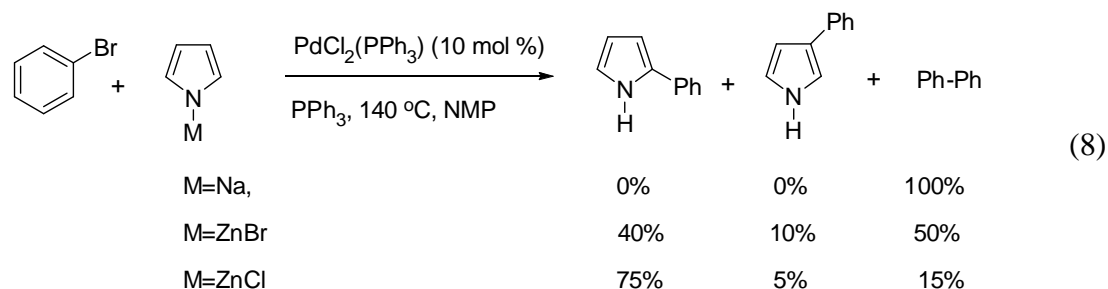
While the use of sodium pyrrole gave the aryl bromide-homocoupled product in

quantitative yield, trans-metalation to a harder pyrrole-1-yl zinc bromide gave the desired

2-substituted pyrrole in 40% yield along with some of the 3-substituted pyrrole and

dimerized bromobenzene product.[11] Further improvement in reaction selectivity was

possible using $ZnCl_2$, which afforded the desired 2-substituted pyrrole product in 75%

yield with very little of the 3-substituted pyrrole and Ullman coupling byproduct.[12]

Sames reported several alternative procedures for the intermolecular C-2 arylation of pyrrole. The first approach uses $ArRh(OPiv)_2[P(p\text{-}CF_3Ph)_3]_2$ as the catalyst system for the C-2 arylation of *NH*-containing pyrrole (Eq 9).[13]

$$\text{(9)}$$

81%
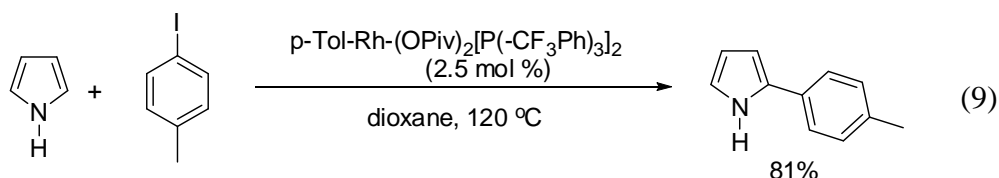
C-vinylated pyrroles are important building blocks for forming porphyrins and related nitrogen macrocycles as well as for serving as precursors for photoactive polymeric materials. Recently Pd catalysts have been found to be particularly versatile in mediation C-H oxidative coupling reactions of substituted pyrroles, pyridines and indoles,[14] where the regioselectivity has often found to be dictated by both the steric and electronic nature of the arene substituents. Elizabeth reported an efficient aerobic palladium oxidation system for C-H bond functionalization of sensitive molecular under ambient conditions (Eq 10).[15]

$$\text{(10)}$$
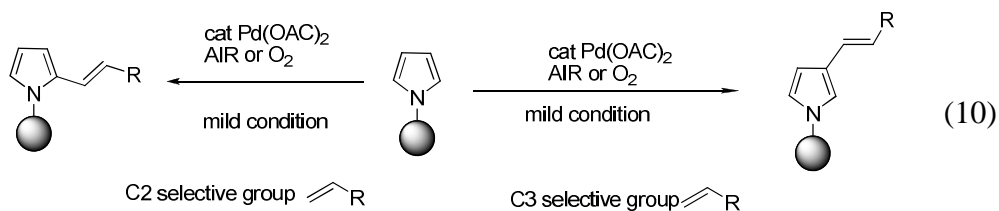
This method can be used to directly generate a range of functionalized and annulated pyrrole architectures and it is possible to control the position of C-H bond

functionalization via simple steric and electronically tuned N-pyrrole protecting groups to form products with either C2 or C3 elaboration.

For the reaction conditions, they identified that 10 mol % Pd (OAc)$_2$ in a dioxane –AcOH– DMSO solvent system and tBuOOBz as oxidant provided an effective system for pyrrole functionalization. They found that N-Bn pyrrole reacted smoothly with benzyl acrylate at only 35 ^{o}C to form the alkenylated products. Although it was expected that the natural reactivity of pyrrole would direct reaction to the C2 position, they observed a mixture of C2 and C3 isomers with the ratio of 2 to 1. They tried different N-group, and found that an electron withdrawing N-protecting group would reduce the reactivity of the pyrrole and yield a more selective process (Eq 11).
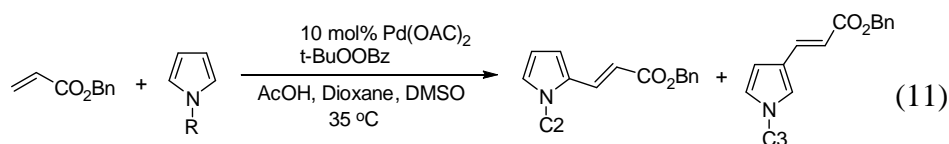
In this reaction, N-Ac, N-Ts(tosyl) and N-Boc pyrrole afforded only the C2 products in good yield under mild conditions. In contrast N-TIPS pyrrole gave only C3 product. The switch in selectivity is attributed to the sterically demanding nature of the TIPS group shields the C2 position from reaction with the palladium catalyst, forcing the reactive pyrrole to palladate at C3. So this is a new method for controlling catalytic activation and functionalization of pyrroles under mild conditions.

They surveyed the catalyst loading and found that the catalyst loading can

reduced to 1 mol %, but the complete conversion takes longer to achieve. The turnover

number (TON) at 60% (96 h) conversion is 55 %, suggesting that the process displays a

high efficiency for palladium (II) processes.
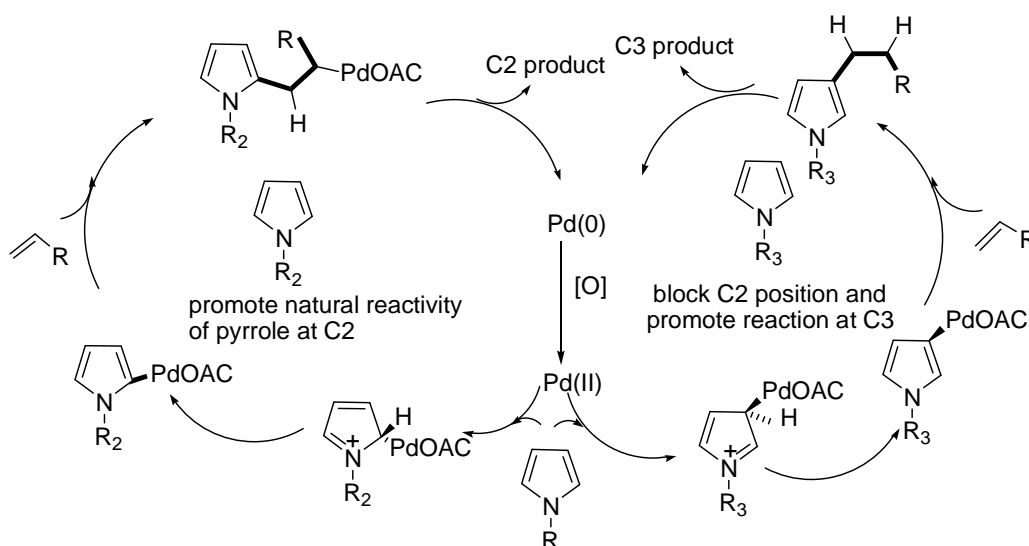
Scheme 3. Stereoelectronic Control Concept: Proposed Mechanism

The catalytic cycle started at the oxidation of Pd (0) complex to generate reactive

species Pd (II). In this catalytic cycle, the key step was the pyrrole insertion to the metal

center and this step is the selectivity-determined step. For the balky R group, the C2

position was blocked and there was strong steric hindrance between the metal complex

and pyrrole. So the pyrrole coordinates to the metal center at C3 position. On the other

hand, with less steric hindrance R group, the C2 position was more reactive than C3

position. Then with the hydrogen elimination and the insertion of alkene, the product was

generated.

Fujiwara reported the pyrroles undergo the addition reaction to C-C triple bond in

the presence of a catalytic amount of Pd(OAc)$_2$ under very mild conditions, affording

cis-heteroarylakenes in most cases (Eq 12). [16]

$$Ar-H \quad + \quad EtO_2C \equiv\!\!\!\equiv R \quad \xrightarrow[\text{HOAc or CH}_2\text{Cl}_2,\text{ r.t.}]{\text{Pd(OAC)}_2} \quad$$

Ar—H = Methylfuran, Pyrroles and Indoles

Ar—H | HOAc, r.t.   (12)
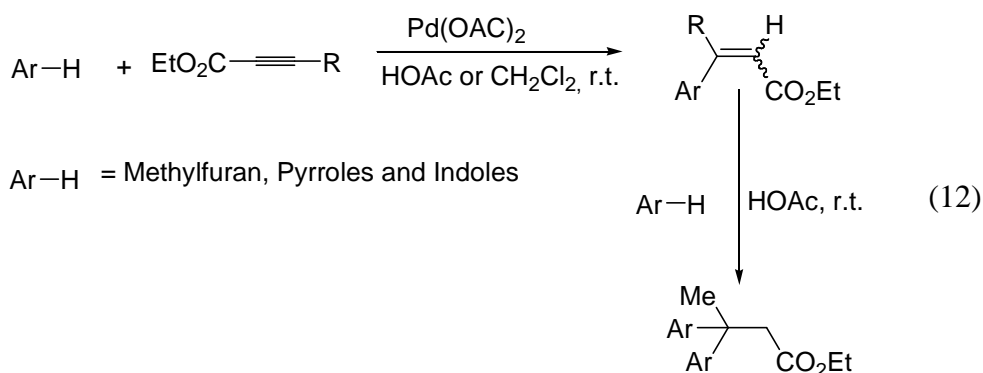
For pyrrole, 1-meththylpyrrole and 2-methylfuran, the substitution of aromatic

C-H bonds occurred at the 2- or 5-position of the arenes, characteristic of electrophilic

substitution (Eq 13).

$$\xrightarrow[\text{HOAc ,r.t., 2 h}]{\text{Pd(OAc)}_2}$$

(13)
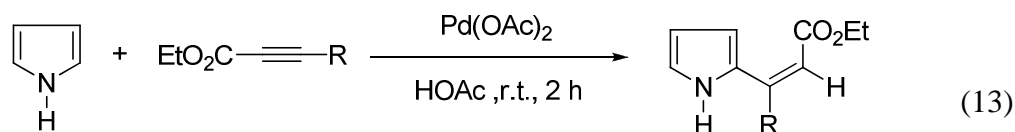
To investigate the possible mechanism of this reaction, they carried out several

isotope experiments using either DOAc as a solvent or d_5-pyrrole as an arene. When the

reaction of pyrrole with ethyl phenylpropiolate was run in the DoAc, D atoms

incorporated into the product **4a** at a rate of 55% at the 2-vinyl position (Eq 14).

$$\text{(14)}$$
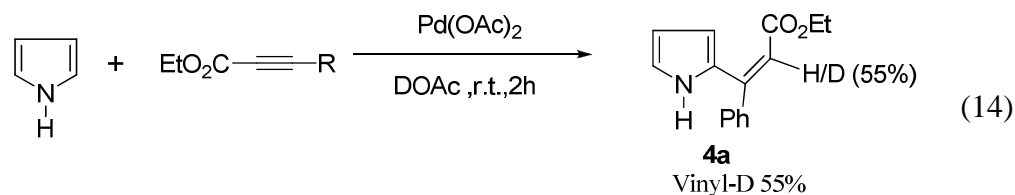
On the other hand, D atoms incorporated into the product **4b** at the rate of 75% at the 2-viny position when the reaction of d_5-pyrrole with ethyl phenylpropiolate was run in dichloromethane. This suggested that the Vinyl-D atoms of the product may result from the protonation of C by DOAc and DOAc itself may be formed from metalation of pyrrole C-H by Pd (II) species (Eq 15).

$$\text{(15)}$$
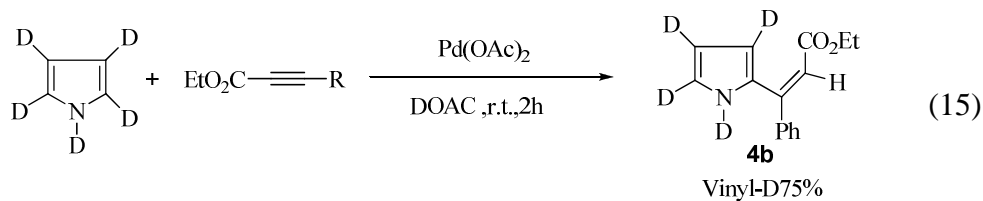
They also noticed that in these two separate reactions the initial rate of the reaction of pyrrole with ethyl phenylpropiolate in dichloromethane was three times faster than that of d_5-pyrrole with ethyl phenylpropiolate in dichloromethane, $k_H/k_D = 3$, which indicated that the cleavage of the pyrrole C-H bonds is the possible rate-determining step in the present reaction.
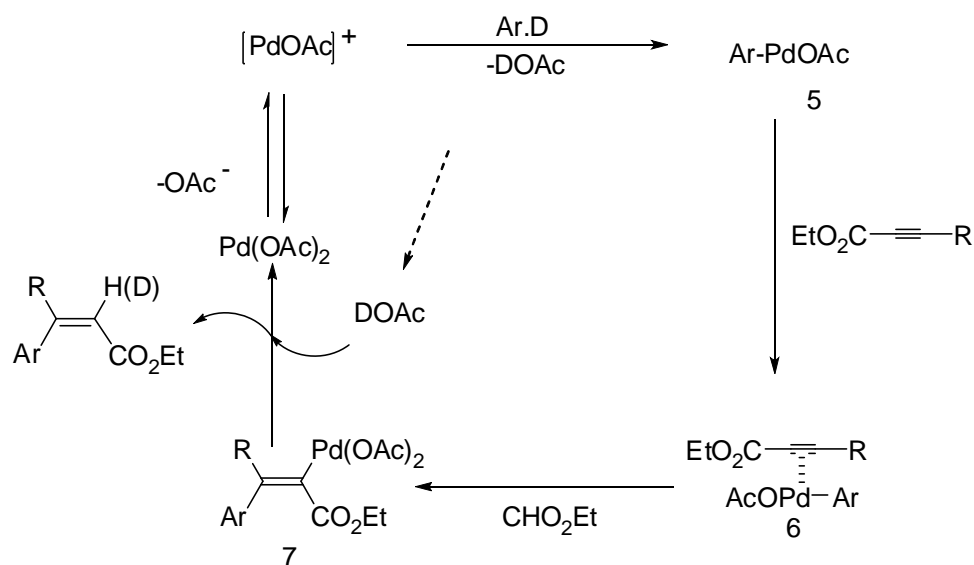
Scheme 4 . Possible Mechanism for the Addition of Heteroarenes to Alkynoates

Based on this information, they showed a possible mechanism in Scheme 4. The electrophilic substitution of the aromatic C-H bond by cationic Pd (II) species would result in the formation of an σ-arylpalladium complex **5** which is followed by coordination of alkyne to give complex **6**. Trans-Insertion of C-C trip bonds to the σ-aryl-Pd bond would afford vinyl-Pd complexes **7**, and upon protonation of complex **7**. The 1:1 coupling product would be released from the Pd (II) species.

Recently Zhang reported that the highly regioselective Palladium–catalyzed oxidative coupling reaction of indolizines and vinylarenes via C-H bond cleavage.[17] In this report, they used the 10 mol % Pd(OAc)$_2$ with one equiv. Ag$_2$CO$_3$ as oxidant and 20 mol % ligand to catalyze the coupling reactions of styrene with indolizines. They found that the ligands added showed the relationship with the selectivity of the product, they got

only the germinal isomer as the product by using 2, 2 -bipyridine, by using PPh$_3$, pyridine

or phenanthroline as ligands, they got the germinal and the (Z)-isomers mixtures (Eq 16)

and the ratio of these two isomers is around 1 to1.

$$\text{(16)}$$
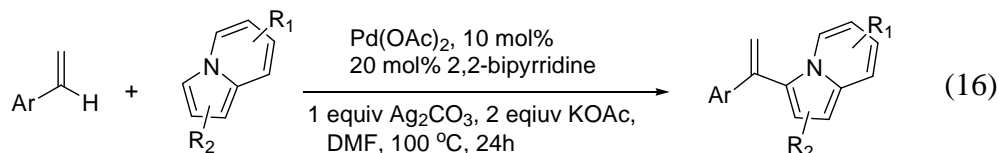
The Friedel-Crafts reaction has gained substantial synthetic and industrial

significance as an immensely powerful tool to effect C-C bond formation. Recently

Jorgensen has reported highly enantioselective Friedel-Crafts reactions of aromatic and

heteroaromatic compounds to trifluoropyruvate. He showed that the reactions of pyrroles

with ethyl trifluoropyruvate in the presence of (s)-t-Bu-BOX-Cu(OTf)$_2$ as the catalyst

show the highly enantioselectivity on the introduction of a chiral

hydroxyl-trifluoromethyl ethyl ester group. Substitution occurred into the 2-position on

the pyrrole ring, and the reaction proceed good yield and high enantioselectivity (Eq

17).[18]

$$\text{(17)}$$

R$_1$=H, Me ; R$_2$=H, COMe,

yield: 42-80%(83-93%ee)
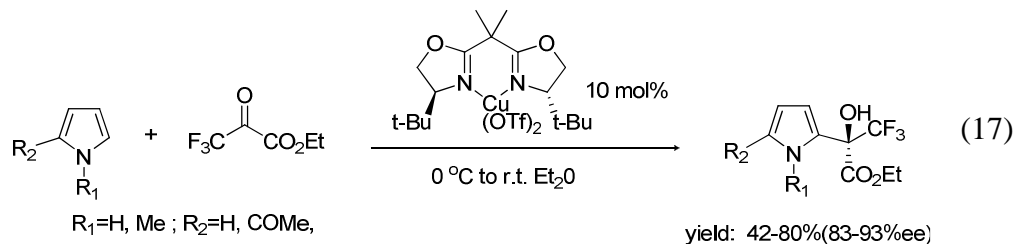
Four years later, Linden reported these highly enantioselective Friedel-Crafts

alkylations of pyrroles and indoles with the enones by using the same catalyst

(s)-*t*-Bu-BOX-Cu(OTf)$_2$ (Eq 18).[19] Compared with Jorgensen's results, Linden's report

shows higher yield and ee value.

R = H, Me ; R' = H, COMe; X, Y = H, CO$_2$R

yield: 80-95%(68-97%ee)
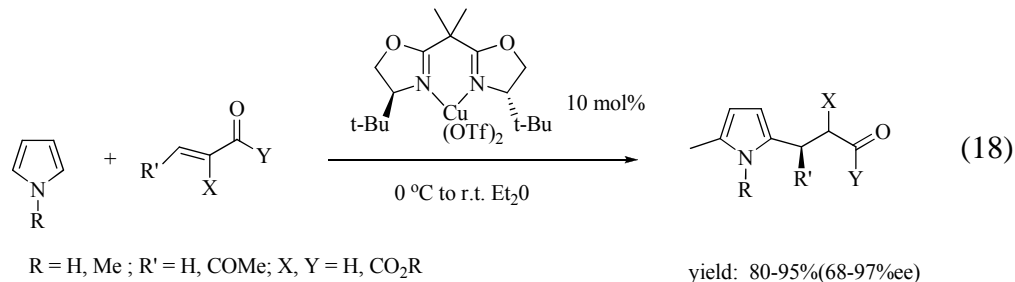
Muller also reported the asymmetric Friedel-Crafts alkylation of pyrroles with

nitroalkenes by using a binuclear zinc catalyst (Eq 19).[20]

R=H, CO$_2$Et,
R$_1$= Ph, Me, iPr, n-Pr, 2-thiophenyl, cyclohexyl, 4-Me-Ph

Yield: 52%-92%
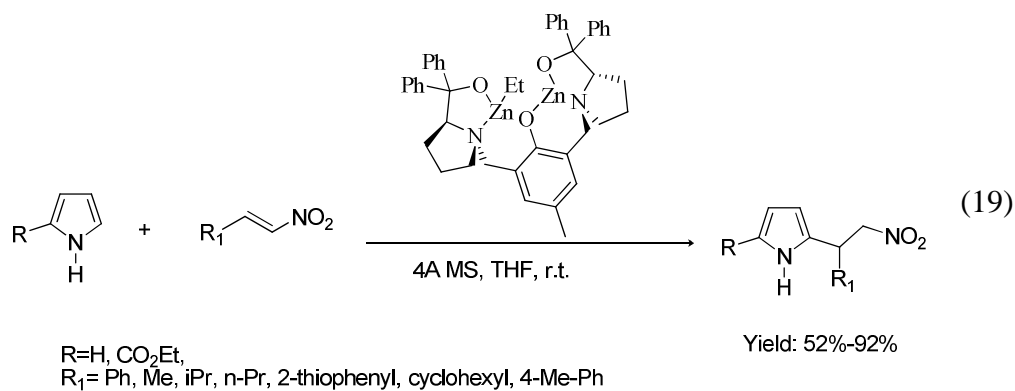
For this reaction, various nitroalkenes were reacted with the pyrrole. When

aromatic substitutes were used, in all these cases, excellent enantioselectivities were

obtained, which ranged from 87% for the o-methoxysubstrate to 97% for the tolyl

substituent compound. The position of the methoxy-substituent of compounds did not

affect either the reactivity or the selectivity of the reaction. An improvement of the yield

was observed by using a furanyl substituent.
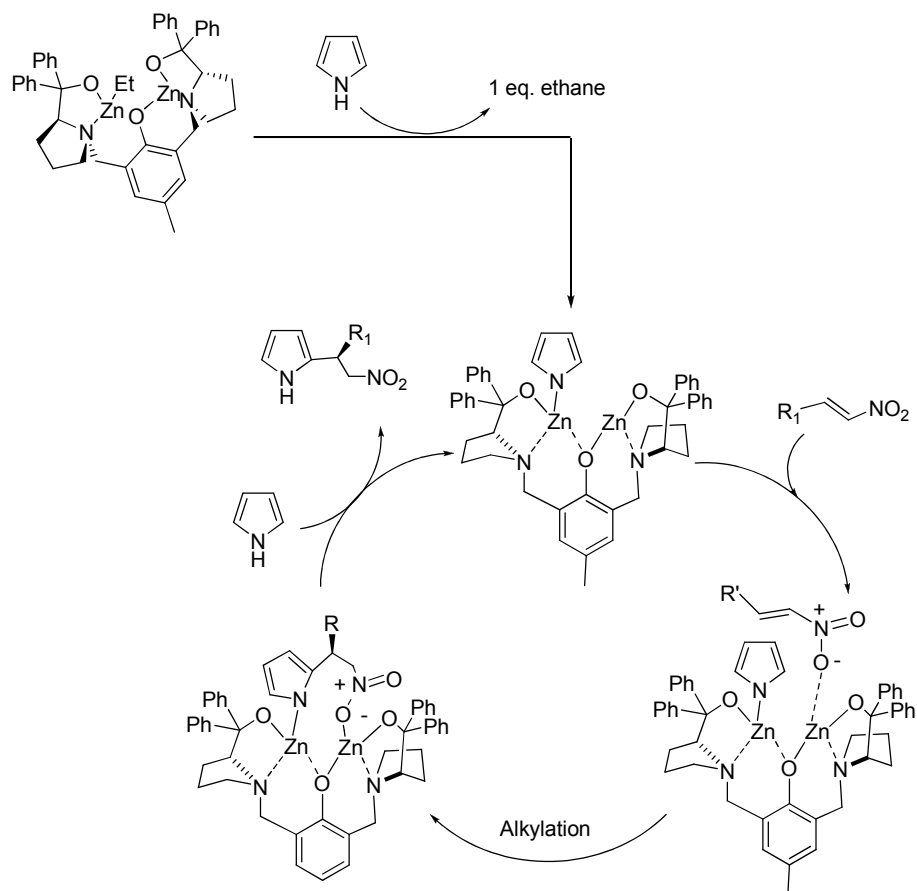
Scheme 5. Proposed the Mechanism for the Reaction of Nitroalkenes and Pyrroles

He proposed a mechanism for this type reaction that involves the deprotonating of

pyrrole by Zinc complex accompanied by the formation of one equiv of ethane (Scheme

5). The nitroalkene coordinates to zinc catalyst and undergoes the alkylation reaction.

The catalytic cycle closed by a proton exchange with an incoming pyrrole to release the

product and reform the active catalyst.

Muller demonstrated the use of the binuclear zinc bis-ProPhenol complex in an

atom economic Friedel-Crafts reaction of unprotected pyrroles with a variety of

substituted nitroalkenes to give both mono- and disubstituted pyrroles. The reactions gave

excellent stereoselectivities in most cases.

Pedro has reported that the complexes of BINOL-based ligands with $Zr(O^tBu)_4$

catalyze the Friedel-Crafts alkylation reaction of indoles and pyrroles with nonchelationg

β-substituted α, β-enones at room temperature affording the expected products with good

yield and above 95% ee in most case (Eq 20).[21]

(20)
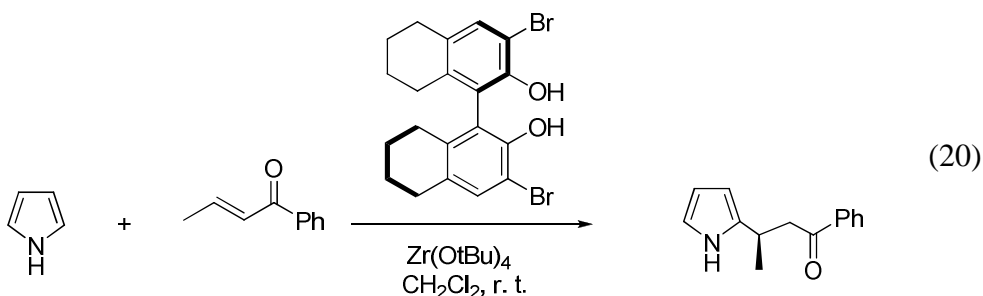
Due to the usefulness on the synthesis, transition- metal catalyzed allylation

chemistry continues to draw attention. The allylation reactions can be carried out by

using allyl carbonate or acetates together with palladium, molybdenum or iridium.

Cationic Ru-ally and vinylidene complexes have been successfully utilized as catalysts

for allylation and alkenylation of indoles and pyridine derivatives, respectively.[22]

Recently Pregosin reported that several Ru(IV) rather than Ru(II)-allyl catalysts readily

tolerate alcohols as substrates in acetonitrile solution.[24] They found that the reactions are

fast and highly regioselective allylation of pyrrole compounds by allyl alcohols using

Ru-Sulfonate as the catalyst (Eq 21).[23]

$$(21)$$
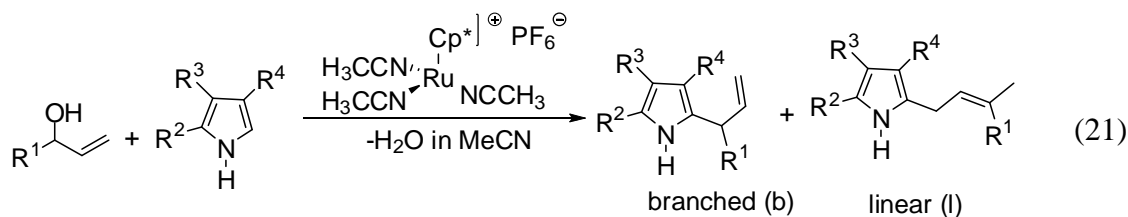
In this reaction, R^1 can be Ph, 1-naphthyl, mesityl, o-MeO-C_6H_4-, o-Me-C_6H_4-,

o-Cl-C_6H_4, R^2 can be Et and Me, R^3 and R^4 can be H, Me and Et. All the reaction can be

done in almost 5-7 min with high conversions. In most case, the others only got the

branched product, when R^1= Ph, R^2= Me, R^3= H, R^4= Me, the ratio of l/b= 1/12, R^1= Ph,

R^2= Me, R^3= Et, R^4= Me, the ratio is 1 to 22.

Grigg reported the first example of the direct arylation of pyrroles using a tethered

aryl iodide under palladium-catalyzed conditions (Eq 22).[24]

$$(22)$$
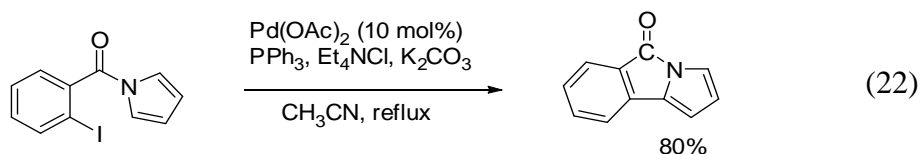
The utility of this type of cyclization has been applied to the synthesis of the core

structure of lamellarin as well as a library of potent cyclin-depent kinase inhibitors (Eq

23).[25]

$$(23)$$
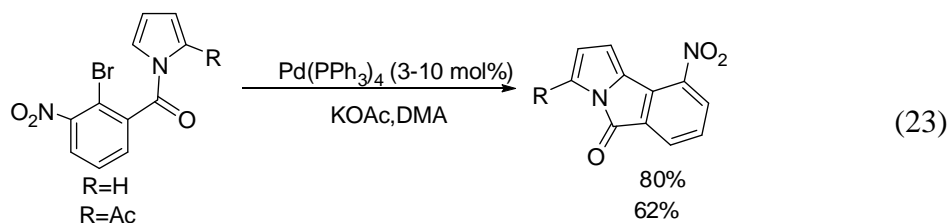
An additional example of the power of this methodology was demonstrated by

Trauner during the total synthesis of rhazinilam.[26] Cyclization of aryl iodide onto the

pyrrole was carried out using catalytic palladium and Buchwald's Davephos ligand to

give the desire rhazinilam precursor. They reported that the introduction of a MOM

protecting group proved necessary to avoid deiodination of the starting material,

presumably via pronation of a stable palladacycle intermediate.

Recently, our group developed a new catalytic coupling reaction between

2,5-disubstituted pyrroles and terminal alkynes which involves multiple C-H bond

activation and cyclization steps (Eq 24).[27]

$$(24)$$
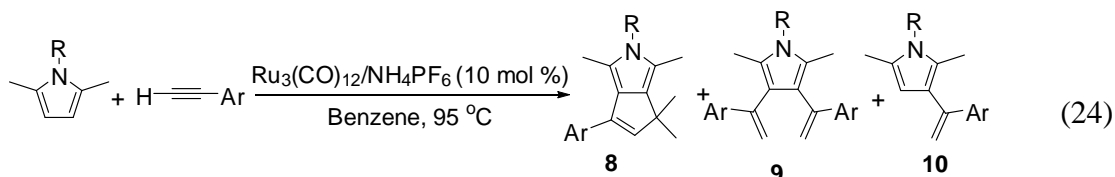
The formation of both 1:1 and 1:2 products suggested that product 1 is resulted

from the cyclization of 1:2 coupling product 2. Through the kinetic studies, we got the

$k_{obs} = 2.1 \times 10^{-2} \, h^{-1.}$ The coupling reaction of 1,2,5-trimethylpyrrole with deuterated

4-ethynylanisole-d_1 (2.0 equiv.) in the presence of $Ru_3(CO)_{12}/NH_4PF_6$ in C_6D_6 shows that

nearly 15% of the deuterium from 4-ethynylanisole-d_1 had exchanged with 35% of the

β-vinyl hydrogen of the unreacted 1,2,5-trimethylpyrrole, prior to the formation of the

coupling products. The product from this reaction contained deuterium at both the

α-methyl (33%) and vinyl (37%) positions. Also in supported of the rapid H/D exchange

between the two substrates, a relatively small deuterium isotope effect was observed from

a separate reaction of 1, 2, 5-trimethylpyrrole with phenylacetylene/phenylacetylene-d_1

when forming 1:1 coupling products. The pseudo first- order plots for the reaction gave

$k_{obs} = 1.65 \times 10^{-2}\,h^{-1}$ and $1.38 \times 10^{-2}\,h^{-1}$, which translated into $k_H/k_D = 1.2$.
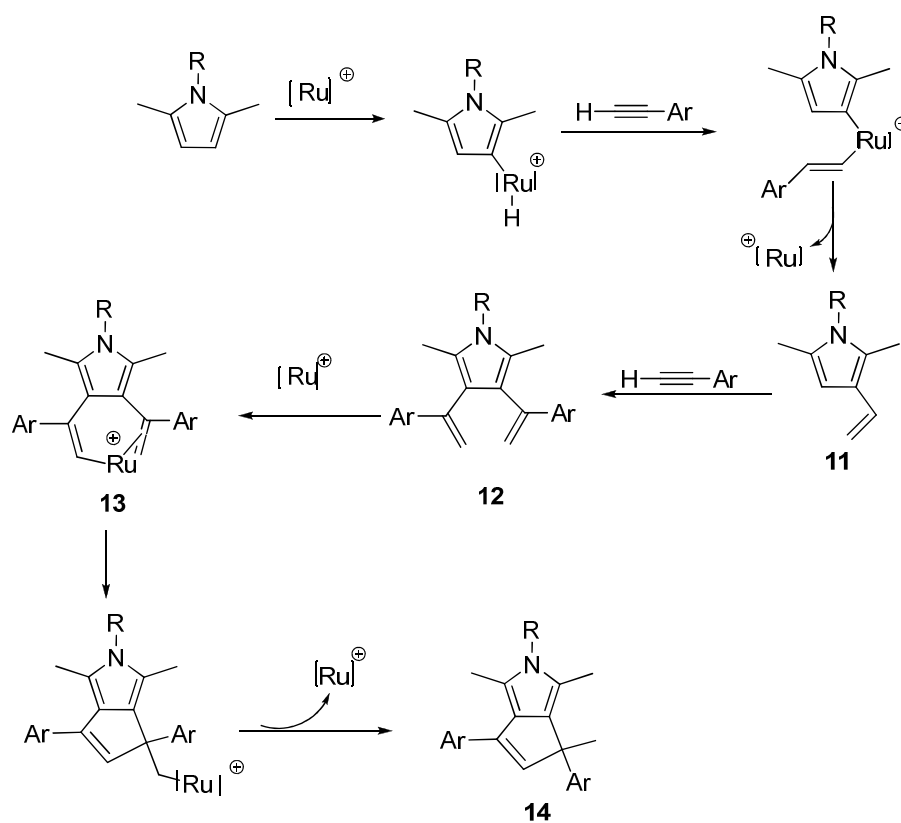
Scheme 6. Proposed Mechanism for the Coupling Reaction of Pyrroles and Alkynes

We proposed the mechanism which involving sequential alkyne insertion and

cyclisation steps (Scheme 6).

The sequential C-H activation and regioselective insertion of alkynes would be mediated by an electrophilic ruthenium catalyst to form 1:2 coupling product **12**. The subsequent ruthenium-mediated vinyl C-H bond activation and cyclization steps should be facilitated by coordination of the adjacent olefin to ruthenium via the formation of alkene-hydride species **13**. Cyclization and reductive elimination would give the product **14**.

1.2.2 C-H Bond Activation of pyridine and other Nitrogen Containing Compounds

Direct oxidative functionalization of tertiary amines is important both enzymatically and synthetically. Propargylic amines are of great pharmaceutical interest and are synthetic intermediates for the synthesis of various nitrogen compound as well as carbohydrates. Li has reported an effective CuBr-catalyzed oxide cross coupling off amines and alkynes via a direct C-H bond alkynylation.[28]

The reaction of N,N-dimethylaniline with phenylacetylene in the presence of a CuBr Catalyst and tert-butyl hydroperoxide to give the product in 77% isolate yield (Eq 25).

$$\text{(25)}$$

77% yield
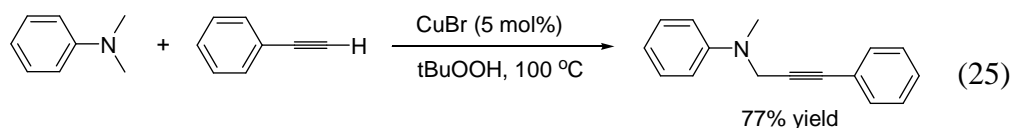
Sames has developed a new system for catalytic arylation and alkenylation of alkane segments (Eq 26).

(26)
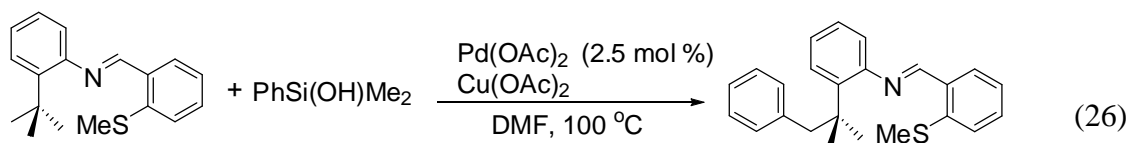
The *ortho-tert*-butylaniline substrates and 2-pivaloylpyridine may be arylated and alkenylated at the *tert*-butyl group, while no functionalization occurred at more reactive C-H and other bonds.[29] Arylation and alkenylation of these substrates are achieved in the presence of $Ph_2Si(OH)Me$ and $PHCHCHSi(OH)Me_2$, with a catalytic amount of $Pd(OAc)_2$ and stoichiometric oxidant $Cu(OAc)_2$ in DMF. He hypothesize that the high selectivity of this system stems from the confluence of directing effect of the Schiff base and unique reactivity properties of phenyl-palladium acetate species.

The addition of 1, 2-diarylazenes to aliphatic or aromatic internal alkynes in the presence of catalytic amount of Wilkinson's catalyst afforded N-(arylamino) indole derivatives (Eq 27).

R1, R2 : electron donating, 55-88%
R1, R2 : electron withdrawing, 6-30%

95   :   5

(27)
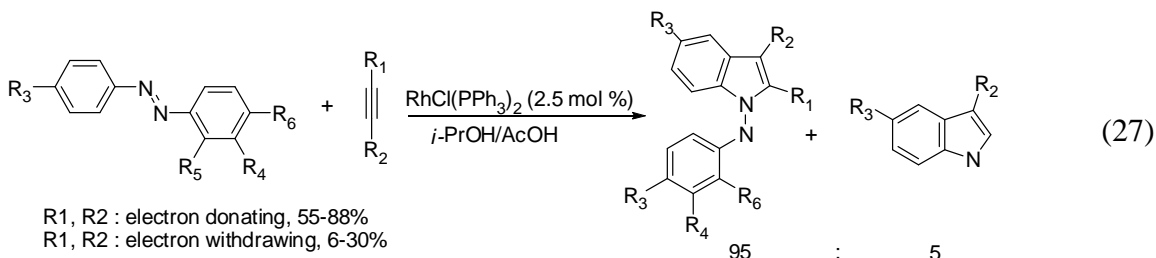
Isolated yield were in the range of 55-85% for symmetrically substituents alkynes with electron-donating substituent. Asymmetrically substituent alkynes and all alkynes with electron-withdrawing substituent gave yield in the range of 6-30%.[30]
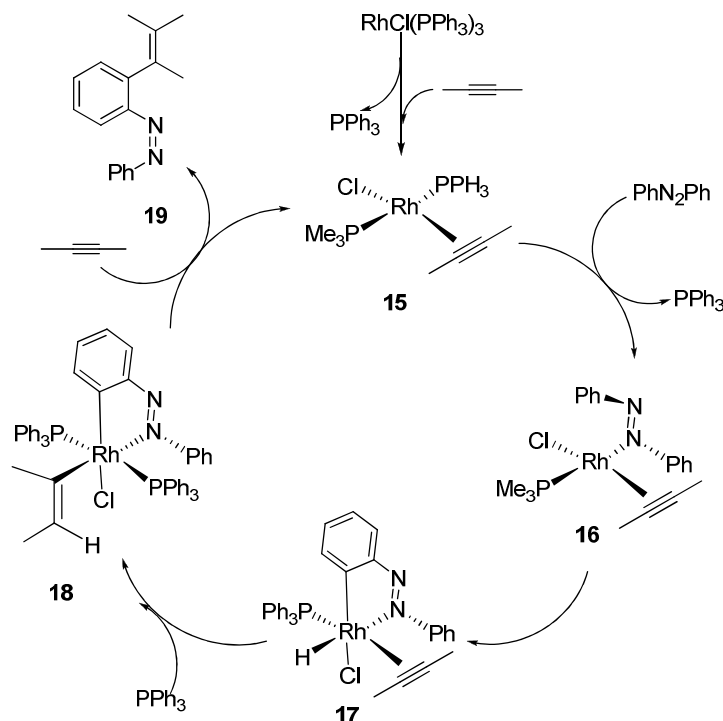
Scheme 7. Proposed Mechanism for the Formation of N-(arylamino) Indole

The mechanism is believed to be essentially the same as that for the olefin hydroarylation. Thus, the key steps are *ortho*-metalation of the diazene followed by insertion of the alkyne into Rh-H bond and reductive elimination to afford the intermediated **19**. This mechanism is substantiated by H NMR experiments. In this particular case, the kinetic measurements tended to show the rate-determining step is the

formation of the cyclometalated complex **17** instead of the usual reductive elimination step.

$Ru_3 (CO)_{12}$ has been reported to selectively activate the *ortho* positions in pyridine. In a typical reaction, pyridine is employed as a solvent and the reaction is conducted at 150 °C under 150 psi of CO_2. Conversion of 1-hexene to pyrodyl ketone mixture results in the high regioselectivity of the reaction (Eq 28). In addition, no other pyridine-containing products are observed.[31]

$$(28)$$
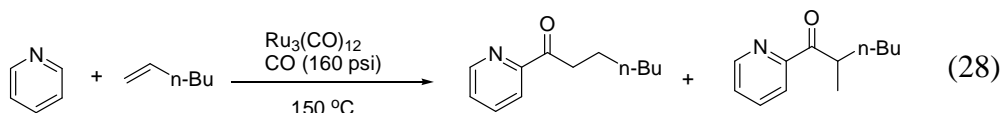
Murakami has reported the alkenylation reaction of pyridine.[32] Heating a cationic ruthenium vinylidene complex $[CpRu(=C=CHR)(PPh_3)_2] PF_6$ in pyridine at 100-125 °C for 24 h affords (E)-2-alkenyl pyridine. Initially, pyridine coordinates to ruthenium by displacement of one of the phosphine ligands. Then, [2+2] heterocycloaddition occurs to form a four-membered ruthenacyclic complex. Deprotonating of the β-hydrogen affords a neutral π-azallyl complex. Protonolysis furnishes the product. As a result, a vinylidene group is inserted into the α-C-H bond of pyridine. The alkenylation reaction is made catalytic in ruthenium by using (alkyn-1-yl) silane as the the vinylidene source.

Treatment of (alkyn-1-yl) trimethylsilane with pyridine in the presence of a cationic ruthenium complex $[CpRu(=C=CHR)(PPh_3)_2] PF_6$ affords the corresponding (E)-2-alkenylpyrine not only in a good yield but also in a region and steroselective

manner (Eq 29).

$$82\%$$
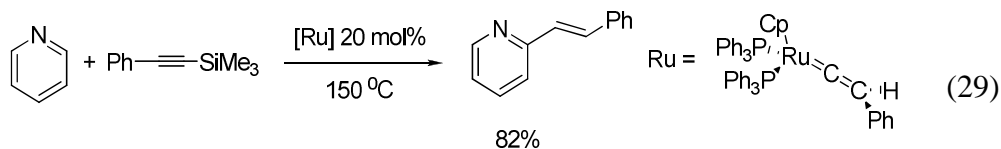
Ames reported the first intramolecular direct arylation reaction involving pyridine

in the eerily 1980s. In this example, treatment of 2-(2-bromphnoxy) pyridine with

Pd(OAc)$_2$ and Na$_2$CO$_3$ afforded the tricyclic compounds in a low 10% yield (Eq 30).[33]
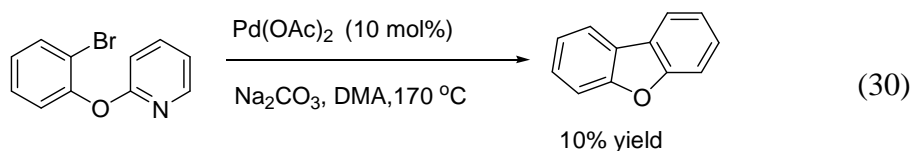
Due to the pyridine moiety is a key component of pharmacophores, nature

products and synthetic building block. Many groups work on pyridine reactions. Sasson

has reported that the access to 2-arylpyridines via an intermolecular coupling has been

achieved using palladium on charcoal in the presence of zinc metal in water (Eq 31).[34]
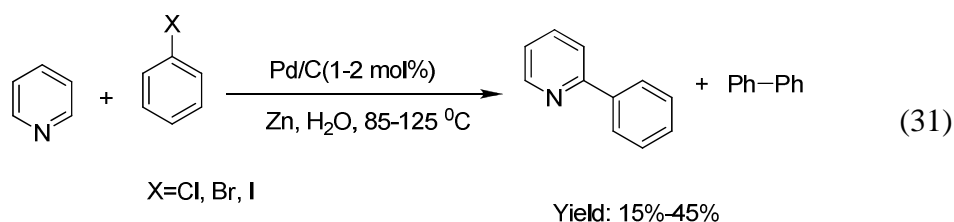
Later, Sames reported that direct and selective catalytic arylation of α- C-H bond

in pyridine with iodobenzene was achieved in up to 70% yield (Eq 32).[89]

$$(32)$$
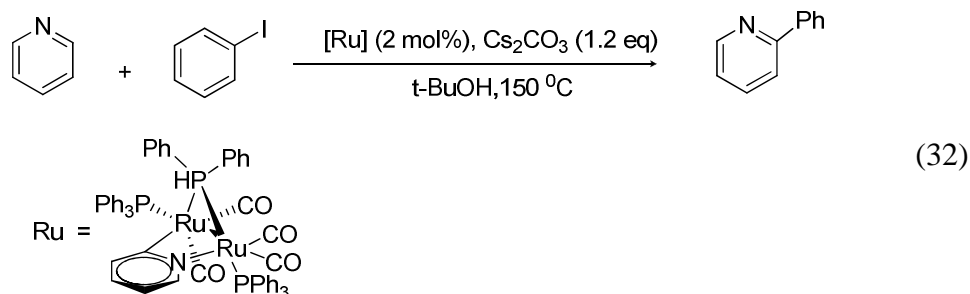
Recently, Fagnou reported that the direct arylation reactions of pyridine N-oxides

occur in excellent yield with complete selectivity for the 2-position with wide range of

aryl bromides (Eq 33).[35] In these reactions, palladium acetate in combination with

tri-tert-butylphosphine emerged as the optimal metal-ligand combination.

$$(33)$$
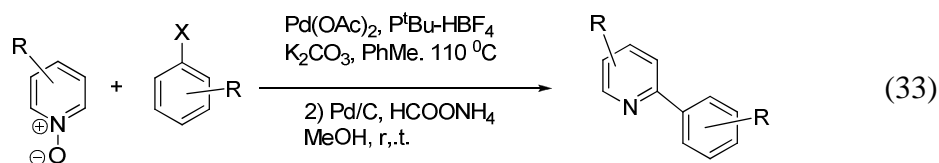
In contrast to reactions performed with many types of organometallics, these

reactions are completely insensitive to the presence of water since 5.0 equiv. of water

added at the reaction outset has no deleterious impact on the reaction outcome. From

these example, they found that these reaction involving pyridine need harsh conditions of

over 150 $^{\circ}$C, and limited to the scope of substrates , and also require the presence of a

direction group or employs N-oxide. Recently, Hiyama reported the C-2 alkenylation of

pyridine by mild nickel catalysis.[36] Since the enhance reactivity of pyridine-N-oxides

compared with that of parent pyridine, is apparently attributed to an electron-deficient

nitrogen that increase the acidity of the C-2 bond, they also reported a similarly activated

pyridine species be generated catalytically in situ by the coordination of the nitrogen to a

Lewis acid(LA) catalyst (Scheme 9). They have reported a combination of nickel and LA

catalyst allows the direct C-2 alkenylation of pyridine under mild conditions. Moreover,

the single or double insertion of alkynes into the C-2-H bond of pyridine is successfully

controlled by simply changing the LA catalyst.
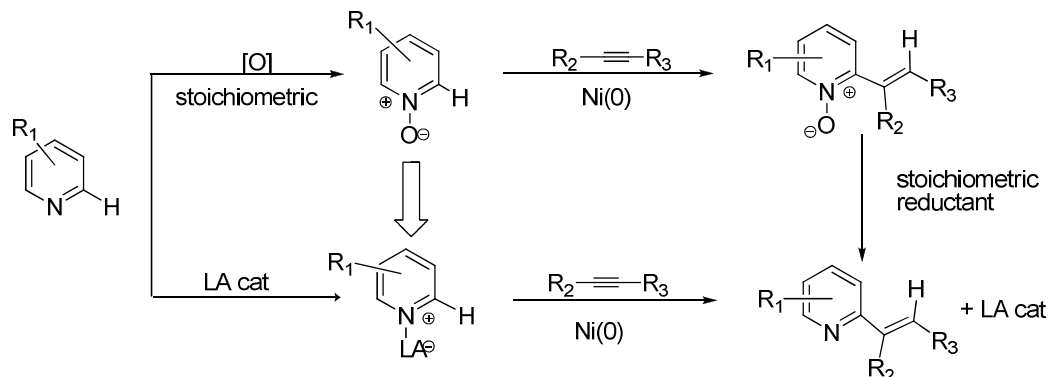
Scheme 8. Mechanism for Alkenylation of Pyridine by Mild Nickel Catalysis

In this report, he found that the zinc and aluminum catalysts with mild Lewis

acidity were highly effective for the alkenylation of pyridine (Eq 34).

$$(34)$$
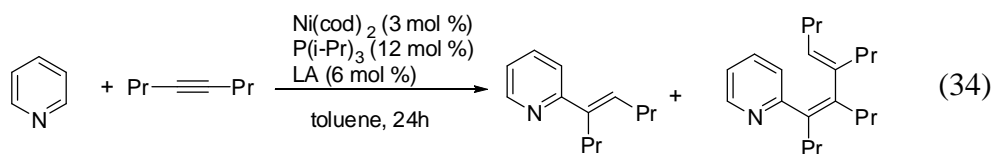
He also gave the plausible Mechanism for this reaction. The pyridine activated by

coordination to a LA would be responsible for the oxidative addition of the C(2)-H bond

to nickel(0) species **20**, a plausible initiation step of the present catalysis.

Hydronickelation across the alkyne coordination to the nickel center in the direction

avoiding a steric repulsion between the bulkier R3 and the pyridyl group in B takes place

to give **22**, which upon reductive elimination affords the product in the presence of zinc

LA catalyst (**path A**). The use of AlMe$_3$, a strong Lewis acid than dioranozincs, or lower

reaction temperature retards the reductive elimination and /or promotes the second

insertion of an additional alkyne into either of the C-Ni bonds in **22** to give **23** or **24**,

resulting in the formation of the product in the **path B**.
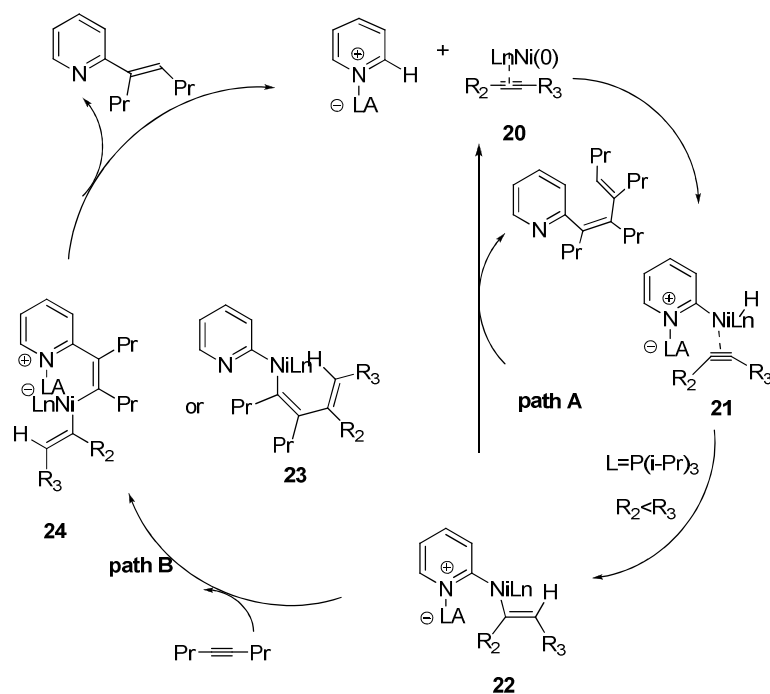
Scheme 9. Mechanism for Alkenylation of Pyridine by Mild Catalysis

1.3 The Formation of Silyl Enol Ether Involving C-H Bond Activation

Due to silyl enol ethers are widely employed in the organic synthesis as the

reactive precursors for carbonyl compounds, they are useful in various synthetic

transformations in a varity of regio-, chemo- and stereo- selective reactions.[37] Over the

past decades, many methods to generate the enol silyl ethers were reported, one of the

early and still one of the mostly frequently used route to (E) or (Z)-silyl enol ethers is the

trapping of ketone or aldehyde enolates generated under the kinetics or

equilibrium–control conditions.[38] And anther mostly used methods are using chlorosilans

with amine as triethyl-amine and amide (as LDA) agent. Although these methods work

well, there still remains a need to look the alternative method with improved efficiency

and can work for an elaborate and practical scale synthesis by generating less waste.

Recently, Tanable and co-workers reported a new method to generate enol silyl ethers

from ketone and aldehydes (Eq 35).[39]

(35)
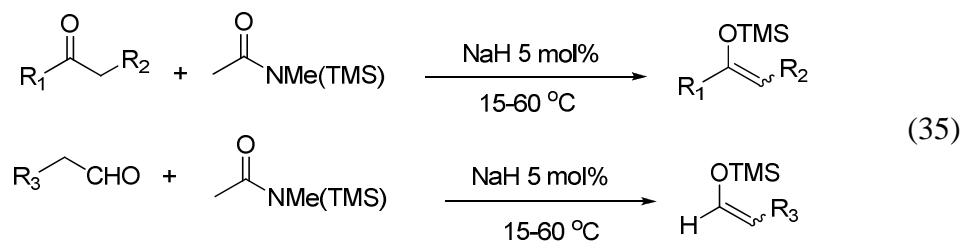
Tanable and the co-workers used NaH to catalyze the reactions under mild

conditions, comparing with the silyl halide method which requires a slightly tedious

work-up procedure to remove HX, their neutral reaction conditions have a practical

advantage of easy isolation of enol silyl ethers.

Due to the convenience and straightforward of the transition-metal catalyzed

isomerization of the ally ether, which can generate the silyl enol ether, [40]many metal

complexes have been reported to syntheses the silyl enol ethers.[41] Recently, Murai

reported the conversion of alkenes to the enol silyl ether by using the iridium carbonyl

complex,[42] which involves the reactions of the alkenes with a hydrosilane and carbon

monoxide to yield the enol silyl ether of acylsilans. These reactions generate the (E) and

(Z)-products, in the most case, the (E) isomers are the major (Eq 36).

$$R' \diagup\diagdown \;\; + \;\; HSiR_3 \;\; + \;\; CO \;\; \xrightarrow[\text{benzene, 140 °C, 48 h}]{Ir_4(CO)_{12}} \;\; R' \diagup\diagup\diagdown \overset{OSiR_3}{\underset{SiR_3}{}} \qquad (36)$$
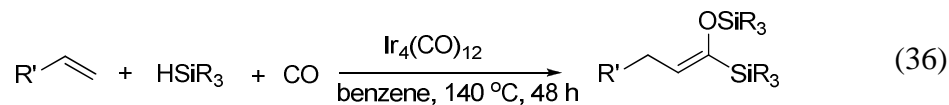
Due to the high temperature and the high pressure of carbon monoxide (50 atm at

25 °C), the reactions require the high pressure tube and some content, it is unsafe for the

people working with the experiments. Later on Milyaura reported the stereoselective

synthesis of the silyl ethers catalyzed by iridium COD complex under the mild conditions

(Eq 37).[43]

$$\underset{R_3}{\overset{R_2}{R_1}}\diagdown\diagup OSiR_3 \;\; \xrightarrow[\text{THF, r.t., 30 min}]{[Ir(cod)(PPh_2Me)_2]PF_6} \;\; \underset{R_3}{\overset{R_2}{R_1}}\diagdown\diagup OSR_3 \;\; + \;\; \underset{R_3}{\overset{R_1 \;\; OSiR_3}{R_2}} \qquad (37)$$
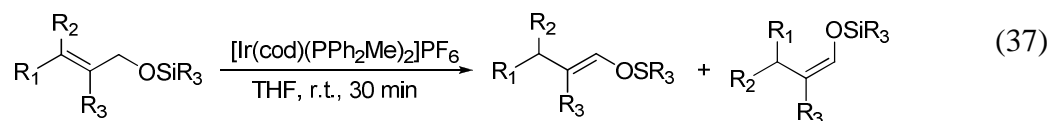
For the less bulky substitutes, the reactions all were carried out the room

temperature and showed the high conversion and the selectivity, but when using more

bulky groups as phenyl ether, the reaction was very slow. These results may due to the

steric hindrance to the coordination to the iridium center. In the report, they also gave the

proposed mechanism for the isomerization reaction. This mechanism involves the

oxidative addition of an allylic C-H bond to the iridium complex to give the ally iridium

intermediates, and next go through the reductive elimination to afford enol ether. In the mechanism, they also mentioned that the isomerization involves two processes: the first and selective formation of the *E* isomer is the kinetically control process, and then following is the equilibration to give a mixture of the (*E*) and (*Z*) isomers. This process can be retarded in a solvent that strongly coordinates to the metal center, but they are fast in the solvent which have the medium donor strength such as CH_2Cl_2 and acetone can favor the formation of the mixture. So they motioned that the formation of the product was highly dependent on the catalyst, the solvent, reaction time and also the substitutes.

As the important synthetic intermediates, the enol silyl ether can be used in the carbon extension reactions. Three carbon chain extensions of the alkynes to geometrically define enol silyl ethers requires stoichiometric conversion to a vinyl halide followed by a heck reaction or to a vinyl organometallic followed by conjugate addition. Recently, Trost reported a simplified protocol to affect a direct catalytic three-carbon chain extension of alkynes to *E*-enol silane (Eq 38) by using ally silly ether.[44]

$$(38)$$
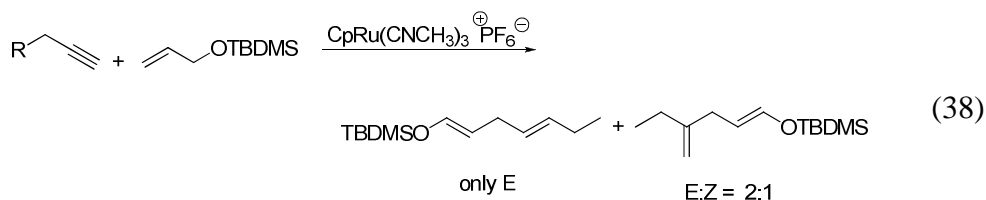
Marciniec reported the silylcarbonylation of vinylsilanes catalyzed by iridium siloxide complexes (Eq 39).[45]

$$(39)$$
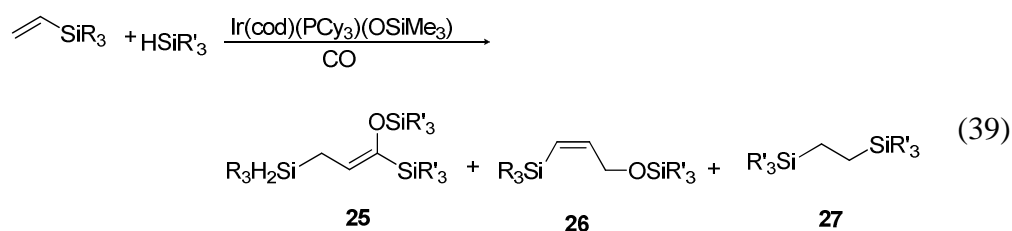
In this reported, the yields of the silylcarbonylation products depends strongly on the reaction conditions such as the ratio of substrates and pressure of the carbon monoxide, as well as the loading of the catalyst.

1.4 Alkyne C-H Bond Activation

1.4.1 The Formation of Enol Esters from the Coupling Reactions of Alkynes and Carboxylic Acids

Enol esters are a versatile class of precursors for a variety of synthetically important organic transformations such as cycloaddition,[46] asymmetric hydrogenation,[47] C-C bond coupling,[48] and Aldol- and Mannich-type of condensation reactions.[49] Since enol esters can also serve as a synthon for aldehydes and ketones, much research efforts has been devoted to develop efficient catalytic methods to control both regio- and stereoselectivity in forming substituted enol esters. From an industrial perspective of increasing synthetic efficiency and tolerating functional groups as well as for reducing

waste byproducts, catalytic methods for producing enol esters are highly desired

compared to the classical methods that utilize stoichiometric amounts of strong base or

toxic Hg salts.[50] Recently Zhang reported the synthesis of enol esters by using gold

complexes as catalyst (Eq 40).[51]
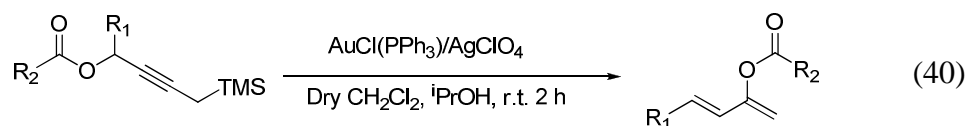
Later on the same author reported the homogeneous oxidative C-O bond

formation by using the different gold catalyst (Eq 41).[52]
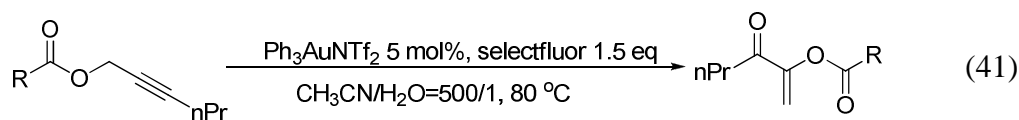
Qian recently reported that the cycloetherification of hydroxyl propargylic esters

by using the Au(I) and Pt (II) complexes (Eq 42).[24d]
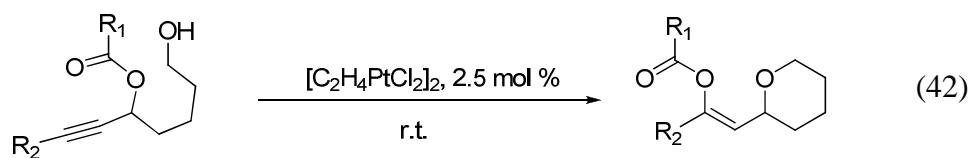
There are also some other examples on the catalytic synthesis of enol esters such

as Zr-catalyzed methyl alumination of alkynes,[53] Au-catalyzed intramolecular

rearrangements of propargylic esters and alcohols[54] Cu-catalyzed oxidative esterification

of aldehydes with β-dicarbonyl compounds,[55] and asymmetric couplings of ketenes with

aldehydes by chiral Fe catalysts.[56]

Transition metal-catalyzed alkyne-to-carboxylic acid coupling reaction offers an

attractive route to enol esters, there has also been a large amount of work on the additions

of carboxylic acids to alkynes to form enolesters. the first report describing this reaction

dates back to 1983 by Youval Shvo,[57] in this report, $Ru_3(CO)_{12}$ was used to catalyze the

coupling reaction of aliphatic and aromatic carboxylic acid to di- and mono-substituted

acetylene and they got the anti-markovnikov (*E* and *Z*) and Markovnikov product by 10

examples with 40% - 95% conversion (Eq 43).
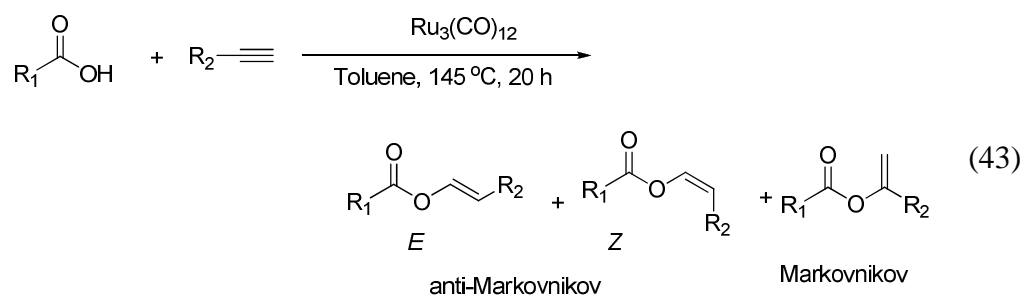
Later on the process has been developed by Mistsudo,[58] Dixneuf,[59] and

Verpoort,[60] although other groups have been and still involved in this field. But its

synthetic potential has not been fully realized in part because the catalytic method

typically produces a mixture of *gem*- and (*E*)/(*Z*)-enol ester products. Considerable

research has been devoted to control both regio- and stereoselectivity in forming the enol

ester products by modulating steric and electronic nature of the metal catalysts.

Generally, late transition metal catalysts have been found to be effective for the coupling

reaction to produce a mixture of (*E*) - and (*Z*)-enol esters from *anti*-Markovnikov

addition of carboxylic acids to terminal alkynes over *gem*-enol ester products.[61] The

regioselectivity of the Markovnikov addition has been significantly increased by using a

variety of ruthenium precursors such as $(C_5H_5)_2Ru$, $(arene)RuCl_2(PR_3)$.[62] Mistsudo use

bis (C_5H_5) ruthenium (PBu_3) as the catalyst, and they found that for the linear alkynes

such as 1-hexyne and 1-pentyne the reactions showed high selectivity for Markovnikov

addition to give the *gem*-enol esters. For other substitute alkynes such as phenylacetylene

addition of acetic acid gave of Markovnikov and anti-Markovnikov products and yields

were around 55 % (Eq 44).[63]

$$
\underset{R}{\overset{O}{\underset{OH}{\|}}} + R' \!\!\!\equiv \quad \xrightarrow[\text{Toluene, 80 °C, 5-24 hrs}]{\text{(COD)}_2\text{Ru/PBu}_3} \quad \underset{\text{Major}}{R\overset{O}{\|}O\diagup\!\!\diagdown R'} + \underset{\text{Minor}}{R\overset{O}{\|}O\diagup\!\!\diagdown R'} \quad (44)
$$
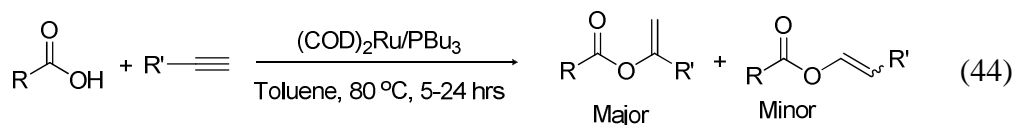
Mitsudo used the bis (C_5H_5) ruthenium-P $(n\text{-}Bu_{3)}$ to generate the geminal product

as the major. Other groups are still working on this type reaction to get the regioselective

formation of *gem*-enol esters by using a variety of metals complexes such as mercury (II),

silver (I), rhodium I) and palladium (II). And the regioselective formation of *gem*-enol

esters has recently been achieved by using cationic Rh catalysts.[64] Bianchini and Dixneuf

got the regioselective formation of 2-(benzoyloxy) propene from the addition of benzoic

acid to propyne in the presence of the trigonal- bipyramidal Rh(I) monohydrides

$(PPh_3)_3RhH$ and $(NP_3)_3RhH$ and they were the first group showed the mechanism study

on this reaction (Eq 45).

$$\text{Ph}\overset{\text{O}}{\underset{\text{OH}}{\bigvee}} + \text{H}_3\text{C}\!\!=\!\!=\!\! \xrightarrow[\text{Toluene, 100 °C,4 h}]{(PPh_3)_3RhH\ 1\ mmol\%}$$

G : Z : E
94% 3% 3%

(45)
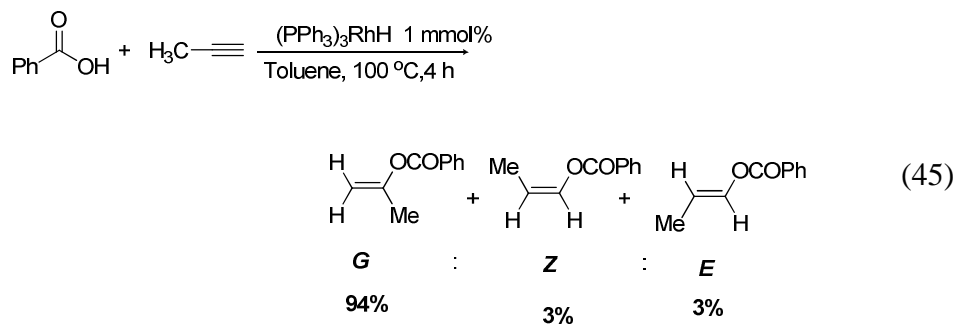
The proposed catalysis cycle for the coupling reaction of carboxylic acid and alkynes was given by Dixneuf (Scheme 10). Firstly, the rhodium (III) dihydride complex was detected by NMR by the reaction of rhodium phosphine complex with the carboxylic acid at the room temperatures. Dixneuf assumed this was the starting point of the catalysis cycle, and the 16- electron systems $[(L)Rh]^+$ was the real catalyst. And then by using rhodium (III) dihydride compound to react with alkyne they detected the H_2 by the GC and get the Rh(I) alkenyl complex that may form upon nucleophilic attact by carboxylate at alkeyne. This Rh(I) alkenyl complex is ready to be protonated at the metal by a second molecule of carboxylic acid. Then with the elimination this cycle generates the geminal product and the 16-electron fragment $[(L)Rh]^+$ are regenerated and the catalysis cycle can continue.

Among these methods all showed high regioselectivity for the Markovnikov addition to form the *gem*-enol esters, but no general preparation of alk-1-en-1-yl esters corresponding to an *anti*-Markovnikov addition of the carboxylic acid to the triple bond was discovered.
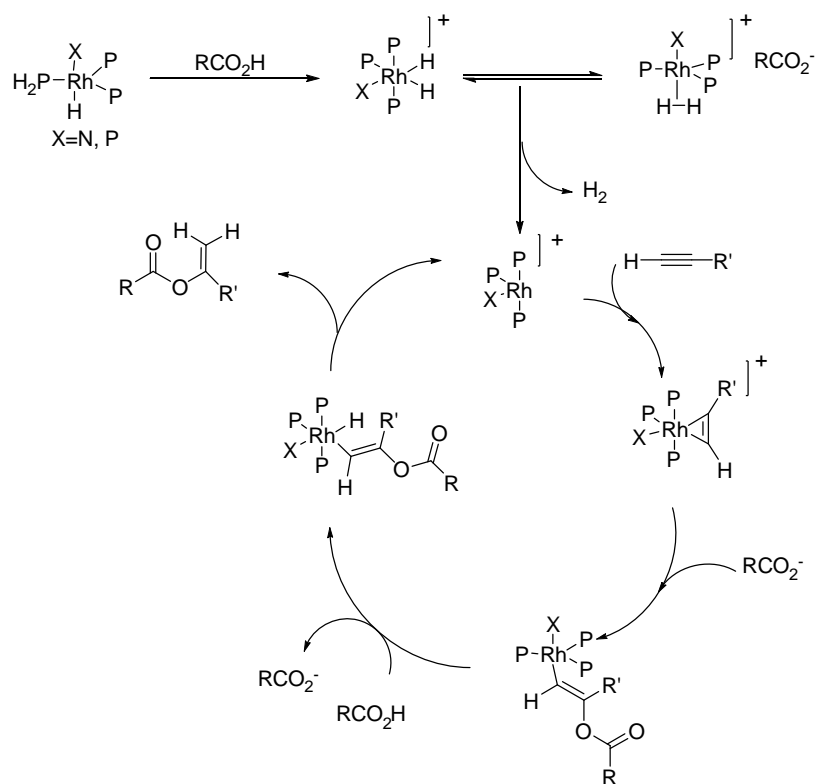
Scheme 10. Proposed Mechanism for the Reaction of Carboxylic Acid and Alkynes

Doherty tried to control the selectivity for the formation of the anti-Markovnikov addition product by changing the ligands of the ruthenium complexes, although they could get the (Z)-isomers as the major, they still got mixtures of three products. Dixneuf and co-workers work on the formation of enol ester reaction since 1995,[24] they got three mixtures at their first report on this type reaction, and later on they focused on the study on the regioselectivity of the this type reaction in presence of ruthenium complexes by changing the ligands. Recently they showed the relationship between steric environment of the ruthenium-phosphine catalysts and the stereoselective formation of the (Z)-enol

esters.[65] They reported that modification of the active ruthenium (II) center by coordination of a chelating diphosphine and labile allylic ligands in complexes $(Ph_2P(CH_2)_2PPh_2)Ru(methallyl)_2$ provides suitable catalyst precursors for the *anti*-Markovnikov addition of carboxylic acid to terminal alkynes to stereoselectivity afford (Z)-alk-1-en-yl esters.

This ruthenium compound **28** was used to demonstrate the mechanism of this reaction (Scheme 11). In presence of carboxylic acid at the reaction temperature, a ligand exchange took place from the ruthenium complex **28** and gave the new ruthenium complex **29**. The addition of benzoic acid to hexyne, carried out at 65 ^{o}C for 3 hours in the presence of 1 mol % of compound **29** as catalyst precursor, led to a complete conversion of the starting materials and formation of (Z)-hex-1-en-1-yl benzoate in 97% selectivity. Moreover this complex **29** was recovered at the end of the reaction and thus appeared to be the actual catalyst precursor or the catalyst itself. Based on these observations, they proposed that the first step is the ligand substitution of the allylic group by the carboxylates with elimination of isobutene to produce complexes **29**, a rearrangement of the carboxylate to get complex **30** would make possible the coordination of the alkyne to give intermediate **31**.
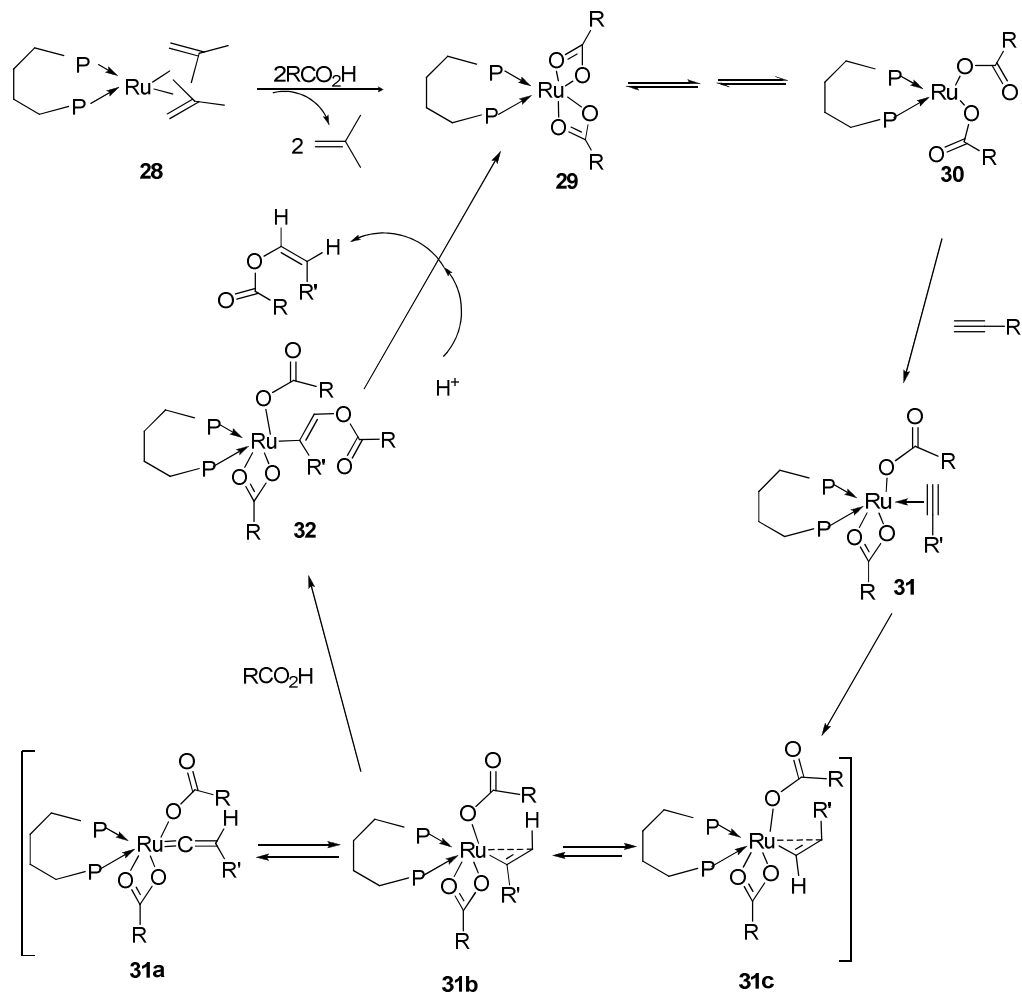
Scheme 11. Proposed Mechanism for the Coupling Reaction of Carboxylic Acid and Alkynes by Ruthenium Complex

From this intermediate, several resonance forms (**31b** and **31c**) and the vinylidene

tautomer **31a** can be postulated, depending on the ancillary bidentate ligands. The

external addition of the carboxylate to the electrophilically actived C (1) of the alkyne

might then take place to form the intermediate **32**. On subsequent protonolysis of the

Ru-C bond, or protonation of the ruthenium center followed by reductive elimination, the

alkyl ester is liberated. The regioselectivity of the reaction may depend on the electron

deficiency of the coordinated triple bond. Its polarization according to **31b** with a positive

charge at the unsubstituted carbon atom of the alkyne due to electronic effects of the

diphosphine ligand, or the formation of the tautomeric ruthenium –vinylidene complex

32, easily formed from a terminal alkyne and ruthenium complex, would favor the

addition of the carboxylate at the electrophilic of C (1) of the terminal alkyne. Due to the

steric interactions between the diphosphine ligands and the substituted the formation of

(Z)-isomers suggested a ruthenium intermediated of type **32**, which on protonation would

lead to a formal trans- addition of carboxylic acid to the terminal alkyne is low with

catalyst **28** (Eq 46).[66]

$$2\ R\!\!=\!\!\!=\!\!\!-H + R'CO_2H \xrightarrow[\text{dioxane, r.t.}]{\text{Cp*Ru(COD)Cl 5 mol\%}} \underset{R'}{\overset{O\quad R}{\bigg\Vert}}\!\!\!\diagdown\!\!\!\diagup\!\!\!O\!\!\!\diagup\!\!\!\diagdown\!\!\!\diagup\!\!\!\diagdown\!\!R \qquad (46)$$
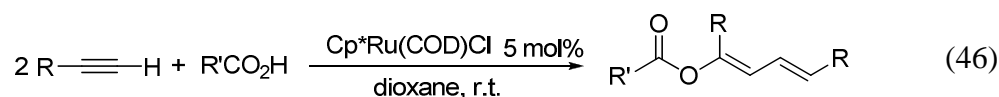
This reaction is proposed to proceed via metallacyclopentadiene intermediate **34**.

Protonation of ruthenium complex **33** followed by addition of the carboxylate produces

ruthenacyclopentene **37**.

A â-hydrogen elimination of Ha followed by a reductive elimination releases the

1,3-diene product and regenerates the active ruthenium catalyst (**33**). For example, aryl

alkyne and acetic acid combine to form 1,3-dienyl ester in 85% yield. Another potential

mechanism for this reaction involves the *trans* addition of a carboxylic acid catalyzed by

ruthenium to generate a vinyl ruthenium which generates *cis* carbometalation of another

alkyne.
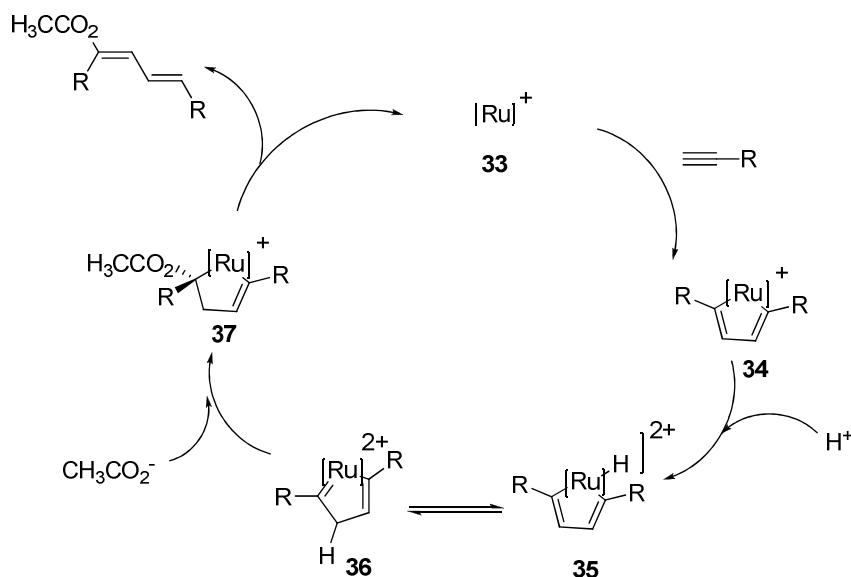
Scheme 12. Proposed Mechanism for the Formation of Dienyl Esters

Both intra- and intermolecular versions of the catalytic alkyne-to-carboxylic

coupling methods have been successfully applied to the synthesis of complex organic

molecules.[67] Burton and the co-workers reported that the reaction of

difluoro-3-iodoacrylic acid with a variety of the terminal acetylenes under cocatalysis of

PdCl$_2$(PPh$_3$) and CuI gave difluoroinated 2- pyrones as the sole product in good yields

(Eq 47) .[68]
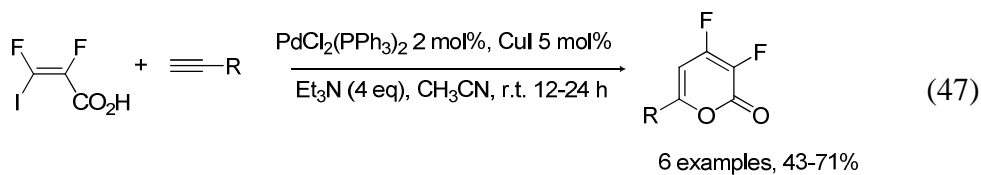
(47)

6 examples, 43-71%

Despite considerable synthetic and mechanistic progress, however, neither the

nature of reactive intermediate species nor controlling factors for the formation of *gem-*

vs (*E*)/(*Z*)-enol esters has been clearly established.

1.4.2 The Hydrosilylation of Alkynes

Vinylsilanes are very useful intermediates in organic synthesis,[69] they have

emerged as versatile building blocks. Because of their low toxicity, low cost, high

stability, and innocuous byproduct vinylsilanes play a growing role in the synthesis and

particularly in metal-catalyzed cross-coupling reactions.[70] Vinylsilanes are very useful as

acceptors in conjugate addition reactions,[71] as masked ketones through Tamao-Fleming

oxidation,[72] and as terminators for cation cyclizations.[73] They can be readily carried

through many synthetic operations. Over the past decades, many groups are working on

the routes to syntheses vinylsilanes, and among the most straightforward and

atom-economical method to assemble vinylsilanes is transition metal catalyzed

hydrosilylation of alkynes. This method started at the addition to the alkynes by both

carbon monoxide and trialkylsilanes in the manner depicted in Eq 48.

$$R\text{---}\!\!\equiv\!\!\text{---}H \ + \ CO \ + \ R'_3SiH \ \xrightarrow{\text{Catalyst}} \ \underset{OHC}{\overset{R}{\diagup}}\!\!=\!\!\underset{SiR'_3}{} \qquad (48)$$
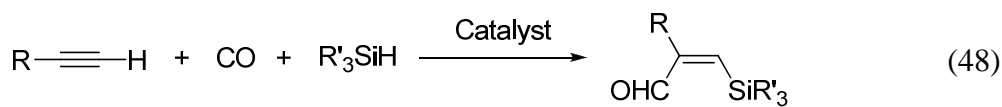
The original discovery of "silylcarbonylation" by Murai[74] using $Co_2(CO)_8$ found

olefin conversion to silyl enol ethers of the homologous aldehydes as the sole

carbonylation products. The same outcome has been reported for enamines catalyzed by

$[RhCl(CO)_2]_2$ and for the terminal alkenes catalyzed by $Ru_3(CO)_{12}$ and $(Ph_3P)_3RhCl$.[75]

And later on Matsuda and Ojima[76] independently reported the silycarbonylation of

alkynes catalyzed by $Rh_4(CO)_{12}$ or Rh-Co mixed metal carbonyl clusters. In contrast

silylcarbonylation reactions catalyzed by $Rh_4(CO)_{12}$ or Rh-Co mixed metal carbonyl

clusters yield the carbon-centered silane exclusively, and with terminal alkynes these

transformations generally occur under mild conditions with a high degree of regiocontrol.

There are many reports on the intramolecular version and intermolecular

silylcarbonylation reactions. Recently Trost reported the intramolecular endo-dig

hydrosilylation catalyzed by ruthenium.[77] For the intramolecular hydrosilylation, there

are two major pathways (Eq 49), one is catalyzed by the platinum compounds to generate

the (E)-vinylsilanes, the other one is catalyzed by the ruthenium complexes to generate

the (Z)-vinylsilanes.

(49)
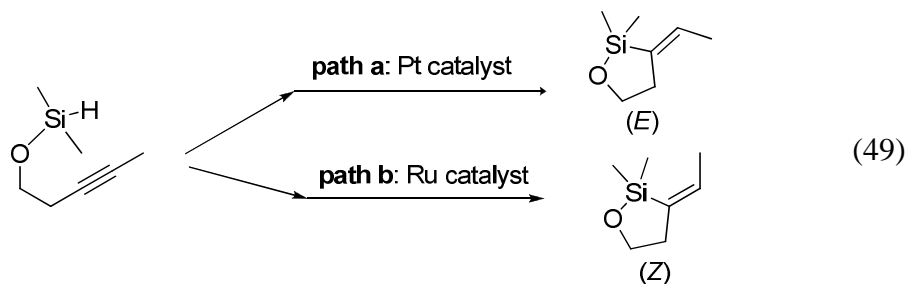
Trost and the co-workers show some details on the pathway in this report, they

extend the scope of the reactions by using function substitutes such as the alcohol, ester

and ether. Moreover, all these reactions show the high selectivity on the formation of (*Z*)

isomer and good yields. For the intermolecular silylcarbonylation reactions, the

hydrosilylation of alkynes is still the simplest and most straightforward method for their

preparation. The main difficulty with this transformation is control of the stereo- and

regiochemistry of the alkenesilane. Generally, these type reactions always generate the

mixture (Eq 50).

$$R\!\!=\!\!=\!\!H + R'_3SiH \xrightarrow{\text{catalyst}} \underset{H}{\overset{R}{\diagdown}}\!\!=\!\!\underset{SiR'_3}{\overset{H}{\diagup}} + \underset{R}{\overset{H}{\diagdown}}\!\!=\!\!\underset{SiR'_3}{\overset{H}{\diagup}} + \underset{R}{\overset{R'_3Si}{\diagdown}}\!\!=\!\!\underset{H}{\overset{H}{\diagup}} \quad (50)$$
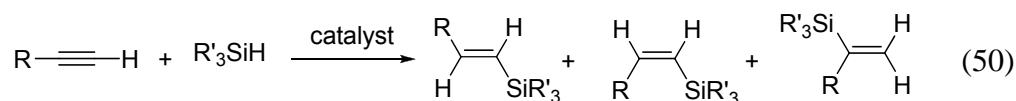
Although radical and Lewis acid [78] induced procedures have been reported, the

transition-metal-catalyzed reaction continues to play a dominant role since it proceeds in

a stereoselective manner. Recently Alami reported platinum oxide catalyzed

hydrosilylation of unsymmetrical internal aryl alkynes under *ortho*-substituent

regiocontrol (Eq 51).[79]

$$Ph\!\!=\!\!R_1 + Et_3SiH \xrightarrow[\text{CH}_2\text{Cl}_2, 60\,^\circ\text{C, 1h}]{\text{Pt complex (5 mol \%)}} \quad (51)$$
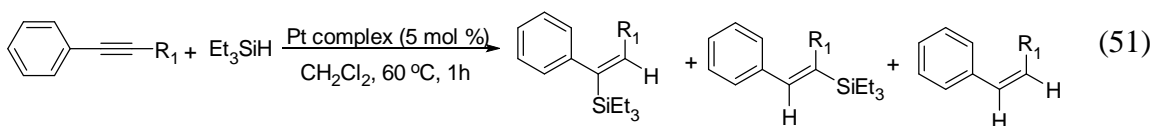
Alami and co-workers compared the reactivity of the catalyst PtO_2 with Speier's

catalyst (H_2PtCl_6) in hydrosilanes of terminal alkynes, and they found that these two

platinum complexes show the good reactivity for hydrosilylation of terminal alkynes, and

in most case PtO_2 shows better reactivity and higher selectivity on the α-isomer and

β-isomer than Speier's catalyst (H_2PtCl_6). They tried to control the selectivity on one

isomer by modifying the reactions conditions, but they still get the mixtures, and they did

not give the explanation on the factor of the formation of the mixtures. Later on Marko[80]

and Folch [81]improved the selectivity on β-hydrosilylation isomers by using platinum

complexes as catalyst. Marko used platinum complex with bulky ligand to get the high

selectivity on the β-(Z) isomers (Eq 52).

$$R_1\!\!=\!\!=\!\!R_2 \;+\; HSiR_3 \quad \xrightarrow[\text{THF},60\,°C,\,30min]{\text{5 mol\% Pt complex}} \quad \underset{R_1}{\overset{H}{\diagdown}}\!\!=\!\!\underset{R_2}{\overset{SiR_3}{\diagup}} \;+\; \underset{R_1}{\overset{R_3Si}{\diagdown}}\!\!=\!\!\underset{R_2}{\overset{H}{\diagup}} \qquad (52)$$
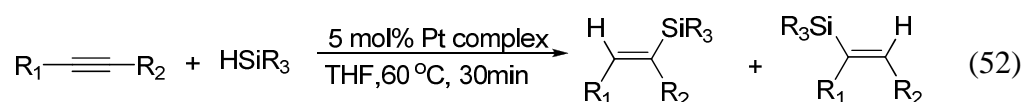
Floch focused on improving the selectivity on the β-(E) isomers by using

platinum (0) phosphine complex as the catalyst (Eq 53).

$$R\!\!=\!\!= \;+\; Et_3SiH \quad \xrightarrow[\text{THF},60\,°C,\,5min]{\text{5 mol\% Pt complex/PPh}_3} \quad \underset{R}{\overset{Et_3Si}{\diagdown}}\!\!=\!\! \;+\; \underset{Et_3Si}{\diagup}\!\!=\!\!\overset{R}{\diagup} \qquad (53)$$
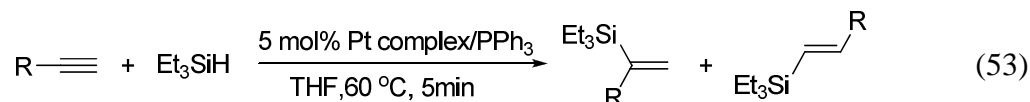
The reactions of terminal alkynes and triethylsilane generate the vinylsilanes in

mild conditions in about 5 min. These reactions generate β-(E) isomers and α-isomer.

Floch found the ratio of these two isomers shows the dependence on the alkynes. When

using less bulky substitutes as linear alkynes the reactions show the high selectivity on

the β-(E) isomers, and the ratio of β-(E) isomer to α-isomer is about 99/1. The ratio of

these compounds decreased by using the bulky substituents, for example the reaction the

phenyl acetylene with triethylsilane generates the mixture of β-(E) isomer and α-isomer,

the ratio of them is around 80/20, but they did not mention the details on the mechanism of these reactions.

Ruthenium complexes are also good catalysts for the hydrosilylation of alkynes and alkenes. In 1986 Muri reported the single-operation synthesis of vinylsilanes from alkenes and hydrosilanes with the aid of ruthenium carbonyl complex (Eq 54).[82]

$$\text{(54)}$$
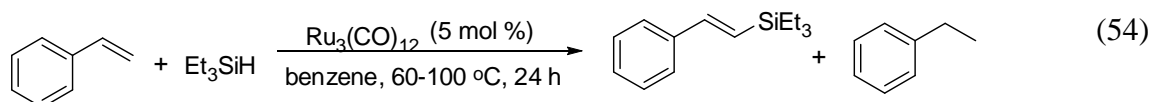
The reaction of excess amount of styrene with triethylsilane gives the *trans*-vinylsilane and one equiv. ethylbenzene as by product. At high temperature, this reaction also generates some amount of alkylsilanes. These reactions show the high limitation on the alkenes, Muri found that, only the terminal alkenes can show the reactivity and generate the products but some substituents need high temperature. Later on, many groups had been working on the synthesis of vinylsilane by hydrosilylation of alkynes and alkenes, but most of them focused on the selectivity for the reactions of alkynes and hydrosilanes. Recently, Chang reported the highly stereoselective and efficient hydrosilylation of terminal alkynes catalyzed by [RuCl$_2$(p-cymene)]$_2$ (Eq 55).[83]

$$\text{(55)}$$
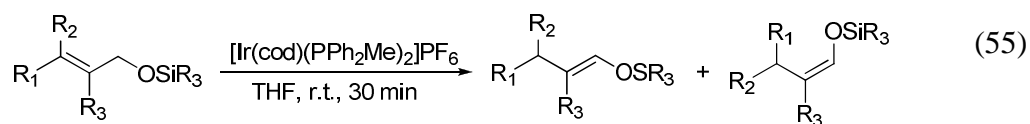
Under mild conditions, the reactions of terminal alkynes with hydrosilane favor to generate the (*Z*)-vinylsilanes and give high yields. However, when Chang uses some

function substitutes such as the hydroxyl groups, the reactions lose the selectivity, they

get α-isomer and β-(Z) isomer as the mixture and the ratio of them changes with the

different substitutes, in this report, they did not mention the factor of these results, and no

mechanistic details were given by them.

Later on Ball reported the Markovnikov alkyne hydrosilylation catalyzed by the

ruthenium cationic complexes, [84] they reported that the reactions of alkynes with

hydrosilanes were smoothly converted in 30 min at ambient temperature to the branch the

(1,1-distubstituted) vinylsilane in good yields without detectable formation of

(1,2-disubstituted) products with only 1 mol % of $CpRu(MeCN)_3{}^+PF_6{}^-$ A variety of

terminal alkynes proved amenable to the reaction, including those with substantial steric

bulky groups. The reaction is tolerant to a wide range of functional groups, including sp^2

halides, alkenes, esters, free alcohol, protected amines and even free carboxylic acid.

Overall good yield and good regioselectivity are maintained through a wide range of

substrates in this report. The details on the mechanism for this reaction have not been

discussed (Eq 56).

$$\text{(56)}$$
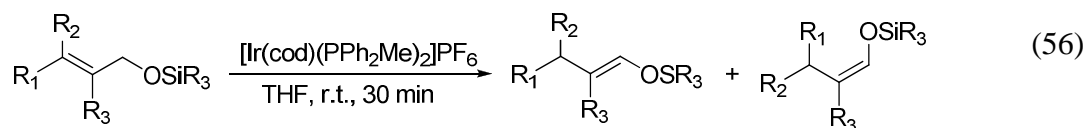
Yamamoto also reported hydrosilylation of the terminal alkynes by using the

$Cp^*RuH_3(PPh_3)$, they observed the similar results as Ball's: the reactions of terminal

alkynes with hydrosilane generate the germinal vinylsilane as the major product with

some amount of ($Z+E$) isomers. The ratio of these products can be 99/1-89/11 (Eq 57).[85]

$$R\!\!=\!\!\equiv \;+\; MeCl_2SiH \xrightarrow[\text{toluene,80 }^{\circ}\text{C, 24 h}]{Cp^*RuH_3(PPh_3)} \quad \underset{R}{\overset{Cl_2MeSi}{>}}\!\!=\!\! \;+\; \underset{Cl_2MeSi}{\overset{R}{/\!\!=\!\!/}} \;+\; \underset{R}{/\!\!=\!\!\overset{}{\underset{SiMeCl_2}{}}} \tag{57}$$
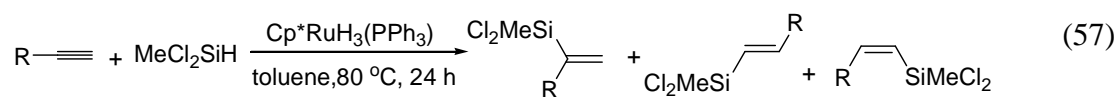
On the basis of these the NMR observation of the stoichmetric mixture of

complex **38** and HSiMeCl$_2$ for liberation of hydrogen, a plausible catalytic loop of the

present hydrosilylation of terminal alkyne is depicted as Scheme 13, where the key

intermediate **39** would originate from the precursor **1**, the hydrosilane, and the substrate

alkyne. Thus they assume that a key step may involve the silylruthenation, probably in a

manner syn to the coordinated alkyne to form either β-silyated alkenylruthenium **40** or

41. And the intermediate **40** would be sterically less demanding and constitutes the major

loop, while B' may be more congested due to an additional steric repulsion between the

ruthenium center and the substituent R, becoming the minor one.
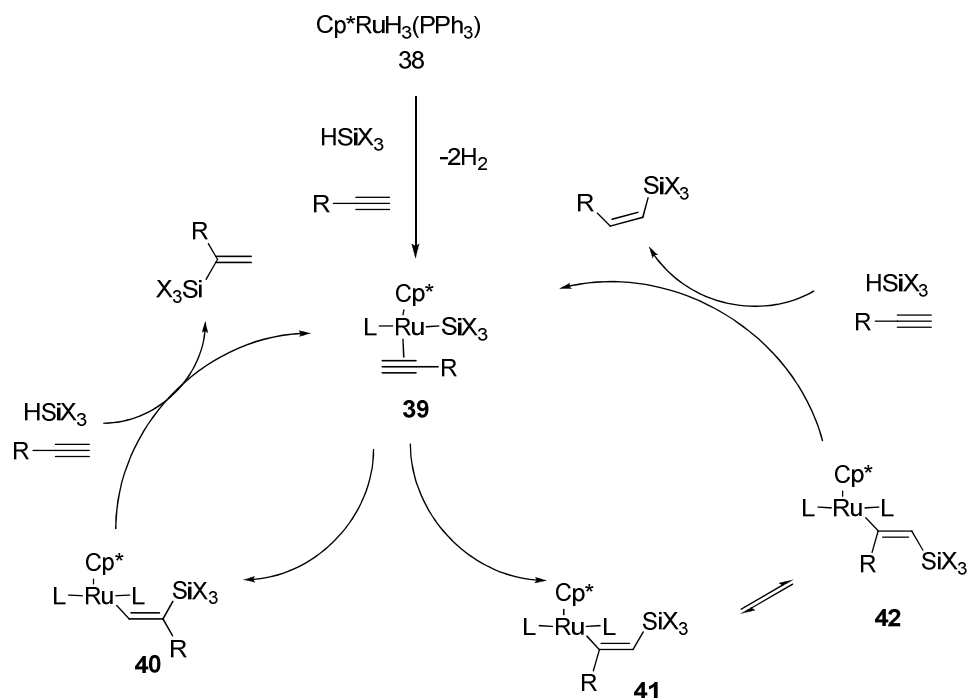
Scheme 13. Proposed Mechanism of the Hydrosilylation of Alkynes

They also did the study on the ligands of the ruthenium, and fond that the presence of a bulk Cp* ligand and PCy$_3$ on the ruthenium center in complex **39** would help silyruthenation proceed highly regioselectivity in favor of **40** rather than **41**. Moreover, this can give the explanation the ratio of the germinal and *cis* vinylsilane products.

Although Yamamoto and the co-workers give some details on the mechanism for the hydrosilylation of alkynes, there are still something unclear for this reaction. Up to now, the better catalyst for mechanistic study on the hydrosilylation of alkynes is the

rhenium complexes. There are four types proposed mechanism for the hydrosilylation

reactions catalyzed by rhenium complexes in Scheme 14 was proposed by Haszeldine,[86]

the catalytic cycle starts at the addition of terminal alkynes to the Rh-Si complex to give

the complex **43**, and with another equiv. $HSiEt_3$ coming, there are two path ways, one is

going through the elimination to generate the trans product, due to the steric conflict

between the silyl group and alkynes this way should favor if there is some bulky

substitutes. The other one is the formation of the *cis* product through β-hydride

elimination of the 1- Et_3Si-hexyl-Rh($SiEt_3$) species **45**, but there are some problems on

this scheme. This step should not favorable since there is a steric conflict between the

silyl and the butyl groups in the transition state, and it is unreasonable to assume that the

sterically more demanding *trans* product selectively substituents the *cis* product from the

intermediate **46**. Overall, it is against thermodynamics to assume isomerization of the

more stable *trans* product to the less stable *cis* product.
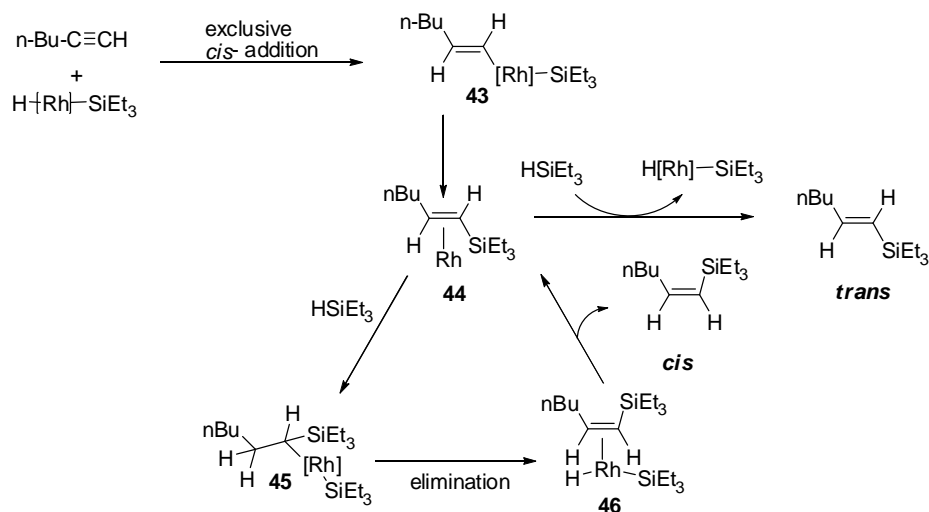
Scheme 14. Proposed Mechanism of the Hydrosilylation of Alkynes by Rhodium Complexes

Nile improved this mechanism (Scheme 15)[87], the first step of the catalytic cycle is the addition of rhenium silane complex to generate the *trans* intermediated **47,** and then the same way to get the *trans* product. For the formation of the *cis* product, he proposed the rotation of the single bond in the zwitterionic carbene intermediated VI to give the *cis*-1-pente-nyl-Rh-(SiR$_3$) complex **48** and then go through the elimination to generate the *cis* product, but the intermediated complex **49** is sterically much more hindered, so it is unflavored, and the n-propyl group would destabilize the negative charge developing on C-2 of VII, so we can see clearly, this mechanism can't explain the formation of the *cis* product.
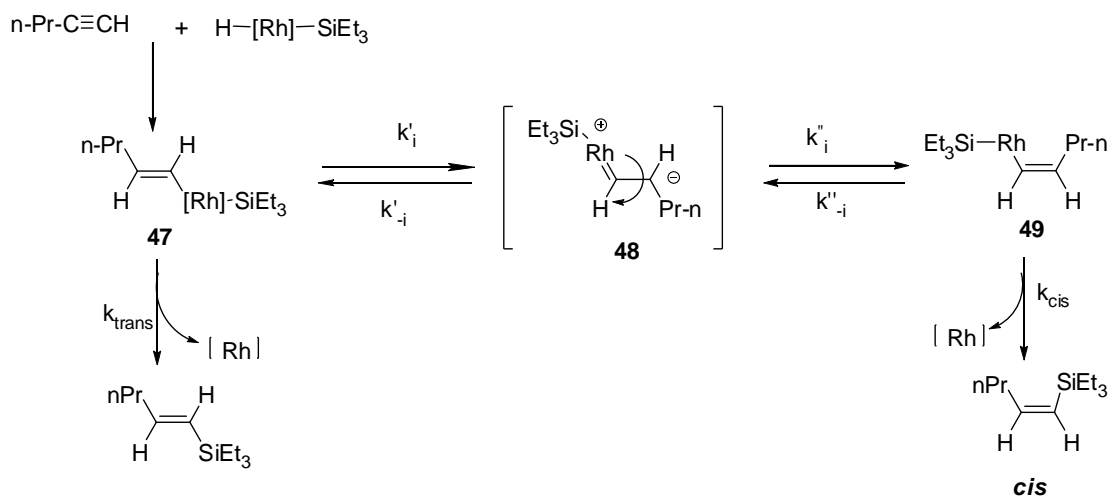
Scheme 15. Nile's Proposed Mechanism of the Hydrosilylation of Alkynes

Later on, Ojima proposed a different mechanistic cycle,[88] which can explain the

formation of the *cis* product.
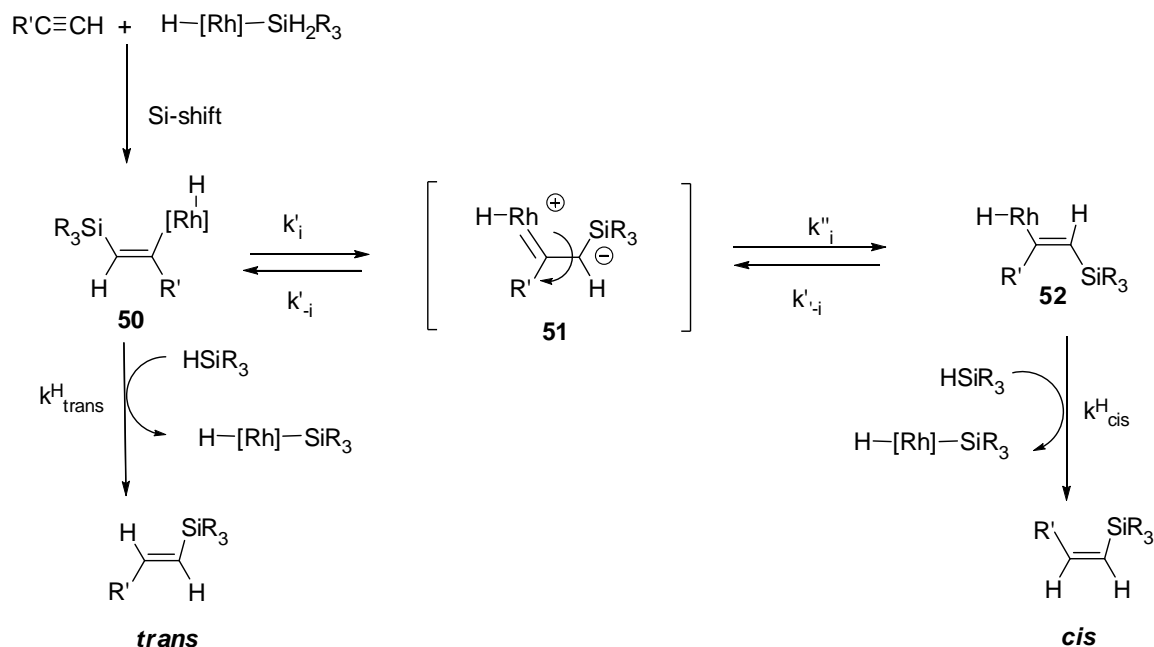
Scheme 16. Ojima's Proposed Mechanism of the Hydrosilylation of Alkynes

The proposed mechanism starts at the insertion of an alkyne into the silicon-rhodium bond in the first place to form the (Z)-l-silyl-l-alken-2-yl-Rh intermediate **50**, instead of the previously proposed insertion into the hydrogen-rhodium, this is one of the most important steps in the whole mechanism. The intermediate **50** thus formed suffers from serious steric hindrance between the silyl group and the rhodium moiety, which are both bulky. Thus, **50** undergoes isomerization to the sterically more favorable (E)-l-silyl-1-alken-2-yl-Rh complex (X) via the zwitterionic carbene complex **51**, which is somewhat similar to the one proposed by Nile, but the silyl group is at C-1, to the rhodium. By the oxidative addition of another molecule of another molecule of the hydrosilane and reductive elimination, the reaction generates the *cis* product. The

formation of *trans* and *cis* product depends on the k'_i and k^H_{trans}. If the oxidative addition

of another molecular of the hydrosilane to **50** is much faster than the isomerization, the

trans product should be formed selectively. So this mechanism can explain the factor of

the formation of the *cis* and *trans* isomers and furthermore, the reaction with the

hydrosilanes bearing electron-withdrawing substituents should be not give any *cis*

products arising from the isomerization of **50** to **52**.

Chapter 2. Regioselective Formation of α-Vinylpyrroles from the Ruthenium-Catalyzed Cross Coupling Reaction of Pyrroles and Terminal Alkynes Involving C-H Bond Activation

C-vinylated pyrroles and indoles are not only important building blocks in formation of biologically active porphyrins and related nitrogen macrocycles but also serve as precursors of electroactive polymeric materials.[89] Allylation and alkenylation of such indoles and pyridine derivatives have been achieved by using cationic Ru-allyl and -vinylidene catalysts, respectively.[90] Pd-catalyzed direct oxidative arylation of indoles and quinoline-*N*-oxides have also been achieved by using Pd catalysts.[91] Despite such remarkable progress, regio- and stero-controlled vinylation still remains as a major problem in the catalytic C-H alkenylation methods. Lack of *cis-* and *gem*-selective vinylation method, *trans*-selective product is formed in most cases. While exploring the scope of the catalytic coupling reactions involving C–H bond activation, here we report a method promoting highly regioselective formation of a-vinylpyrroles from ruthenium-catalyzed cross coupling reaction of pyrroles and terminal alkynes.[92]

2.1 Results and Discussion

The initial activity studies showed the cationic ruthenium catalyst

$Ru_3(CO)_{12}/NH_4PF_6$ was effective for the regioselective intermolecular coupling reaction of pyrroles and terminal alkynes to give α-vinylpyrroles (Eq 58).

(58)

Yield: 70-99%
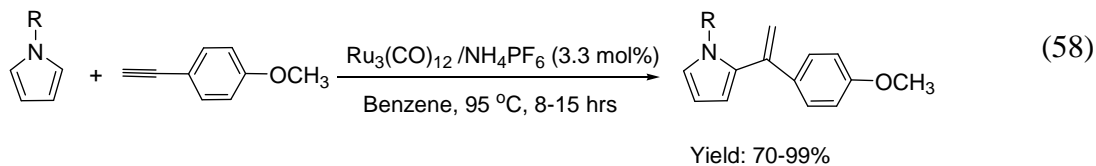
The treatment of methyl pyrrole (143 mg, 1 mmol) with excess 4-ethynylanisole (2 mmol) in the presence of $Ru_3(CO)_{12}/NH_4PF_6$ (3.3 mol %) in benzene at 95 ^{o}C for 12 hours cleanly produced 1:1 ratio product (α-position) almost exclusively (99% yield achieved).

When R=Ph, the yield is 83%, and the following are the characterized data.
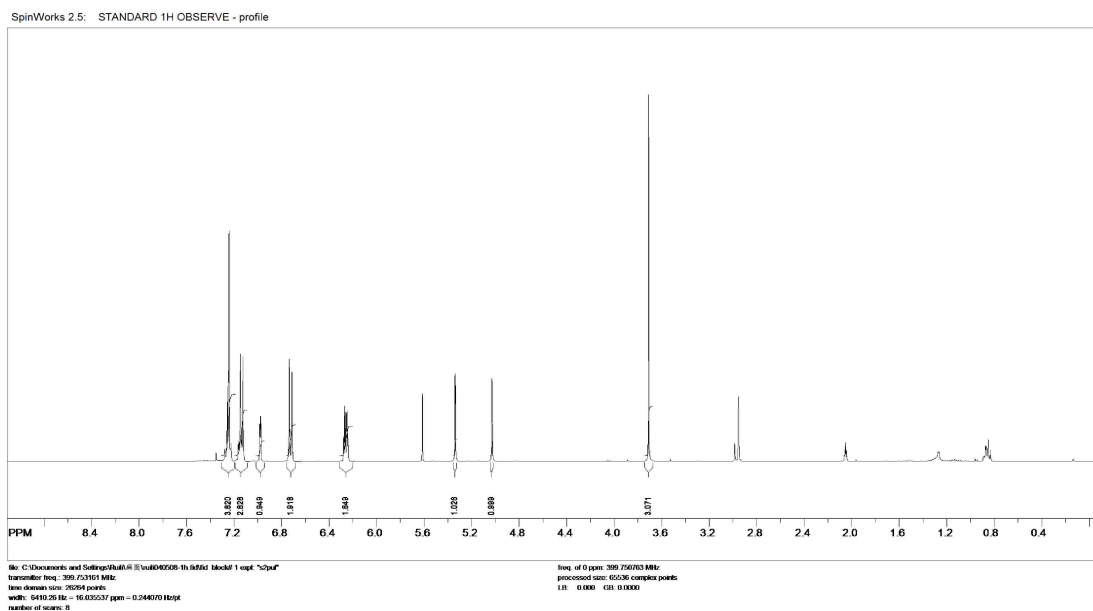
Figure 1. ^{1}H NMR Spectroscopy for complex **53c**

In the ^{1}H NMR (Acetone-d_6, 400 MHz), the singlet peak at δ 3.71ppm is assigned to the 3H of OCH_3. The peaks at δ 5.34 ppm and 5.03 ppm respond the two vinyl proton, they are showed as doublets, and their coupling constant are the same (J = 1.6 Hz). The peaks at δ 6.26 ppm are from the two β-hydrogens, and the peak at δ 6.98 ppm belongs to the other α-position, the other peaks are from the aromatic H.

Needle-like crystals of Compound **53c** formed after slow evaporation of a sample dissolved in CH_2Cl_2/n-hexane mixture. X-ray crystallography shows that it is α-vinylpyrroles (Figure 2) and its C(2A)-C(3A) bond length is 1.4815 Å.
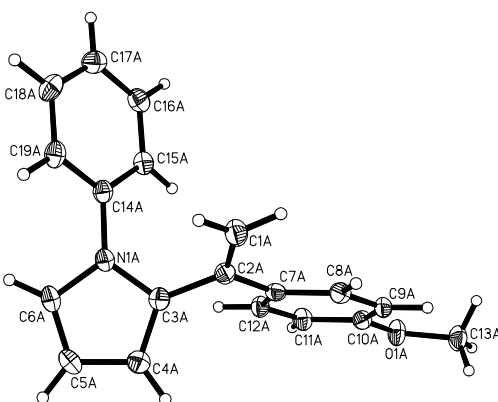
Figure 2. X-ray Crystal Structure of **53c**

2.2 Scope of the Coupling Reactions of Pyrroles with Terminal Alkynes

2.2.1 Catalyst Survey

In order to find the best condition for this coupling reaction, we used the reaction of N-methyl pyrrole (143 mg, 1 mmol) with 4-ethynylanisole (2 mmol) to test the activity of ruthenium complexes (10 mol %). The amount of the coupling product was determined by GC/MS. This catalyst activity survey showed that $Ru_3(CO)_{12}$ /NH_4PF_6 (1:3 molar ratio) has the highest activity in this coupling reaction among selected ruthenium complexes (Table 1).

$Ru_3(CO)_{12}$/NH_4PF_6 and $Ru_3(CO)_{12}$/HBF_4OEt_2 showed high yield while $Ru_3(CO)_{12}$ alone produced only 30% coupling product. Other common ruthenium complexes such as $RuH_2(PPh_3)_4$, $RuHCl(CO)(PCy_3)_2$ and $RuCl_3 \cdot 3H_2O$ showed no activity to the coupling reaction under similar reaction conditions. Although $Ru_3(CO)_{12}$/HBF_4OEt_2 shows similar yield of coupling products as the $Ru_3(CO)_{12}$/NH_4PF_6, we chose $Ru_3(CO)_{12}$/NH_4PF_6 as the catalyst for this coupling reactions, since HBF_4OEt_2 is liquid and not easy to handle.

Table 1. Catalyst Activity Survey for Coupling Reaction of Pyrroles with Alkynes[a]

Entry	Catalyst	Additive	yield(%)[b]
1	None	None	0
2	$Ru_3(CO)_{12}$	None	30
3	$Ru_3(CO)_{12}$	NH_4PF_6	>99
4	$Ru_3(CO)_{12}$	HBF_4OEt_2	96
5	$RuCl_3.3H_2O$	None	0
6	$(PCy_3)_2(CO)RuHCl$	None	0
7	$(PCy_3)_2(CO)RuHCl$	HBF_4OEt_2	0
8	$(PCy_3)_2(CO)RuHCl$	NH_4PF_6	0
9	$(PPh_3)_3(CO)RuH_2$	None	0
10	$(PPh_3)_3RuCl_2$	None	0
11	$(PPh_3)_3RuHCl$	None	0
12	$[RuCl_2(COD)]_x$	None	0
13	$(PCy_3)_2(CH_3CN)_2(CO)Ru\overset{\oplus}{H}$ $\overset{\ominus}{BF4}$	None	0

[a] Reaction condition: 0.1 mmol of methyl pyrrole, 0.2 mmol 4-ethynylanisole, [Ru] 10 mol %, benzene 2 mL, 95 °C, 12 h. [b] GC yields based on N-methylpyrrole.

2.2.2 Solvent Effects

A variety of solvents was tested to optimize the reaction condition. Methyl

pyrrole (0.1 mmol) was reacted with 4-ethynylanisole (0.2 mmol) in the presence of 3.3

mol % $Ru_3(CO)_{12}/NH_4PF_6$ (1:3 molar ratio) and the yield of the product was determined

by GC-MS. It was found that the nature of the solvent affects reaction efficiency

significantly. Benzene was found to be the best among the tested solvents. Toluene and

dichloromethane also showed respectable yield, but with some byproducts. Coordinating

solvents such as THF, MeCN showed low conversion in this reaction.

Table 2. Solvent Effect Survey on Coupling Reaction of Pyrroles with Alkynes

entry	solvent	yield(%)[b]
1	benzene	>99
2	CH_2Cl_2	95
3	Toluene	90
4	THF	20
5	MeOH	20
6	MeCN	5
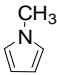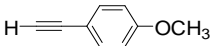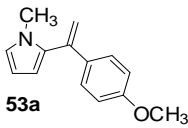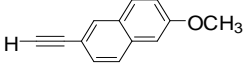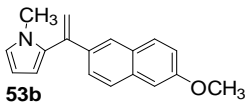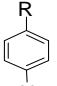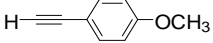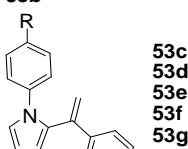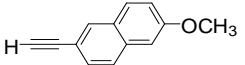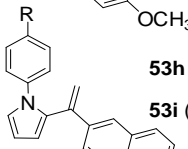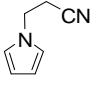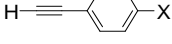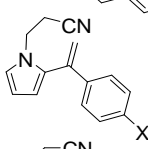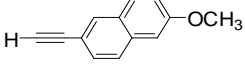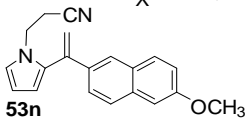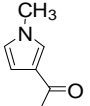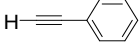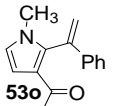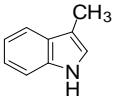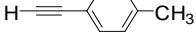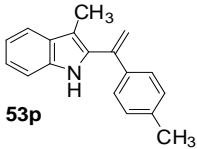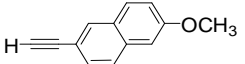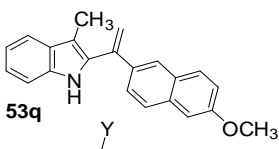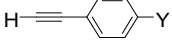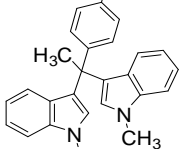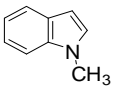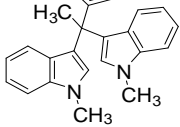
[a] Reaction condition: 0.1 mmol of methyl pyrrole, 0.2 mmol 4-ethynylanisole, 10 mol %, $Ru_3(CO)_{12}$ /NH_4PF_6 (3.3 mol %) (1:3 molar ratio); 2 mL solvent; 95 $^{\circ}$C; 12 h. [b] GC yields based on N-methyl pyrrole.

2.2.3 Reaction Scope

To demonstrate the synthetic utility of the catalyst $Ru_3(CO)_{12}$/NH_4PF_6 (1:3 molar ratio), we explored the scope of this coupling reaction (Table 3). All of the tested reactions yielded only one to one coupling product and alkyne-trimer as byproduct. We also performed the survey on coupling reactions of different N-pyrrole substrates (0.1 mmol) with 4-Ethynylanisole (0.2 mmol) in the presence of 3.3 mol % $Ru_3(CO)_{12}$ /NH_4PF_6 (1:3 molar ratio). Results showed that existence of an electron donating group (EDG) in an N-pyrrole would promote the reaction. For those with electron withdrawing group (EWG) at N-prroles, the conversion was low, which was usually less than 10% and isolation of products was thus impractical. So, here we show only the results from the coupling reaction of the N-pyrroles with electron donating substrates with the alkynes. For terminal alkynes, we scanned reactions of methyl-N-pyrrole with triethyl(ethynyl)silane, phenylacetylene, 1,2-diphenylethyne, pent-2-yne, pent-1-yne under the same condition and checked the reaction by GC-MS. The reaction involving phenylacetylene produced 1:1 coupling product in good yields. For 1-pentyne, only trace amount of product was observed.

Table 3. Coupling Reactions of Pyrroles with Terminal Alkynes[a]

Entry	Pyrrole	Alkyne	Product	Yield (%)[b]
1	N-CH₃ pyrrole	H—≡—C₆H₄—OCH₃	**53a**	99
2		H—≡—naphthyl—OCH₃	**53b**	95
3	R-phenyl-N-pyrrole	H—≡—C₆H₄—OCH₃	**53c** (R=H)	83
4			**53d** (R=CH₃)	80
5			**53e** (R=OCH₃)	78
6			**53f** (R=Cl)	73
7			**53g** (R=F)	70
8		H—≡—naphthyl—OCH₃	**53h** (R=H)	75
9			**53i** (R=OCH₃)	75
10	N-CH₂CH₂CN pyrrole	H—≡—C₆H₄—X	**53j** (X=H)	80
11			**53k** (x=CH₃)	83
12			**53l** (x=OCH₃)	85
13			**53m** (x=NMe₂)	75
14		H—≡—naphthyl—OCH₃	**53n**	78
15	1-CH₃-3-acetylpyrrole	H—≡—Ph	**53o**	81
16	3-CH₃-indole	H—≡—C₆H₄—CH₃	**53p**	78
17		H—≡—naphthyl—OCH₃	**53q**	80
18	N-CH₃-indole	H—≡—C₆H₄—Y	**53r** (Y=H)	85
19			**53s** (Y=CH₃)	87

[a] Reaction condition:1.0 mmol pyrrole; 2.0 mmol alkyne; 3 mL benzene; Ru₃(CO)₁₂/NH₄PF₆ (3.3 mol %) (1:3 molar ratio); [b] isolated yield.

For triethyl(ethynyl)silane and 1,2-diphenylethyne pent-2-yne, there were no

coupling products formation was observed, the GC-MS showed only peaks of starting

materials and trimerized byproducts, even after prolonged reaction time. Therefore, we

focused our effort on the phenyl acetylene and different substrates on the *para*-X-phenyl

acetylene, such as 1-ethynyl-4-methylbenzene, 4-ethynylanisole,

1-bromo-4-ethynylbenzene, 1-chloro-4-ethynylbenzene and 1-ethynyl-4-fluorobenzene.

All these reactions generated products at 1:1 ratio. We performed kinetic analysis on

these reactions, and it was found that electron donating groups such as OMe and Me

group can promote this reaction, while the electron withdrawing groups (such as Br, Cl,

and F,) showed low conversion. There were no reactions observed for furan, thiophene

with the phenylacetylene, and N-methyl pyrrole with the alkynes.

2.3 Mechanism Studies

2.3.1 Hammett Study

Hammett studies were performed on *para*-substituted N-phenylpyrroles and

alkynes to determine the electronic effects on the pyrrole substrates in the coupling

reaction. It was found that the substituents at *para*-position of the aromatic ring could

transfer their electronic information through bonds. During the reaction, the substituents

create a dipole interaction at the α-carbon, influencing the energy associated with the

development of possible charge at the reaction center. Charge development occurs during

formation of the most stable transition state of the reaction through bond formation or

rupturing. The effect that electron-donating and electron-withdrawing substituents have

on the reactions rates is correlated to the nature of the transition state.[93]

Encouraged by the differences in the appearance of the reaction mixtures for the

coupling reactions, we performed a Hammett study using a series of *para*-substituted

phenyl pyrroles (X = OMe, CH_3, H, Cl, F). We monitored the coupling reactions using

the initial rate method. In the study, $Ru_3(CO)_{12}$ (0.003 mmol), NH_4PF_6 (0.01 mmol),

pyrrole (0.1 mmol), alkyne (0.25 mmol) and hexamethylbenzene (26 mg as the internal

standard) were dissolved in 0.5 mL benzene-d_6 solution and transferred into Wilmad

J-Young NMR tubes with a Teflon screw cap. The tubes were cooled in liquid nitrogen

twice, and were degased three times. The tubes were gradually warmed to room

temperature and then heated in oil bath at 95 ^{o}C. The reactions were monitored every

hour by ^{1}H NMR spectroscopy. The rates were measured by integration of the product ^{1}H

peak (OCH_3 δ 3.71 ppm), and the results were normalized against the internal standard.

The k_{obs} was estimated from a first–order log-linear plot of ln[product] vs. reaction time.

Through these reactions, we found that an electron-donating group on the phenyl pyrroles

could accelerate the rate of the reaction. A Hammett plot was constructed by plotting the

$\log(k_x/k_H)$ vs σ_ρ and a Hammett value of $\rho = -0.9$ was obtained from the correlation of

para-substituted p-X-C_6H_4N (X=OMe, CH$_3$, H, Cl, F) with 4-ethynylanisole (Figure 3).
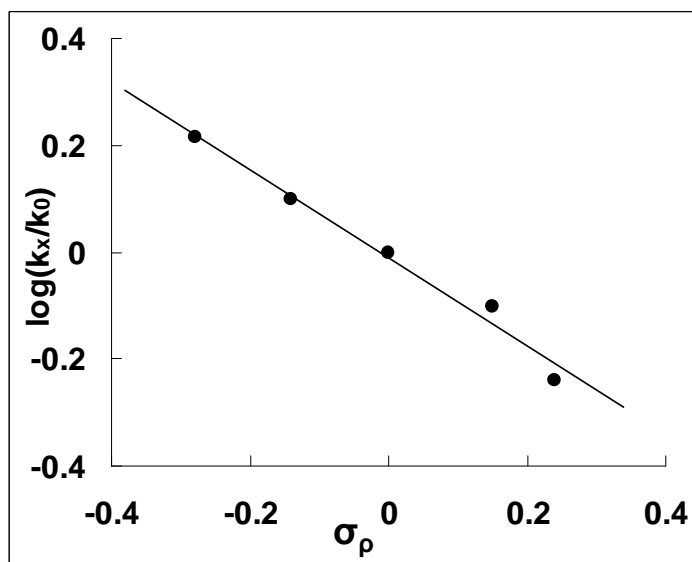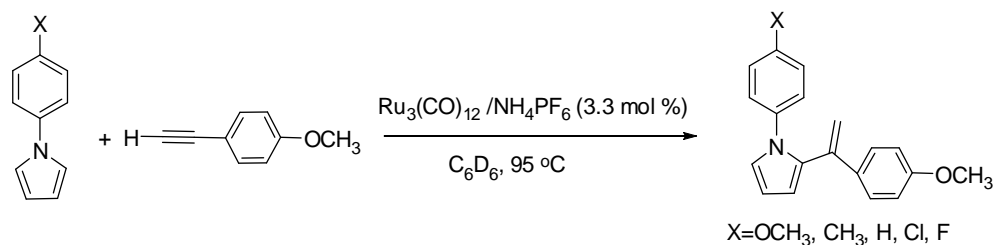
Figure 3. Hammett Plot of the Coupling Reaction of *para*-Substituted p-X-C_6H_4N (X = OMe, CH$_3$, H, Cl, F) with 4-ethynylanisole Catalyzed by $Ru_3(CO)_{12}/NH_4PF_6$ (1:3 molar ratio).

Generally, Hammett plot having a sharp change in the direction of the slope is an

indication of a change in the rate-determining step of the mechanism, or alludes to the

possible existence of a different mechanism together. The negative ρ value for pyrroles

suggests considerable cationic character of the transition state. Because of the developing

positive charge on the transition state, electron-donating groups stabilizing the transition

state enhanced the overall rate of the reaction and the promotional effect by

electron-releasing group is indicative of a nucleophilic nature of the pyrrole group.

In order to learn the electronic effects on the alkyne substrates for the coupling

reactions we also performed analysis the Hammett studies of *para*-substituted phenyl

acetylene. Analogous correlation from the reaction of *N*-phenylpyrrole with

aryl-substituted alkynes p-X-$C_6H_4C\equiv CH$ (X = OMe, CH_3, H, Br, F) resulted in a

considerably less negative Hammett ρ value of -0.42 (Figure 4). In this case, the negative

ρ value suggests a considerable cationic characteristic on the transition state of the C-C

bond formation step, which is stabilized by electron-releasing group of the alkyne

substituent. These results are consistent with the notion that the C-C bond formation step

is promoted by both a nucleophilic pyrrole and electrophilic alkyne substrate via a

cationic transition state.
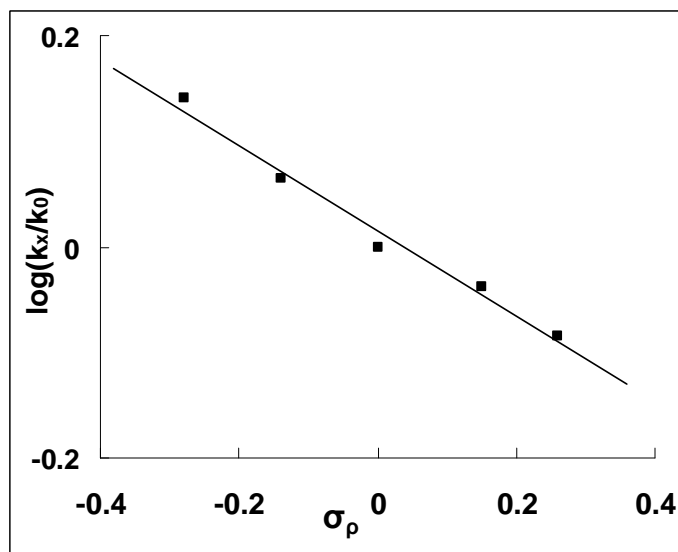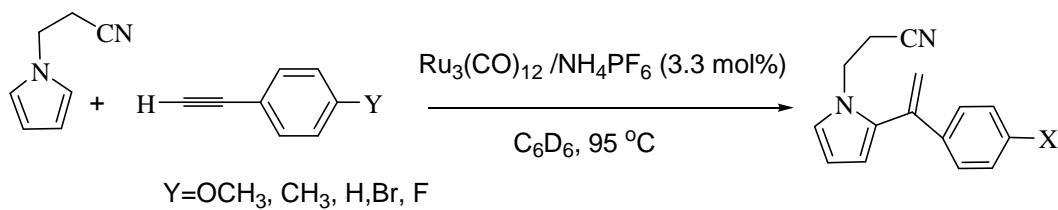
Figure 4. Hammett Plot of the Coupling Reaction of *para*-Substituted p-X-C$_6$H$_4$CCH (X = OMe, CH$_3$, H, Br, F) with Pyrrole Catalyzed by Ru$_3$(CO)$_{12}$ /NH$_4$PF$_6$ (1:3) at 95 ^{o}C

2.3.2 Isotope Effect Study

To determine the possibility of a rate-limiting C-H bond cleavage step in the

coupling reaction of alkynes and pyrroles, a series of experiments based on kinetic

isotope effect on were performed. Again, the initial rate method was used to calculate the

rate for each reaction. In this investigation, the N-phenyl 2,4-dideuteopyrrole was made

using *n*-Buli and D$_2$O (for the procedure, see the experiment section). The crude

deuterium product was purified though the silica gel column, and the product was

characterized by ^{1}H and ^{2}H NMR spectroscopy (Figure 5). In this figure, the 2 α-position

hydrogen and the ^{2}H from aromatic rings were deuterated.

Figure 5. ^{1}H and ^{2}H NMR Spectra for the Deuterated N-phenyl Pyrrole

The top one is the ^{1}H NMR for the N-phenyl pyrrole, spectrum in the middle

show the ^{1}H NMR of the deuterium product, and the bottom one is the ^{2}H NMR spectrum

of the deuterium product. The peaks at 7.6 ppm was signed for the α-position H of the

phenyl pyrrole.

The coupling reactions of $C_6H_5NC_4H_4$ with the 4-ethynylanisole and

$C_6H_3D_2NC_4H_2D_2$ with 4-ethynylanisole were performed separately, and the reaction was

monitored by NMR spectroscopy. These type reactions were set up in the same condition.

$Ru_3(CO)_{12}$ (0.003 mmol), NH_4PF_6 (0.01 mmol), pyrrole (0.1 mmol) and alkyne (0.25 mmol) and hexamethylbenzene (26 mg as the internal standard) were dissolved in 0.5 mL benzene-d_6 solution in a Wilmad J-Young NMR tube with a Teflon screw cap. The tube was cooled in the liquid nitrogen, and degassed for three times. The tube was gradually warmed to room temperature and was heated in 95 ^{o}C oil bath. We monitored the reaction every hour by NMR spectroscopy. The rate was measured by monitor the ^{1}H integration of the product peak (OCH_3 δ 3.71ppm) signal, and the values were normalized against the internal standard. The k_{obs} was estimated from a first–order log-linear plot of ln[product] vs. reaction time. A normal deuterium isotope effect was observed for the $C_6H_5NC_4H_4$ and $C_6H_3D_2NC_4H_2D_2$. The pseudo-first order plots of the catalytic reaction of both $C_6H_5NC_4H_4$ and $C_6H_3D_2NC_4H_2D_2$ with the 4-ethynylanisole, at 95 ^{o}C in C_6D_6 led to $k_{obs} = 0.1424$ h^{-1} and $k_{obs} = 0.1392$ h^{-1} (Figure 6) respectively, from which a $k_{CH}/k_{CD} = 1.0 \pm 0.1$ was calculated. This is different from the predicted value of k_{CH}/k_{CD}, which should be larger than 1, if the C-H bond cleavage is the rate-limiting step. This low KIE values suggest the C-H bond cleavage in the α-position of the pyrrole is not the rate-limiting step. And the isotope effect of $k_{CH}/k_{CD} = 1.0 \pm 0.1$ was observed from the coupling reactions of C_6H_5CCH and C_6H_5CCD with the $C_6H_5NC_4H_4$ (Figure 6) and this means C-H bond cleavage in the alkyne is not the rate-limiting step. Based on these isotope effect data, we concluded that the C-H bond cleavage of both the pyrrole and the alkyne is not the rate-limiting step.
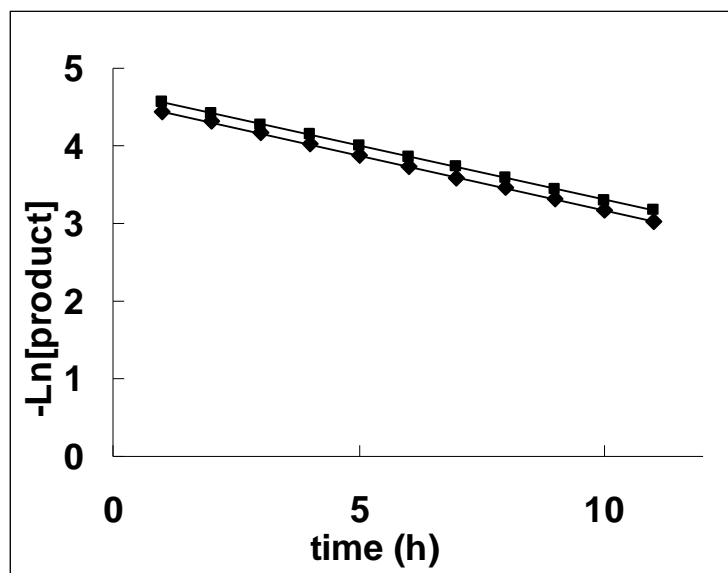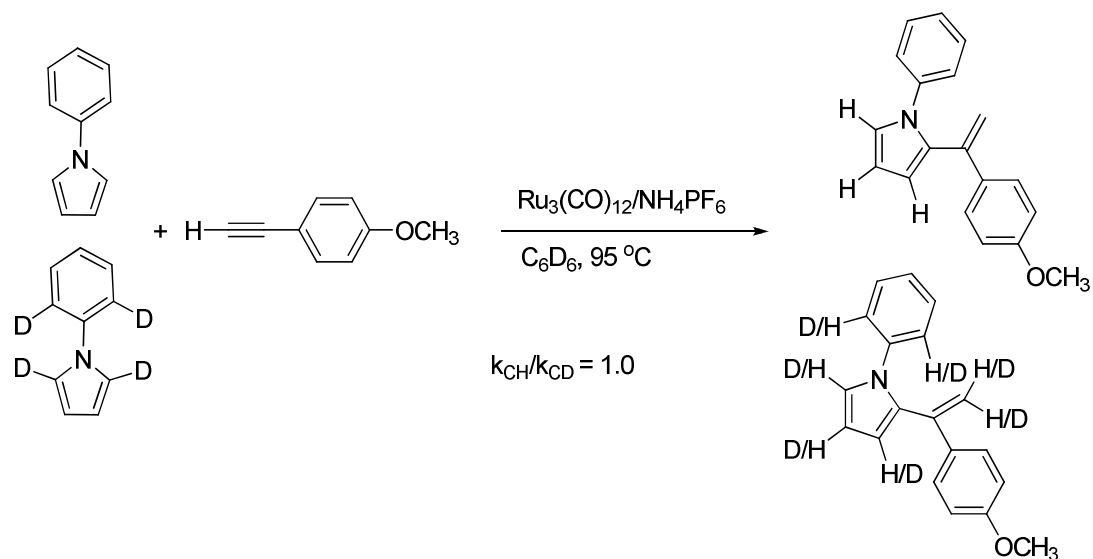
Figure 6. First Order Plot of –ln[product] vs Reaction Time for the Coupling Reaction; ◆-Phenyl pyrrole-d_4; ■-Phenyl pyrrol

2.3.3 Deuterium Labeling Studies

Though the isotope effect studies indicated that the C-H bond cleavage of the pyrrole and the alkyne was not the rate-limiting step, the mechanism is still largely

unknown. To learn more about the reaction mechanism, the following deuterium labeling

studies were performed (Eq 59).

(59)
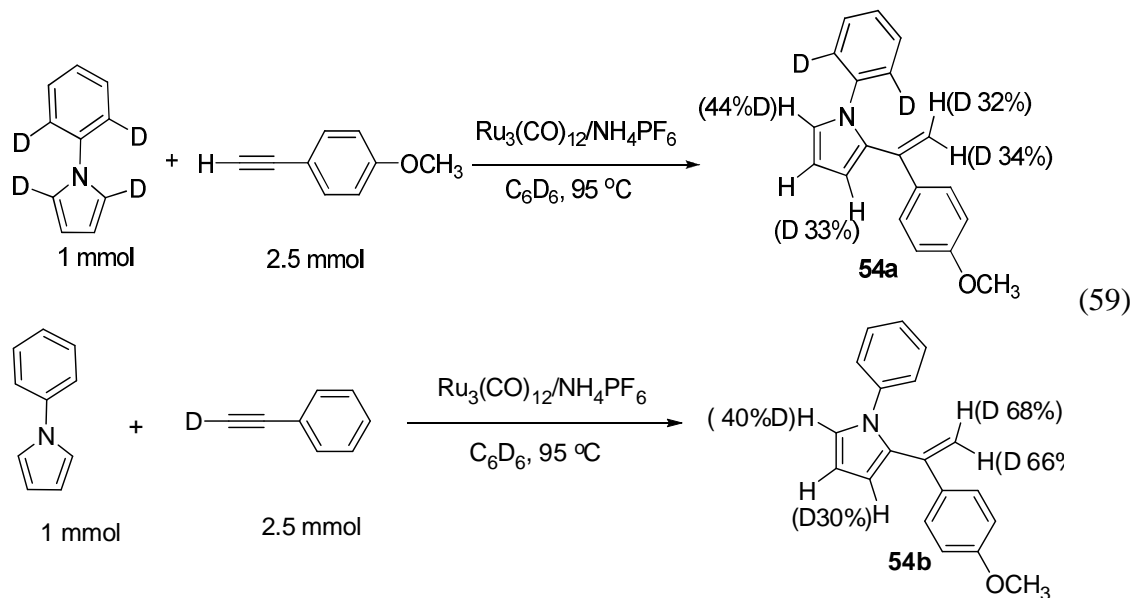
The reaction of the $C_6H_3D_2NC_4H_2D_2$ with excess 4-ethynylanisole (2.5 equiv.)

and $Ru_3(CO)_{12}/NH_4PF_6$ (1:3 molar ratio) in benzene at 95 $^{\circ}$C for 15 hours yielded product

54a with extensive deuterium incorporation at terminal alkene (D 32% and 34%) and at

the β position (D 33%) of the phenyl pyrrole as well as on the α position (D 44%) of the

phenyl pyrrole as measured by both ^{1}H and ^{2}H NMR. Conversely, 68% and 66% on the

terminal alkene and 30% on the β position of the phenyl pyrrole as well as 44% on the α

position of the phenyl pyrrole were found to contain the deuterium when phenyl pyrrole

was reacted with 2.5 equiv. of phenyl acetylene-d_1 in benzene at 95 $^{\circ}$C for 15 hours

yielded product **54b**.
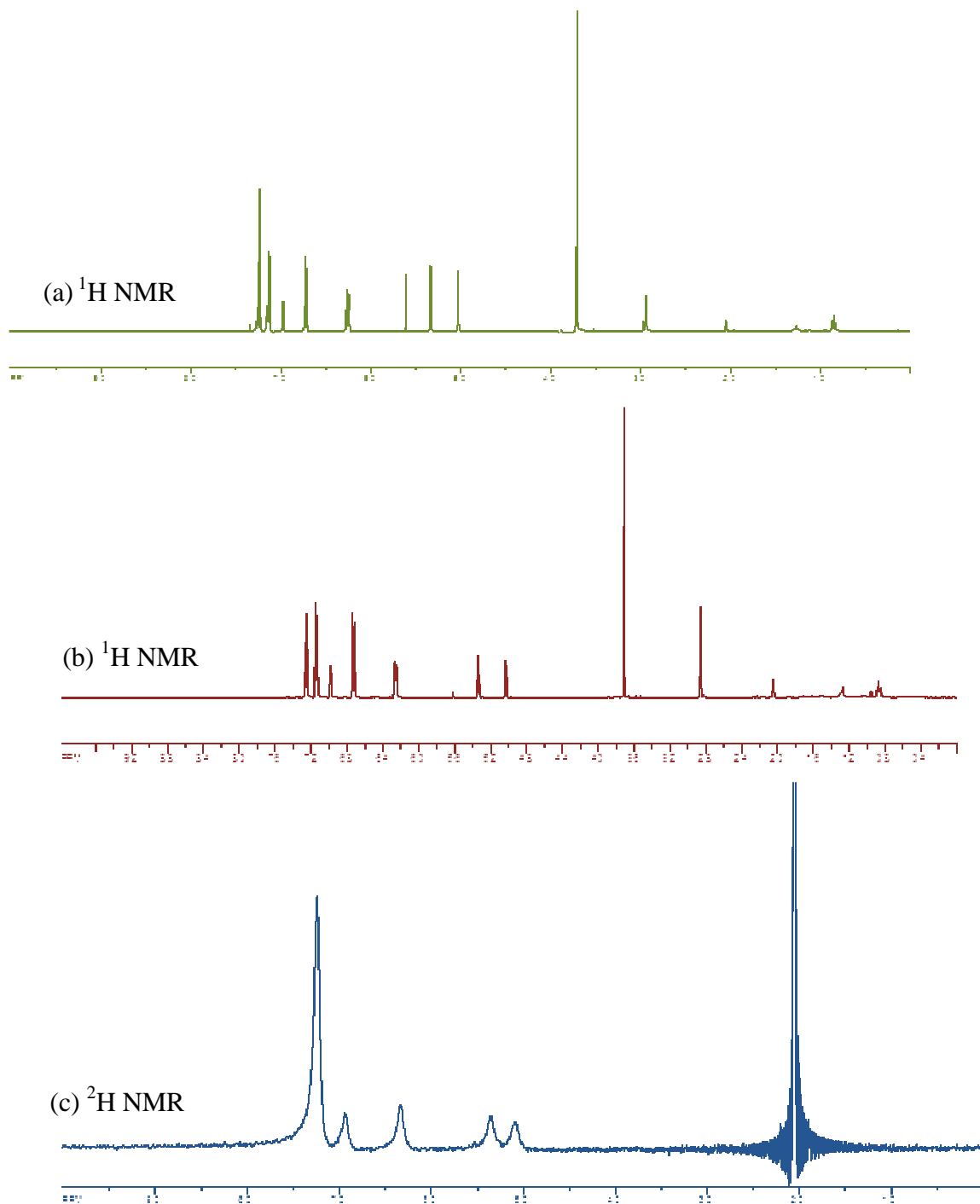
Figure 7. (a) ¹H NMR Spectrum of the Undeuterated Compound; (b) ¹H NMR Spectrum of the Compound **54a**; (c) ²H NMR Spectrum of the Compound **54a**.
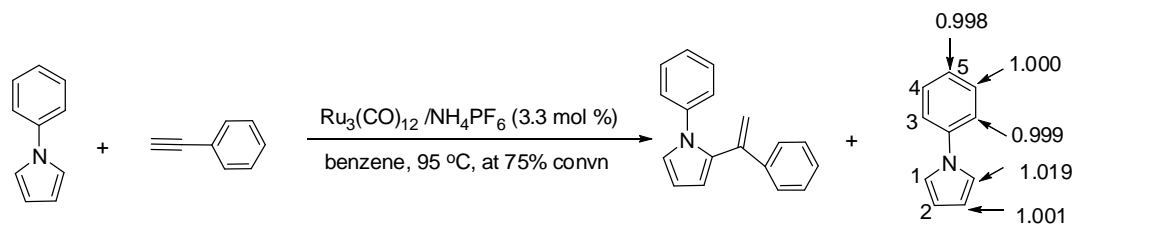
Figure 7a is the ^{1}H NMR spectrum of the non-deuterated compound and Figure 7b is the ^{1}H NMR spectrum of the compound **54a.** The intensities of the peaks at δ 5.33 ppm, 5.02 ppm and 6.25 ppm corresponds to vinyl and β position of the phenyl pyrrole resonances, respectively, which were significantly decreased due to extensive deuterium incorporation. As show in Figure 7c), the existence of deuterium at each position was further confirmed by ^{2}H NMR.

There are two possibilities for the proton and deuterium exchange: one is that the rate of deuterium and proton exchange is faster than the rate of the formation of the coupling products and the other one is the rate of deuterium and proton exchange is slower than the rate of forming the coupling products. If the rate of exchange is slower than the rate of product formation, there should be little D/H exchange between reagents, which would give less amount of deuterium in the product. However, from the studies, we can see that there are large amount of D in the coupling products. This faster D and H exchanges indicate that C-H bonds activation step in both alkyne and pyrrole are reversible.

2.3.4 Carbon Isotope Effect Study

In order to get information about the rate-determining step, experiments based on carbon isotope effect study were also performed. In a glove box, $Ru_3(CO)_{12}$ (0.03 mmol), NH_4PF_6 (0.1 mmol), *N*-phenylpyrrole (1.0 mmol) and 4-ethynylanisole (2.5 mmol) were dissolved in 3 mL benzene solution in a 25 mL Schlenk tube equipped with a magnetic stirring bar. The tube was brought out of the glove box. The reaction tube was heated in an oil bath at 95 °C for 15 h. The tube was opened to air at room temperature, and the crude product mixture was analyzed by GC/MS (75% conversion). And the solvent was removed under a rotary aspirator, and the unreacted *N*-phenylpyrrole was isolated by a column chromatograph on silica gel (CH_2Cl_2/*n*-hexanes).

The ^{13}C NMR analysis of the recovered and virgin samples of N-phenylpyrrole was performed according to Singleton's method.[94] The NMR sample of virgin and recovered *N*-phenylpyrrole was prepared identically by adding *N*-phenylpyrrole (75 mg) in $CDCl_3$ (0.5 mL) in a 5 mm high precision NMR tube. The ^{13}C {^1H} NMR spectra were recorded with H-decoupling and 45 degree pulses. A 60 s delay between pulses was imposed to minimize T_1 variations (d1 = 60 s, at = 5.0 s, np = 245098, nt = 512). The average ^{13}C integration ratio of the recovered and virgin samples of *N*-phenylpyrrole is shown in Table 4.

Table 4. Average^{13}C Integration of the Recovered and Virgin Samples of N-phenylpyrrole

C#	Virgin	Recovered (75% conv.)	Recovered/Virgin	Change (%)
1	0.998(5)	1.017(5)	1.019(5)	1.90(5)
2	1.020(3)	1.025(3)	1.005(3)	0.49(3)
3	1.009(4)	1.008(4)	0.999(4)	0.11(4)
4(ref)	1.000	1.000	1.000	0.00
5	0.469(3)	0.468(3)	0.998(3)	0.22(3)
C#	Virgin	Recovered (70% conv.)	Recovered/Virgin	Change (%)
1	0.998(5)	1.011(5)	1.013(5)	1.30(5)
2	1.020(3)	1.025(3)	1.005(3)	0.47(3)
3	1.009(4)	1.007(4)	0.998(4)	0.19(4)
4(ref)	1.000	1.000	1.000	0.00
5	0.469(3)	0.468(3)	0.998(3)	0.24(3)

From this study, the most significant carbon isotope effect was observed at the α-position carbon of the phenyl pyrrole. This isotope effect indicates that the reaction step involving α-position carbon of the phenyl pyrrole is slow. Since ^{13}C is heavier than

^{12}C, and in the slow reaction step, the migration rate of ^{13}C should be slower than that of

^{12}C, thus results in that the abundance of ^{13}C α-position carbon of the recovered phenyl

pyrrole would be more than the unused phenyl pyrrole. The experimental data agrees well

with the theory. With the isotope effect studies, which indicated that the C-H bond

cleavage is not the rate-limiting step and deuterium labeling studies, which showed the H

and D exchange is faster than the formation of the coupling product, we reached the

conclusion: C-C bond formation involving in the α-position carbon of the phenyl pyrrole

should be the rate-limiting step.

2.3.5 Proposed Mechanism of the Coupling Reactions of Pyrroles and Alkynes

We provided a mechanistic rationale for the coupling reaction based on these

results (Scheme 17). Here, we propose that the catalytically active cationic Ru-pyrrole

species **57** is initially formed from an *ortho*-metallation followed by the elimination of an

arylalkene. In support of this hypothesis, catalytic coupling reaction of *N*-phenylpyrrole

with PhC≡CH was performed.

The formation of styrene (3%) was detected by both ^{1}H NMR and GC-MS. Both

neglible k_H/k_D isotope effect and rapid H/D exchange pattern on the coupling reaction are

consistent with a rapid and reversible C–H bond activation step.
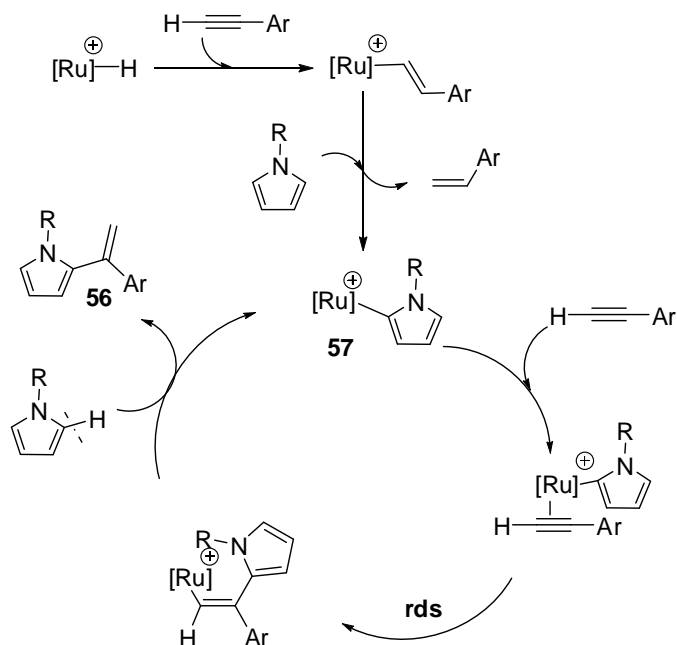
Scheme 17. Proposed Mechanism for the Coupling Reactions of Pyrrole and Alkynes

The observation of a significant α-carbon isotope effect on the pyrrole substrate

provides a strong evidence for the rate-limiting C–C bond formation step. A relatively

strong negative Hammett ρ value from the correlation of *para*-substituted *N*-arylpyrroles

also supports that the C–C bond formation step is promoted by the nucleophilicity of the

pyrrole substrate. The regioselective insertion of pyrrole to the internal alkynyl carbon

would be dictated by the formation of sterically less demanding Ru-vinyl species to yield

the 1,1-disubstituted vinylpyrrole product **56**. The C-C bond forming step has been

commonly observed as the rate determining step in other C-H insertion reactions.

2.4 Conclusions

In summary, the cationic ruthenium catalyst $Ru_3(CO)_{12}/NH_4PF_6$ was found to be effective for the regioselective intermolecular coupling reaction of pyrroles and terminal alkynes to give α-vinylpyrroles. The mechanistic studies on the coupling reaction revealed a rate-limiting C-C bond formation step and electronic origin of the regioselective formation of the coupling products. This catalytic method provides a predictable way to introduce synthetically useful *gem*-vinyl group to pyrroles and related nitrogen heterocycles.

**Chapter 3. Scope and Mechanistic Investigations on the Solvent-Controlled Regio-
and Stereoselective Formation of Enol Esters from the Ruthenium-Catalyzed
Coupling Reaction of Terminal Alkynes and Carboxylic Acids**

Enol esters are a versatile class of precursors for a variety of synthetically

important organic transformations such as cycloaddition,[95] asymmetric hydrogenation,[96]

C-C bond coupling,[97] and Aldol- and Mannich-type of condensation reactions.[98] Since

enol esters can also serve as a synthon for aldehydes and ketones, much research efforts

has been devoted to develop efficient catalytic methods to control both regio- and

stereoselectivity in forming substituted enol esters. From an industrial perspective of

increasing synthetic efficiency and tolerating functional groups as well as reducing waste

byproducts, catalytic methods for producing enol esters are highly desired compared to

the classical methods that utilize stoichiometric amounts of strong base or toxic Hg

salts.[99]

Transition metal-catalyzed alkyne-to-carboxylic acid coupling reaction offers an

attractive route to enol esters, but its synthetic potential has not been fully realized, in

part because this catalytic method typically produces a mixture of *gem*- and (*E*)/(*Z*)-enol

ester products.[100] Considerable research has been devoted to control both regio- and

stereoselectivity in forming the enol ester products by modulating steric and electronic

nature of the metal catalysts. Generally, late transition metal catalysts have been found to

be effective for the coupling reaction to produce a mixture of (*E*)- and (*Z*)-enol esters

from *anti*-Markovnikov addition of carboxylic acids to terminal alkynes over *gem*-enol

ester products,[101] though the regioselective formation of *gem*-enol esters has recently

been achieved by using cationic Rh catalysts.[102] Despite considerable synthetic and

mechanistic progress, however, neither the nature of reactive intermediate species nor

controlling factors for the formation of *gem*- vs (*E*)/(*Z*)-enol esters have been clearly

established. Here we report the coordinatively unsaturated ruthenium-hydride complex

$(PCy_3)_2(CO)RuHCl$ (**1**) as a highly effective catalyst for the alkyne-to-carboxylic acid

coupling reaction to form synthetically useful enol esters.[103] This chapter delineates

kinetic and mechanistic insights as well as the solvent-controlled regio- and

stereoselective formation of the enol ester products that are mediated by the

ruthenium-hydride catalyst (Eq 60).
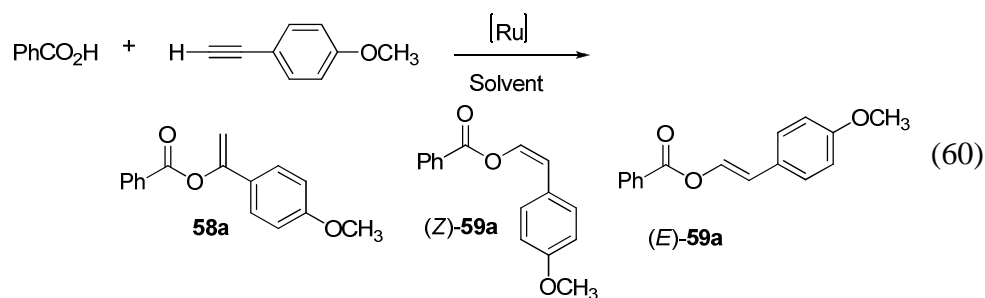
3.1 Results and Discussion

We found that the ruthenium hydride complex $(PCy_3)_2(CO)RuHCl$ (**1**) showed the high activity on the coupling reaction of carboxylic acid with terminal alkynes to give product in a 1:1 ratio, and in different solvent it can give different product. For example, treating benzoic acid (122 mg, 1 mmol) with excess 4-ethynylanisole (1.5 mmol) in the presence of complex **1** in 3 mL dichloromethane at 95 ^{o}C for 8 hours could cleanly produce germinal olefin with 98% yield (Eq 61). When using THF as the solvent, the *cis*-olefin (*Z*)-**59a** was isolated as product (Eq 62).

$$(61)$$

$$(62)$$
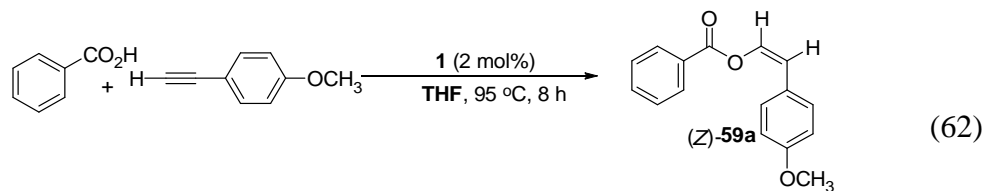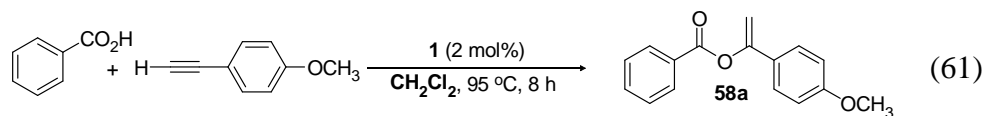
3.2 Optimization Studies for the Coupling of Carboxylic acid with Terminal Alkynes

3.2.1 Catalyst Activity Survey

The catalytic activity of selected ruthenium complexes was initially screened for the coupling reaction of benzoic acid and 4-ethynylanisole.

Table 5. Catalyst Survey on the Coupling Reaction of Benzoic Acid and 4-Ethynylanisole.[a]
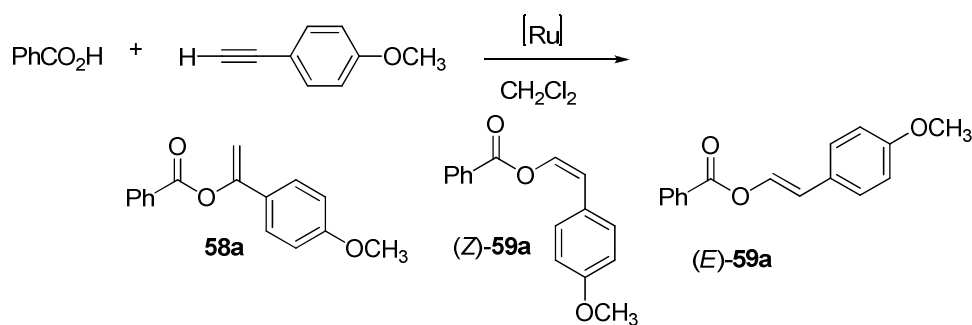
Entry	Catalyst	Yield (%)[b]	58a:(Z)-59a:(E)-59a
1	None	0	
2	$(PCy_3)_2(CO)RuHCl$	>95	100:0:0
3	$(PPh_3)_3(CO)RuH_2$	0	
4	$(PPh_3)_3RuCl_2$	0	
5	$RuCl_3 \cdot 3H2O$	0	
6	$[RuCl_2(COD)]_x$	0	
7	$Ru_3(CO)_{12}$	90	8:17:75
8	$Cp*Ru(PPh_3)_3Cl$	50	15:50:35
9	$Cp*Ru(COD)Cl$	60	27:78[c]
10	PCy_3	0	
11	$(PCy_3)_2(CO)(CH_3CN)_2HRu^{\oplus} BF_4^{\ominus}$	0	
12	$(p\text{-Cymene})RuCl_2$	0	

[a] Reaction condition: benzoic acid (0.10 mmol), 4-ethynylanisole (0.15 mmol), catalyst (2 mol %), CH_2Cl_2 (2 mL), 95 °C, 8 h. [b] GC yields based on benzoic acid. [c] The ratio of **58a** and 1:2 coupling products.

Among the selected ruthenium catalysts, complex **1** exhibited uniquely high catalytic activity and selectivity, giving the *gem*-enol ester product **58a** exclusively in CH$_2$Cl$_2$ within 5 h at 95 °C (Table 5). Both Ru$_3$(CO)$_{12}$ and Cp*Ru(PPh$_3$)$_2$Cl showed significant activity, but suffered from low selectivity. The catalyst Cp*Ru(COD)Cl, on the other hand, produced a mixture of 1:1 and 1:2 coupling products, which is in line with the previously reported results on the formation of 1:2 coupling products.

3.2.2 Solvent Effects

Solvent effect on catalyst activity and selectivity in coupling reaction of benzoic acid and 4-ethynylanisole was examined (Table 6). A remarkably strong solvent influence on the ruthenium catalyst **1** was observed in modulating the selectivity of the enol ester products. Thus, the coupling reaction in a relatively non-polar and non-coordinating solvent tended to favor formation of germinal coupling product **58a** over (*E*)- and (*Z*)-**59a**, of which CH$_2$Cl$_2$ was found to be the best in producing the germinal product **58a** among these non-coordinating solvents (entry 4, Table 6).

Table 6. Solvent Effect on the Coupling Reaction of Benzoic Acid and 4-Ethynylanisole[a]
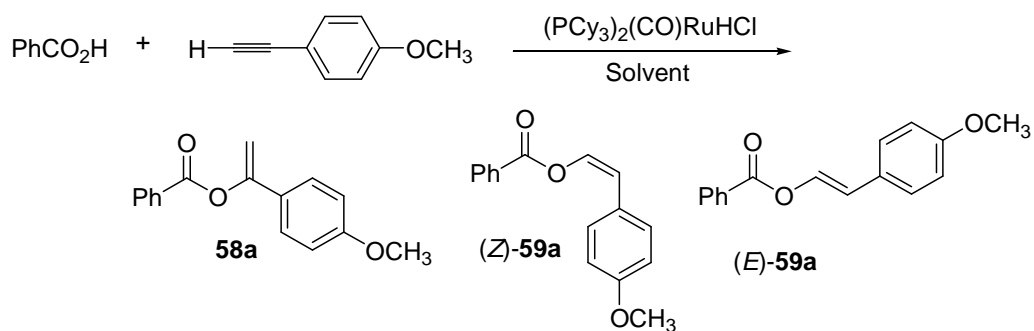
entry	solvent	**58a:(Z)-59a:(E)59a**	yield[b]
1	benzene	51:40:9	80
2	toluene	68:26:6	70
3	*n*-hexane	71:18:11	75
4	**CH$_2$Cl$_2$**	99:1:0	>99
5	Et$_2$O	13:20:67	60
6	CH$_3$CN	33:55:13	55
7	DME	5:74:21	50
8	DMSO	2:48:50	53
9	H$_2$O	3:44:53	73
10	**THF**	0:100:0	>99

[a] Reaction conditions: benzoic acid (0.10 mmol), 4-ethynylanisole (0.15 mmol), **1** (14 mg, 2 mol %), solvent (2 mL), 95 °C, 8 h. [b] GC yields based on benzoic acid.
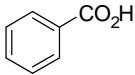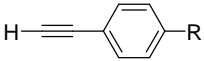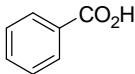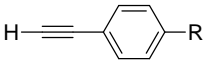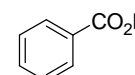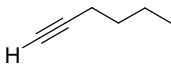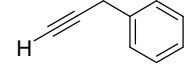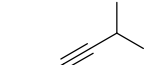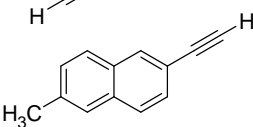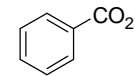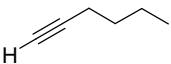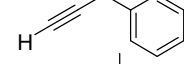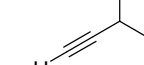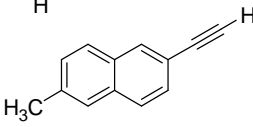
In contrast, among polar coordinating solvents, which tended to favor the formation of (*Z*)-enol ester product (*Z*)-**59a**, THF was found to be the most selective in giving (*Z*)-**59a** (entry 10). It should be emphasized that the formation of 1:2 coupling products was not observed in the coupling reaction catalyzed by **1**. Other ruthenium catalysts such as $Ru_3(CO)_{12}$, $Cp*Ru(PPh_3)_2Cl$ and $Cp*Ru(COD)Cl$ surveyed in Table 5 did not exhibit similar degree of solvent control in forming the coupling products. It is imperative to mention about the recent research progress in controlling the activity and selectivity of products by using solvents with different polarity and coordinating ability. Coordinately unsaturated transition metal complexes have been found to be particularly sensitive to the nature of solvents in mediating unreactive bond activation reactions. For example, Milstein discovered a remarkable solvent effect of electrophilic pincer-ligated (PCP)Rh complexes in directing C-H vs. C-C bond activation and C-I vs C-CN reductive elimination reactions.[104] Jones studied the mechanistic aspects of solvent effects in C-C vs. C-H bond cleavage of butenenitriles by using well-defined Ni-diphosphine complexes.[105] The regioselectivity of a number of synthetically useful catalytic coupling reactions of alkenes and alkynes such as Heck-type coupling and allylic substitution reactions, has been successfully controlled by using different solvents.[106]

3.3 Reaction Scope

The scope of the coupling reaction was surveyed by using the catalyst **1** in both CH$_2$Cl$_2$ and THF (Table 7). Excellent solvent-control in regio- and stereoselective formation of the enol ester products was observed in the coupling reaction of both aryl- and aliphatic terminal alkynes with carboxylic acids. Thus, the coupling reaction in CH$_2$Cl$_2$ led to the exclusive formation of the *gem*-enol ester product **58** for both aliphatic and aryl-substituted terminal alkynes. In contrast, the coupling reaction in THF predominantly gave the (*Z*)-enol ester product (*Z*)-**59** for aryl-substituted alkynes. The electronic nature of the alkynes was found to be an important factor in dictating regioselective formation of *gem*-enol ester products **58** from the reaction with the aliphatic terminal alkynes, even when the reaction was performed in THF (Table 7, entries 15, 30, 32). In most cases, a relatively low catalyst loading (1-2 mol %) was used to obtain the enol ester products, which were readily isolated in high yields after a simple column chromatography on silica gel. The coupling reactions in CH$_2$Cl$_2$ show the high selectivity for the formation of the germinal product. In this system, a variety of alkynes were tested, such as phenylacetylene, the linear alkynes 1-hexyne (Table 7, entry13), bulky alkynes 2-ethynyl-6-methoxynaphthalene (entry 16) and both the electron withdrawing substitutes (entry 1 and 2) and electron donating substitutes (entry 4 and 5) only generate germinal coupling products.

Table 7. Alkyne-to-Carboxylic Acid Coupling Reaction Catalyzed by Complex **1**.[a]

$$RCO_2H \ + \ H \!-\!\!\equiv\!\!-\ R' \ \xrightarrow[\text{Solvent}]{(PCy_3)_2(CO)RuHCl} \ \underset{\textbf{58}}{R\text{-}CO_2\text{-}C(=CH_2)R'} \ + \ \underset{(Z)\textbf{-59}}{R\text{-}CO_2\text{-}CH\!=\!CH\text{-}R'} \ + \ \underset{(E)\textbf{-59}}{R\text{-}CO_2\text{-}CH\!=\!CH\text{-}R'}$$

Entry	Acid	Alkyne	Solvent	Product Ratio 58:(Z)-59:(E)-59	Yield (%)[b]
1				R = OMe **58a**:(Z)-**59a**:(E)-**59a** = 100:0:0	91
2				R = Me **58b**:(Z)-**59b**:(E)-**59b** = 100:0:0	87
3		H—≡—C₆H₄—R	CH₂Cl₂	R = H **58c**:(Z)-**59c**:(E)-**59c** = 100:0:0	98
4				R = Br **58d**:(Z)-**59d**:(E)-**59d** = 100:0:0	98
5				R = CF₃ **58e**:(Z)-**59e**:(E)-**59e** = 100:0:0	98
6				R = F **58f**:(Z)-**59f**:(E)-**59f** = 100:0:0	98
7				R = OMe **58a**:(Z)-**59a**:(E)-**59a** = 0:100:0	95
8				R = Me **58b**:(Z)-**59b**:(E)-**59b** = 0:86:14	90
9		H—≡—C₆H₄—R		R = H **58c**:(Z)-**59c**:(E)-**59c** = 0:87:13	98
10				R = Br **58d**:(Z)-**59d**:(E)-**59d** = 0:94:6	89
11				R = CF₃ **58e**:(Z)-**59e**:(E)-**59e** = 0:93:7	90
12				R = F **58f**:(Z)-**59f**:(E)-**59f** = 0:90:10	87
13				**58g**:(Z)-**59g**:(E)-**59g** = 100:0:0	97
14				**58h**:(Z)-**59h**:(E)-**59h** = 100:0:0	96
15			CH₂Cl₂	**58i**:(Z)-**59i**:(E)-**59i** = 100:0:0	97
16				**58j**:(Z)-**59j**:(E)-**59j** = 100:0:0	89
17				**58g**:(Z)-**59g**:(E)-**59g** = 100:0:0	97
18				**58h**:(Z)-**59h**:(E)-**59h** = 100:0:0	96
19			THF	**58i**:(Z)-**59i**:(E)-**59i** = 100:0:0	97
20				**58j**:(Z)-**59j**:(E)-**59j** = 0:100:0	89

Entry	Acid	Alkyne	Solvent	Product Ratio 58:(Z)-59:(E)-59		Yield (%)[b]
21	4-R-C6H4-CO2H	H–≡–Ph	CH2Cl2	R = OMe	**58k**:(*Z*)-**59k**:(*E*)-**59k** = 100:0:0	83
22				R = Me	**58l**:(*Z*)-**59l**:(*E*)-**59l** = 100:0:0	90
23				R = Br	**58m**:(*Z*)-**59m**:(*E*)-**59m** = 100:0:0	68
24				R = CN	**58n**:(*Z*)-**59n**:(*E*)-**59n** = 100:0:0	89
25				R = CF3	**58o**:(*Z*)-**59o**:(*E*)-**59o** = 100:0:0	90
26	4-R-C6H4-CO2H	H–≡–Ph	THF	R = OMe	**58k**:(*Z*)-**59k**:(*E*)-**59k** = 0:90:10	95
27				R = Me	**58l**:(*Z*)-**59l**:(*E*)-**59l** = 0:90:10	93
28				R = Br	**58m**:(*Z*)-**59m**:(*E*)-**59m** = 0:92:8	90
29				R = CN	**58n**:(*Z*)-**59n**:(*E*)-**59n** = 3:92:5	83
30				R = CF3	**58o**:(*Z*)-**59o**:(*E*)-**59o** = 8:81:11	85
31	Ph,Ph-C=C(Ph)-CO2H	H–≡–Ph	CH2Cl2		**58p**:(*Z*)-**59p**:(*E*)-**59p** = 100:0:0	90
32	Ph,Ph-C=C(Ph)-CO2H	H–≡–C3H7			**58q**:(*Z*)-**59q**:(*E*)-**59q** = 100:0:0	93
33	Ph,Ph-C=C(Ph)-CO2H	H–≡–Ph	THF		**58p**:(*Z*)-**59p**:(*E*)-**59p** = 100:0:0	97
34	Ph,Ph-C=C(Ph)-CO2H	H–≡–C3H7			**58q**:(*Z*)-**59q**:(*E*)-**59q** = 100:0:0	96
35	cyclohexyl-CO2H	H–≡–Ph	CH2Cl2		**58r**:(*Z*)-**59r**:(*E*)-**59r** = 88:12:0	90
36	cyclohexyl-CO2H	H–≡–Ph	THF		**58r**:(*Z*)-**59r**:(*E*)-**59r** = 0:97:3	93
37	CH3(CH2)12CO2H	H–≡–Ph	CH2Cl2		**58s**:(*Z*)-**59s**:(*E*)-**59s** = 89:11:0	91
38	CH3(CH2)12CO2H	H–≡–Ph	THF		**58s**:(*Z*)-**59s**:(*E*)-**59s** = 0:90:10	91
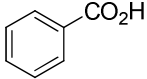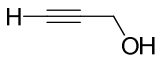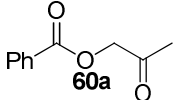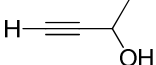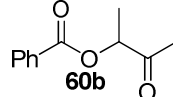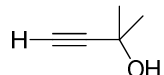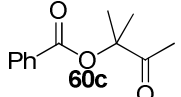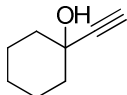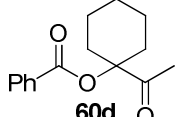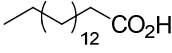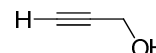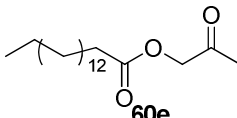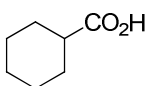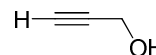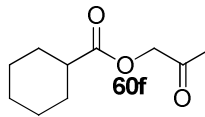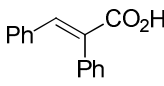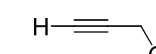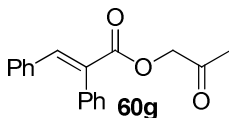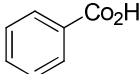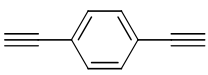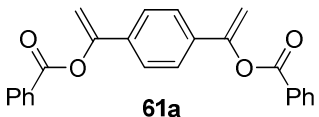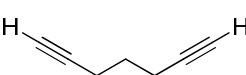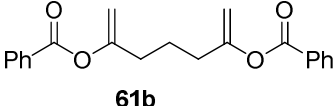
[a] Reaction conditions: acid (1.0 mmol), alkyne (2.0 mmol), **1** (14 mg, 2 mol %), solvent (2-3 mL), 90-95 °C, 8-12 h. *[b]* Isolated yield.

Internal alkynes such as 1-phenyl-1-propyne show no reactivity in the coupling

reactions. Most carboxylic acid reactants give the germinal product, but when

unbranched linear aliphatic carboxylic acids is used (entry 37), we detected the formation

of the (Z)-59s isomer as a minor product. In THF, the reactions favor the

anti-Markovnikov addition to generate the (E) and (Z) isomers, with the (Z) isomer is the

major coupling product, but the less bulky alkynes such as 1-hexyne (entry17),

3-phenyl-1-propyne (entry 18) and 3-methyl-3-buten-1-yne (entry 19), only generate the

germinal coupling products. For *para*-substituted benzoic acid reactants,

electron-donating substituents strongly favor anti-Markovnikov addition. For

para-substituted benzoic acid with strongly electron withdrawing substituents (entry 29

and 30), a small amount of the germinal was also detected.

To further demonstrate the synthetic utility of the ruthenium catalyst **1**, we next

examined the coupling reaction of carboxylic acids with both propargylic alcohols and

diynes (Table 8).

Catalyst **1** was found to catalyze coupling reactions of carboxylic acids with

propargylic alcohols to give acetomethyl ester products **60** in high yields. In this case, the

ketone product was formed exclusive from the Markovnikov-selective hydration of the

alkynes. Such Markovnikov-selectivity has been generally preferred for the hydration of

terminal alkynes,[107] though *anti*-Markovnikov selective hydration of alkynes has been

achieved more recently by using late transition metal catalysts.

Table 8. Coupling Reaction of Carboxylic Acids with Propargyl Alcohols and Diynes.[a]

entry	acid	alkyne	product	yield(%)[b]
1			60a	98
2			60b	95
3			60c	97
4			60d	90
5			60e	89
6			60f	83
7			60g	85
8[c]			61a	90
9[c]			61b	94

[a] Reaction conditions: carboxylic acid (1.0 mmol), alkyne (2.0 mmol), **1** (14 mg, 2 mol %), CH$_2$Cl$_2$ (2-3 mL), 90-95 °C, 8-12 h. [b] Isolated yield. [c] 48 h of the reaction time.

The analogous coupling reaction with an aryl-substituted diyne,

1,4-diethynylbenzene, in CH$_2$Cl$_2$ predictably yielded the corresponding *gem*-dienol

diester product **61a** (entry 8), while a mixture of *gem*-, (*E*)- and (*Z*)-dienol diester

products were formed in THF (*gem*:(*E*):(*Z*) = 18:32:50, 91% combined yield). In contrast,

an aliphatic diyne produced *gem*-dienol diester **61b** exclusively in both CH$_2$Cl$_2$ and THF

(entry 9).

3.4 Mechanistic Study

3.4.1 Phosphine Inhibition Study

We performed a series of PCy$_3$ inhibition experiments to gain further insight into

the mechanism of coupling reaction of alkynes and carboxylic acid. It is well documented

that PCy$_3$ ligands reversibly dissociates from the reactive metal centers. This reversible

association/dissociation occurs more rapidly at higher temperature, creating vacant

coordination sites on the catalyst. Under such conditions, PCy$_3$ is most likely to inhibit

substrate coordination to the active metal sites. In order to observe this phenomenon,

experiments analogous to the substrate rate dependence experiments were performed.
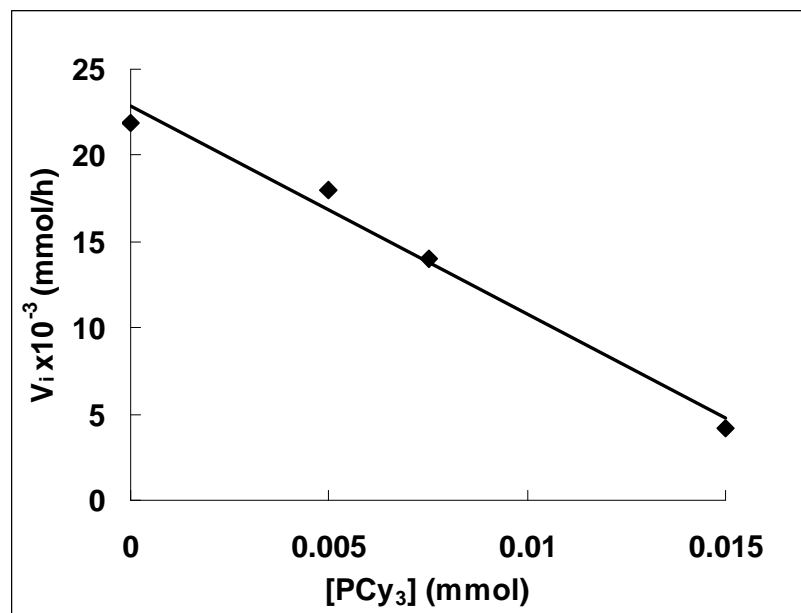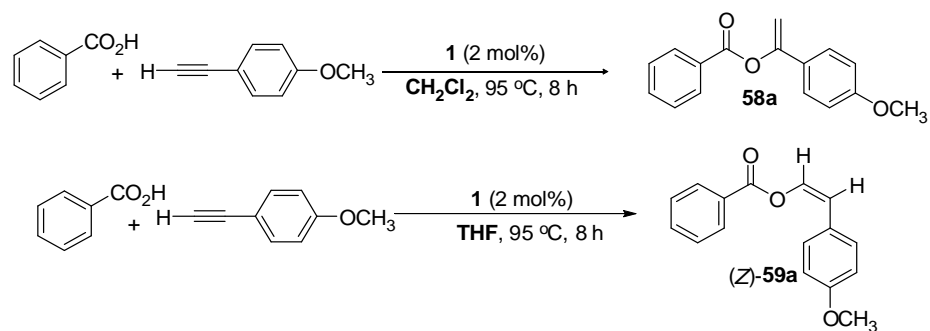
Figure 8. Plot of the Initial Rate (v_i) vs. [PCy$_3$] for the Coupling Reaction of Benzoic Acid and Phenylacetylene. Reaction conditions: benzoic acid (0.20 mmol), phenylacetylene (0.40 mmol), **1** (3 mg, 2 mol %), CDCl$_3$ (0.5 mL).

The initial rate method was used to monitor the rate of formation of enol ester in

the presence of increasing PCy$_3$ concentration of inhibitor. Benzoic acid (0.20 mmol),

phenylacetylene (0.40 mmol), **1** (3 mg, 2 mol %) and C$_6$Me$_6$ (2 mg, internal standard)

were dissolved in 0.5 mL of CDCl$_3$ solution and tranfered into a J-Young NMR tube with

a Teflon screw cap. A solution of PCy$_3$ in CDCl$_3$ (5 μL, 1.0 *M*) was added to the tube via

syringe. The tube was brought out of the glove box and was heated in oil bath at 95 °C.

The reaction was monitored by ^{1}H NMR spectroscopy in 30 min intervals. The rate was

measured by the ^{1}H integration of the product peak at δ 5.61 ppm (=CH$_2$), and was

normalized against the internal standard peak.

The initial rates (v_i) were estimated from a first-order plot of *ln*[product] vs.

reaction time. The plot of the initial rates (v_i) as a function of [PCy$_3$] showed a linear

dependency on [PCy$_3$] (Figure 8). Addition of PCy$_3$ (5-15 μmol, 2.5-7.5 mol %) to the

reaction mixture under otherwise similar conditions led to a steady decrease of k_{obs} from

1.8×10^{-2} h^{-1} (without PCy$_3$) to 4.0×10^{-3} h^{-1} (15 μmol of PCy$_3$). These results indicate

that the active Ru catalyst is formed by an initial dissociation of the phosphine ligand.

3.4.2 Deuterium Labeling Study

In order to determine the possibility of a rate-limiting step of the catalytic reaction,

the following experiments on the deuterium labeling study were performed. The

treatment of PhCO$_2$D with PhC≡CH (2.0 equiv.) and **1** (2 mol %) in CH$_2$Cl$_2$ at 95 °C

yielded the *gem*-enol ester product **58a** with 30% D on both vinyl positions as determined

by both ^{1}H and ^{2}H NMR spectroscopy (Scheme 18). The analogous reaction in THF also

formed the product (*Z*)-**59a** with a similar amount of deuterium on the vinyl positions. On

the other hand, the reaction of $PhCO_2H$ with $PhC\equiv CD$ (2 equiv.) in CH_2Cl_2 produced the

gem-enol ester product **58a** with nearly equal amount of the deuterium (63-67%) at the

vinyl positions, while the reaction in THF resulted in the production of (*Z*)-**59a** with the

similar H/D exchange at the vinyl positions. In a separate experiment, the H/D exchange

reaction between $PhCO_2D$ with $PhC\equiv CH$ (2.0 equiv.) and **1** (2 mol %) was almost

complete within 10 min at 95 °C prior to the product formation.
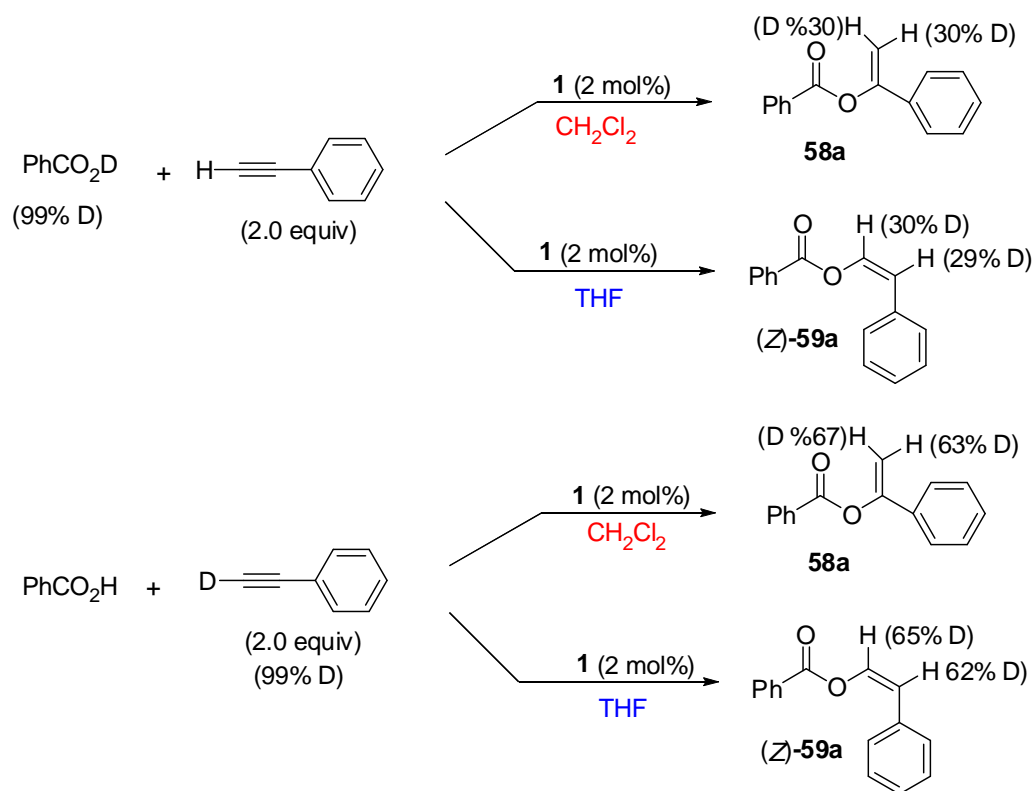
Scheme 18. Deuterium Labeling Study on the Coupling Reaction of Alkyne and
Carboxylic Acid

The ruthenium catalyst was found to facilitate the H/D exchange, since no significant H/D exchange between $PhCO_2D$ with $PhC \equiv CH$ was observed in the absence of **1** under otherwise similar conditions. These results indicate that the H/D exchange between the acid and alkynyl hydrogen is rapid and reversible, and that the alkynyl C–H bond activation step is not a rate-limiting step of the coupling reaction.

3.4.3 Hammett Study

To discern the electronic effects on the product formation, the Hammett ρ values were measured for the coupling reaction in both $CDCl_3$ and THF. In a glove box, a *para*-substituted acid p-X-$C_6H_4CO_2H$ (X = OMe, CH_3, H, CF_3) (0.20 mmol), phenylacetylene (40 mg, 0.4 mmol), **1** (3 mg, 2 mol %) and C_6Me_6 (2 mg, internal standard) were dissolved in $CDCl_3$ (0.5 mL) solution and transferred into a J-Young NMR tube with a Teflon screw cap. The tube was then heated in 95 °C oil bath. The reaction was monitored in 10 min intervals by ^{1}H NMR spectroscopy. The k_{obs} was estimated from a first-order plot of ln[product] vs. reaction time by measuring the ^{1}H integration of the product peak (=CH_2, δ 5.61 ppm), which was normalized against the peak of internal standard. For the reaction in THF, *para*-substituted acid p-X-$C_6H_4CO_2H$ (X = OMe, CH_3, H, CF_3 and CN) (1.0 mmol), phenylacetylene (200 mg, 2.0 mmol) and **1**

(14 mg, 2 mol %) and C_6Me_6 (26 mg, internal standard) were dissolved in 3 mL of THF

solution in a 25 mL Schlenk tube equipped with a Teflon stopcock and a magnetic

stirring bar. The tube was then heated in 95 °C oil bath. The reaction was monitored by

GC in 10 min intervals.
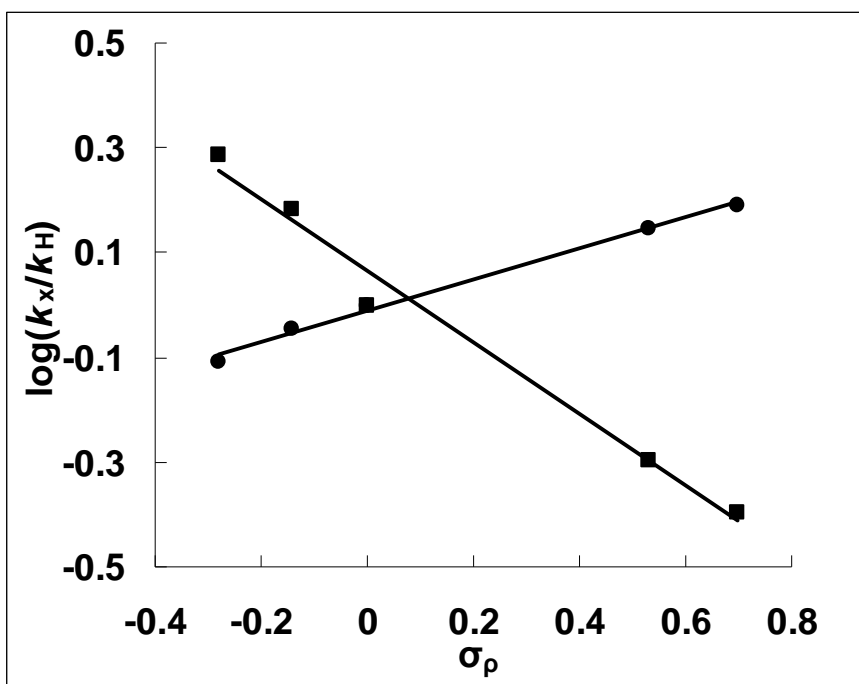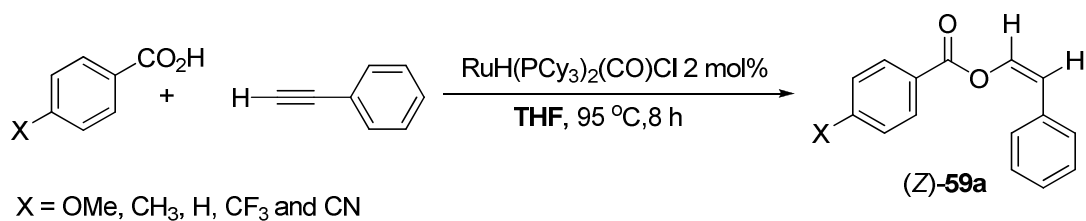
Figure 9. Hammett Plot of the Coupling Reaction of *para*-Substituted p-X-$C_6H_4CO_2H$ (X
= OMe, CH_3, H, CF_3, CN) with Phenylacetylene in $CDCl_3$ (●) and in THF (■)
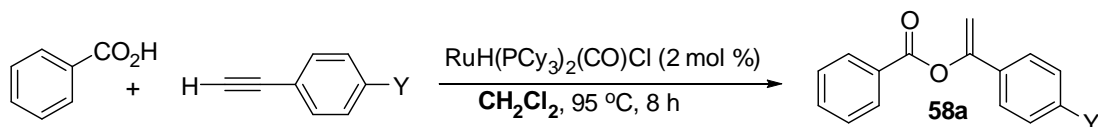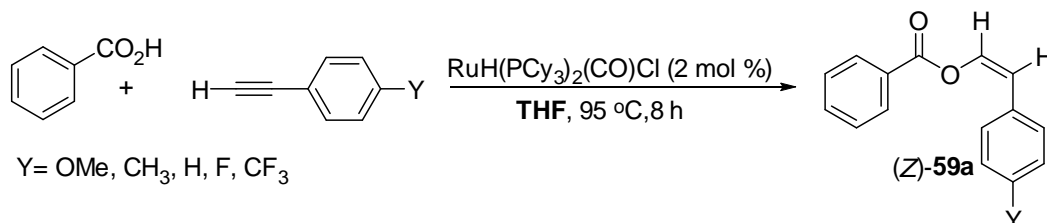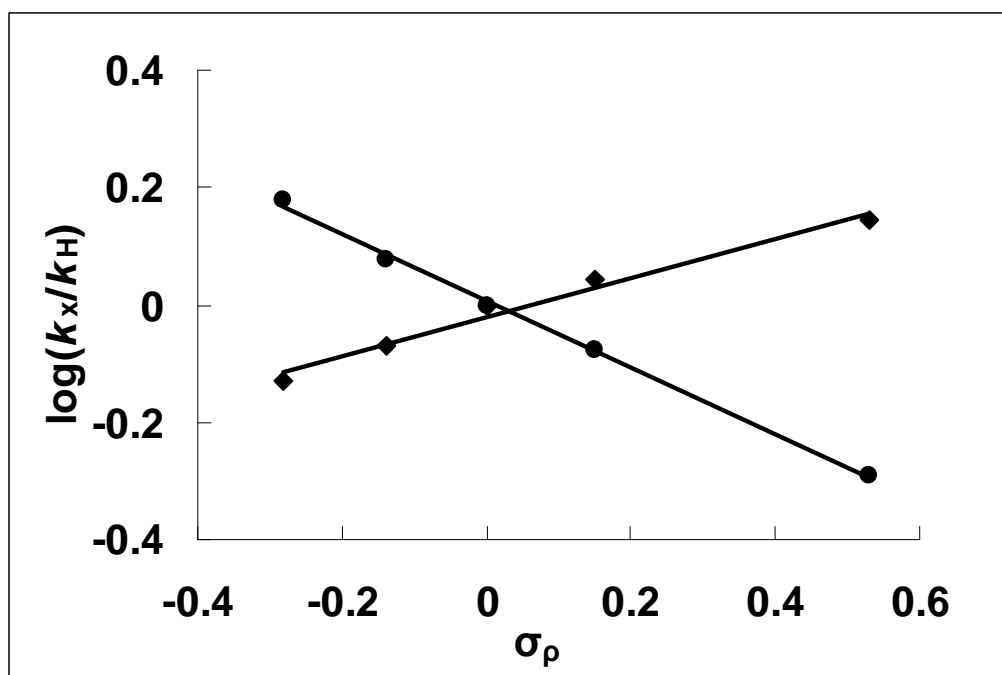
Figure 10. Hammett Plot of the Coupling Reaction of *para*-Substituted p-X-C$_6$H$_4$C≡CH (X = OMe, CH$_3$, H, CF$_3$, F) with Benzoic Acid in CDCl$_3$ (●) and in THF (■)

The k_{obs} was estimated from a first-order plot of ln[product] vs. reaction time by measuring the amount of the products against the internal standard. Thus, correlation of the relative rates with ρ for a series of *para*-substituted benzoic acids p-X-C$_6$H$_4$CO$_2$H (X = OMe, CH$_3$, H, CF$_3$, CN) with phenylacetylene in the presence **1** (2 mol %) at 95 °C led to

the opposite trend between the reaction in CDCl$_3$ (ρ = +0.30) and in THF (ρ = –0.68,

Figure 9). An analogous correlation of the reaction rates of benzoic acid with a series of

para-substituted alkynes *p*-Y-C$_6$H$_4$C≡CH (Y = OMe, CH$_3$, H, F, CF$_3$) also resulted in the

opposite slope between two solvents (ρ = –0.57 in CDCl$_3$ vs ρ = +0.33 in THF, Figure 10).

The opposite Hammett ρ value indicates a different mechanistic pathway for the

coupling reaction between CDCl$_3$ and THF. The positive ρ value observed from the

correlation of *para*-substituted benzoic acids *p*-X-C$_6$H$_4$CO$_2$H in CDCl$_3$ matches well with

the nucleophilicity of the carboxylic oxygen atom due to a developing negative charge on

the carbonyl oxygen, resulted from the direct migratory insertion of the acid to the

coordinated terminal alkyne.

On the other hand, a negative ρ value from the reaction in THF indicates

considerable cationic character build-up on the transition state, and this can be explained

via formation of Ru-vinylidene species, where α-vinylidene carbon has been well known

to be electrophilic. The analogous opposite trend from the correlation of the alkynes

p-Y-C$_6$H$_4$C≡CH can be explained similarly in terms of charges development on the

alkynyl carbon. Thus, a negative ρ value in CDCl$_3$ is consistent with the positive charge

build-up on the internal alkynyl carbon, while the positive ρ value in THF suggests a

partial positive charge build-up on the terminal alkynyl carbon. Once again, the latter

case is consistent with the formation of a Ru-vinylidene species and the addition of the

carboxylate group to the electrophilic α-vinylidene carbon in the transition state.

3.4.4 Synthesis of Catalytically Relevant Ruthenium-Carboxylate

A catalytically relevant ruthenium-carboxylate complex was successfully isolated from the reaction of **1** with a carboxylic acid. Thus, the treatment of **1** (72 mg, 0.10 mmol) with phenylacetylene in CH_2Cl_2 (2 mL) at room temperature for 10 min form the complex **64** in 95% isolated yield. And the treatment of complex **64** (0.1 mmol) with p-OMe-$C_6H_4CO_2H$ (0.11 mmol) in CH_2Cl_2 (2 mL) at room temperature for 10 h led to the clean formation of ruthenium-carboxylate complex **62**, which was isolated in 87% yield after recrystallization in CH_2Cl_2/n-hexanes (Scheme 19).
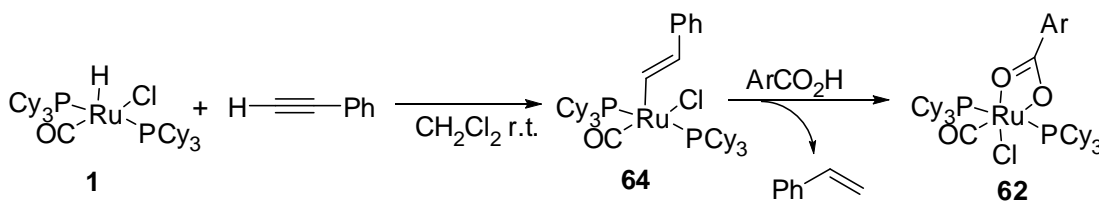
Scheme 19. Synthesis of Ruthenium Vinylidene and Carboxylate Complexes

Complex **62** exhibited two sets of aryl protons at δ 7.88 (d, J = 8.7 Hz) and 6.89 (d, J = 8.7 Hz) in ^1H NMR spectroscopy, as well as two carbonyl peaks at δ 208.8 (t, J_{PH} = 13.3 Hz, CO) and 179.0 (s, CO_2) in ^{13}C {^1H} NMR spectroscopy. A single phosphine peak at δ 28.7 was also observed by ^{31}P {^1H} NMR spectroscopy.

The structure of **62** was further established by X-ray crystallography (Figure 11).

The molecular structure showed a relatively acute *cis* geometry between CO and Cl⁻

ligands (bond angle = 96.4°) to accommodate κ^2-bonding mode of the carboxylate ligand.

Isolated complex **62** was found to be an active catalyst for coupling reactions of alkyne.
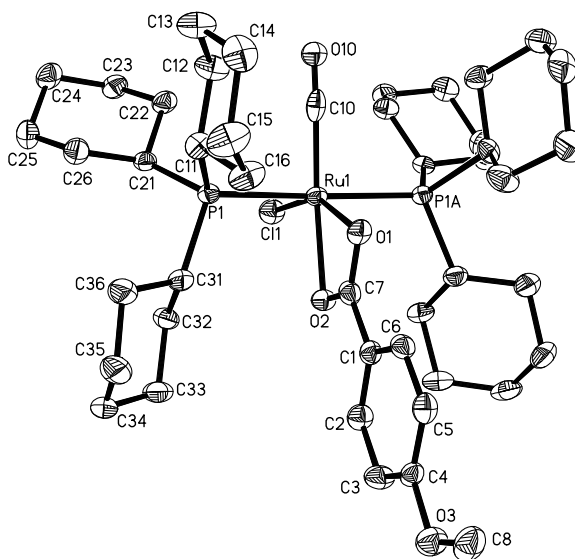
Figure 11. Molecular Structure of **62**

3.4.5 Synthesis of Catalytically Relevant Ruthenium–Vinylidene-Carboxylate Complexes

The reaction of the ruthenium-carboxylate complex **62** with terminal alkynes was

performed in THF to form a catalytically relevant ruthenium-vinylidene complex.

Complex **62** (44 mg, 0.050 mmol) was heated with phenylacetylene (1.2 equiv) in THF to

95 °C for 10 h led to the coupling product **63**, which was isolated in 85% yield as a

yellow-colored solid (Scheme 20).

^{1}H NMR of complex **63** showed a diagnostic vinyl peak at δ 6.24 (br s), and two

distinct K-carbonyl peaks at δ 208.8 (t, J_{PH} = 14.4 Hz, Ru-CO) and 190.2 (t, J_{PH} = 12.1

Hz, Ru-*C*(O)CHPh) were also observed in the ^{13}C{^{1}H} NMR spectroscopy.
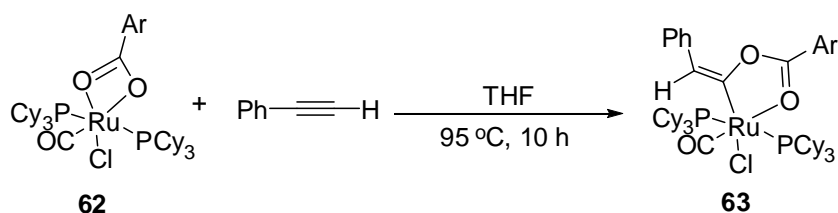
Scheme 20. Synthesis of Catalytically Relevant Ruthenium -Vinylidene-Carboxylate
Complexes

The Structure of **63** was further established by X-ray crystallography (Figure 12).

The molecular structure of **63** showed a *syn* orientation between the carboxylate oxygen

atom and the phenyl group, which was resulted from the coupling between the

carboxylate and the vinylidene ligand. The structure clearly implicates the formation of

the (*Z*)-enol ester product (*Z*)-**59k** from the protonation by another carboxylic acid. To

show the enol ester product formation, complex **63** was treated with an equivalent of

benzoic acid in THF at 90 $^{\circ}$C, which produced carboxylate complex **62** and (*Z*)-**59k** along

with another unidentified ruthenium complexes. Furthermore, catalytic activity of **63** for

the coupling reaction was found to be virtually identical as **1**.
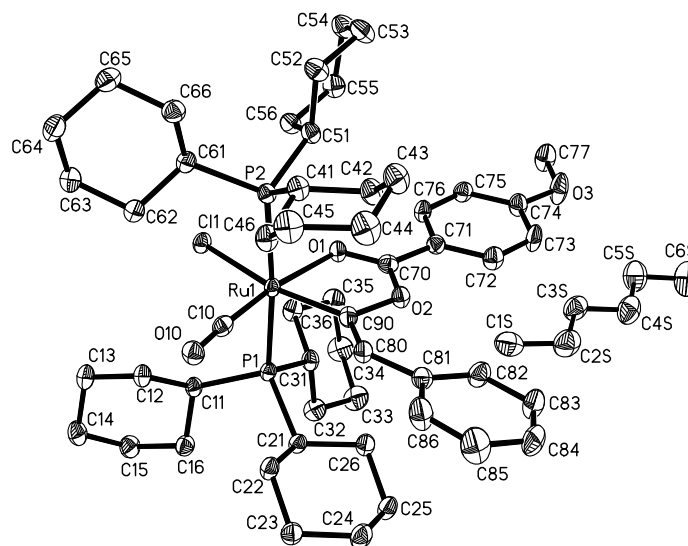
Figure 12. Molecular Structure of **63**

3.4.6 Kinetic Experiments on the Conversion of Complex 64 to Complex 62 and Complex 63
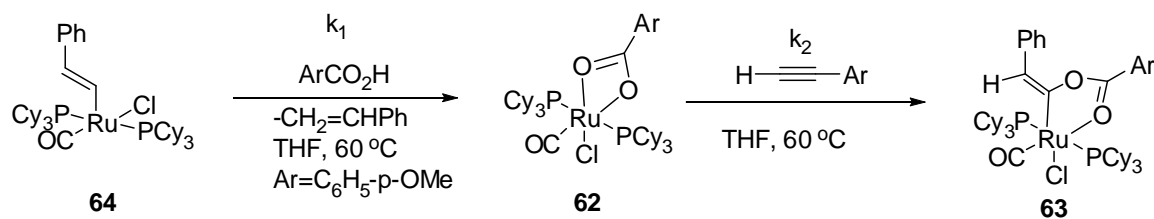
Scheme 21. Synthesis of Complex **62** and Complex **63** from Complex **64**

The successful isolation of the catalytically relevant complexes **62** and **63** enabled

us to further examine the kinetics of the formation of these complexes. The treatment of **1**

(14 mg, 0.02 mmol) with an excess amount of p-OMe-$C_6H_4CO_2H$ (10 equiv.) and

HC≡CPh (15 equiv.) in THF was followed by ^{1}H and ^{31}P NMR spectroscopy (Scheme

21).
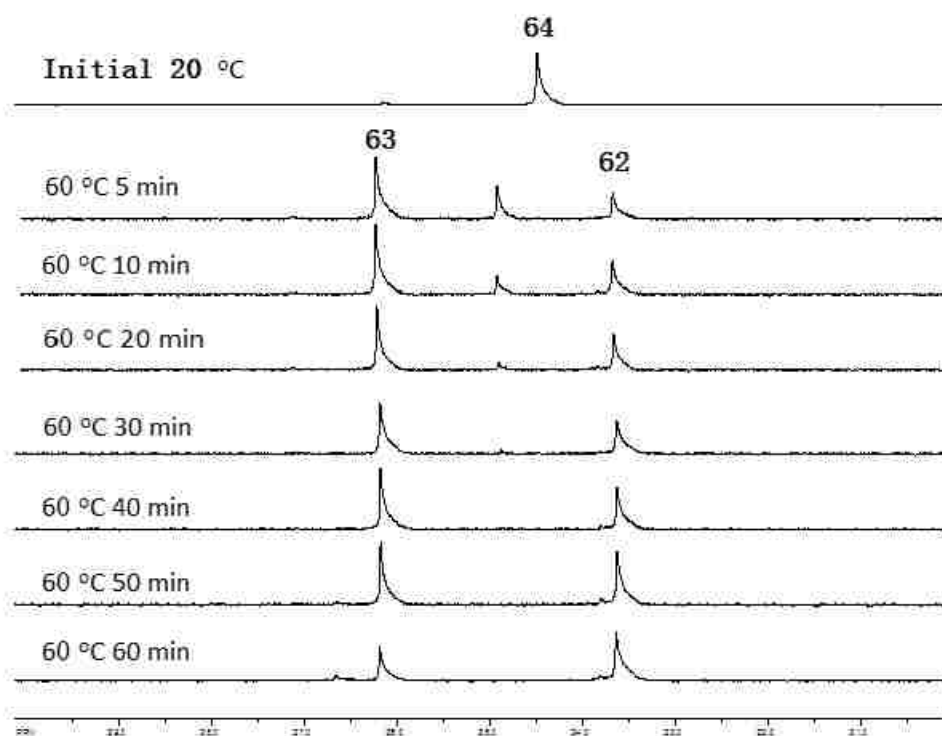
Figure 13. High-temperature VT-NMR of the Conversion of Complex **62** and **63** from
Complex **64**

As expected, the formation of the previously synthesized ruthenium-vinyl

complex **64** was observed after 15 min at room temperature.[109] For ^{31}P NMR, here was

only one peak at 24.5 ppm in THF. The formation of complex **62** can happen at 20 ^{o}C,

but it is slow. Upon warming up to 60 °C, the vinyl complex **64** was converted to

carboxylate complex **62** within 30 min along with formation of styrene. And the signal

(P2 at 26.3 ppm) due to vinylidene-carboxylate complex **63** gradually appeared at the

expense of carboxylate complex **62**. Formation of complex **63** from complex **62** went

smoothly and took couple hours (Figure 13). At these periods the formation of coupling

product was not detected. After 3 hours, the mixtures was heated up to 90 °C for 2 hour,

formation of the coupling product (Z)-**59k** was detected by ^{1}H NMR spectroscopy and

about 10% of $Cy_3PH^+PhCO_2^-$ was detected by ^{31}P NMR spectroscopy.

3.4.7 Derivation of the Kinetic Equation of the Conversion of 64 to 63

The derivation for two consecutive first-order reactions was followed as described[108].

d[**64**]/dt = -k_1t

d[**62**]/dt = k_1[**64**] - k_2[**62**]

d[**63**]/dt = k_2[**62**]

[**64**] = [**64**]$_0$e^{-k1t}

d[**62**]/dt = k_1[**64**]$_0$e^{-k1t} - k_2[**62**]

[**62**] = [**64**]$_0$$k_1$(e^{-k1t} - e^{-k2t})/($k_2$ - k_1)

d[**64**]/dt + d[**62**]/dt + d[**63**]/dt = 0

Since:

$[\mathbf{64}] + [\mathbf{62}] + [\mathbf{63}] = [\mathbf{64}]_0$

$[\mathbf{62}]_0 = [\mathbf{63}]_0 = 0$

$[\mathbf{63}] = [\mathbf{64}]_0 - [\mathbf{64}] - [\mathbf{62}]$

$= [\mathbf{64}]_0[1 + (k_2e^{-k_1t} - k_1e^{-k_2t})/(k_1 - k_2)$

$d[\mathbf{63}]/dt = [\mathbf{64}]_0 k_1 k_2[(e^{-k_1t} - e^{-k_2t})/(k_1 - k_2)$

Figure 14. Kinetic Profile of the Conversion of **64** to **63**. Notations: **64** (▲), **62** (●), **63** (■)

The experimental data was globally fitted to the kinetic equation by non-linear regression techniques (Sigmaplot V. 10). The rate constants $k_1 = 0.039$ min^{-1} and $k_2 = 0.013$ min^{-1} were obtained and from this analysis, which led to

$$d[\mathbf{63}]/dt = [\mathbf{64}]_0 * 0.039 * 0.013 * (e^{-0.039t} - e^{-0.013t})/(0.039 - 0.013)$$

$$= [\mathbf{64}]_0 * 0.0195 * (e^{-0.039t} - e^{-0.013t})$$

The kinetics of the conversion of the vinyl complex **64** to the carboxyl complex **63** was followed by ^{31}P NMR spectroscopy (Figure 14). In a J-Young NMR tube, **1** (14 mg, 0.020 mmol), 4-methoxybenzoic acid (30 mg, 0.20 mmol) and phenylacetylene (31 mg, 0.30 mmol) in THF was dissolved in THF (0.5 mL). Formation of the vinyl complex **64** was completed within 10 min at room temperature. The appearance of **62** and **63** was monitored by ^{31}P NMR spectroscopy at 60 °C in 5 min intervals.

The experimental data was globally fitted to the kinetic equation for two consecutive reactions kinetics by non-linear regression techniques for the conversion from **64** to **63** (Sigmaplot Version 10). The rate constants $k_1 = 0.039$ min^{-1} and $k_2 = 0.013$ min^{-1} were obtained and from this analysis. A relatively smaller value of k_2 compared to k_1 is consistent with the rate-limiting C-O bond formation step.

3.4.8 Proposed Mechanism

We proposed a mechanism for the coupling reaction involving a coordinative unsaturated ruthenium-carboxylate complex **65** as one of the key intermediate species (Scheme 22). The phosphine inhibition study suggests that the catalytically active 16 e-complex **65** is formed from the Ru-carboxylate complex **62** by reversible phosphine dissociation. For the coupling reactions in a non-coordinating solvent such as CH_2Cl_2, direct migratory insertion of the carboxylate oxygen atom to an internal carbon of the alkyne substrate is preferred over the terminal ones to give the germinal ester product **58**. The dative coordination of carboxylic oxygen atom would promote such insertion by stabilizing the intermediate species.

On the other hand, formation of (*Z*)-enol ester product (*Z*)-**59** is rationalized via formation of Ru-vinylidene species **66**. It is well-established that the acetylene-to-vinylidene rearrangement is relatively facile for aryl-substituted alkynes. The X-ray crystal structure of **63** provided a direct evidence for the cis addition of carboxylate oxygen to the Ru-vinylidene ligand. The ability to promote the acetylene-to-vinylidene rearrangement for the ruthenium-catalyst in a coordinating solvent such as THF appears to be an important factor for the stereoselective formation of (*Z*)-enol ester products.

Scheme 22. Proposed Mechanism of the Coupling Reaction of Carboxylic Acids and Terminal Alkynes

The Hammett study suggested that C-O bond formation in catalytic coupling reaction is strongly influenced by the electronic nature of the substrates. For the coupling reaction in CH_2Cl_2, this implies a direct migratory insertion of the coordinated terminal alkyne to the Ru-carboxylic oxygen bond, where both steric and electronic factors dictate the Markovnikov-selective formation of the gem-enol ester product **58**. The dative coordination of the carbonyl oxygen to the Ru center would also facilitate this

transformation by avoiding the formation of a high-energy 14-electron species. The successful isolation of **62** and **63** and their kinetic reaction profile provided a mechanistic rationale for the formation of (*Z*)-enol ester products (*Z*)-**59**. It is reasonable to extrapolate that the coordinating THF solvent promotes the acetylene-to-vinylidene rearrangement for aryl-substituted alkynes by stabilizing unsaturated Ru-vinylidene complex **66**. The reversible dissociation of PCy_3 from both complexes **62** and **63** would form the catalytically active species for the coupling reaction. A slow formation of Cy_3PH^+ apparently from the protonation reaction with the carboxylic acid substrate would also prohibit the re-coordination of the dissociated PCy_3 ligand. The syn geometry of the vinylidene-carboxylate ligand of **63** clearly indicates that the formation of (*Z*)-enol ester product (*Z*)-**3** is electronically controlled during the addition of carboxylate group to the vinylidene ligand of the ruthenium-vinylidene species **66**. From a purely steric perspective, such *syn* addition step would be favored over the anti- Markovnikov addition due to sterically demanding Ru center, and would also be facilitated by the dative coordination of the carboxylate oxygen atom. Since these catalytically active species are not easily detected by spectroscopic methods, corresponding computational study on realated catalytic coupling reactions would be prudent in identifying these catalytically active intermediate species.

3.5 Conclusions

      The ruthenium-hydride complex **1** was found to be a highly effective catalyst for the alkyne-to-carboxylic acid coupling reaction to give synthetically valuable enol esters. Regio- and stereoselective pattern of the catalyst **1** was successfully controlled by using CH_2Cl_2 and THF. The salient features of the ruthenium catalyst **1** are: its ability to control the activity and selectivity on the enol ester products as well as a broad substrate scope and mild reaction condition. A detailed mechanism of the coupling reaction has been established from the kinetic and mechanistic investigations as well as the successful isolation of ruthenium-carboxylate and -vinylidene complexes **62** and **64**. The mechanistic knowledge gained from these studies should provide new insights in designing the next generation of the metal catalysts.

Chapter 4. Catalytic Formation of Silyl Enol Ethers from the Reaction of Ketones with Vinylsilanes and Their Use in Aldol-Type Condensation and Fluorination Reactions

Enol silyl ethers are widely employed in the organic synthesis as the reactive precursors for for a number of synthetically useful C-C and C-heteroatom bond forming reactions. They are useful in various synthetic transformations in the various region-, chemo- and stereoselective reactions. Silyl enol ethers have been commonly utilized as precursors for Aldol-type condensations and other a-functionalization reactions of ketones and bulk material synthesis.[109] Over the past decades, methods have been developed to generate the enol silyl ethers. One of the early and still one of the mostly frequently used route to (E) or (Z)-silyl enol ethers is trapping ketone or aldehyde enolates generated under the kinetics or equilibrium controlled conditions. Another widely used method to generate enol silyl ethers is by deprotonation of acidic α-proton of carbonyl compounds and trapping the corresponding enolates with R_3SiCl. Since a stoichiometric amount of strong base is required to form enolates, the method is generally incompatible with highly functionalized ketone substrates and controlling stereochemistry of *E/Z* mixture of the enol ethers has often been a problematic. The transition metal catalyzed silylation methods offer significant advantages in forming silyl enol ethers, because these methods do not require strong base and generate less waste. The most widely used catalyst for the formation of enol silyl ether is iridium complexes,

but the problem is that the reaction conditions require high temperature, high pressure

and high catalyst loading. We are working on the methods to generate the enol silyl ether

in the mild conditions by the ruthenium complexes. We previously reported that the

well-defined ruthenium-hydride complex $(PCy_3)_2(CO)RuHCl$ (**1**) is an effective catalyst

precursor for oxidative silylation of terminal alkenes and alkynes.[110] Here we report a

highly regioselective formation of silyl enol ethers from the coupling reaction of ketones

and vinylsilanes. The synthetic utility of the silyl enol ethers formed in this reaction has

been demonstrated by Mukaiyama Aldol condensation and fluorination reactions. More

details on the mechanistic study will allow to be discussed.

4.1 Results and discussion

Recently, we found that the ruthenium hydride complex **1** was effective for the

coupling reactions of ketones and vinylsilane to generate the enol silyl ether. From the

initial study, the treatment of acetophenone (1 mmol) with excess vinyltrimethylsilane (2

mmol) in the presence of **1** (0.5 mol %) in toluene at 120 $^{\circ}$C for 12 hours cleanly

produced the enol silyl ether in 95% conversion and the ethylene gas as byproduct (Eq

63).

$$\text{(phenyl methyl ketone)} + \text{Si(Me)}_3 \xrightarrow[\text{Toluene, 120 °C}]{\text{RuHCO(PCy}_3)_2\text{Cl (0.5 mol \%)}} \text{(silyl enol ether)} + \text{H}_2\text{C=CH}_2 \quad (63)$$

The details on the reactions scope, the synthetic utility for the silyl enol ethers and more details on the mechanistic study will be discussed.

4.2 Optimization Studies for the Coupling of Ketones with Vinylsilane

4.2.1 Catalyst Activity Survey

The catalytic activity of selected ruthenium complexes were initially screened for the coupling reaction of phenyl acetone and vinyltrimethylsilane (Eq 64).

$$\text{(phenyl methyl ketone)} + \text{Si(Me)}_3 \xrightarrow[\text{Toluene, 120 °C}]{\text{[Ru] (0.5 mol \%)}} \text{(silyl enol ether)} + \text{H}_2\text{C=CH}_2 \quad (64)$$

The survey of the catalysts showed that ruthenium hydride complex **1** has the highest activity in the formation of the enol ether among selected ruthenium complexes (Table 9, entry 5). (PCy$_3$)$_2$(CO)RuHCl (**1**) complex exhibited uniquely high activity for silylation reaction, giving >99% conversion with less than 0.5 mol % catalyst loading (Table 9). The ruthenium complex RuH$_2$(CO)(PPh$_3$)$_3$ (entry 7) showed a modest activity,

giving the coupling product in 20% yield under similar reaction condition. Other

commonly ruthenium complexes such as $Ru_3(CO)_{12}$, $Ru(CO)H_2(PPh_3)_3$, $RuCl_3 \cdot 3H_2O$,

$[(COD)RuCl_2]_x$ and $[(PCy_3)_2(CO)(MeCN)_2RuH]^+BF_4^-$, were not effective in giving

coupling products under similar reaction condition.

Table 9. Catalyst Activity Survey for the Coupling Reaction of Vinyltrimethylsilane and Acetophenone.[a]

Entry	Catalyst	Additive	Yield (%)[b]
1	None	None	0
2	$Ru_3(CO)_{12}$	None	0
3	$Ru_3(CO)_{12}$	NH_4PF_6	0
4	$RuCl_3 \cdot 3H_2O$	None	0
5	**$(PCy_3)_2(CO)RuHCl$**	**None**	**99**
6	$(PCy_3)_2(CO)RuHCl$	HBF_4OEt_2	<5
7	$(PPh_3)_3(CO)RuH_2$	None	0
8	$(PPh_3)_3RuCl_2$	None	0
9	$(PPh_3)_3(CO)RuHCl$	None	0
10	$[RuCl_2(COD)]_x$	None	0
11	$[(PCy_3)_2(CO)(CH_3CN)_2HRu]^{\oplus}BF_4^{\ominus}$	None	<3
12	$(p\text{-Cymene})RuCl_2$	None	0
13	PCy_3	None	0

[a] Reaction conditions: 0.1 mmol of acetophenone, 0.2 mmol vinyltrimethylsilane, catalyst (0.5 mol %), toluene (2 mL), 120 °C, 12 h. [b] GC yields based on acetophenone.

4.3 The Scope for the Reactions of Ketones with Vinylsilane and the Reaction of Enol Ether with Aldehyde under the Titanium (IV) Chloride

To demonstrate the synthetic utility of the catalyst $(PCy_3)_2(CO)RuHCl$ on the reactions of ketones and vinylsilane, the scope of the reaction was explored by using $(PCy_3)_2(CO)RuHCl$ (**1**) as the catalyst (Table 10). A variety of ketones was explored in this reaction; both alkyl- and aryl-substituted ketones were found reacting smoothly with vinyltrimethylsilane to give enol silyl ether products. In general, the conversion the products determined by GC-MS was found to be quite high with a relatively small catalyst loading (0.5-1 mol % of Ru). Since many of silyl enol ether products were found to be thermally unstable and could not be isolated by column chromatography, isolated yields of the products were determined from the Mukaiyama Aldol condenstion reaction with an aldehyde. Thus, treatment of the silyl enol ether (entry 7) product with p-NO_2-C_6H_4CHO in the presence of a stoichiometric amount of $TiCl_4$ led to β-hydroxyketone products (Eq 65).[111]

$$(65)$$

In a typical reaction, after evaporating the solvent from the silyl enol ether solution under high vacuum, and the crude product was dissolved in CH_2Cl_2 (2-3 mL). In a separate 100 mL Schlenk flask, $TiCl_4$ (3 mmol) was added to a cooled CH_2Cl_2 solution (5 mL) of 4-nitrobenzaldehyde (3 mmol) at 0 °C. After stirring for about 15 min, the solution was cooled to -78 °C, and the CH_2Cl_2 solution of crude silyl enol ether was added dropwise via a syringe to the reaction flask. After stirring at -40 °C for 1 h, water (3 mmol) was added to the reaction flask, and the resulting mixture was stirred at 0 °C for 8 h. The reaction mixture was quenched by adding saturated Na_2CO_3 solution (10 mL), and the organic layer was extracted with Et_2O (3 × 20 mL). The ether solution was dried with anhydrous $MgSO_4$, and the Aldol product was isolated by a column chromatograph on silica gel (*n*-hexanes/CH_2Cl_2) and the product was characterized by NMR in Figure 15.

Figure 15. ^{1}H NMR Spectroscopy of Product **67g**

For aliphatic ketones, enone products were obtained under similar reaction conditions. Regioselective formation of silyl enol ether with more substituted α-carbon was implicated in the formation of products **67i** and **67m** (Table 10, entries 16, 17). These both substrates produce enol silyl ether in high conversion level according to GC-MS data. For Mukaiyama Aldol condenstion reaction with an aldehyde, they generate *syn-* and *anti-* mixtures and the anti- product was the major. But for 2-heptanone (entry 6), the reaction generated the *syn*-isomer as the major product. For 1-indanone and a-tetralone (entry 14 and 15), the reaction gave the highly *anti*-diastereoselective formation of β-hydroxyketones was resulted from the condensation to the α-carbon of the ketones. Other ketones showed high diastereoselectivity of the formation of β-hydroxyketone products on Mukaiyama Aldol condenstion reaction. Cyclohexanone, cyclopentanone and 4-tert-butylcyclohexanone (Table 10, entry 1, 2 and 3), with the treatment of enol silyl ether with benzaldehyde under Mukaiyama Aldol condensation reaction conditions generate dienes as products.

Table 10. Coupling Reaction of ketones with Vinyltrimethylsilane [a] and the Reaction of Enol Ether with Aldehyde under the Titanium (IV) Chloride.[b]

Entry	Ketone	Enol	Conv(%) [c]	Product	Yield(%) [d]
1			99	**67a**	93
2			97	**67b**	83
3			99	**67c**	85
4			95	**67d**	89
5			85	**67e** anti : syn = 85:15	65
6			90	**67f** anti : syn = 10:90	78
7			98	**67g**	85
8			95	**67h**	75

9		94	**67i**	73
10		90	**67j**	80
11		90	**67k**	81
12		93	**67l** anti : syn= 70:30	83
13		96	**67m** anti : syn= 83:17	75
14		98	**67n**	85
15		97	**67o**	87
16		97	**67p**	88
17		94	**67q**	80

[a] Reaction conditions: ketone (1.0 mmol), vinyltrimethylsilane (2.0 mmol), **1** (0.5 mol %), toluene (3 mL), 120 °C, 12-15 h. [b] Reaction conditions enol ether (2.0 mmol), aldehyde (3.0 mmol), $TiCl_4$ (3.0 mmol), CH_2Cl_2 (10 mL). [c] Conversion based on ketone by GC-Ms. [d] Isolated yield based on the ketones.

4.3.1 The Use of Enol Silyl Ether in Fluorination Reactions and Diketone Reactions

To further demonstrate the synthetic utility of the silyl enol ether formation, we next performed a set of C-C and C-F bond forming reactions. For example, acetophenone was treated with vinyltromethylsilane in the presence of the catalyst **1** to produce the enol ether product, as indicated in Table entry **7**. The crude product of enol silyl ether (1.0 mmol) was subsequently reacted with acetyl chloride (80 mg, 1.1 mmol) in the presence of TiCl$_4$ (1.1 mmol) to form the 1,3-diketone product in 43 % yield (Eq 66). The other substrates were treated with this reaction, but only acetophenone can generated the diketone product.

(66)

In an anologous fashion, in a 50 mL Schlenk flask, the crude silyl enol ether product residue (2.0 mmol) was dissolved in CH$_3$CN (2 mL), and the solution was cooled to 0 °C in an ice bath. Selectfluor® (2.0 mmol) was added in several portions to the

solution under N_2 purge. The reaction mixture was stirred while it was allowed to

gradually warm to room temperature over 8 h. The solvent was evaporated, water (10

mL) was added to the residue, and the organic layer was extracted with Et_2O (3×20

mL). The combined organic layers were washed with brine solution, dried over

anhydrous Na_2SO_4, and the solvent was evaporated. The pure product **67s** was isolated by

a column chromatography on silica gel (EtOAc/*n*-hexanes) in 65% isolated yield after

silica chromatography (Et_2O/*n*-hexane) (Eq 67)[112].

67s, n = 0, (65%)
67t, n = 1, (68%)
67u, n = 2, (76%)

(67)

The products were characterized by NMR in Figure16, which show 46.9 Hz as the

coupling constant between F and H.

Figure 16. ^{1}H NMR Spectroscopy for complex **67s**

In both cases, the reaction can be carried out in tandem in a one-pot without isolating the enol ether products.

(68)

67v, n = 0, (60%)
67w, n = 1, (53%)
67x, n = 2, (72%)

Next, the aminomethylation reaction of the silyl enol ethers was performed by following a recently reported procedure (Eq 68). Thus, in a 100 mL Schlenk flask, t-BuOOH (0.10 mL, 5-6 M in decane) was added dropwise to a mixture of N,N-dimethylanilines (1.5 mmol), CuBr (4 mg, 0.025 mmol), crude silyl enol ether product (0.5 mmol) and CH$_3$CN (5 mL) at room temperature. The resulting mixture was stirred at 50 °C for 12 h. The mixture was filtered

through a pad of celite, and the solvent was removed under a reduced pressure. The residue was

purified by a column chromatography on silica gel to afford the desired product **67v-67x** in

60-72% isolated yields.

4.4 Mechanistic Study on the Reaction of Ketones and Vinylsilanes

4.4.1 Deuterium Labeling Study

We performed the following kinetic experiments to gain mechanistic insights on

this coupling reaction. First, the deuterium labeling experiment was performed from

treatment of $PhCOCD_3$ with $CH_2=CHSiMe_3$ (2 equiv.) and **1** (0.5 mol %) in toluene (3

mL) at 120 °C (Eq 69).

The NMR spectroscopy of the product **67y** was acquired, and the crude coupling

product showed 50% D on the vinyl positions as determined by both ^{1}H and ^{2}H NMR

spectroscopy (Figure 17).

Figure 17. A- ^{1}H NMR Spectroscope of the Reaction Mixtures; B- ^{2}H NMR Spectroscope of the Reaction Mixtures.

The two vinyl protons of enol silyl ether were signed to 4.34 ppm and 4.86 ppm in the ^{1}H NMR spectroscope (Figure 17A), in the same region, there are deuterium signals which were assigned to vinyl protons of enol silyl ether in the ^{2}H NMR spectroscope (Figure 17B). In the ^{2}H NMR spectroscopy, there are deuterium signals assigned to

unreacted vinyltrimethylsilane. In addition, the deuterium signal at 5.3 ppm was assigned

to ethylene gas.

These results show that D/H exchange happens between $C_6D_5COCD_3$ and

vinyltrimethylsilane. This exchange should be rapid and reversible, and should be done

before the formation of the enol silyl ether. The extensive H/D exchange pattern at the

vinyl positions is consistent with the rapid and reversible keto-enol tautomerization of the

ketone substrate and its exchange with the vinyl group of $CH_2=CHSiMe_3$.

4.4.2 Deuterium Isotope Effect Study

Experiments based on kinetic isotope effect were performed on the reaction of

ketone and vinylsilanes to determine the possibility of a rate-determining C-H bond

cleavage step. Again, the initial rate method was used to determine the rate of each

reaction. Thus, $RuH(CO)(PCy_3)_2Cl$ (**1**) (0.5 mol %), acetophenone-d_8 (0.2 mmol) and

vinyltrimethylsilane (0.4 mmol, 2.0 equiv.) and hexamethylbenzene (26 mg as the

internal standard) were dissolved in 0.5 ml toluene-d_8 solution in a Wilmad J-Young

NMR tube with a Teflon screw cap. The tube was kept stirred in oil bath set at 120 °C.

The reaction mixture was monitored every 30 min by NMR spectroscopy. The rate was

measured by ^1H integration of the product peak vinyl protons signal which shows 4.34

ppm in the ^{1}H NMR spectroscopy and the data were normalized vinyl protons against the internal standard. The k_{obs} was estimated from a first–order plot of ln[product] vs. reaction time and gave k_{obs} = 0.1237 h^{-1}. The other reaction of acetophenone with vinyltrimethylsilane was setup and monitored under the similar condition as the former reaction, and this reaction gave k_{obs} = 0.1265 h^{-1} which translated to k_{CH}/k_{CD} = 1.0±0.1 (Scheme 23).

Scheme 23. The Kinetics Study on the Reaction of Ketone and Vinylsilane

This low KIE value suggests that the keto-enol tautomerization involving C-H bond cleavage of is fast and not the rate -limiting step. This deuterium isotope effect study also supported the notion of rapid H/D exchange in deuterium labeling study.

4.4.3 Phosphine Inhibition Study

We next performed a series of phosphine inhibition experiments to gain further

insight into the mechanism of the reaction of ketone and vinylsilanes. Experiments

analogous to the PCy_3 rate dependence experiments were performed. The initial rate

method was used to monitor the rate of the reactions. Therefore, the treatment of

acetophonone and vinyltrimethylsilane with various concentrated PCy_3 (5-15 μmol) in the

presence of the catalyst **1** (0.5 mol %) in toluene-d_8 at 120 °C was monitored by ^{1}H NMR

spectroscope every 30 min intends at room temperature.

The initial rate (v_i) of each reaction was constructed from the first–order plot of

ln[product] vs reaction time. The initial rate (v_i) as a function of added [PCy_3] showed a

linear rate dependence on [PCy_3] (Figure 18). The addition of PCy_3 (5-15 μmol, 1.5-7.0

mol %) to the reaction mixture under otherwise similar conditions led to a steady

decrease from $k_{obs} = 8.34 \times 10^{-2}$ h^{-1} (without PCy_3) to 4.38×10^{-2} h^{-1} (15 μmol of PCy_3).

These results indicate that the active Ru catalyst is formed by the initial dissociation of

the phosphine ligand. Reaction conditions: acetophonone (0.20 mmol),

vinyltrimethylsilane (0.40 mmol) with various concentrations of PCy_3 in the presence of

the catalyst **1** (0.5 mol %) in toluene-d_8 at 120 °C.

Figure 18. Plot of the Initial Rate (vi) vs. [PCy$_3$] for the Coupling Reaction of Acetophonone and Vinyltrimethylsilane

4.4.4 Hammett Study

Hammett studies of *para*-substituted acetophenones were performed in order to determine the electronic effects on thereaction mechanism. Therefore, in the glove-box, (PCy$_3$)$_2$(CO)RuHCl (1 mg 0.5 mol %), *para*-substituted acetophenones (0.2 mmol), Vinyltrimethylsilane (0.4 mmol) and hexamethylbenzene (26 mg as the internal standard) were dissolved in 0.5 ml toluene-d$_8$ solution in a Wilmad J-Young NMR tube with a Teflon screw cap (Eq 70).

X=CH$_3$, OCH$_3$, H, Cl, Br

The tube was taken out and was heated in oil bath at 120 $^\circ$C. ^{1}H NMR of the reactions mixtures were monitored every 30 min at room temperature. The initial rate method was used to determine the rate of each reaction. The rates were measured by integration of the vinyl protons peak of the product (=CH$_2$), which gives 4.34 ppm on ^{1}H NMR spectroscopy, and these were normalized against vinyl protons of the internal standard. The k_{obs} was estimated from a first-order plot of ln[product] vs reaction time.

Other reactions were monitored under the same condition. A Hammett plot was constructed by plotting the log (k_x/k_H) vs σ_ρ and a positive Hammett value of $\rho = 0.97$ was obtained from the correlation of *para*-substituted *p*-X-C$_6$H$_4$COCH$_3$ (X = OMe, CH$_3$, H, Cl, Br) with Vinyltrimethylsilane (Figure 19).

Figure 19. Hammett Plot of the Reaction of *p*ara-Substituted *p*-X-C$_6$H$_4$COCH$_3$ (X = OMe, CH$_3$, H, Cl, Br) with Vinylrimethylsilane

The rate of the reaction can be accelerated by adding electron-withdrawing group on the acetophenone and the promotional effect by electron-withdrawing group is indicative of an electrophilic nature of the carbonyl carbon which is stabilized by the Ru catalyst. The results are consistent with the notion that a buildup of negative charge on transition state of C-Si bond formation step.

4.5 Proposed Mechanism of the Reaction of Ketone and Vinylsilanes

A plausible mechanistic rationale for the silyl enol ether formation is illustrated

on the basis of these results (Scheme 24).

Scheme 24. Proposed Mechanism of the Coupling Reaction of Ketones and
Vinyltrimethylsilane

From the phosphine inhibition study, we learned that PCy_3 ligand show strong

inhibition on enol silyl ether formation, the dissociation of phosphine ligand is necessary

to give the open active site to the substitutes to coordinate to the ruthenium center. And

the dissociation of PCy_3 should be the first step and at high temperature this step is rapid

and reversible. With the dissociation of PCy_3 from the ruthenium complex **1,** there is one

open active site in the ruthenium center in the ruthenium complex **68a**, so complex **68a** is

active. We proposed that the catalytically active cationic Ru-silyl species **68c** was

initially formed from an alkene insertion followed by the elimination of ethylene molecule. The elimination of ethylene happened before the formation of the enol silyl ether and was detected by ^{1}H NMR spectroscopy. The ^{13}C isotope effect study also indicates that elimination of ethylene and form ruthenium-silyl complex is not the rate–limiting step. But we did not detect the formation of ruthenium-silyl species, which hints this step to be reversible and rapid. Next step is the keto-enol tautomerization and insertion of an enol substrate to the ruthenium-silyl complex to form a Ru-enolate species. The low KIE value from the kinetic isotope effect study on the reaction of acetophenone and vinyltrimethylsilane indicates that the the keto-enol tautomerization which involves the C-H bond cleavage is not the rate-limiting step. The Ru-enolate species **68d** would then undergo reductive elimination to yield the silyl enol ether product **68e**. A relatively positive high Hammett value from the correlation of *para*-substituted arylketones supports the notion that a buildup of negative charge on transition state of the Ru-enolate species **68d** and the O-Si bond formation step the rate–limiting step.

4.6 Conclusions

We successfully developed an effective catalytic method to produce synthetically useful vinylsilyl ethers through coupling reaction of ketones and vinylsilane by using well-defined ruthenium-hydride catalyst **1**. As demonstrated from both Mukaiyama Aldol condensation and aminomethylation reactions, the catalytic method of silyl enol ether formation should find useful applications in α-functionalization reactions of ketones. Phosphine inhibition and kinetics studies give the useful inforamtion on the mechanism. The highly positive Hammett value from the correlation of *para*-substituted arylketones on vinyltrimethylsilanes support the O-Si bond formation step being the rate-limiting step.

Chapter 5. Highly Stereoselective and Regioselective Hydrosilylation of Alkynes and Alkenes Catalyzed by $(PCy_3)_2(CO)RuHCl$

Vinylsilanes have emerged as versatile building blocks in organic synthesis. Because of their low toxicity, low cost, high stability, and innocuous byproduct, vinylsilanes play an increasingly important role in the synthesis and particularly in metal-catalyzed cross-coupling reactions. Over the past decades, many groups have been working on routes to syntheze vinylsilanes, and among them, hydrosilylation of alkynes catalyzed by transition metals is the most straightforward and atom-economical method. Generally, the hydrosilylation of alkynes generates a mixture of three compounds. There are still things to improve in such hydrosilylation reactions. Though recently the selectivity of the germinal products has been improved by using Pd catalyst, Firstly, generation of highly selective *cis* or *trans* coupling products remains difficult. Moreover, the high catalyst loading is typically required in these reactions and mechanism of the hydrosilylation is still unclear. Here, we have been working to improve the selectivity on the formation of *cis* and *trans* vinylsilane, as well as learning the factor to the selectivity of vinylsilanes formation and the mechanism of the hydrosilylation reactions.

5.1 Results and Discussion

Due to the synthetic utility of vinysilane, we have been working on the methods to generate selective vinylsilanes by transition metal catalysts. Recently, we observed that $(PCy_3)_2(CO)RuHCl$ (**1**) shows a considerably high selectivity and reactivity toward hydrosilylation of alkynes and alkenes. For example, the treatment of phenylacetylene (1.0 mmol) and triethylsilane (2.0 mmol) in the presence of 1 mol % ruthenium catalyst **1** in CH_2Cl_2 generated (*Z*)- vinylsilanes **69a** in 99% yield (Eq 71). On the other hand, the treatment of styrene with 2.0 equiv. triethylsilane at 40 ^{o}C forms the (*E*)-vinylsilanes **70a** at a high yield (Eq 72). More details on experimental conditions, reaction scope, and mechanism of these reactions, will be discussed in this chapter.

$$HSiEt_3 \quad + \quad H \!\!\equiv\!\! \underset{}{\bigcirc} \quad \xrightarrow[CH_2Cl_2,\ r.t,\ 4\ h]{\textbf{1}\ (1\ mol\ \%)} \quad \underset{\textbf{69a}}{\bigcirc\!\!\!\sim\!\!SiEt_3} \qquad (71)$$

$$\underset{}{\bigcirc\!\!\!\sim} \quad + \ HSiEt_3 \quad \xrightarrow[CH_2Cl_2,\ 40\ ^oC,\ 8\ h]{\textbf{1}\ (1\ mol\ \%)} \quad \underset{\textbf{70a}}{\bigcirc\!\!\!\sim\!\!SiEt_3} \quad + \quad \bigcirc\!\!\!\sim \qquad (72)$$

5.2 Scope of the Hydrosilylation of Alkynes

5.2.1 Catalyst Survey

The catalytic activity of selected ruthenium complexes was initially screened for the coupling reaction of phenylacetylene and triethylsilane (Eq 73). The survey of catalysts showed that ruthenium hydride complex $(PCy_3)_2(CO)RuHCl$ (**1**) has the highest activity in the formation of the vinylsilanes among selected ruthenium complexes in 4 hours at room temperature with 99 % conversion determined by GC-MS and NMR (Table 11, entry 5).

$$HSiEt_3 \quad + \quad H\!\!=\!\!\!\!\!\equiv\!\!\!\!\!-\!\!\bigcirc \quad \xrightarrow[\text{CH}_2\text{Cl}_2,\ \text{r.t, 4 h}]{\text{[Ru] (1 mol \%)}} \quad \bigcirc\!\!-\!\!\!\diagup\!\!\!\!\diagdown_{SiEt_3} \qquad (73)$$

69a

Under similar conditions, $Ru_3(CO)_{12}$ (entry 4) and [(p-cymene)RuCl$_2$]$_2$ (entry 12) showed some activity on the hydrosilylation products, but the conversion is low (around 5%). Other commonly ruthenium complexes such as $Ru(CO)H_2(PPh_3)_3$, $RuCl_3 \cdot 3H_2O$, [(COD)RuCl$_2$]$_x$ and [(PCy$_3$)$_2$(CO)(MeCN)$_2$RuH]$^+$BF$_4^-$, were not effective in giving coupling products under similar reaction conditions.

Table 11. Catalyst Activity Survey for the Coupling Reaction of Phenylacetylene and Triethylsilane

Entry	Catalyst	Additive	yield(%)[b]
1	None	None	0
2	$Ru_3(CO)_{12}$	None	3
3	$Ru_3(CO)_{12}$	NH_4PF_6	4
4	$RuCl_3.3H_2O$	None	0
5	**$(PCy_3)_2(CO)RuHCl$**	**None**	**99**
6	$(PCy_3)_2(CO)RuHCl$	HBF_4OEt_2	< 5
7	$(PPh_3)_3(CO)RuH_2$	None	0
8	$(PPh_3)_3RuCl_2$	None	0
9	$(PPh_3)_3RuHCl$	None	0
10	$[RuCl_2(COD)]x$	None	0
11	$(PCy_3)_2(CH_3CN)_2(CO)Ru \overset{\oplus}{H} BF_4 \ominus$	None	0
12	$[(p\text{-}cymene)RuCl_2]_2$	None	5

[a] Reaction conditions: 1.0 mmol of phenylacetylene, 2.0 mmol triethylsilane, [Ru] 1 mol %, CH_2Cl_2 2 mL, room temperature, 4 hours. [b] GC yields based on phenylacetylene.

5.2.2 Scope of the Hydrosilylation of Alkynes

To demonstrate the synthetic utility of the catalyst **1**, we explored the scope of the hydrosilylation of alkynes. The reactions of phenylacetylene with different silanes such as triethylsilane, diethylmethylsilane, the more bulky substituted triphenyl silane were tested under the similar conditions and all gave only (z)-vinylsilane isomers (Eq 71).

$$HSiEt_3 \quad + \quad H \!\!=\!\!=\!\! \bigcirc \quad \xrightarrow[\text{CH}_2\text{Cl}_2, \text{ r.t, 4 h}]{\text{RuCl(CO)(PCy}_3)_2\text{H (1 mol \%)}} \quad \bigcirc \!\!=\!\! SiEt_3 \qquad (71)$$

A variety of terminal and internal alkynes were proven to be amenable for the hydrosilylation reaction. We found that these alkynes showed a strong steric effect on the selectivity of the coupling products. For phenylacetylene (entry 1) and 1-hexyne (entry 10), (*Z*)- vinylsilanes were detected by ^{1}H NMR. But for the steric bulky alkynes as 3-methyl-1-butyne (entry 11), a mixture of both (*Z*) and (*E*) isomers at a ratio of 3:2 was detected. When we treated the more bulky substrate 3,3-dimethyl-1-butyne in entry 21, only *trans* vinylsilanes was formed. So the selectivity of formation of vinylsilane has significant dependence on alkynes. Bulky substrates generally favor formation of *trans* vinylsilane (Table 12), which may due to the steric hindrance between the alkynes and the ruthenium complex.

We also tried to explore the utility of these hydrosilylation reactions by some internal alkynes (enty 17 and 18). They all showed the high activity and conversion to vinylsilane products. For prop-1-yne benzene (entry 17), we determined the product to be the (*E*)-isomer based on NOSEY and ^{1}H NMR data. We also detected a signal of the

methyl with the ethyl group, and for ^{1}H NMR the signals signed to methyl show the doublet with a small coupling constant (1.7 Hz). This result is also consistent with the prediction based on stereo effect, in which the bulky group favors formation of *trans* product. So, at this point, the reaction of diphenylethyne with triethylsilane should give *trans* vinylsilane. For 1,4-diethynylbenzene (entry 16), it generates a mixture of *cis* and *trans* products at a ratio of 3:1. We also tried 1, 6-heptadiyne, but the selectivity of the reaction was poor, as multiple isomers were detected.

Table 12. The Coupling Reaction of Alkynes and Triethylsilane [a]

Entry	Alkyne	Silane	Product	Yield (%)
1		$HSiEt_3$	**69a**	99
2	H—≡—Ph	$HSiEt_2CH_3$	**69b**	98
3		$HSiPh_3$	**69c**	95
4	H—≡—⟨ ⟩—X	$HSiEt_3$	**69d-69g** X=CH_3	99
5			X=OCH_3	96
6			X=F	98
7			X=CF_3	97
8	H—≡— (o-tolyl)	$HSiEt_3$	**69h**	98
9	H—≡— (m-tolyl)	$HSiEt_3$	**69i**	98
10	H—≡— (butyl)	$HSiEt_3$	**69j**	98
11	H—≡— (sec-butyl)	$HSiEt_3$	**69k** 1 : 1.5	90
12	H—≡—$C(CH_3)_3$	$HSiEt_3$	**69l**	91
13	H—≡—CH_2Ph	$HSiEt_3$	**69m**	96
14	H—≡—(isopropenyl)	$HSiEt_3$	**69n**	85

15	(6-methoxynaphthalen-2-yl-ethyne)	HSiEt₃	**69o** *Cis* : *tran* 1:2	93
16	(ethynylcyclohexane)	HSiEt₃	**69p** 4:5	98
17	(1,4-diethynylbenzene)	HSiEt₃	**69q** *cis* : *tran* 3:1	94
18	(1-phenylpropyne)	HSiEt₃	**69r**	98
19	(diphenylacetylene)	HSiEt₃	**69s**	95
20	(ethynylestradiol)	HSiEt₃	**69t**	67

a Reaction conditions: alkyne (1.0 mmol), hydrosilane (1.5 mmol), **1** (1 mg, 1 mol %), CH₂Cl₂ (2-3 mL), room temperature, 6 h. *b* Isolated yield. *c* 60 °C, 15 h.

5.2.3 The Scope of the Hydrosilylation of Alkenes

In another case, the treatment of 1.0 mmol styrene with 2.0 mmol triethylsilane in

the presence of 1 mol % catalyst **1** in CH₂Cl₂ at 40 °C for 8 h smoothly generates *trans*

vinylsilane **70a** as coupling product along with one equiv. of ethyl benzene as the

byproduct (Eq 72).

$$HSiEt_3 \; + \; \underset{\text{1.0 mmol}}{\text{[styrene]}} \; \xrightarrow[\text{CH}_2\text{Cl}_2, \, 40 \, ^\circ\text{C}, \, 8 \, \text{h}]{\text{RuCl(CO)(PCy}_3)_2\text{H (1 mol \%)}} \; \underset{\textbf{70a}}{\text{[styryl-SiEt}_3]} \; + \; \text{[ethylbenzene]}$$

(72)

2.0 mml

To demonstrate the synthetic utility of the catalyst $(PCy_3)_2(CO)RuHCl$ on the

hydrosilylation of alkenes, we explored the reaction scope. Firstly, triethysilane,

diethylmethylsilane and triphenylsilane were explored by the reaction with styrene,

which all give *trans*-vinysilylane. Triethoxy(vinyl)silane show the low conversion under

similar conditions. A variety of alkenes was used in this reaction. The Table 13 shows

that both less bulky substitutes as 1-hexene (entry 11) and more bulky substitutes as

2-methoxyl-6-vinylnaphthalene (enty 8) and vinylcyclohexane (enty 9) give only *trans*

products. So unlike the hydrosilylation of alkynes, there is no steric effect on the

formation of coupling products. On the other hand, those internal alkenes showed no

reactivity in the hydrosilylation reactions.

Table 13. The Coupling Reaction of Alkenes and Hydrosilane. [a]

Entry	Alkene	Silane	Product	Yield(%)[b]
1		HSiEt$_3$	**70a**	98
2		HSiEt$_2$Me	**70b**	96
3		HSiPh$_3$	**70c**	87
4		HSiEt$_3$	**70d**	97
5		HSiEt$_3$	**70e**	95
6		HSiEt$_3$	**70f**	94
7		HSiEt$_3$	**70g**	95
8		HSiEt$_3$	**70h**	90
9		HSiEt$_3$	**70i**	96
10		HSiEt$_3$	**70j**	95
11		HSiEt$_3$	**70k**	87
12		HSiEt$_3$	**70l**	93
13		HSiEt$_3$	**70m**	92

14		HSiEt$_3$	**70n**	83
15		HSiEt$_3$	**70o**	93
16		HSiEt$_3$	**70p**	69
17		HSiEt$_3$	**70q**	73
18		HSiEt$_3$	**70r**	85

[a] Reaction conditions: alkenes (2.0 mmol), HSiEt$_3$ (1.0 mmol), **1** (1 mg, 1 mol %), CH$_2$Cl$_2$ (2-3 mL), 40 ^{o}C, 8 h. [b] Isolated yield.

We explored the reaction scope by using some functional substituents such as ethyl arylate (entry12), carbazole (entry 18) and 1-vinylpyridin-2-one (entry 17). They all show very high selectivity towards *trans* products. However, in the reactions of but-3-en-2-one, isoprene, and but-3-en-2-ol, only a trace amount of *trans*-product was detected. This may result from the fact that these substitutes are highly reactive, thus favoring self-isomerization.

5.3 Mechanistic Study on the Hydrosilylation of Alkynes

5.3.1 Deuterium Labeling Study on the Hydrosilylation of Alkynes

In order to get insight on the mechanism of these reactions, we performed a series

of deuterium labeling study experiments. The treatment of triethylsilane (2.0 mmol) with

PhC≡CD (1.0 mmol) in the presence of **1** (1 mol %) in CH_2Cl_2 at room temperature

yielded coupling product **69a** without H/D exchange and **69a** was determined by both ^{1}H

and ^{2}H NMR (Eq 74 and Figure 20).

$$\text{(74)}$$

$$\underset{\text{2.0 mmol}}{\text{HSiEt}_3} \quad + \quad \underset{\text{1.0 mmol}}{\text{D}\!\!=\!\!\!\!-\!\!\!\bigcirc} \quad \xrightarrow[\text{CH}_2\text{Cl}_2,\text{ r.t, 4 h}]{\textbf{1} \text{ (1 mol \%)}} \quad \bigcirc\!\!-\!\!\!=\!\!\!\overset{\text{D}}{\underset{\text{SiEt}_3}{}}$$

In Figure 19, there are only two deuterium signal, one (2.05 ppm) was the

reference acetone-d_6 and the other (5.81 ppm) the vinyl proton of complex **69a.** Since no

signal at this position was observed in ^{1}H NMR spectroscopy. It is clear that this

deuterium is from PhC≡CD, and there should be no H/D exchange between

phenylacetylene and triethylsilane during this reaction. This indicated that for

phenylacetylene, there should be no C-H bond cleavage during the reaction.

Figure 20. ^{1}H and ^{2}H NMR for the Deuterated Complex **69a**. A-^{1}H NMR Spectroscopy of *cis*-vinylsilane **69a**; B–^{1}H NMR Spectroscopy of Deuterium Vinylsilane; C- Deuterium NMR Spectroscopy of Deuterium Product and Acetone-d_6 is the Reference.

5.3.2 Phosphine Inhibition Study on the Hydrosilylation of Alkynes.

We next performed a series of phosphine inhibition experiments to gain further insight into the reaction mechanism. Therefore, in order to observe such phosphine inhibition, phenylacetylene (0.20 mmol), triethylsilane (0.40 mmol), **1** (2 mg, 1 mol %) and C$_6$Me$_6$ (2 mg, internal standard) were dissolved in 0.5 mL of CDCl$_3$ solution in a J-Young NMR tube with a Teflon screw cap. A pre-dissolved PCy$_3$ in CDCl$_3$ solution (5 μL, 1.0 *M*) was added to the tube via syringe. The reaction was monitored by ^{1}H NMR

spectroscopy with 30 min interval at room temperature. The initial rate method was used

to measure the rate of each reaction. The rate was measured by the ^{1}H integration of the

product peak at δ 5.81 (=CHSi), and was normalized against the internal standard peak.

The k_{obs} was estimated from the first order plot of *ln*[product] vs. reaction time.

Figure 21. The Phosphine Inhibition for the Coupling Reaction of Phenylacetylene and Triethylsilane; [a] Reaction conditions: phenylacetylene (0.20 mmol), triethylsilane (0.40 mmol), **1** (1 mol %), PCy$_3$ (0.0-0.014 mM).

The catalytic reaction was found to be strongly inhibited by the phosphine ligand.

The initial rate was estimated from [product] vs. time plots for each sample with different

[PCy$_3$] (Figure 21). The addition of PCy$_3$ (2.7-8.3 mol, 2.7-8.3 mol %) to the reaction

mixture under otherwise similar conditions led the rate to a steady decrease from 4.1 x

10^{-5} h^{-1} (without PCy$_3$) to 8.7 x 10^{-6} h^{-1} (0.014 M of PCy$_3$). These results indicate that

active Ru catalyst formed by initial dissociation of a phosphine ligand.

Figure 22. Plot of the Initial Rate vs. [PhC≡CH] at different PCy$_3$ Concentrations
 No PCy$_3$ (■); 0.004 mM (0.8 equiv.) PCy$_3$ (◆); 0.009 mM (1.8 equiv.) PCy$_3$(●); 0.014
mM (2.8 equiv.) PCy$_3$(▲).

In order to determine the nature of such inhibition, a series of kinetic experiments

were performed. Therefore the reaction of phenylacetylene (0.04-0.2 mmol) and excess

amount of triethylsilane with various concentrations of PCy$_3$ (0-0.14 M, 0-2.8 equiv.

compared to **1**) in presence of **1** (1 mol %) in CDCl$_3$ at room temperature was monitored

using ^{1}H NMR over the internal standard. Rate vs. the concentration of phenylacetylene

plot (Figure 22) was constructed from a linear, pseudo-first order plot of product

formation vs. time.

Figure 23. Lineweaver-Burke Plot of 1/vi vs. 1/[PhCCH]

In order to determine the nature of the inhibition, the inhibition data was fitted to

Michaelis-Menten equation to determine the kinetic parameters for the addition. A series

of Lineweaver-Burke plot (Figure 23) were constructed.

$$[Ru] + S \rightleftharpoons |RuS| \longrightarrow [Ru] + A$$
$$+$$
$$P$$
$$|RuS|$$
$$P$$

Scheme 25. General Kinetic Scheme for an Uncompetitive Inhibitor[113]

The reciprocal plots show non-intersecting lines, indicating that PCy_3 acts as an uncompetitive inhibitor. As illustrated in Scheme 25, where [Ru] is the catalytically active species, [S] is the substrate, P is PCy_3 ligand and A is the vinylsilane products.

In this scheme, the inhibitor reversibly coordinates to the catalyst-substrate complex [RuS], creating inactive catalyst-substrate-inhibitor complex [RuSP]. Reduction of the amount of catalyst-substrate complex from the formation of inactive catalyst-substrate-inhibitor complex [RuSP] increases the apparent affinity of the substrate. In this reaction condition, there always is some of the inactive complex in solutions, which decreases the overall apparent V_{max}.

5.3.3 Rate Dependence on the Substrate Concentration

The rate dependence on alkynes would provide valuable insights into the mechanism for hydrosilylation of alkynes. The initial rate method was used to determine the rate of reaction. The treatment of 0.06-0.8 M phenylacetylene with excess amount of triethylsilane in the presence of 2 mg of **1** at room temperature in $CDCl_3$ was monitored by ^1H NMR spectroscopy. The initial rates of the reactions were determined from linear, pseudo-first order plots of product formation rate vs. time.

Figure 24. Plot of the Initial Rate vs. [PhC≡CH]

In Figure 24, the rate does not show any dependence on the concentration of phenylacetylene in 0.06 M-0.20 M, the k_{obs} is 4.3 x $10^{-5} h^{-1}$. However, from 0.2 M, with the concentration of phenylacetylene to 0.8 M, the k_{obs} was decreased from 4.3 x $10^{-5} h^{-1}$

(0.2 M) to 1.0×10^{-5} h^{-1} (0.8 M). These results indicate that the rate of reaction shows no

dependence on concentration of phenylacetylene under the dilute condition. However,

with the concentration increasing, the phenylacetylene coordinates to the catalyst center

by creating inactive catalytic species and will eventually prevent the substrate from the

coordination to the ruthenium center to generate the products.

We next performed a kinetic study on the rate dependency on triethylsilane.

Treatment of 0.06-0.8 M of phenylacetylene with excess amount of triethylsilane in the

presence of 2 mg of **1** at room temperature in $CDCl_3$ was monitored by ^{1}H NMR

spectroscopy. The initial rate method was used to determine the rate of the reactions. The

initial rates of the reactions were determined from linear, pseudo-first order plots of rate

of the product formation vs. time.

Figure 25. Plot of the initial rate vs. [HSiEt$_3$]

Figure 25 indicated that the rates of reaction of hydrosilylation of alkynes showed

no dependence on the concentration of triethylsilane. We monitored the rate of the

reactions with the different concentration of triethylsilane from 0.04 M to 0.7 M at

similar conditions, and found all the reactions giving similar k_{obs} value as 4.3 x 10^{-5} h^{-1}.

5.3.4 Rate Dependence on the Catalyst Concentration

In order to get insight into the mechanism, the rate dependence of ruthenium

hydride concentration was performed. The treatment of 1.4-11 mM ruthenium hydride **1**

with 0.4 M triethylsilane and 0.2 M phenylacetylene at room temperature in CDCl$_3$ was

monitored by ^{1}H NMR spectroscopy. The initial rate method was used to determine the

rates of the reactions. The initial rates of the reactions were determined from linear,

pseudo-first order plots of rate of the product formation vs. time.

The rate of the reactions of hydrosilylation of alkynes showed dependence on the

concentration of catalyst. We monitored the rates of reaction with different concentration

of catalyst from 1.4 mM to 11 mM under similar conditions, and we found that the k_{obs}

increased from 7.5 x 10^{-6} h^{-1} to 6.8 x 10^{-5} h^{-1}. The plot of v_i vs. concentration of

ruthenium hydride is linear, which indicated that there was a first order rate dependence

on the concentration of catalyst. So in the dilution, we can drive the kinetics equation rate

$= k \, [\text{Ru}]^1 [\text{Alkyne}]^0 [\text{silane}]^0$.

Figure 26. Plot of the initial rate vs. [RuH]

5.4 Mechanistic Study on the Hydrosilylation of Alkenes

5.4.1 Deuterium Labeling Study on the Hydrosilylation of Alkenes

To explore the mechanism of hydrosilylation of alkenes, we first performed

deuterium labeling study experiments. The treatment of triethylsilane (1.0 mmol) and

styrene-d_8 (1.0 mmol) in CH_2Cl_2 at 40 ^{o}C was monitored by ^{1}H NMR spectroscopy. The

coupling product **70a** was characterized by ^{1}H and ^{2}H NMR spectroscopy. For the

product **70a**, a similar amount of deuterium on the two vinyl positions was detected by [1]H

and ^{2}H NMR spectroscopy which gives the 77% and 71% deuterium (Scheme 26). Under

similar conditions, the reaction of styrene-d_8 (1.0 mmol) with triethylsilane (2.0 mmol)

gave the product with 70% and 64% deuterium on the vinyl positions.

Scheme 26. Deuterium Labeling Study on the Hydrosilylation of Alkenes

As shown in Figure 27, A is the ^{1}H NMR spectroscopy of trans-vinylsilane;

B is the ^{1}H NMR of deuterium vinylsilane and C is ^{2}H NMR spectroscopy of deuterium

product two deuterium signals at 2.6 ppm and 0.8 ppm were detected, which were

assigned to the ethylbenzene. In ^{1}H NMR spectroscopy, two signals were detected at the

same chemical shift. In addition, there was also a deuterium signal assigned to the unused

triethylsilane. These H/D exchange results indicate that the H/D exchange is rapid and

done before the formation of the coupling products.

Figure 27. ^{1}H and ^{2}H NMR for the complex **70a**

5.4.2 Isotope Effect Study on the Hydrosilylation of Alkenes

In order to determine the possibility of a rate-limiting C-H bond cleavage step, the

kinetic isotope effect for the hydrosilylation of alkenes was performed. Again, the initial

rate method was used in order to determine the reaction rates. Here, the treatment of

styrene (0.1 mmol) and triethylsilane (0.2 mmol) in the presence of 1.0 mol % of **1** in

CDCl$_3$ was monitored by ^{1}H NMR spectroscopy at 40 ^{o}C (Scheme 27).

Figure 28. Kinetics Plot of the Reaction of Styrene and HSiMe$_3$

The rate of reaction was then determined from linear, pseudo-first order plots of the product formation vs. time (Figure 28), which gave the k_{obs} as 1.1×10^{-5} h^{-1}. Under similar conditions, the reaction of deuterated styrene-d_8 (0.1 mmol) and triethylsilanes (0.2 mmol) was monitored by NMR spectroscopy at 40 ^{o}C, and gave the k_{obs} as 9.8×10^{-6} h^{-1}. The kinetic isotope effect study gave us a similar k_{obs} value for the deuterated and regular reactions, which gave the k_{CH}/k_{CD} as 1.1 ± 0.1. This low KIE value suggested that C-H bond cleavage of the styrene is not the rate-limiting step.

Scheme 27. Kinetic Isotope Effect Study on the Hydrosilylation of Alkenes

5.4.3 Carbon Isotope Effect Study

In order to get more information on the rate limiting step, we used singleton's

method in carbon isotope effect study. In glove box, styrene (2.0 mmol), triethylsilane

(3.0 mmol), **1** (14 mg, 1 mol %) were dissolved in 3 mL CH_2Cl_2 solution in two 25 mL

Schlenk tubes equipped with a magnetic stirring bar. The reaction tube was then heated in

oil bath at 40 °C for 10 min and was opened to air at room temperature, and the crude

product mixture was analyzed by GC/MS (10 % conversion). The other reaction tube was

heated in an oil bath at 40 °C for 8 hr and was opened to the air at room temperature. The

crude product mixture was analyzed by GC/MS (98 % conversion). The solvent was

removed under a rotary aspirator, and the product *trans* vinylsilane was isolated by a

column chromatograph on silica gel (*n*-hexanes) (Scheme 28).

Scheme 28. Carbon Isotope Effect Study on the Hydrosilylation of Styrene

The ^{13}C NMR analysis of *trans* vinylsilane of both 98% conversion and 15%

conversion was performed by following Singleton's ^{13}C NMR method. The NMR

samples were prepared identically by adding *trans* vinylsilane (198 mg) in CDCl$_3$ (0.5

mL) in a 5 mm high precision NMR tube. The ^{13}C {^{1}H} NMR spectra were recorded with

H-decoupling and 45 degree pulses. A 60 s delay between pulses was imposed to

minimize T_1 variations (d1 = 60 s, at = 5.0 s, np = 245098, nt = 512). The average ^{13}C

integration ratio of the samples of *trans* vinylsilane **70a** is shown in Table 14.

Table 14. Average ^{13}C Integration of the Samples of trans-vinylsilane **70a**

HSiEt$_3$ + [styrene] $\xrightarrow[\text{CH}_2\text{Cl}_2,\ 40\ ^\circ\text{C},\ 8\ \text{h}]{\text{RuCl(CO)(PCy}_3)_2\text{H (1mol\%)}}$ [PhCH=CHSiEt$_3$] + [ethylbenzene]   98 % conv.

HSiEt$_3$ + [styrene] $\xrightarrow[\text{CH}_2\text{Cl}_2,\ 40\ ^\circ\text{C},\ 10\ \text{min}]{\text{RuCl(CO)(PCy}_3)_2\text{H (1mol\%)}}$ [PhCH=CHSiEt$_3$] + [ethylbenzene]   10 % conv.

C#	98% conv.	18% conv.	18% conv./98% conv.	change (%)
1	2.9936 (3)	2.9925 (3)	0.9996 (3)	0.04 (3)
2	2.9827 (4)	2.9823 (4)	0.9998 (4)	0.02 (4)
3	0.9314 (5)	0.9208 (5)	0.9886 (5)	1.14 (5)
4	1.0084 (3)	1.0060 (3)	0.9976 (3)	0.24 (3)
5	0.9288 (4)	0.9272 (4)	0.9983 (4)	0.17 (4)
6	2.0000 (5)	2.0000 (5)	1.0000 (5)	0.00 (5)
7	1.9892 (3)	1.9884 (3)	0.9996 (5)	0.04 (5)
8	0.9938 (3)	0.9923 (3)	0.9985 (3)	0.15 (3)
C#	98% conv.	10% conv.	10% conv./98% conv.	change (%)
1	2.9936 (4)	2.9915 (4)	0.9993 (4)	0.07 (4)
2	2.9827 (4)	2.9813 (3)	0.9995 (3)	0.05 (3)
3	0.9314 (5)	0.9198 (5)	0.9875 (5)	1.25 (5)
4	1.0084 (3)	1.0074 (3)	0.9990 (3)	0.10 (3)
5	0.9288 (4)	0.9266(4)	0.9976 (4)	0.24 (4)
6	2.0000 (5)	2.0000 (5)	1.0000 (5)	0.00 (5)
7	1.9892 (3)	1.9879(3)	0.9993 (5)	0.07 (5)
8	0.9938 (3)	0.9953 (3)	1.0015 (3)	0.15 (3)

In Table 14, the most significant carbon isotope effect was observed at the

CH=CH-Si of the product. We can see that at 10 % conversion, the integration of the

carbon **3** which was signed to CH=CH-Si is 0.9198 at five runs, comparing with 0.9314

at 98% conversion the integration of carbon **3** is change by 1.25 %. But other carbons

change by 0.05 %-0.15%. At 18 % conversion, the results is similar, the carbon **3**

changed by 1.14 %, and others changes even less. This result indicates that the reaction

step involving this C-Si carbon is slow and should be rate limiting. This is based on an

assumption that the migration of ^{13}C is slower than the migration of ^{12}C in such slow

steps, which results that the abundance of ^{13}C of the product at low conversion will

become less than the ^{13}C of the product from the completed reaction.

Compound **70a**

5.4.4 Hammett Study on the Hydrosilylation of Alkenes

Hammett studies of *para*-substituted styrene were performed to determine the

electronic effects on the alkene substrates for the hydrosilylation of alkenes. The

treatment of the *para*-substituted styrene p-X-C$_6$H$_4$CH=CH (X = OMe, CH$_3$, H, Br, Cl)

(0.2 mmol), Triethylsilane (0.3 mmol) and hexamethylbenzene (26 mg as the internal

standard) was monitored by [1] H NMR spectroscopy at 40 $^{\circ}$C.

X = OMe, CH$_3$, H, Br, Cl

Scheme 29. The Hammett Study on the Hydrosilylation of Alkenes

The initial rate method was used to determine the rate of each of reactions. The

rates were measured by the integration of the products vinyl peak (6.48 ppm). The

integration of product peak was normalized against the internal standard. The k_{obs} was

estimated from a pseudo first-order plot of ln[product] vs reaction time. The Hammett

plot of the log (k_x/k_H) vs the σ_ρ gave the Hammett ρ value of 0.59 (Figure 31).

In Figure 29, the Hammett plot of the log (k_x/k_H) vs the σ_ρ gave a positive

Hammett ρ value of 0.59, which indicated that the rate of the reaction increased with the

electron-withdrawing substitutes. By using styrene, the reaction gave $k_{obs} = 1.1 \times 10^{-5}\,h^{-1}$.

The reaction with the electron-donating substitutes as 4-methoxyl styrene, gave $k_{obs} = 7.3$

$\times 10^{-6}\,h^{-1}$. But when using the electron-withdrawing substitutes as the 4-bromo-styrene,

the reaction gave a $1.5 \times 10^{-5}\,h^{-1}$ as the k_{obs} value. This positive Hammett ρ value

indicated that possible anionic nature of the transition state.

Figure 29. Hammett Plot of the Coupling Reaction of *para*-Substituted p-X-$C_6H_4CH=CH_2$ (X = OMe, CH_3, H, Cl, F) with Triethylsilane

Here, we propose the structure of possible transition state of the intermediate (Figure 30), where X can be either electron-withdrawing or the electron-donating substitutes. When X are electron-withdrawing substitutes, the Ru-C bond will become weak and easy to break. Besides, the electrophonic addition of silyl group to the carbon will become easy. So in this case, the rate of the reaction will increase. These results indicate that the transition state is stable and the formation of C-Si bond is slow and rate-determining. These results are also consistent with the carbon isotope effect study, which suggests that the formation of the C-Si bond is the rate-determining step.

Figure 30. Possible Transition State for the Intermediate of the Hydrosilylation of Alkenes

5.4.5 Phosphine Inhibition Study on the Hydrosilylation of Alkenes

We next performed a series of phosphine inhibition experiments to gain the further insights into the reaction mechanism. The phosphine inhibition is common in our ruthenium hydride catalyst system, we observed a strong phosphine inhibition in the reaction of alkynes with triethylsilane and the reaction of alkynes with carboxylic acid. This phenomenon may also happen in the hydrosilylation of the alkenes. Therefore, to observe this phosphine inhibition, the mixtures of styrene (0.20 mmol), triethylsilane (0.40 mmol), **1** (2 mg, 1 mol %) and C_6Me_6 (2 mg, internal standard) were dissolved in 0.5 mL of $CDCl_3$ solution in a J-Young NMR tube with a Teflon screw cap. A pre-dissolved PCy_3 in $CDCl_3$ solution (5 μL, 1.0 M) was added to the tube via syringe. The tube was brought out of the glove box. The reaction was monitored by ^{1}H NMR at 10 min interval at 40 $^\circ$C. The initial rate method was used to measure the rate of each reaction. The rate was measured by integration of product peak at δ 5.81 ppm (=CHSi), and was normalized against the internal standard peak. The k_{obs} was estimated from the first order plot of *ln*[product] vs. reaction time.

The catalytic reaction was found to be strongly inhibited by the phosphine ligand.

The initial rate was estimated from the [product] vs. time for each added [PCy$_3$] (Figure

31). Addition of PCy$_3$ (2.7-1.0 μmol, 2.7-1.0 mol %) to the reaction mixture under the

similar conditions led the rate to a steady decrease from 3.6 x 10^{-5} h^{-1} (without PCy$_3$) to

1.2 x 10^{-6} h^{-1} (1.0 mM of PCy$_3$). These results indicated that active Ru catalyst formed by

initial dissociation of one phosphine ligand.

Figure 31. The Phosphine Inhibition for the Reaction of Styrene and Triethylsilane

In order to determine the type of inhibition, a series of kinetic experiments were

performed. The treatment of styrene (0.05-1.0 mmol) and excess amount of triethylsilane

with various concentrations of PCy$_3$ (0-1.0 mM, 0-2.2 equiv. compared to **1**) in presence

of **1** (1 mol %) in CDCl$_3$ at room temperature was monitored by ^{1}H NMR. The rate vs.

[styrene] plot (Figure 32) was constructed from linear, pseudo-first order plot of product

formation vs. time.

Figure 32. Plot of the Initial Rate vs. [styrene] at Different PCy$_3$ Concentrations. Without
PCy$_3$ (■); 0.21 mM (0.4 equiv) PCy$_3$ (▲); 0.42 mM (0.8 equiv) PCy$_3$(◆); 1.01 mM (1.8
equiv) PCy$_3$(○);

The inhibition data was fitted to the Michaelis-Menten equation to determine the

kinetic parameters. A series of Lineweaver-Burke plots (Scheme 30) were constructed.

The reciprocal plots indicated that PCy$_3$ acts as a noncompetitive inhibitor, as illustrated

in Scheme 30, where [Ru] is the catalytic active species, [S] is the substrate, P is PCy_3

ligand and A is the vinylsilane product.

$$[Ru] + S \underset{}{\overset{K_s}{\rightleftharpoons}} [RuS] \xrightarrow{K_p} [Ru] + A$$

$$+ \qquad\qquad +$$

$$P \qquad\qquad P$$

$$K_i \Big\updownarrow \qquad\qquad \Big\updownarrow K_i$$

$$[Ru\text{-}P] + S \underset{}{\overset{K_s}{\rightleftharpoons}} [\underset{P}{RuS}]$$

Scheme 30. General Kinetic Scheme for the Noncompetitive Inhibitor[114]

In order to conform this, replot of the slope and Dixon plot of 1/v vs. $[PCy_3]$ were

constructed (Figure 33 and 34).

Figure 33. Lineweaver-Burke Plot of 1/vi vs. 1/[styrene]. No PCy₃ (■); 0.21 mM (0.4 equiv.) PCy₃ (▲); 0.42 mM (0.8 equiv.) PCy₃ (◆); 1.01 mM (1.8 equiv.) PCy₃ (○);

The following reciprocal equation is for noncompetitive inhibition.

$$\frac{1}{v} = \frac{K_m}{V_{max}}(1+\frac{[I]}{K_i})\frac{1}{[S]} + \frac{1}{V_{max}}(1+\frac{[I]}{K_i})$$

And this equation may be rearranged to:

$$\frac{1}{v} = (1+\frac{K_m}{[S]})\frac{[I]}{V_{max}K_i} + \frac{1}{V_{max}}(1+\frac{K_m}{[S]})$$

A plot of 1/v versus [I] will be a straight line. The slope of the Dixon plot is given

by

$$slope = \frac{K_m}{V_{max}K_i}\frac{1}{[S]} + \frac{1}{V_{max}K_i}$$

Figure 34. Dixon plot of 1/v versus [PCy$_3$]

From the equations, the replot of slope vs. 1/[S] should be a straight line with a slope of $K_m/V_{max}K_i$, and an intercept of $1/V_{max}K_i$. So K_m can be figured out from Figure 35 by slope/intercept which gave 3.033. The value of K_i is from the Figure 34. The plot of 1/v vs. [I] gave a straight line with a slope of $(1+K_m/[S])/V_{max}K_i$ and an intercept of $(1+K_m/[S])/V_{max}$. So K_i = intercept/slope which gave 0.16 and V_{max} is 10.42. Therefore the kinetic equation can be derived by using these parameters.

Figure 35. The replot of slope vs. 1/[S]

Scheme 31. General Kinetic Scheme for the Non-competitive Inhibitor[115]

Where [Ru] is the catalytically active species, [S] is the substrate, P is PCy_3 ligand

and A is the vinylsilane products. In this scheme, the inhibitor reversibly coordinates to

the catalyst-substrate complex [RuS], creating inactive catalyst-substrate-inhibitor

complex [RuSP]. The catalyst-substrate-inhibitor complex [RuSP] can release the S to

form the catalyst-inhibitor complex [RuP], which can generate the catalytically active

species [Ru] by the dissociation of inhibitor PCy_3.

Kinetics data for the hydrosilylation of alkenes can be explained using a

non-competitive inhibitor model. The Lineweaver-Burke plots, Dixon plot and slope

secondary plot are consistent with this non-competitive inhibitor model: A

non-competitive inhibitor has no effect on the affinity the [RuP] complex has for the

coordination of alkene. The overall effect for a non-competitive inhibitor is to lower the

V_{max} of the reaction.

5.4.6 Rate Dependence on the Substrate Concentration

The rate dependence on alkenes would provide valuable insights into the

mechanism for the hydrosilylation of alkynes. The initial rate method was used to

determine the rate of reactions. The treatment of 0.06-0.8 M styrene with excess amount

of triethylsilane in the presence of 2 mg **1** at 40 $^{\mathrm{o}}$C in $CDCl_3$ was monitored by ^{1}H NMR

spectroscopy. The initial rates of the reactions were determined from linear, pseudo-first

order plots of product formation rate vs. time.

In Figure 36, the rate showed the linear dependence on the concentration of styrene as first order.

Figure 36. Plot of the initial rate vs. [styrene]

We next performed a kinetic study on the rate dependency on triethylsilane. Treatment of 0.04 M to 0.7 M triethylsilane with excessive amount styrene in the presence of 2 mg **1** at room temperature in $CDCl_3$ was monitored by ^1H NMR spectroscopy. The initial rate method was used to determine the rate of the reactions. The initial rates of the reactions were determined from linear, pseudo-first order plots of rate of the product formation vs. time.

The Figure 37 indicated that the rates of reaction of hydrosilylation of alkynes showed no dependence on the concentration of silane. We monitored the rate of the

reactions with the different concentration of silanes from 0.04 M to 0.7 M at similar

conditions, and found all the reactions giving similar k_{obs} value as 7.3 x 10^{-5} h^{-1}.

Figure 37. Plot of the initial rate vs. [HSiEt$_3$]

5.4.7 Rate Dependence on the Catalyst Concentration

In order to get insight into the mechanism, the rate dependence on ruthenium

hydride concentration was performed. The treatment of 1.4-11 mM of ruthenium hydride

1 with 0.4 M of triethylsilane and 0.2 M of phenylacetylene at room temperature in

CDCl$_3$ was monitored by ^{1}H NMR spectroscopy. The initial rate method was used to

determine the rates of the reactions. The initial rates of the reactions were determined

from linear, pseudo-first order plots of rate of the product formation vs. time.

The rate of the reactions of hydrosilylation of alkenes showed dependence on the concentration of catalyst. We monitored the rates of reaction with different concentration of catalyst from 0.0014 M to 0.011 M at similar conditions, and find the k_{obs} increasing from 5.0 x 10^{-5} h^{-1} to 3.82 x 10^{-4} h^{-1}. The plot of v_i vs. concentration of ruthenium hydride is linear, which indicates that there was a first order rate dependence on the concentration of catalyst.

Figure 38. Plot of the initial rate vs. [RuH]

5.5 The Reaction of Triethylsilane with Ruthenium Vinyl Complex

In order to get insight into the mechanism, we made the immediate species ruthenium vinyl complex in Eq 75. Thus, in glove box, 100 mg ruthenium complex **1**, excess amount of phenylacetylene were dissolved in 3 mL CH_2Cl_2 solution in two 25 mL Schlenk tubes equipped with a magnetic stirring bar, at room temperature for 30 min this reaction led to the clean formation of the ruthenium-vinyl complex **2**, which was isolated in 87% yield after recrystallization in CH_2Cl_2/*n*-hexanes (Eq 75).

We tested the activity of complex **2** for both the reaction of triethylsilane with styrene and the reaction of triethylsilane with phenylacetylene, they showed the same activity as the complex **1**, for the hydrosilylation of phenylacetylene, the reaction generates *cis* product, for the styrene case, it generates *trans* product. We performed the reaction of complex **2** (0.1mmol) with styrene (0.2 mmol) in the $CDCl_3$, and monitored the reaction by the VT-NMR from -40 ^{o}C to 80 ^{o}C, and observed no change on both the ^{1}H NMR and ^{31}P NMR. On the other hand, we also observed by VT-NMR that no reaction of complex **2** with triethylsilane took place at temperatures below 70 ^{o}C. However, when heated above 70 ^{o}C, the formation of the *trans* vinylsilane was detected, and the complex **2** was detected to turn back to complex **1** (Eq 76).

$$\text{(76)}$$
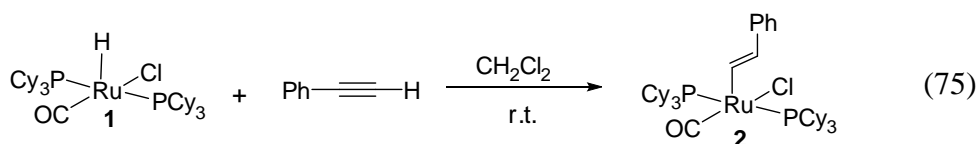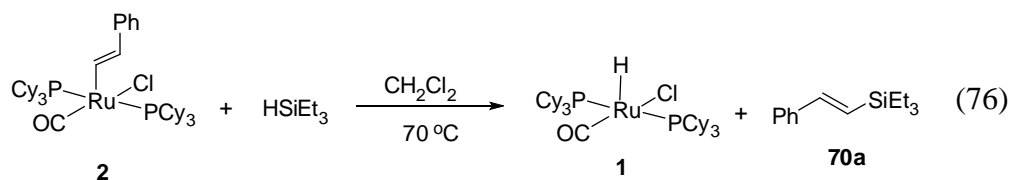
The Figure 39 showed the ^{31}P NMR signal change at 70 $^{\circ}$C, before the reaction, there was only one signal at 27.8 ppm, which belonged to ruthenium vinyl complex **2**. And then we observed ruthenium hydride signal at 45.8 ppm and for the ^{1}H NMR, we observed the formation of complex **70a.** After 3hr the reaction was done, all the complex 2 convers to the ruthenium hydride complex **1**.
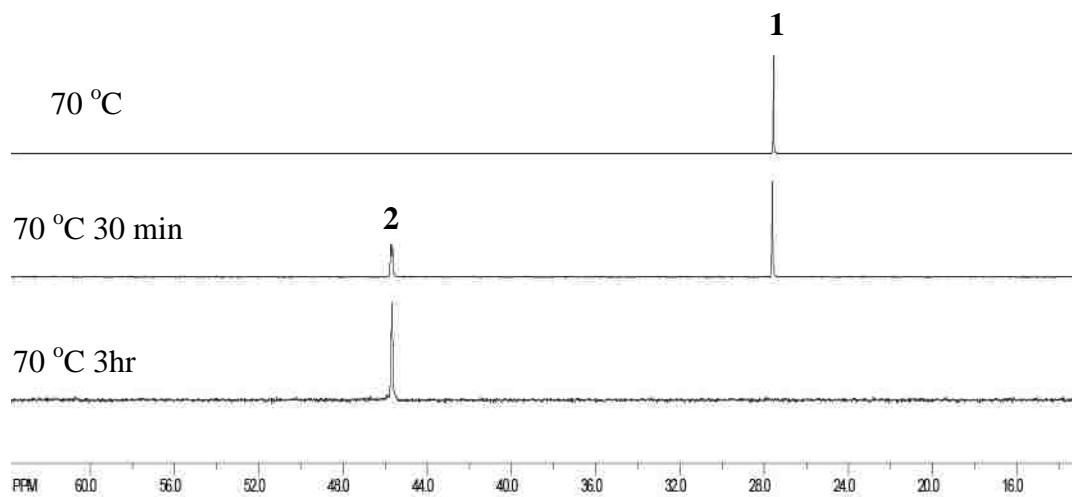
Figure 39. ^{31}P NMR of the Formation of Ruthenium Hydride Complex **1** from Rutheniumvinyl Complex **2**

Since this reaction is slower than the catalytic reactions, which can generate the product at room temperature, the following kinetic experiments are performed to get more information on this reaction. In a glove box, triethylsilane (0.3 mmol) with complex

2 (0.2 mmol), C_6Me_6 (2 mg, internal standard) were dissolved in 0.5 mL $CDCl_3$ in J-Young tube. This tube was taken out and was monitored by the ^1H NMR, The rate was measured by integration of the product ^1H peak at δ 5.81 (=CHSi), and was normalized against the internal standard peak. The k_{obs} was estimated from the first order plot of [product] vs. reaction time. Under similar conditions, we monitored the rate change by adding PCy_3 and by adding styrene. We found that this reaction shows the strong phosphine inhibition (Figure 40).
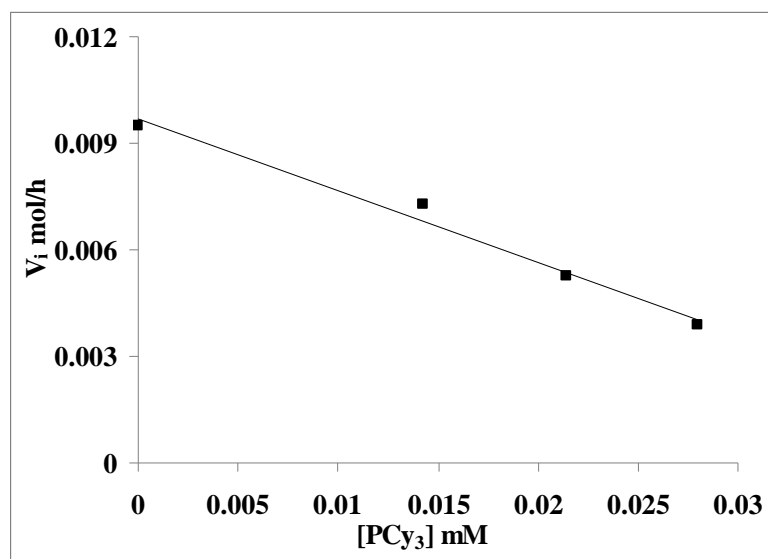
Figure 40. The Plot of the Reaction Rate vs the Concentration of PCy_3

The k_{obs} of this reaction of triethylsilane with ruthenium vinyl complex is 0.0095mol/h. By adding 0.005 mmol PCy_3 the reaction gives a k_{obs} 0.007 mmol/h. These

results are consistent with the catalytic reactions which were observed the strong

phosphine inhibition.

Meanwhile, we observed that the reaction can be promoted by adding styrene. By

adding the styrene, k_{obs} of the reaction are 0.016 mmol/h (0.01 mmol styrene), 0.016

mmol/h (0.035 mmol styrene) 0.016 mmol/h (0.046 mmol styrene) (Figure 41).
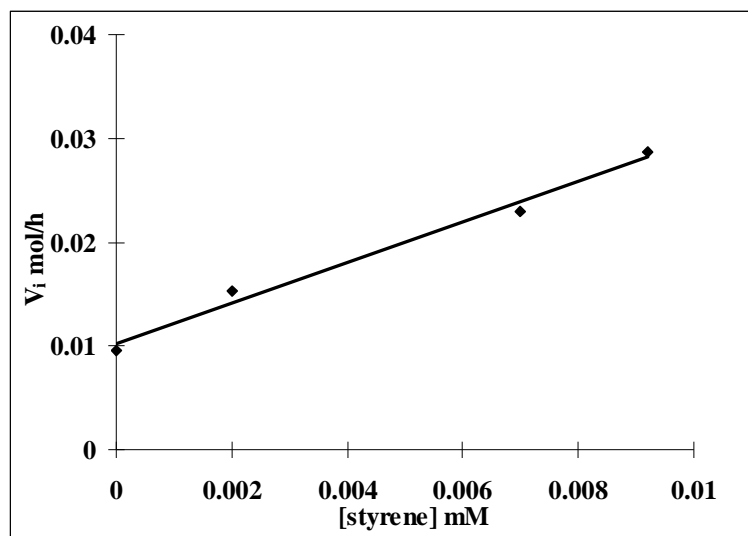
Figure 41. The Plot of Reaction Rate vs the Concentration of Styrene

So these indicated that the formation of intermediate **72c** (Eq 77) through the

intermediate **72b** requires phosphine dissociation and styrene addition, as styrene can be

coordinated to the ruthenium center and promote the dissociation of PCy_3. Without

styrene, the dissociation of the PCy_3 does not favor. This can explain that the reaction of

complex **2** with treithylsilane needs being heated to 70 $^{\circ}$C to generate the product but a

catalytic reaction can finish just at room temperature.

5.6 Computation Studies on the Hydrosilylation of Alkynes

For the mechanism of the hydrosilylation of alkynes, deuterium labeling study

was carried out and the results indicated that there was no D/H exchange during the

reaction, which means there should not be C-H cleavage of the alkynes during the

reaction. We also detected the formation of ruthenium vinyl complex, which showed

similar activity and selectivity as complex **1** on the hydrosilylation of alkyne. So we

proposed that the catalytic reaction starts at the formation of the ruthenium vinyl complex

by adding alkyne to the ruthenium center. Then with the coordination of silane to the

ruthenium center, the key intermediate ruthenium-silyl complex was generated by the

eliminating styrene. This step was monitored by ^{1}H NMR and ^{31}P NMR, only the

formation of styrene was detected, there was no information on the formation of

ruthenium silyl complex. This may be due to the high reactivity of 14 electron ruthenium

silyl complex. In order to get more details on the selectivity and mechanism of the

hydrosilylation of alkynes, density functional calculations were carried out. All

calculations were carried out with Gaussian 09 program. First of all, all geometries of the

reactants, transition structures and intermediates were fully optimized by B3LYP method.

The 6-31G (d) basis set was used for H, C, O, P, Si and Cl atoms, while the Lanl2dz basis

set and ECP were used for Ru atom. The Ru atom was augmented with f-polarization

functions. The harmonic vibration frequency calculation was performed for each

structure, from which the zero-point energy, thermal energy, entropy and free energy

were derived. In order to minimize computation time, $RuH(PMe_3)_2Cl(CO)$ was chosen to

be the catalyst, with trimethylsilane and phenylacetylene as the reacting silane and

alkyne.

First we considered two mechanism pathways: two phosphine ligand system

(Scheme 32) and one phosphine ligand system (Scheme 33).

In the two phosphine ligands system (Scheme 32), there was no phosphine ligand

dissociation during the reaction, while the one phosphine ligand system with the

dissociation of phosphine ligand. The reaction started at the formation of ruthenium vinyl

complex **71a**, and this step gave $\Delta G = -28.00$ kcal mol^{-1}. Then ruthenium silyl complex

71b was formed with the elimination of styrene by giving negative ΔG. With the alkyne

coordination the ruthenium center, complex **71c** was generated, which was followed by

the migration of silyl group and elimination to give the *cis* or *trans* vinyl silane. But this

mechanism cannot explain the strong phosphine inhibition which was detected by

experiments and indicated that there should be the dissociation of phosphine ligand or

one more phosphine ligand coordinating to the ruthenium center. Due to the steric

hindrance between the ligands, there was no way to build up the ruthenium complex with

three phosphine ligands based on the computational studies.
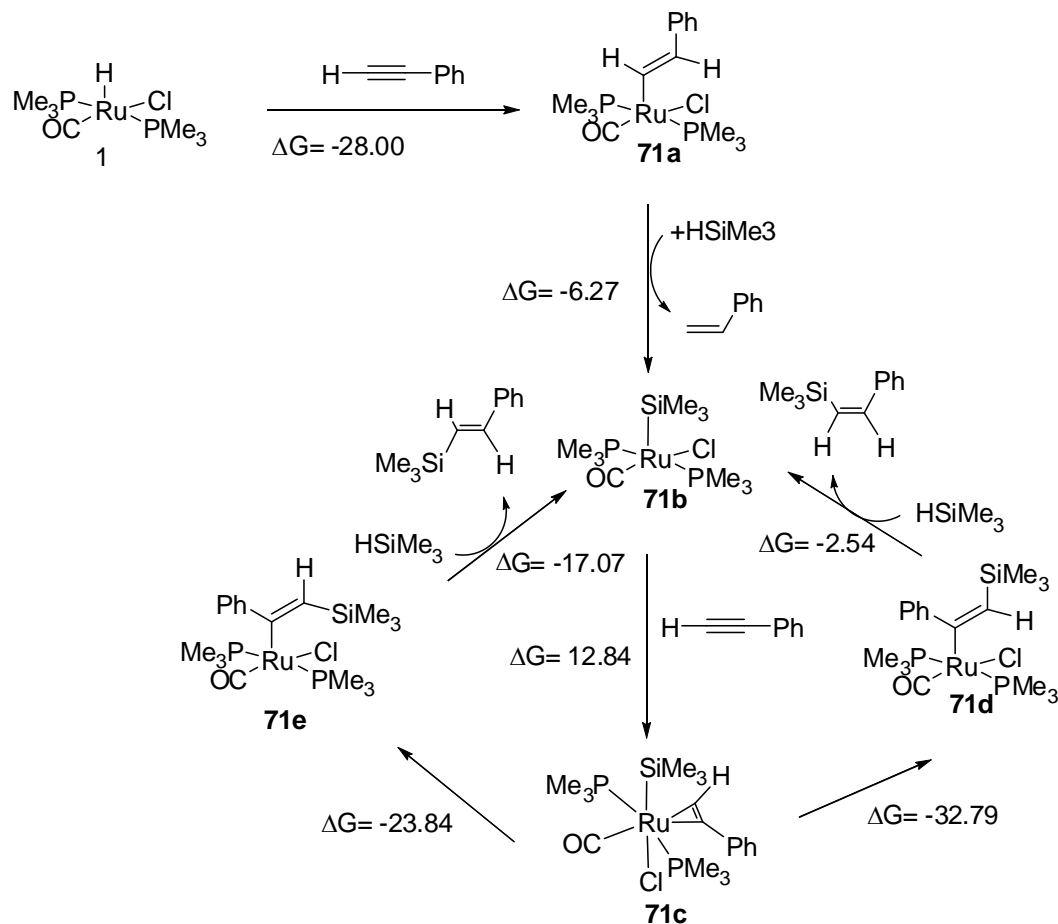
Scheme 32. Proposed Mechanism of the Hydrosilylation of Alkyne with Two Phosphine Ligand

Here we proposed the other mechanism which involves the dissociation of the

phosphine ligand (Scheme 33) and our computational results, with the computed reaction

free energies given in kcal mol^{-1} were shown in Scheme 34.

In this monophosphine catalytic cycle, the first step was the formation of ruthenium vinyl complex **71a** by the addition of alkyne to ruthenium center. This step was done in seconds at room temperature by mixing ruthenium hydride with alkyne. For complex **71a**, the ruthenium center was coordinated by five ligands and there was strong steric hindrance between the ligands. Due to there was no active site left, so complex **71a** was stable and inactive. Complex **71a** was isolated and characterized by ^{1}H NMR and ^{31}P NMR. With the dissociation of one phosphine ligand active complex **71f** was generated, and then trimethylsilane coordinated to ruthenium center to form complex **71g**. Next, the high active 14 electron ruthenium silyl complex **71h** was formed with the elimination of styrene, which was detected by NMR. And then the alkyne coordinated to the ruthenium center to form complex **71i** with the π-bonding between ruthenium and alkyne. Next step was the silyl group migration to the alkyne to form η^2- vinyl complex **71j** or **71l**.

Scheme 33. Proposed Mechanism of the Hydrosilylation of Alkynes with the Dissociation of Phosphine

+CHCPh
ΔG= -28.00
ΔH= −40.43

1

71a

-PMe₃
ΔG= 28.39
ΔH= 41.29

71f

ΔG = -6.32
ΔH = −17.43
+HSiMe₃

-CH₂CHPh
ΔG= -3.36
ΔH= 7.14

71g

Cis-
CHSiMe₃CHPh

71h

Trans-
CHSiMe₃CHPh

ΔG= -11.91
ΔH= 2.78

ΔG= -11.61
ΔH= −24.44

+CHCPh

ΔG= 2.00
ΔH= 13.88

71m

71i

71k

ΔG= -6.01
ΔH= −18.79

+HSiMe₃

ΔG= 1.48
ΔH= 0.766

ΔG= -10.28
ΔH= −9.92

ΔG= -2.6
ΔH= −14.34

+HSiMe₃

71l

71j

Scheme 34. Proposed Mechanism of the Hydrosilylation of Alkyne with the Dissociation of Phosphine

Based on the experimental results, this reaction has high selectivity, when R was less steric group as phenyl, there was only *cis* complex formed, whiles R was bulky group as t-butyl, there was trans product formed. In order to get the details on the selectivity factors, the computational studies were performed. First of all, all the stable intermediate species in Scheme 34 were optimized by B3LYP method by Gaussian 09 and the harmonic vibration frequency calculation was performed for each structure, from which the zero-point energy, thermals energy, entropy and free energy were derived and the ΔG and ΔH of each step was calculated and showed in Scheme 35.

In Scheme 35, which showed the entropy and free energy of all the structure, the entropy and free energy of ruthenium with phenylacetylene were considered as zero. The ruthenium vinyl complex **71a** has low entropy and free energy, and this was constant with the experimental results. And with the dissociation of one phosphine ligand, more active intermediate **71f** formed and the free energy increased to 0.39 kcalmol^{-1}. Based on Scheme 34 and Scheme 35, it was clear that, the first step which gave -28.00 kcalmol^{-1} as the Gibbs free energy was thermal favor while the dissociation of phosphine gave the 28.39 kcalmol^{-1}. Comparing with other steps, the dissociation of phosphine which needs more energy should be the rate-determining step. We tried to look for the transition state for the phosphine dissociation, unfortunately we failed. Here we proposed that the high active intermediate **71h** was the real starting catalyst for the catalytic cycle, with the

alkyne coordinating to the ruthenium center, the intermediate **71i** was more stable and

this step was thermal favor.
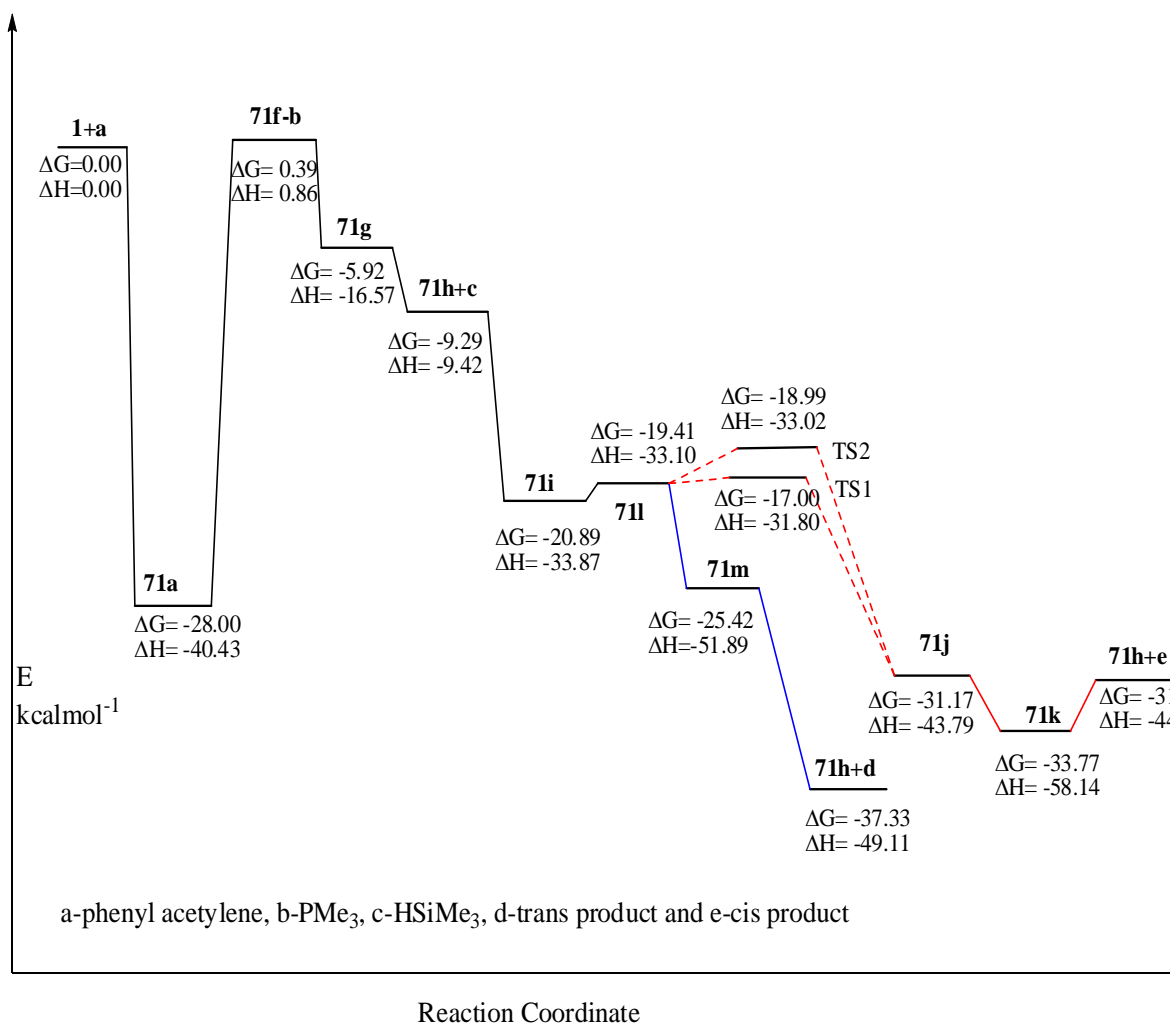
Scheme 35. Calculated Energy of the Reaction Pathway

The silyl group migration was the key step for the formation the selective product.

We proposed two pathways to form the selective product. One is that the silyl group

migration determining the selectivity of the product by directly forming the *cis* η^2-vinyl

species **71j** or *tran* η^2-vinyl species **71l** which was determined by the steric hindrance

between the ligands. We tested this possibility by using phenenylacetylene as alkyne, but

we could not get the *cis* η^2-vinyl by the silyl group migration, what we got was only the

tran η^2-vinyl species **71l**. Based on these computational results, if the silyl group

migration was the selectivity demanding step, there should be only *trans* product

formation without *cis* product. But there was only *cis* product formed as the experimental

results. So the step of the silyl group migration should not be the selectivity determining

step.

Based on these, we proposed the other possibility: intermediate **71i** went through

the silyl group migration to form the *tran* η^2-vinyl species **71l** first and then **71l** went

through the isomerization to form *cis* η^2-vinyl species **71j**. The intermediates **71i** and **71l**,

had close entropy and free energy and the ΔG for the silyl group migration to form the

tran η^2-vinyl species **71l** was only 1.48 kcalmol^{-1}. The free energy of *tran* η^2-vinyl

species **71l** was higher than the *cis* η^2-vinyl species 71j by 11.78 kcalmol^{-1} and the

isomerization from *trans* η^2-vinyl species **71l** to *cis* η^2-vinyl species **71j** step gave -11.78

kcalmol^{-1} and was thermal favored. After the isomerization, the trimethylsilane

coordinates to the ruthenium center by forming the hydrogen bridge bond to form more

stable species which had -33.77 kcalmol^{-1} as free energy. Finally, the *cis* product was

generated by the elimination with 2.00 kcalmol^{-1} as free energy, and the catalyst came

back to the 14 electron high active ruthenium silyl intermediate **71h**. Although the cis

product was only detected, the pathway to form the *trans* vinylsilane product was also

calculated and the results were summarized in Scheme 35 (in blue). The Gibbs free

energy for the formation of **71m** from *trans* η^2-vinyl species **71l** was -25.42 kcalmol^{-1},

comparing with the Gibbs free engery for the isomerization, it was higher by 5.75

kcalmol^{-1}. So after the formation of *tran* η^2-vinyl species **71l**, it was favorite to go

through the isomerization to generate the *cis* product. These computational results were

constant with our experimental results and can explain that in phenyl acetylene case,

there was only *cis* product formed.

One of the importances of this catalytic pathway is that how the isomerization

happened. In order to get more details, more computational work was done on looking for

the transition state of the isomerization. Firstly, we considered the phenylacetylene as the

alkyne. We monitored the rotation of silyl group and vinyl proton and we found that the

rotation of vinyl proton related to the isomerization. The transition state between complex

71l and complex **71j** (Scheme 36) was detected by scanning the dihedral angle.
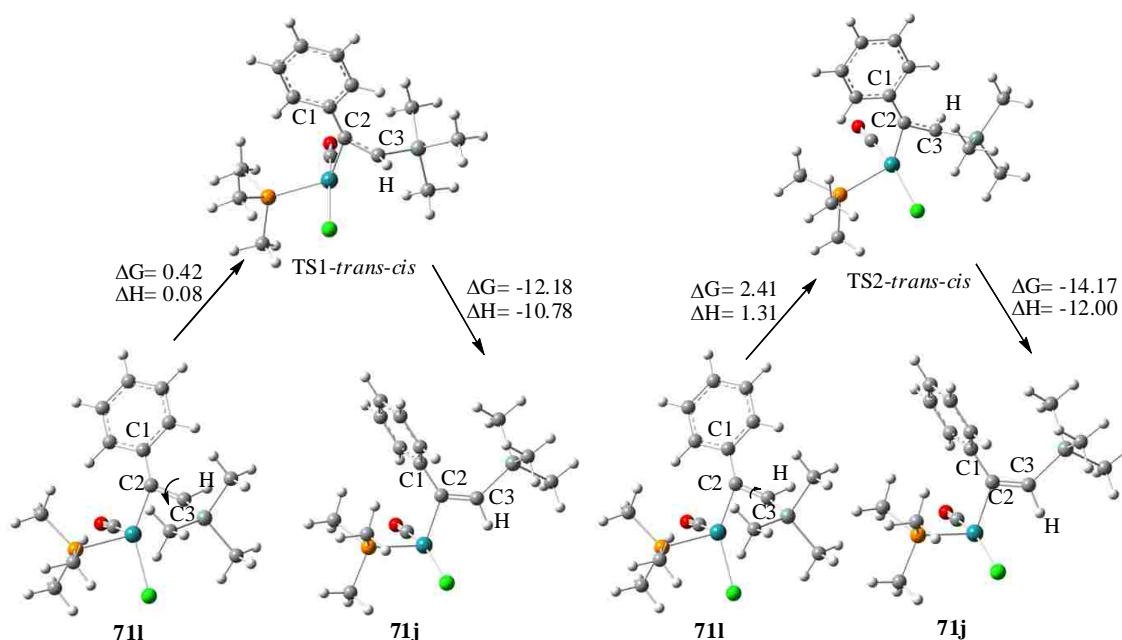
Scheme 36. Model I for the Isomerization of the Hydrosilylation of Phenylacetylene

In this model, the transition state (TS1) was figured out by scanning the

anti-clockwise rotation of the dihedral angle of C1, C2, C3 and H. Here we considered

the free energy and entropy of the *cis* complex **71j** as 0.00 kcalmol^{-1}, so the trans

complex **71l** gave ΔG = 11.76 kcalmol^{-1} while the transition state (TS1) gave 12.18

kcalmol^{-1} in Figure 43 which indicated the formation of *cis* complex was thermal favor.

In the Scheme 36, the *trans* complex **71l** went through the rotation to reach the transition

state (TS1) by giving a smooth energy barrier as 0.42 kcalmol^{-1}, but there was -12.18

kcalmol^{-1} between the transition state and the *cis* complex **71j**. So based on these

computational results, it was clear that the isomerization from *tran* η^2-vinyl species **71l** to

cis η^2-vinyl species **71j** was thermal and dynamic favorite.
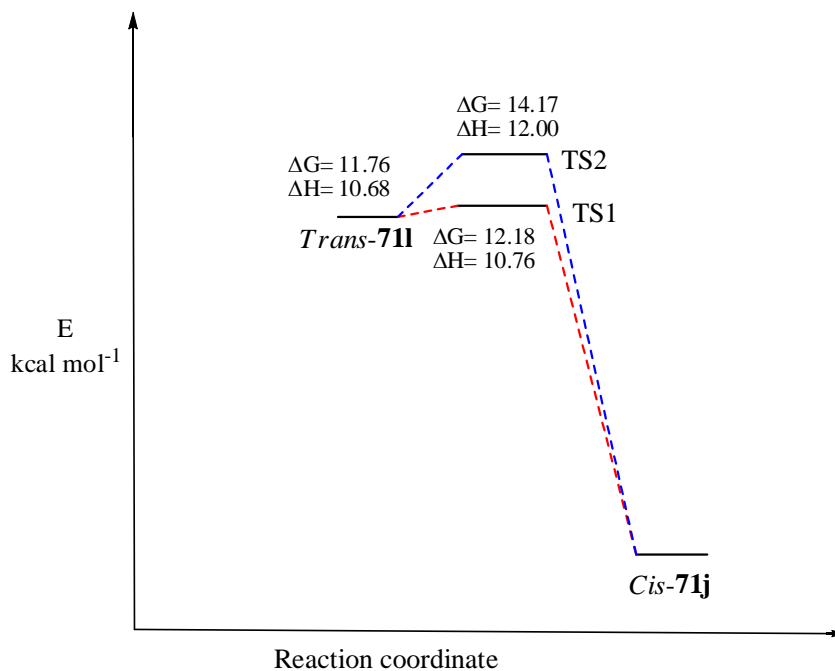
Figure 42. The Energy of intermediate **71l**, **71j** and Transition State 1 and Transition State 2

On the other hand, the clockwise rotation of dihedral angle was considered which

gave transition state (TS2) with higher energy comparing with transition state 1 (TS1). In

Figure 42 (in blue), the transition state had free energy as 14.17 kcalmol^{-1} which was

higher than TS1 by 2.0 kcalmol^{-1}. The Scheme 36 demonstrated that activation energy of

the isomerization, in the transition state 2, *tran* η^2-vinyl species **71l** need to go through an

energy barrier as 2.41 kcalmol^{-1} to reach the transition state and activation energy for the

transition state to the *cis* η^2-vinyl species **71j**. These results indicated that the

isomerization going through the transition state 2 was thermal and dynamic favorite.

Comparing with transition state 1, *tran* η^2-vinyl species **71l** need around 2 kcalmol^{-1} more

than in Scheme 36 to reach the transition state. Although the model of transition state 2

can indicated that the isomerization was thermal and dynamic favorite, it required higher

energy barrier to reach the transition state comparing with the model of transition state 1.

So we chose the model of transition state 1 as the isomerization transition state.

Comparing with phenylacetylene, 3,3-dimethylbutyne gave only the *trans*

vinylsilane when reacting with trimethylsilane, we also did the computational studies on

finding the transition state of the isomerization. The same scan method was used to get

the crude transition state structure and then the structure was optimized to get the

transition state structure.

The model II in Scheme 37 demonstrated the two transition states of the

isomerization for 3,3-dimethylbutyne, the transition state (TS3) was figured out by

scanning the anti-clockwise rotation of the dihedral angle of C1, C2, C3 and H. Here we

considered the free energy and entropy of the *cis* η^2-vinyl species as 0.00 kcalmol^{-1}, so

the *trans* η^2-vinyl species gave free energy $\Delta G = 5.42$ kcalmol^{-1} while the transition state

(TS3) gave 13.33 kcalmol^{-1} in Figure 43.
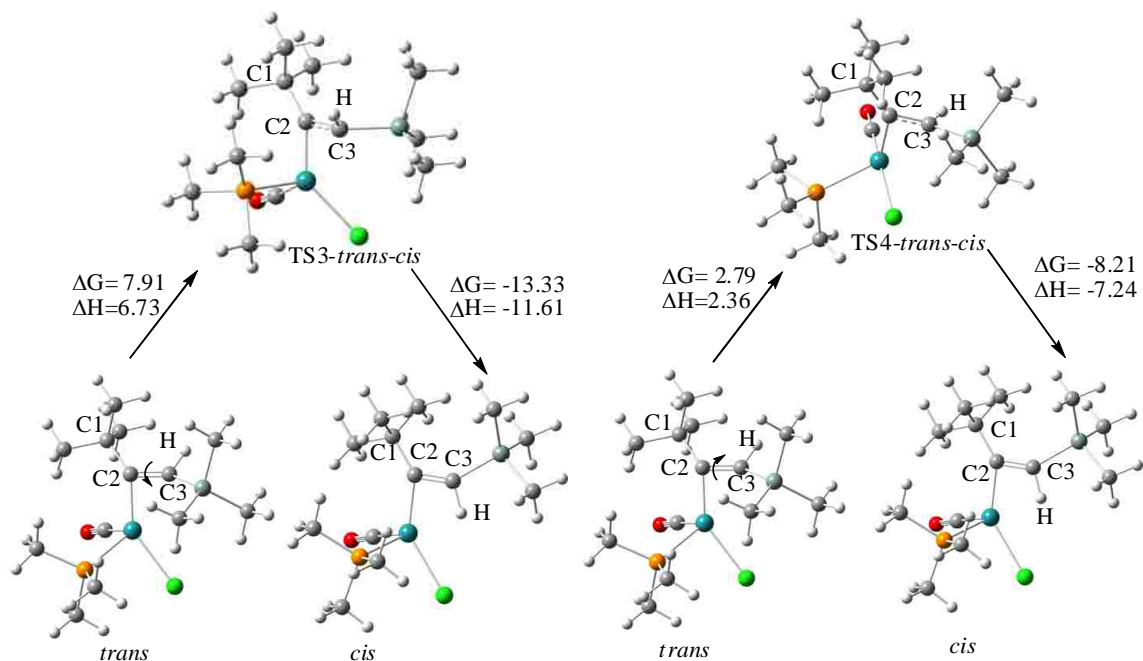
Scheme 37. Model II for the Isomerization

One the other hand, the clockwise rotation of dihedral angle (C1, C2, C3 and H) was considered which gave transition state (TS4) with lower energy comparing with transition state 3 (TS3). In Figure 44 (in red), the transition state had free energy as 8.21 kcalmol[-1] which was higher than TS3 by 5.21 kcalmol[-1]. The Scheme 37 demonstrated that activation energy of the isomerization, *tran* η^2-vinyl species need to go through a energy barrier as 2.79 kcalmol[-1] to reach the transition state and activation energy for the transition state to the *cis* η^2-vinyl species was -13.33 kcalmol[-1], which indicated that the step to form the *cis* η^2-vinyl species from transition state 4 was thermal favorite. Due to

the lower energy barrier comparing with TS3, TS4 was considered as the transition state

of the isomerization from *trans* η^2-vinyl species *cis* η^2-vinyl species.
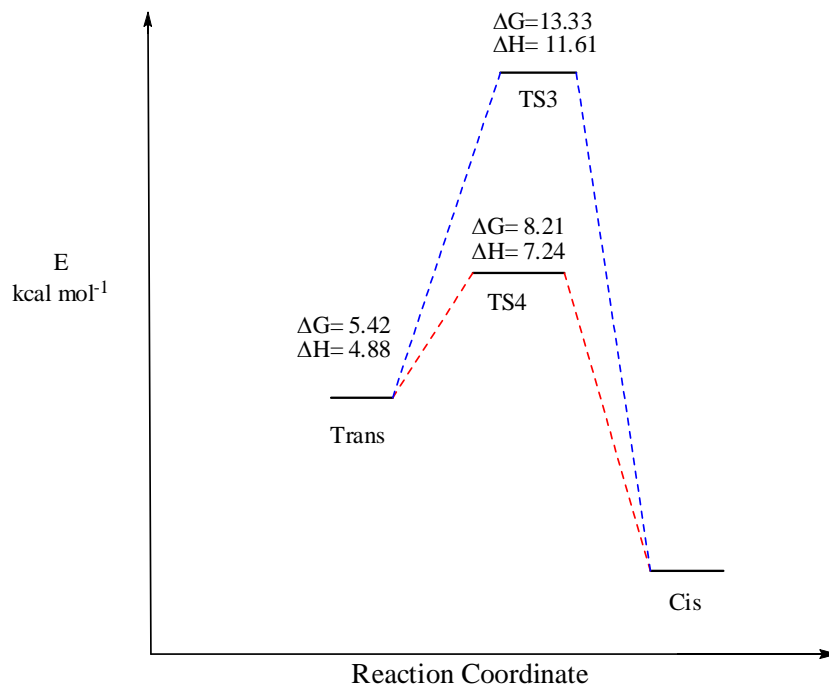
Figure 43. The Energy of *cis* and *trans* Intermediate and Transition State 1 and
Transition State 2 for 3,3-Dimethylbutyne

For 3, 3-dimethyl butyne, there was only *trans* product detected by the

experiment. There was 2.79 kcalmol^{-1} energy barrier for the isomerization, although it is

not significant, comparing to the phenyl acetylene case with 0.42 kcalmol^{-1} energy

barrier, it still can explain the isomerization is less favor in 3,3-dimethylbutyne case, and

the reaction attends to form to *trans* product. One more important thing is that all the

computation calculation was done in gas phase while the experiment was done in solvent,

which would case the difference between the experimental results and computational

results. On the other hand, for the computation calculation, we used PMe$_3$ as the

phosphine ligand in order to save computation time, and can also case the difference. So

we can see that the computation results can match the experimental results.

5.7 Proposed Mechanism of the Hydrosilylation of Alkenes

Here, we propose a mechanism for the coupling reaction of alkenes and

triethylsilane (Scheme 38). This catalytic cycle starts at the coordination of styrene to the

ruthenium center. Then, the alkenes add to the metal center to form complex **72a**. This

addition of alkene to the ruthenium center should be rapid and reversible. We tried to

detect the formation of complex **72a** by VT NMR from -40 $^{\mathrm{o}}$C to 60 $^{\mathrm{o}}$C. Unfortunately,

we did not detect any signal of complex **72a**. But when we treated the ruthenium hydride

complex with excess amount ethylene, we detected a new phosphine peak (26.5 ppm),

which was assigned to the ruthenium-ethyl complex. This ruthenium–ethyl complex was

active for the reaction of alkene and triethylsilane to generate the *trans* vinylsilane

product. Next, another equiv. styrene was added to ruthenium center by eliminating one

equiv. ethylbenzene to form the ruthenium vinyl complex and this step should be rapid.

We syntheses this ruthenium vinyl complex **72b** by using phenylacetylene with

ruthenium hydride complex, this complex **72b** showed a similar activity as the ruthenium

hydride (**1**) on the coupling reaction of styrene and triethylsilane to generate the

trans-vinylsilane product under the similar conditions. In order to get insight into the

mechanism of this step, we treated the complex **72b** and styrene as 1:3 ratios, and

monitored the mixture by VT NMR from -40 °C to 60 °C. However, we observed no

reaction between them. On the other hand, when complex **72b** is treated with excess

amount of triethylsilane, a slow formation of *trans* vinylsilane was detected at 70 °C.

These results are consistent with the carbon isotope effect study which indicated that the

formation of the Si-C bond is the rate-determining step.
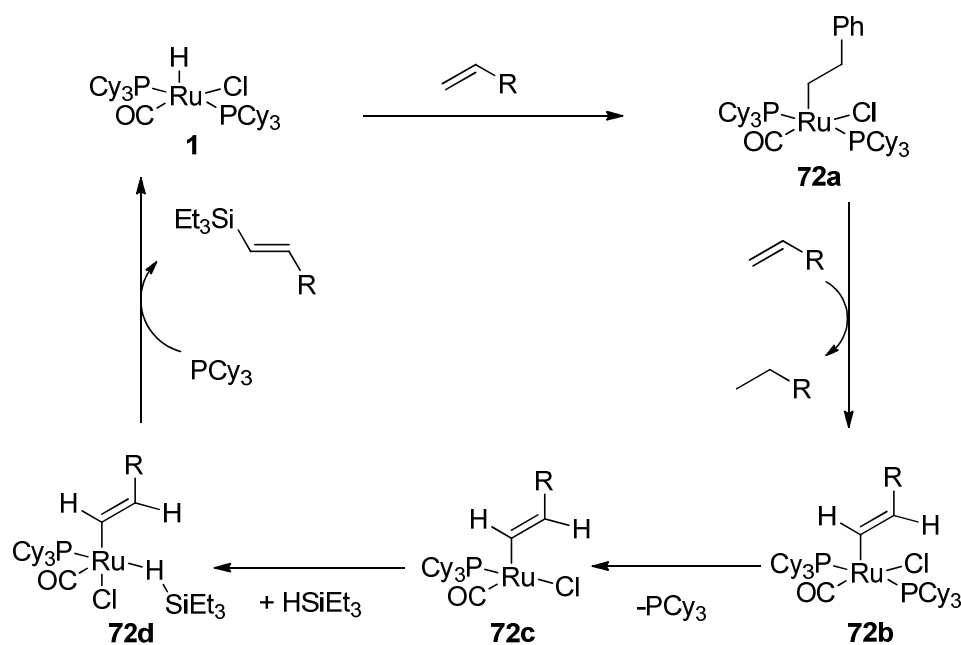
Scheme 38. Proposed Mechanism of the Coupling Reaction of Alkene and Triethylsilane

We also detected the strong phosphine inhibition on the reaction of intermediate **72b** with triethylsialne, which indicated that the formation of the intermediate **72d** involved the phosphine dissociation. Then, with the migration of silyl to the alkene, the *trans* vinylsilane product was generates and the ruthenium complex comes back to complex **1**. Recovered ruthenium complex was identified by ^{1}H NMR and ^{31}P NMR spectroscopy, and they are all consistent with that of the ruthenium hydride complex. The step of the migration of silyl group to the alkene to form the Si-C bond which involving the intermediate **72d** should be the rate limiting step. The observation of the carbon isotope effect study on the products provides the strong evidence for this, which showed significant abundance change of ^{13}C of the product. Moreover, the reaction of ruthenium vinyl complex and triethylsilane also supported this step to be rate-determining. Besides, the relatively positive Hammett value from the *para*-substituted styrene also proved this conclusion.

5.8 Conclusions

The ruthenium–hydride complex **1** was found to be a highly effective catalyst for hydrosilylation of the alkynes and alkenes to form selective vinylsilane under mild conditions. The mechanistic studies on the coupling reactions of alkenes with triethylsilane revealed C-Si bond formation as the rate-limiting step. The Hammett study, carbon isotope effect study, and the treatment of the ruthenium vinyl complex with triethylsilane also gave the strong evidence for this conclusion. For the mechanism study on hydrosilylation of alkyne, the isomerization of η^2-vinyl complex was key point for the selectivity determining by the computation calculation. Other kinetics studies provided important and useful information on the mechanism. Hereby, we believe our catalytic method provides a promising way to generate synthetically useful vinylsilane in a highly selective fashion.

Chapter 6. Experimental Sections

6.1 General Information

All operations were carried out in an inert-atmosphere glove box or by using standard high vacuum and Schlenk techniques. Benzene, tetrahydrofuran were distilled from purple solution of sodium and benzophenone immediately prior to use. Hexane and dichloromethane were distilled from $CaH_2.$ The NMR solvent was dried from the activated molecular sieves (4Å). All the ketones and vinyltrimethylsilane were received from commercial sources and used without further purification. The ^1H, ^2H and ^{13}C NMR spectra were recorded on a Varian Mercury 300 MHz or 400 MHz FT-NMR spectrometer. Mass spectras were recorded from a Hewlett-Packard HP 5970 GC/MS spectrometer. Elemental analyses were performed at the Midwest Microlab, Indianapolis, IN. High-resolution FAB mass spectra were obtained at the center of Mass Spectrometry, Washington University, St, Louis, MO.

6.2 For Chapter 2

6.2.1 Typical Procedure of the Catalytic Reaction

In a glove box, $Ru_3(CO)_{12}$ (0.03 mmol), NH_4PF_6 (0.1 mmol), pyrrole (1.0 mmol) and alkyne (2.0 mmol) were dissolved in 3ml benzene solution in a thick-walls 25 mL Schlenk tube equipped with a magnetic stirring bar. The tube was brought out of the glove box. The reaction tube was heated in an oil bath at 95 ^{o}C for 8-15 hours. The tube was opened to the air at room temperature, and the crude product mixture was analyzed by GC/MS. The solvent was removed under a rotary aspirator, and the organic product was isolated by a column chromatograph on silica gel (n-hexane/dichloromethane).

6.2.2 Hammett Study of the Catalytic Reaction

$Ru_3(CO)_{12}$ (3 μmol), NH_4PF_6 (0.01 mmol), pyrrole (0.1 mmol), 4-ethynylanisole (0.25 mmol) and hexamethylbenzene (26 mg as the internal standard) were dissolved in 0.5 mL benzene-d_6 solution in a Wilmad J-Young NMR tube with a Teflon screw cap. The tube was cooled in liquid nitrogen bath, and degassed for three times. The tube was gradually warmed to the room temperature and was heated in an oil bath at 95 ^{o}C. The reaction was monitored every hour by ^{1}H NMR spectroscopy. The rate was measured by monitor the ^{1}H integration of the product peak (OCH$_3$ δ 3.71 ppm) signal, and these were normalized against the internal standard. The k_{obs} was estimated from a first-order plot of ln[product] vs. reaction time.

6.2.3 Isotope Effect Study

Ru$_3$(CO)$_{12}$ (0.003 mmol), NH$_4$PF$_6$ (0.01 mmol), phenylpyrrole-d_4 (0.1 mmol), 4-ethynylanisole (0.25 mmol) and hexamethylbenzene (26 mg as the internal standard) were dissolved in 0.5 mL benzene-d_6 solution in a Wilmad J-Young NMR tube with a Teflon screw cap. The tube was cooled in the liquid nitrogen bath, and degased for three times. The tube was gradually warmed to room temperature and was heated in an oil bath at 95 ^{o}C. The reaction was monitored every hour by NMR. The rate was measured by monitor the ^{1}H integration of the product peak (OCH_3 δ 3.71 ppm) signal, and these were normalized against the internal standard. The k_{obs} was estimated from a first -order plot of ln[product] vs reaction time.

6.2.4 Preparation of the Phenylpyrrole-d_4

Phenylpyrrole-d_4 was prepared form the following procedure: 1.0 mmol phenylpyrrole was dissolved in 25 mL dry THF in the Schlenk flask, n-BuLi (2 mmol, 2.5 M in hexane) was added in this solution under nitrogen gas in the acetone-dry ice bath, and then the mixtures were warmed to room temperature and kept stirring for 30 min. Then, the excess amount of D$_2$O was added in to the solution in the acetone-dry ice

bath, and this solution was stirred by the magnetic stirring bar for 3 hours at room

temperature until the solution became clear. The reaction was quenched by adding water.

The organic layer was extract from ether, and the water solution was washed for three

times by ether. The organic product was isolated by a column chromatograph on silica

gel (hexane/dichloromethane), and was characterized by ^{1}H NMR spectroscopy and ^{2}H

NMR spectroscopy.

6.2.4.1 Deuterium Labeling Study

In a glove box, $Ru_3(CO)_{12}$ (22 mg, 0.030 mmol), NH_4PF_6 (16 mg, 0.10 mmol),

pyrrole (1.0 mmol) and DC≡CPh (2.5 mmol, 2.5 equiv.) were dissolved in 3.0 mL

benzene solution in a 25 mL Schlenk tube equipped with a magnetic stirring bar. The

tube was brought out of the glove box, and was stirred in an oil bath set at 95 °C for 8-15

h. The tube was cooled to room temperature, and the crude product mixture was analyzed

by GC-MS. The solvent was removed under a rotary aspirator, and analytically pure

organic product was isolated by a column chromatograph on silica gel

(n-hexanes/CH_2Cl_2). The ^{1}H and ^{2}H NMR was taken at room temperature.

6.2.4.2 Carbon Isotope Effect Study

In a glove box, $Ru_3(CO)_{12}$ (0.03 mmol), NH_4PF_6 (0.1 mmol), phenylpyrrole (1.0 mmol) and 4-ethynylanisole (2.5 mmol) were dissolved in 3 mL benzene solution in a thick-wall 25 mL Schlenk tube equipped with a magnetic stirring bar. The tube was brought out of the glove box. The reaction tube was heated in an oil bath at 95 ^{o}C for 15 hours. The tube was opened to the air at room temperature, and the crude product mixture was analyzed by GC/MS and the conversion was 75%. The solvent was removed under a rotary aspirator, and the unreacted phenylpyrrole was isolated by a column chromatograph on silica gel (*n*-hexane/dichloromethane).

The ^{13}C NMR analysis of the recovered and virgin samples of N-phenylpyrrole was performed by following Singleton's ^{13}C NMR method. The NMR sample of virgin and recovered N-phenylpyrrole was prepared identically by N-phenylpyrrole (75 mg) in $CDCl_3$ (0.5 mL) in a 5 mm high precision NMR tube. The ^{13}C{^{1}H} NMR spectra were recorded with H-decoupling and 45 degree pulses. A 60 s delay between pulses was imposed to minimize T_1 variations (d_1 = 60 s, at = 5.0 s, np = 245098, nt = 2400).

C#	Virgin	Recovered (75% conv.)	Recovered/Virgin	Change (%)
1	0.998(5)	1.017(5)	1.019(5)	1.90(5)
2	1.020(3)	1.025(3)	1.005(3)	0.49(3)
3	1.009(4)	1.008(4)	0.999(4)	0.11(4)
4(ref)	1.000	1.000	1.000	0.00
5	0.469(3)	0.468(3)	0.998(3)	0.22(3)
C#	Virgin	Recovered (70% conv.)	Recovered/Virgin	Change (%)
1	0.998(5)	1.011(5)	1.013(5)	1.30(5)
2	1.020(3)	1.025(3)	1.005(3)	0.47(3)
3	1.009(4)	1.007(4)	0.998(4)	0.19(4)
4(ref)	1.000	1.000	1.000	0.00
5	0.469(3)	0.468(3)	0.998(3)	0.24(3)

6.3 Characterization Data of Selected Organic Products

For **53a**: ^{1}H NMR (400 MHz, acetone-d_6) δ 7.25 and 6.92 (m, 4H,), 6.70 (m, 1H), 6.05 (m, 2H), 5.46 and 5.15 (d, $J = 1.6$ Hz, 2H), 3.81 (s, 3H), 3.30 (s, 3H); ^{13}C{^{1}H} NMR (75 MHz, acetone-d_6) δ 160.5, 142.4, 134.6, 134.4, 129.1, 114.8, 124.4, 113.8, 110.9, 107.9, 55.4, 35.1 (CH$_3$); HREI (m/z): Calcd for $C_{14}H_{15}NO$ (M)$^+$ 213.1154. Found 213.1144.

For **53b**: ^{1}H NMR (400 MHz, acetone-d_6) δ 7.70- 7.15 (m, 6H), 6.80 (m, 1H), 6.30 (m, 2H), 5.65 and 5.33 (d, J = 1.6 Hz, 2H), 3.39 (s, 3H), 3.13 (s, 3H); ^{13}C{^{1}H} NMR (75 MHz, acetone-d_6) δ 159.5, 143.1, 137.7, 135.9, 134.9, 131.0, 130.2, 128.2, 127.2, 125.0, 120.4, 115.8, 111.5, 108.4, 107.0, 56.1, 35.6; GC-MS m/z = 263 (M$^+$); Anal. Calcd for $C_{18}H_{17}NO$: C, 82.10; H, 6.51. Found C, 81.98; H, 6.59.

For **53c**: ^{1}H NMR (400 MHz, acetone-d_6) δ 7.25, 7.15 and 6.73 (m, 9H), 6.98 (m, 1H), 6.26 (m, 2H), 5.34 and 5.03 (d, J = 1.6 Hz, 2H), 3.71 (s, 3H); ^{13}C{^{1}H} NMR (75 MHz, acetone-d_6) δ 160.3, 142.4, 141.6, 134.4, 134.2, 129.7, 129.3, 127.2, 125.6, 124.7.9, 114.2, 114.1, 113.4, 109.6, 55.6; GC-MS m/z = 275 (M$^+$); Anal. Calcd for $C_{19}H_{17}NO$: C, 82.88; H, 6.22. Found C, 82.92; H, 6.27.

For **53d**: ^{1}H NMR (300 MHz, CDCl$_3$) δ 7.25- 6.73 (m, 8H), 6.98 (m, 1H), 6.26 (m, 2H), 5.21 and 4.90 (d, J = 1.6 Hz, 2H), 3.71 (s, 3H), 2.21 (s, 3H); ^{13}C{^{1}H} NMR (75 MHz, CDCl$_3$) δ 159.3, 140.7, 138.3, 136.2, 133.8, 129.4, 128.7, 125.0, 124.0, 114.2, 113.4, 112.5, 108.5, 55.3, 21.1; GC-MS m/z = 289 (M$^+$); Anal. Calcd for $C_{20}H_{19}NO$: C, 83.01; H, 6.62. Found C, 82.92; H, 6.71.

For **53e**: ^{1}H NMR (400 MHz, CDCl$_3$) δ 7.15-6.73 (m, 8H), 6.91 (m, 1H), 6.22 (m, 2H), 5.31 and 4.98 (d, J = 1.6 Hz, 2H), 3.73 (s, 3H), 3.72 (s, 3H); ^{13}C{^{1}H} NMR (75 MHz, acetone-d_6) δ 160.3, 159.1, 142.1, 134.7, 134.4, 134.3, 129.4, 127.0, 124.8, 114.7, 114.1, 114.0, 112.8, 109.1, 55.7, 55.5; HREI (m/z): Calcd for $C_{14}H_{15}NO$ (M) $^+$ 305.1416, found 305.1408.

For **53f**: ^{1}H NMR (300 MHz, CDCl$_3$) δ 7.25-6.73 (m, 8H), 6.98 (m, 1H), 6.26 (m, 2H), 5.41 and 5.18 (d, 2H, J = 1.6Hz), 3.71 (s, 3H); ^{13}C {^{1}H} NMR (75 MHz, CDCl$_3$) δ 159.3, 140.7, 139.3, 134.0, 133.4, 132.0, 129.0, 128.6, 123.8, 114.6, 113.5, 113.0, 109.2, 55.3; GC-MS m/z = 309 (M$^+$); Anal. Calcd for C$_{19}$H$_{16}$ClNO: C, 73.66; H, 5.21. Found C, 72.68; H, 5.15.

For **53g**: ^{1}H NMR (300 MHz, CDCl$_3$) δ 7.25 - 6.73 (m, 8H), 6.98 (m, 1H), 6.43 (m, 2H), 5.43 and 5.18(d, 2H, J = 1.6Hz), 3.78 (s, 3H); ^{13}C {^{1}H} NMR (75 MHz, CDCl$_3$) δ 162.2, 159.8, 140.7, 136.8, 134.4.0 133.4, 128.5, 126.6, 128.6, 123.8, 115.6, 114.6, 113.5, 112.6, 108.9, 55.3; GC-MS m/z = 293 (M$^+$).

For **53h**: ^{1}H NMR (400 MHz, CDCl$_3$) δ 7.70-7.15 (m, 11H), 6.98 (m, 1H), 6.30 (m, 2H,), 5.48 and 5.28 (d, 2H, J = 1.6Hz), 3.89 (s, 3H); ^{13}C {^{1}H} NMR (75 MHz, CDCl$_3$) δ 157.9, 141.3, 140.8, 136.4, 134.2, 134.0, 129.9, 128.9, 127.8, 126.7, 126.6, 126.2, 125.3, 124.2, 119.0, 115.7, 112.9, 108.9, 105.7, 56.1; GC-MS m/z = 325 (M$^+$); Anal. Calcd for C$_{23}$H$_{19}$NO: C, 84.89; H, 5.89. Found C, 85.09; H, 6.05.

For **53i**: ^{1}H NMR (400 MHz, CDCl$_3$) δ 7.70-7.15, 6.78 (m, 10H), 6.98 (m, 1H), 6.26 (m, 2H), 5.51 and 5.15 (d, 2H, J = 1.6Hz), 3.89 (s, 3H), 3.66 (s, 3H); ^{13}C {^{1}H} NMR (75 MHz, CDCl$_3$) δ 159.4, 159.3, 143.0, 137.4, 135.6, 134.8, 130.9 129.9, 127.7, 127.5, 127.4, 127.0, 125.3, 120.0, 115.9, 115.1, 113.4, 109.7, 106.9, 56.1; GC-MS m/z = 355 (M$^+$); Anal. Calcd for C$_{24}$H$_{21}$NO$_2$: C, 81.10; H, 5.96. Found C, 80.88; H, 6.02.

For **53j**: ^{1}H NMR (300 MHz, CDCl$_3$) δ 7.40-7.28 (m, 4H), 6.77 (m, 1H), 6.23-6.21 (m, 2H), 5.62 and 5.41 (d, 2H, J = 1.6Hz), 3.82 (t, 2H, J = 7.0Hz), 2.43 (t, 2H, J = 7.0Hz); ^{13}C{^{1}H} NMR (75 MHz, CDCl$_3$) δ 141.9, 141.3, 133.5, 129.2, 128.6,127.6, 123.3, 118.0, 116.7, 111.7, 108.7, 43.5, 19.9; GC-MS m/z = 222 (M$^+$); Anal. Calcd for C$_{15}$H$_{14}$N$_2$: C, 81.05; H, 6.35. Found C, 81.25; H, 6.30.

For **53k**: ^{1}H NMR (400 MHz, acetone-d_6) δ 7.24 -7.18 (m, 4H), 6.91 (m, 1H), 6.15 (m, 2H), 5.62 and 5.40 (d, 2H, J = 1.6Hz), 3.91 (t, 2H, J = 7.0 Hz), 2.64 (t, 3H, J = 7.0Hz), 2.34 (s, 3H); ^{13}C{^{1}H} NMR (75 MHz, acetone-d_6) δ 141.9, 138.8, 138.7, 133.9, 130.1, 127.7, 123.3, 118.3, 116.1, 111.7, 108.7, 43.5, 21.2, 19.9; GC-MS m/z = 236 (M$^+$); Anal. Calcd for C$_{16}$H$_{16}$N$_2$: C, 81.32; H, 6.82. Found C, 81.47; H, 7.02.

For **53l**: ^{1}H NMR (400 MHz, acetone-d_6) δ 7.25 - 6.92 (m, 4H), 6.92 (m, 1H), 6.15 (m, 2H), 5.56 and 5.26 (d, 2H, J = 1.6 Hz), 3.91 (t, 2H, J = 7.0Hz), 3.81 (s, 3H), 2.64 (t, 2H, J = 7.0Hz,); ^{13}C{^{1}H} NMR (75 MHz, acetone-d_6) δ 160.3, 141.1, 133.5, 133.4, 128.4, 114.3, 123.0, 117.8, 114.3, 111.2, 108.3, 55.4, 43.5, 19.9; GC-MS m/z = 252 (M$^+$); Anal. Calcd for C$_{16}$H$_{16}$N$_2$: C, 76.16; H, 6.39. Found C, 75.73; H, 6.45.

For **53m**: ^{1}H NMR (300 MHz, CDCl$_3$) δ 7.25- 6.64 (m, 4H), 6.67 (m, 1H), 6.23 (m, 2H), 5.45 and 5.21 (d, 2H, J = 1.6Hz), 3.88 (t, 2H, J = 7.0Hz), 2.99 (s, 6H), 2.46 (t, 2H, J = 7.0Hz); ^{13}C {^{1}H} NMR (75 MHz, CDCl$_3$) δ 150.7, 140.6, 133.8, 128.1, 127.9, 112.3, 122.2, 117.5, 113.7, 111.4, 108.6, 43.2, 40.6, 19.9; GC-MS m/z = 265 (M$^+$).

For **53n**: ^{1}H NMR (300 MHz, CDCl$_3$) δ 7.70 - 7.15 (m, 6H), 6.80 (m, 1H), 6.30 (m, 2H), 5.72 and 5.45 (d, 2H, J = 1.6Hz), 3.93 (s, 3H), 3.84 (t, 2H, J = 7.0Hz), 2.46 (t, 2H, J = 7.0Hz); ^{13}C {^{1}H} NMR (75 MHz, CDCl$_3$) δ 159.2, 142.1, 136.7, 135.6, 134.0, 130.7, 128.1, 126.7, 126.2, 120.1,116.7, 123.5, 118.3, 111.9, 109.0, 106.6, 55.7, 43.8, 20.2; GC-MS m/z = 302 (M$^+$); Anal. Calcd for C$_{20}$H$_{18}$N$_2$O: C, 79.43; H, 6.00. Found C, 78.93; H, 5.99.

For **53o**: ^{1}H NMR (400 MHz, CDCl$_3$) δ 7.25 (m, 6H), 6.60 (d, 2H, J = 2.03Hz), 6.00 and 5.36 (d, 2H, J = 1.6 Hz), 3.22 (s, 3H), 2.36 (s, 3H); ^{13}C {^{1}H} NMR (75 MHz, CDCl$_3$) δ 193.2, 140.3, 139.8, 135.5, 128.6 128.4, 128.2, 126.8, 124.8, 117.5, 110.4, 43.9, 35.6, 27.0, 21.1; GC-MS m/z = 225 (M$^+$); Anal. Calcd for C$_{15}$H$_{15}$NO: C, 79.97; H, 6.71. Found C, 79.89; H, 6.48.

For **53p**: ^{1}H NMR (300 MHz, CDCl$_3$) δ 7.80 (s, 1H), 7.61- 6.85 (m, 8H), 5.62 and 5.42 (d, J = 1.6 Hz), 3.86 (s, 3H), 2.26 (s, 3H); ^{13}C{^{1}H} NMR (75 MHz, CDCl$_3$) δ 160.0, 141.1, 135.5, 134.2, 133.0, 129.8, 129.4, 122.6, 119.6, 119.2, 115.1, 114.1, 110.9, 110.8, 55.6, 10.1; GC-MS m/z = 288 (M$^+$); Anal. Calcd for C$_{18}$H$_{17}$NO: C, 82.09; H, 6.50. Found C, 81.99; H, 6.42.

For **53q**: ^{1}H NMR (300 MHz, CDCl$_3$) δ 7.80 (s, 1H), 7.65 - 7.05 (m, 10H), 5.67 and 5.42 (d, J = 1.6 Hz), 3.86 (s, 3H), 2.26 (s, 3H); ^{13}C{^{1}H} NMR (75 MHz, CDCl$_3$) δ 160.0, 141.1, 137.4, 135.5, 134.2, 133.0, 130.9, 129.8, 129.4, 127.7, 127.5, 127.4, 127.0,

122.6, 119.6, 119.2, 115.1, 114.1, 110.9, 110.8, 55.6, 10.1; GC-MS m/z = 313 (M$^+$);

Anal. Calcd for $C_{22}H_{19}NO$: C, 84.31; H, 6.11. Found C, 84.49; H, 6.14.

For **53r**: ^{1}H NMR (400 MHz, CDCl$_3$) δ 7.46-6.95 (m, 12H), 6.53 (s, 1H), 3.70 (s, 6H), 2.40 (s, 6H); ^{13}C{^{1}H} NMR (75 MHz, CDCl$_3$) δ 145.4, 138.0, 135.1, 128.4, 128.0, 127.1, 123.6, 122.5, 118.6, 109.5, 43.9, 32.9, 29.4, 21.1; GC-MS m/z = 378 (M$^+$); Anal. Calcd for $C_{18}H_{17}N$: C, 85.67; H, 6.92. Found C, 85.69; H, 6.82.

For **53s**: ^{1}H NMR (300 MHz, CDCl$_3$) δ 7.46 and 6.95 (m, 13H), 6.53 (s, 2H), 3.70 (s, 3H), 2.40 (s, 3H); ^{13}C{^{1}H} NMR (75 MHz, CDCl$_3$) δ 148.6, 138.0, 128.4, 128.0, 127.1, 126.0, 123.6, 122.5, 121.3, 118.6, 109.5, 43.9, 32.9, 29.4; GC-MS m/z = 363 (M$^+$).
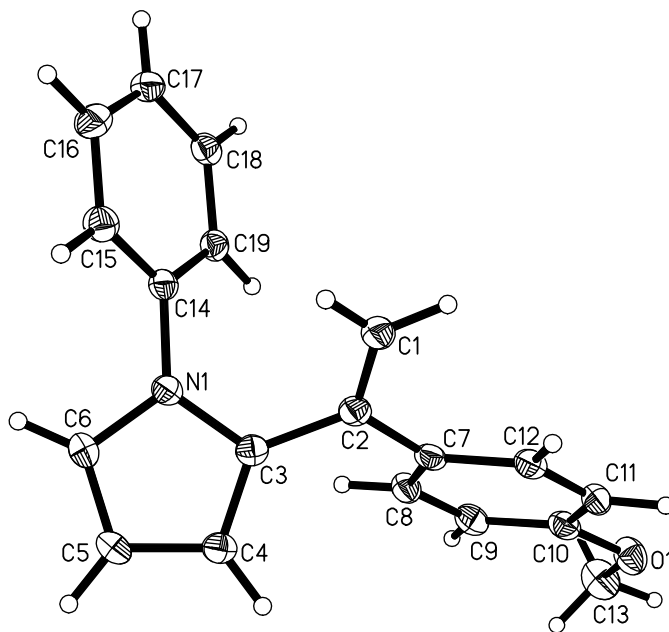
Molecular Structure of **53**

Crystal Data and Structure Refinement for **53c**.

Identification code	yis	
Empirical formula	$C_{19}H_{17}NO$	
Formula weight	275.34	
Temperature	100(2) K	
Wavelength	1.54178 Å	
Crystal system	Monoclinic	
Space group	P21/c	
Unit cell dimensions	a = 19.3228(3) Å	= 90°.
	b = 17.3708(2) Å	= 96.4510(10)°.
	c = 8.83840(10) Å	= 90°.
Volume	2947.85(7) Å3	
Z	8	
Density (calculated)	1.241 Mg/m3	
Absorption coefficient	0.596 mm-1	
F(000)	1168	
Crystal size	0.50 x 0.40 x 0.20 mm3	
Theta range for data collection	3.43 to 67.84°.	
Index ranges	-23<=h<=23, 0<=k<=20, 0<=l<=10	
Reflections collected	24399	
Independent reflections	5215 [R(int) = 0.0186]	
Completeness to theta = 67.84°	97.20%	
Absorption correction	Semi-empirical from equivalents	
Max. and min. transmission	0.8901 and 0.7548	
Refinement method	Full-matrix least-squares on F2	
Data / restraints / parameters	5215 / 0 / 516	
Goodness-of-fit on F2	0.993	
Final R indices [I>2sigma(I)]	R1 = 0.0310, wR2 = 0.0768	
R indices (all data)	R1 = 0.0335, wR2 = 0.0787	
Extinction coefficient	0.00105(10)	
Largest diff. peak and hole	0.194 and -0.165 e.Å-3	

6.4 For Chapter 3

6.4.1 General Procedure of the Catalytic Reaction

In a glove box, a carboxylic acid (1.0 mmol), a terminal alkyne (2.0 mmol) and the ruthenium catalyst **1** (14 mg, 2 mol %) were dissolved in 3 mL of CH_2Cl_2 (or THF) in a 25 mL Schlenk tube equipped with a Teflon stopcock and a magnetic stirring bar. The reaction tube was brought out of the glove box, and was stirred in an oil bath at 90-95 °C for 10-12 h. The tube was opened to the air at room temperature, and the crude product mixture was analyzed by GC-MS. Analytically pure organic product was isolated by a column chromatography on silica gel (*n*-hexane/EtOAc).

6.4.1.1 Hammett Study

In a glove box, a *para*-substituted acid p-X-$C_6H_4CO_2H$ (X = OMe, CH_3, H, CF_3) (0.20 mmol), phenylacetylene (40 mg, 0.4 mmol), **1** (3 mg, 2 mol %) and C_6Me_6 (2 mg, internal standard) were dissolved in $CDCl_3$ (0.5 mL) solution in a J-Young NMR tube with a Teflon screw cap. The tube was brought out of the glove box and was heated in an oil bath set at 95 °C. The reaction was monitored in 10 min intervals by ^{1}H NMR. The k_{obs} was estimated from a first-order plot of ln[product] vs. reaction time by measuring the ^{1}H integration of the product peak (=CH_2, δ 5.61 ppm), which was normalized against

the internal standard peak. For the THF system, in a glove box, *para*-substituted acid

p-X-C$_6$H$_4$CO$_2$H (X = OMe, CH$_3$, H, CF$_3$) (1.0 mmol), phenylacetylene (200 mg, 2.0

mmol) and **1** (14 mg, 2 mol %) and C$_6$Me$_6$ (26 mg, internal standard) were dissolved in 3

mL of THF solution in a 25 mL Schlenk tube equipped with a Teflon stopcock and a

magnetic stirring bar. The tube was brought out of the glove box, and was heated in an oil

bath at 95 °C. The reaction was monitored by GC in 10 min intervals. The k_{obs} was

estimated from a first-order plot of ln[product] vs. reaction time by measuring the amount

of the products against the internal standard.

6.4.1.2 Isotope Labeling Study

In a glove box, benzoic acid (122 mg, 1.0 mmol) and DC≡CPh (206 mg, 2.0

mmol) were added via a syringe to a 25 mL Schlenk tube equipped with a magnetic

stirring bar and Teflon stopcock. The catalyst **1** (14 mg, 2 mol %) and the solvent (3 mL)

were added to the reaction tube. The reaction tubes were brought out of the box was

stirred in an oil bath at 95 °C for 10 h. The solvent was removed from a rotary

evaporator, and the organic product was isolated by a column chromatography on silica

gel (n-hexanes/CH$_2$Cl$_2$ = 3:2). The deuterium content of the product was measured by

both ^{1}H NMR (CDCl$_3$ with 10 mg cyclohexane as the external standard) and ^{2}H NMR (CH$_2$Cl$_2$ with 50 μL CDCl$_3$).

6.4.1.3 Phosphine Inhibition Study

In a glove box, benzoic acid (0.20 mmol), phenylacetylene (0.40 mmol), **1** (3 mg, 2 mol %) and C$_6$Me$_6$ (2 mg, internal standard) were dissolved in 0.5 mL of CDCl$_3$ solution in a J-Young NMR tube with a Teflon screw cap. A pre-dissolved PCy$_3$ in CDCl$_3$ solution (5 μL, 1.0 *M*) was added via syringe to the tube via the syringe. The tube was brought out of the glove box and was heated in an oil bath at 95 °C. The reaction was monitored by ^{1}H NMR in 30 min intervals. The rate was measured by the ^{1}H integration of the product peak at δ 5.61 (=CH$_2$), and was normalized against the internal standard peak. The k_{obs} was estimated from the first order plot of *ln*[product] vs reaction time.

6.4.1.4 Kinetic Profile Experiment

In a glove box, **1** (14 mg, 0.02 mmol), 4-methoxybenzoic acid (30 mg, 0.20 mmol) and HC≡CPh (31 mg, 0.30 mmol) in THF were dissolved in THF in a J-Young NMR tube with a Teflon screw cap (0.5 mL). The tube was brought out of the glove box,

and was placed in NMR probe which was preset at 60 °C. The appearance and

disappearance of the phosphine signals for **64** (δ =24.4 ppm), **62** (δ = 25.9 ppm) and **63** (δ

= 23.4 ppm) were monitored by ^{31}P NMR at 60 °C in 5 min intervals. The rate of the

product formation was determined by measuring the integration of the product peaks

against the disappearance of the complex **64**. The experimental data was globally fitted to

the kinetic equation by using a non-linear regression technique (Sigmaplot V. 10). The

rate constants k_1= 0.039 min^{-1} and k_2 = 0.013 min^{-1} were obtained and from this analysis.

6.4.1.5 Synthesis of (PCy₃)₂(CO)(Cl)Ru(κ²-O₂CC₆H₄-p-OMe) (62)

In a glove box, 4-methoxybenzoic acid (13 mg, 0.10 mmol), phenylacetylene (10

mg, 0.10 mmol), and complex **1** (72 mg, 0.10 mmol) were dissolved in CH_2Cl_2 (3 mL) in

a 25 mL Schlenk tube equipped with a Teflon screw cap stopcock and a magnetic stirring

bar. The tube was brought out of the box, and was stirred for 10 h at room temperature.

The solvent was evaporated and the residue was washed with hexanes (3 mL × 3 times)

to obtain **62** in 87% yields. Single crystals suitable for X-ray crystallographic study were

obtained from hexanes/CH_2Cl_2.

For **62**: ^{1}H NMR (300 MHz, CDCl₃) δ 7.88 (d, J = 8.7 Hz, 2H), 6.89 (d, J = 8.7

Hz, 2H), 3.86 (s, 3H), 2.30-1.01 (m, 72H); ^{13}C{^{1}H} NMR (100 MHz, CDCl₃) δ 208.8 (t,

J_{PH} = 13.3 Hz,), 179.0, 162.9, 130.3, 125.1, 113.6, 55.5, 34.1, 30.2, 29.7, 28.3, 26.8;

$^{31}P\{^1H\}$ NMR (161 MHz, CDCl$_3$) δ 28.7 (s, PCy$_3$); IR (KBr) v_{CO} = 1913 cm^{-1}.

Crystal Data and Structure Refinement for 62.

Identification code	yi1ka
Empirical formula	C45 H73 Cl O4 P2 Ru
Formula weight	876.49
Temperature	100(2) K
Wavelength	1.54178 Å
Crystal system	Orthorhombic
Space group	A b m 2
Unit cell dimensions	a = 9.7750(2) Å a= 90°.
	b = 24.8661(4) Å b= 90°.
	c = 17.6805(3) Å g = 90°.
Volume	4297.53(13) Å3
Z	4
Density (calculated)	1.355 Mg/m3
Absorption coefficient	4.543 mm-1
F(000)	1864
Crystal size	0.12 x 0.09 x 0.04 mm3
Theta range for data collection	3.55 to 67.20°.
Index ranges	-11<=h<=0, -22<=k<=27, -17<=l<=21
Reflections collected	10054
Independent reflections	3201 [R(int) = 0.0231]
Completeness to theta = 67.20°	98.20%
Absorption correction	Numerical
Max. and min. transmission	0.8392 and 0.6117
Refinement method	Full-matrix least-squares on F2
Data / restraints / parameters	3201 / 1 / 263
Goodness-of-fit on F2	1.015
Final R indices [I>2sigma(I)]	R1 = 0.0323, wR2 = 0.0793
R indices (all data)	R1 = 0.0349, wR2 = 0.0808
Absolute structure parameter	0.450(8)
Largest diff. peak and hole	d -0.422 e.Å-3

6.4.1.6 Synthesis of $(PCy_3)_2(CO)(Cl)RuC(=CHPh)OC(O)C_6H_4$-p-OMe (63)

In a glove box, the Ru-carboxylate complex **62** (44 mg, 50 μmol) and phenylacetylene (6 mg, 60 μmol) were dissolved in THF (3 mL) in a 25 mL Schlenk tube equipped with a Teflon screw cap stopcock and a magnetic stirring bar. The tube was brought out of the glove box and was heated in an oil bath at 95 °C for 10 h. The solvent was removed under high vacuum, and the residue was washed with hexanes (3 mL × 3 times) to obtain analytically pure **63** in 85% yield. Single crystals suitable for X-ray crystallographic study were obtained from hexanes/CH_2Cl_2.

For **63**: ^{1}H NMR (400 MHz, C_6D_6) δ 8.44 (d, J = 8.7 Hz, 2H), 7.76 (d, J = 7.7 Hz, 2H), 7.36-6.63 (m, 5H), 6.24 (s,1H), 2.98 (s, 3H), 2.71-0.8 (m, 72H); ^{13}C{^{1}H} NMR (100 MHz, CDCl$_3$) 209.8 (t, J_{PC} = 14.4 Hz), 190.2 (t, J_{PC} = 12.2 Hz), 173.8, 167.9, 165.4, 138.4, 133.8, 129.1, 125.0, 122.5, 120.0, 115.1, 55.4, 35.2, 31.1, 30.6, 29.8, 28.8, 27.3; ^{31}P{^{1}H} NMR (400 MHz, CDCl$_3$) δ 27.0 (PCy$_3$); IR (KBr) ν_{CO} = 1922 cm^{-1}.

Table 15. Crystal Data and Structure Refinement for **63**

Identification code	yi1na
Empirical formula	C59 H93 Cl O4 P2 Ru
Formula weight	1064.79
Temperature	100(2) K
Wavelength	1.54178 Å
Crystal system	Triclinic
Space group	P -1

Unit cell dimensions	a = 10.9925(2) Å a= 103.0180(10)°
	b = 12.9129(2) Å
	c = 21.9786(5) Å
Volume	2815.46(9) Å3
Z	2
Density (calculated)	1.256 Mg/m3
Absorption coefficient	3.558 mm-1
F(000)	1140
Crystal size	0.40 x 0.23 x 0.17 mm3
Theta range for data collection	3.74 to 67.81°.
Index ranges	-13<=h<=12, -15<=k<=15, 0<=l<=26
Reflections collected	23248
Independent reflections	9565 [R(int) = 0.0242]
Completeness to theta = 67.81°	93.50%
Absorption correction	Numerical
Max. and min. transmission	0.5897 and 0.3317
Refinement method	Full-matrix least-squares on F2
Data / restraints / parameters	9565 / 0 / 607
Goodness-of-fit on F2	1.012
Final R indices [I>2sigma(I)]	R1 = 0.0295, wR2 = 0.0722
R indices (all data)	R1 = 0.0321, wR2 = 0.0735

6.5 Characterization Data of Selected Organic Products

For **58a:** ^{1}H NMR (300 MHz, CDCl$_3$) δ 8.15-6.70 (m, 9H), 5.37 (d, 1H, J = 2.1 Hz), 4.98 (d, 1H, J = 2.1 Hz), 3.69 (s, 3H); ^{13}C{^{1}H} NMR (75 MHz, CDCl$_3$) δ 165.1, 160.5, 153.2, 133.8, 130.4, 129.8, 128.8, 127.2, 126.6, 114.2, 100.7, 55.5; GC-MS *m/z* = 254 (M$^+$).

For **58b:** ^{1}H NMR (300 MHz, CDCl$_3$) δ 8.25-7.10 (m, 9H), 5.57 (d, 1H, J = 2.1 Hz), 5.14 (d, 1H, J = 2.1 Hz), 2.37 (s, 3H); ^{13}C {^{1}H} NMR (100 MHz, CDCl$_3$) δ 164.9, 153.3, 139.0, 133.6, 131.6, 130.1, 129.6, 129.3, 128.5, 124.8, 100.4, 21.3; GC-MS m/z = 238 (M$^+$).

For **58c:** ^{1}H NMR (300 MHz, CDCl$_3$) δ 8.05-7.10 (m, 10H), 5.57 (d, 1H, J = 1.9 Hz), 5.09 (d, 1H, J = 1.9 Hz); ^{13}C{^{1}H} NMR (75 MHz, CDCl$_3$) δ 164.9, 153.3, 134.4, 133.8, 130.2, 129.5, 129.1, 128.8, 128.7, 125.0, 102.5; GC-MS m/z = 224 (M$^+$).

For **58d:** ^{1}H NMR (300 MHz, CDCl$_3$) δ 8.25-7.38 (m, 9H), 5.60 (d, 1H, J = 2.4 Hz), 5.21 (d, 1H, J = 2.4 Hz); ^{13}C{^{1}H} NMR (75 MHz, CDCl$_3$) δ 165.1, 152.5, 134.0, 133.6, 132.0, 130.4, 129.5, 126.8, 123.4, 103. (CH$_2$=C); GC-MS m/z = 303 (M$^+$).

For **58e:** ^{1}H NMR (400 MHz, CDCl$_3$) δ 8.25-7.38 (m, 9H), 5.69 (d, 1H, J = 2.4 Hz), 5.30 (d, 1H, J = 2.4 Hz); ^{13}C{^{1}H} NMR (100 MHz, CDCl$_3$) δ 163.8, 153.2, 135.4, 135.0, 134.1, 132.8, 130.7, 129.4, 128.8, 125.9, 122.4, 102.8; GC-MS m/z = 292 (M$^+$).

For **58f:** ^{1}H NMR (300 MHz, CDCl$_3$) δ 8.25-7.00 (m, 9H), 5.53 (d, 1H, J = 2.4 Hz), 5.16 (d, 1H, J = 2.4 Hz); ^{13}C{^{1}H} NMR (75 MHz, CDCl$_3$) δ 165.1, 161.7, 152.5, 133.9, 130.8, 130.3, 129.5, 128.9, 127.1, 115.7, 102.4; GC-MS m/z = 242 (M$^+$); Anal. Calcd for C$_{15}$H$_{11}$FO$_2$: C, 74.37; H, 4.58. Found: C, 73.27; H, 4.50.

For **58g:** ^{1}H NMR (300 MHz, CDCl$_3$) δ 8.15-7.38 (m, 5H), 4.87 (s, 2H), 4.83 (s, 2H), 2.34 (t, 2H), 1.53 (m, 2H), 1.39 (m, 2H), 0.92 (t, 3H); ^{13}C{^{1}H} NMR (75 MHz,

CDCl$_3$) δ 164.8, 156.9, 133.3, 130.0, 129.6, 128.5, 101.3, 33.2, 28.7, 22.2, 13.9; GC-MS

m/z = 204 (M$^+$).

For **58h**: ^{1}H NMR (400 MHz, CDCl$_3$) δ 8.15-7.30 (m, 10H), 5.08 (d, 1H, J = 2.4

Hz), 4.90 (d, 1H, J = 2.4 Hz, 3.75 (s, 2H); ^{13}C{^{1}H} NMR (100 MHz, CDCl$_3$) δ 164.8,

155.8, 137.0, 133.5, 130.0, 129.8, 129.6, 128.6, 126.9, 103.6, 40.1; GC-MS m/z = 238

(M$^+$).

For **58i**: ^{1}H NMR (300 MHz, CDCl$_3$) δ 8.20-7.38 (m, 5H), 5.22 (d, 1H, J = 2.4

Hz), 5.03 (d, 1H, J = 2.4 Hz), 2.0 (s, 3H); ^{13}C{^{1}H} NMR (75 MHz, CDCl$_3$) δ 164.6,

153.7, 136.6, 133.5, 130.0, 129.5, 128.6, 113.9, 103.6, 19.4; GC-MS m/z = 188 (M$^+$).

For **58j**: ^{1}H NMR (300 MHz, CDCl$_3$) δ 8.35-7.10 (m, 11H), 5.70 (d, 1H, J = 2.4

Hz), 5.23 (d, 1H, J = 2.4 Hz), 3.90 (s, 3H); ^{13}C{^{1}H} NMR (75 MHz, CDCl$_3$) δ 165.2,

158.4, 153.5, 135.0, 133.8, 130.3, 129.7, 129.6, 128.8, 127.4, 124.1, 123.4, 119.4 , 105.9,

102.1, 55.5 (OCH$_3$); GC-MS m/z = 304 (M$^+$); Anal. Calcd for C$_{16}$H$_{14}$O$_2$: C, 78.93; H,

5.30. Found: C, 78.76; H, 5.37.

For **58k**: ^{1}H NMR (300 MHz, CDCl$_3$) δ 8.25-6.95 (m, 9H), 5.62 (d, 1H, J = 2.4

Hz), 5.19 (d, 1H, J = 2.4 Hz), 3.87 (s, 3H); ^{13}C{^{1}H} NMR (75 MHz, CDCl$_3$) δ 164.6,

164.0, 153.3, 134.5 132.3, 129.0, 128.6, 125.0, 121.8, 114.2, 102.3, 55.5; GC-MS m/z =

254 (M$^+$).

For **58l**: ^{1}H NMR (400 MHz, CDCl$_3$) δ 8.20-7.32 (m, 9H), 5.66 (d, 1H, J = 2.1

Hz), 5.23 (d, 1H, J = 2.1 Hz), 2.48 (s, 3H); ^{13}C {^{1}H} NMR (100 MHz, CDCl$_3$) δ 164.9,

153.3, 144.5, 134.4, 132.2, 130.1, 129.6, 129.0, 128.5, 126.8, 102.4, 21.8; GC-MS m/z = 238 (M$^+$)

For **58m:** ^{1}H NMR (300 MHz, CDCl$_3$) δ 8.00-7.20 (m, 9H), 5.50 (d, 1H, J = 2.4 Hz), 5.07 (d, 1H, J = 2.4 Hz); ^{13}C{^{1}H} NMR (75 MHz, CDCl$_3$) δ 164.3, 153.2, 134.2, 132.2, 131.8, 129.3, 129.0, 128.8, 128.5, 125.0, 102.7; GC-MS m/z = 303 (M$^+$).

For **58n:** ^{1}H NMR (400 MHz, CDCl$_3$) δ 8.30-7.00 (m, 9H), 5.52 (d, 1H, J = 2.4 Hz), 5.10 (d, 1H, J = 2.4 Hz, =CH$_2$); ^{13}C{^{1}H} NMR (100 MHz, CDCl$_3$) δ 163.3, 153.2, 133.9, 133.3, 132.7, 130.7, 129.3, 128.8, 128.5, 125.0, 118.0, 117.1, 102.7; GC-MS m/z = 249 (M$^+$); Anal. Calcd for C$_{16}$H$_{11}$NO$_2$: C, 77.10; H, 4.45. Found: C, 77.30; H, 4.47.

For **58o:** ^{1}H NMR (300 MHz, CDCl$_3$) δ 8.38-7.32 (m, 9H), 5.64 (d, 1H, J = 2.4 Hz), 5.20 (d, 1H, J = 2.4 Hz); ^{13}C{^{1}H} NMR (75 MHz, CDCl$_3$) δ 163.8, 153.2, 135.4, 135.0, 134.1, 132.8, 130.7, 129.5, 128.8, 125.9, 122.4, 102.8; GC-MS m/z = 292 (M$^+$); Calcd for C$_{16}$H$_{11}$F$_3$O$_2$: C, 65.76; H, 3.80. Found: C, 65.51; H, 3.82.

For **58p:** ^{1}H NMR (400 MHz, CDCl$_3$) δ 7.92 (s, 1H), 7.40-6.90 (m, 15H), 5.38 (d, 1H, J = 2.4 Hz), 5.01 (d, 1H, J = 2.4 Hz); ^{13}C{^{1}H} NMR (100 MHz, CDCl$_3$) δ 166.1, 153.4, 142.1, 135.7, 134.5, 134.4, 132.0, 131.0, 129.9, 129.6, 129.0, 128.9, 128.6, 128.4, 125.0, 102.8; GC-MS m/z = 326 (M$^+$); Calcd for C$_{23}$H$_{18}$O$_2$: C, 84.64; H, 5.56. Found: C, 84.40; H, 5.55.

For **58q:** ^{1}H NMR (300 MHz, CDCl$_3$) δ 7.97 (s, 1H), 7.47-7.08 (m, 15H), 4.86 (d, 1H, J = 2.4 Hz), 4.79 (d, 1H, J = 2.4 Hz), 2.43 (t, 2H), 1.55 (m, 4H), 1.03 (t, 3H);

^{13}C{^{1}H} NMR (75 MHz, CDCl$_3$) δ 166.1, 157.0, 141.3, 135.7, 134.5, 132.4, 130.8, 129.9, 129.3, 1287, 128.4, 101.0, 33.1, 28.7, 14.0, 2.1; GC-MS *m/z* = 306 (M$^+$).

For **58r:** ^{1}H NMR (400 MHz, CDCl$_3$) δ 7.52-7.30 (m, 5H), 5.53 (d, 1H, *J* = 2.4 Hz), 5.01 (d, 1H, *J* = 2.4 Hz), 2.56 (m, 1H), 2.09-1.83 (m, 4H), 1.7-1.2 (m, 6H); ^{13}C{^{1}H} NMR (100 MHz, CDCl$_3$) δ 174.2, 153.1, 134.7, 129.0, 128.6, 125.0, 102.0, 43.4, 29.1, 25.8, 25.5; GC-MS *m/z* = 230 (M$^+$); Calcd for C$_{15}$H$_{18}$O$_2$: C, 78.22; H, 7.87. Found: C, 78.09; H, 7.66.

For **58s:** ^{1}H NMR (400 MHz, CDCl$_3$) δ 7.52-7.30 (m, 5H), 5.48 (d, 1H, *J* = 2.4 Hz), 5.01 (d, 1H, *J* = 2.4 Hz), 2.56 (t, 2H), 1.74 (m, 2H), 1.44-1.20 (m, 24H), 0.89 (t, 3H); ^{13}C{^{1}H} NMR (100 MHz, CDCl$_3$) δ 172.2, 153.1, 134.7, 129.0, 128.6, 125.0, 102.4, 34.5, 31.2, 30.0, 29.9, 29.8, 29.7, 29.6, 29.5, 29.4, 29.3, 25.1, 22.9, 14.3; GC-MS *m/z* = 230 (M$^+$); Calcd for C$_{24}$H$_{38}$O$_2$: C, 80.40; H, 10.68. Found: C, 80.55; H, 10.46.

For (*Z*)-**59a:** ^{1}H NMR (300 MHz, CDCl$_3$) δ 8.10-6.63 (m, 9H), 7.38 (d, 1H, *J* = 7.4 Hz,), 5.71 (d, 1H, *J* = 7.4 Hz), 3.73 (s, 3H); ^{13}C{^{1}H} NMR (75 MHz, CDCl$_3$) δ 163.8, 159.1, 133.8, 133.0, 130.8, 130.3, 129.3, 129.0, 127.1, 114.2, 112.5, 55.5; GC-MS *m/z* = 254 (M$^+$).

For (*Z*)-**59b**: ^{1}H NMR (400 MHz, CDCl$_3$) δ 8.05-7.05 (m, 9H), 7.98 (d, 1H, *J* = 12.8 Hz,), 6.47 (d, 1H, *J* = 12.8 Hz), 2.25 (s, 3H); ^{13}C{^{1}H} NMR (75 MHz, CDCl$_3$) δ 163.7, 137.4, 135.9, 133.7, 133.6, 131.1, 130.0, 129.5, 129.0, 128.6, 115.8, 21.3; GC-MS *m/z* = 238 (M$^+$); Anal. Calcd for C$_{16}$H$_{14}$O$_2$: C, 80.65; H, 5.92. Found: C, 80.74; H, 5.99.

For (*Z*)-**59c**: ^{1}H NMR (300 MHz, CDCl$_3$) δ 8.05-7.10 (m, 10H), 7.40 (d, 1H, *J* = 7.4 Hz,), 5.76 (d, 1H, *J* = 7.4 Hz); ^{13}C{^{1}H} NMR (75 MHz, CDCl$_3$) δ 163.5, 134.2, 134.1, 133.8, 130.2, 129.2, 128.9 128.8, 128.5, 127.4, 112.7; GC-MS *m/z* = 224 (M$^+$).

For (*Z*)-**59d:** ^{1}H NMR (300 MHz, CDCl$_3$) δ 8.15-7.24 (m, 9H), 7.50 (d, 1H, *J* = 7.4 Hz), 5.80 (d, 1H, *J* = 7.4 Hz); ^{13}C{^{1}H} NMR (75 MHz, CDCl$_3$) δ 163.8, 159.1, 133.8, 133.0, 130.8, 130.3, 129.3, 129.0, 127.1, 114.2, 112.5, 55.5; GC-MS *m/z* = 303 (M$^+$); Calcd for C$_{15}$H$_{11}$BrO$_2$: C, 59.42; H, 3.66. Found: C, 59.06; H, 3.64.

For (*Z*)-**59e:** ^{1}H NMR (400 MHz, CDCl$_3$) δ 8.20-7.50 (m, 9H), 7.53 (d, 1H, *J* = 7.4 Hz,), 5.89 (d, 1H, *J* = 7.4 Hz); ^{13}C{^{1}H} NMR (75 MHz, CDCl$_3$) δ 163.8, 159.1, 133.8, 133.0, 130.8, 130.3, 129.3, 129.0, 127.1, 114.2, 112.5, 55.5; GC-MS *m/z* = 292 (M$^+$).

For (*Z*)-**59f:** ^{1}H NMR (400 MHz, CDCl$_3$) δ 8.24-7.00 (m, 9H), 7.50 (d, 1H, *J* = 7.4 Hz), 5.83 (d, 1H, *J* = 7.4 Hz); ^{13}C{^{1}H} NMR (100 MHz, CDCl$_3$) δ 163.6, 163.2, 160.8, 134.1, 134.0, 131.1, 130.3, 129.0, 128.8, 115.7, 111.7; GC-MS *m/z* = 242 (M$^+$); Calcd for C$_{15}$H$_{11}$FO$_2$: C, 74.37; H, 4.58. Found: C, 73.27; H, 4.50.

For (*E*)-**59b**: ^{1}H NMR (400 MHz, CDCl$_3$) δ 8.05-7.05 (m, 9H), 7.98 (d, 1H, *J* = 12.8 Hz), 6.47 (d, 1H, *J* = 12.8 Hz), 2.25 (s, 3H); ^{13}C{^{1}H} NMR (75 MHz, CDCl$_3$) δ 163.7, 137.4, 135.9, 133.7, 133.6, 131.1, 130.0, 129.5, 129.0, 128.6, 115.8, 21.3; GC-MS *m/z* = 238 (M$^+$).

For (*E*)-**59c**: ^{1}H NMR (300 MHz, CDCl$_3$) δ 8.05-7.10 (m, 10H), 8.05 (d, 1H, *J* = 12.8 Hz), 5.76 (d, 1H, *J* = 12.8 Hz); ^{13}C {^{1}H} NMR (75 MHz, CDCl$_3$) δ 163.7, 136.1, 133.7, 133.5, 130.1 130.0, 128.9, 128.6 127.5, 126.3, 115.9; GC-MS *m/z* = 224 (M$^+$).

For (*E*)-**59d**: ^{1}H NMR (300 MHz, CDCl$_3$) δ 8.15-7.24 (m, 9H), 8.09 (d, 1H, *J* = 12.8 Hz), 6.53 (d, 1H, *J* = 12.8 Hz); ^{13}C{^{1}H} NMR (75 MHz, CDCl$_3$) δ 163.7, 137.4, 134.7, 134.0, 133.2, 132.0, 130.9, 130.2, 128.8, 127.9, 111.5; GC-MS *m/z* = 303 (M$^+$).

For **60a:** ^{1}H NMR (300 MHz, CDCl$_3$) δ 8.08-7.38 (m, 5H), 4.84 (s, 2H), 2.18 (s, 3H); ^{13}C{^{1}H} NMR (75 MHz, CDCl$_3$) δ 201.9, 165.9, 133.5, 129.9, 129.2, 128.5, 68.8, 26.6; GC-MS *m/z* = 178 (M$^+$).

For **60b:** ^{1}H NMR (300 MHz, CDCl$_3$) δ 8.10-7.38 (m, 5H), 5.29 (m, 1H), 2.22 (s, 3H), 1.53 (d, 3H, *J* = 7.1 Hz); ^{13}C{^{1}H} NMR (75 MHz, CDCl$_3$) δ 205.9, 165.9, 133.5, 129.9, 129.5, 128.5, 75.6, 25.8, 16.2; GC-MS *m/z* = 192 (M$^+$).

For **60c:** ^{1}H NMR (300 MHz, CDCl$_3$) δ 8.10-7.38 (m, 5H), 2.12 (s, 3H), 1.55 (s, 6H); ^{13}C{^{1}H} NMR (75 MHz, CDCl$_3$) δ 206.7, 165.9, 133.5, 129.7, 129.5, 128.5, 84.2, 23.6, 23.4; GC-MS *m/z* = 206 (M$^+$).

For **60d:** ^{1}H NMR (300 MHz, CDCl$_3$) δ 8.10-7.38 (m, 5H), 2.14 (m, 2H), 2.06 (s, 3H), 1.74-1.50 (m, 8H); ^{13}C{^{1}H} NMR (75 MHz, CDCl$_3$) δ 206.9, 165.9, 133.3, 129.7, 129.5, 128.5, 85.5, 30.8, 25.5, 23.5, 21.3; GC-MS *m/z* = 247 (M$^+$).

For **60f:** ^{1}H NMR (300 MHz, CDCl$_3$) δ 4.60 (s, 2H), 2.60 (m, 2H), 2.40 (s, 3H), 2.15 (m, 26H), 0.85 (t, 3H); ^{13}C{^{1}H} NMR (75 MHz, CDCl$_3$) δ 201.8, 175.2, 68.3, 51.9,

34.1, 34.0, 32.1, 29.9, 29.8, 29.7, 29.6, 29.5, 29.4, 29.3, 26.2, 22.9, 25.0, 14.3; GC-MS

$m/z = 276$ (M$^+$).

For **60g:** ^{1}H NMR (300 MHz, CDCl$_3$) δ 4.60 (s, 2H), 2.40 (m, 1H), 2.13 (s, 3H),

2.0-1.10 (m, 10H); ^{13}C {^{1}H} NMR (75 MHz, CDCl$_3$) δ 202.2, 175.5, 68.2, 42.9, 29.1,

26.3, 25.5, 25.9 (CO*C*H$_3$); GC-MS $m/z = 184$ (M$^+$).

For **60h:** ^{1}H NMR (300 MHz, CDCl$_3$) δ 7.93 (s,1H), 7.40-7.08 (m, 10H), 4.75 (s,

2H), 2.10 (s, 3H); ^{13}C{^{1}H} NMR (75 MHz, CDCl$_3$) δ 201.6, 166.8, 141.4, 135.4, 134.3,

131.5, 130.6, 129.9, 129.2, 128.5, 128.1, 127.8, 68.8, 25.9; GC-MS $m/z = 280$ (M$^+$).

For **61a:** ^{1}H NMR (300 MHz, CDCl$_3$) δ 8.25-7.45 (m, 14H), 5.6 (d, 2H, $J = 2.4$

Hz), 5.22 (d, 2H, $J = 2.4$ Hz); ^{13}C{^{1}H} NMR (75 MHz, CDCl$_3$) δ 164.9, 152.7, 135.0,

133.8, 130.3, 129.4, 128.8, 125.3, 103.1; GC-MS $m/z = 370$ (M$^+$).

For **61b:** ^{1}H NMR (300 MHz, CDCl$_3$) δ 8.10-7.35 (m, 10H), 4.91 (d, 4H, $J = 2.4$

Hz), 2.45 (t, 4H, $J = 7.5$ Hz), 1.78 (m, 2H); ^{13}C{^{1}H} NMR (75 MHz, CDCl$_3$) δ 164.7,

155.8, 133.4, 130.0, 129.8, 128.5, 102.2, 32.7, 23.5; GC-MS $m/z = 336$ (M$^+$).

6.6 For Chapter 4

6.6.1 Typical Procedure of the Catalytic Reaction

In a glove box, RuH(CO)(PCy$_3$)$_2$Cl (0.5 mol %), ketone (2.0 mmol) and

vinylsilane (3.0 mmol) were dissolved in 3mL toluene solution in a thick-walls 25 mL

Schlenk tube equipped with a magnetic stirring bar. The tube was brought out of the

glove box. The reaction tube was heated in an oil bath at 120 ^{o}C for 8-15 hours. The tube

was opened under nitrogen gas at room temperature and the crude product mixture was

analyzed by GC-MS.

6.6.2 Typical Procedure of the Aldol-Type Condensation Reaction

When the catalytic reaction of ketone with vinylsilane was done, the toluene was

evacuated, and the crude product was dissolved in 2 mL CH$_2$Cl$_2$. 3.0 mmol

4-nitrobenzaldehyde was dissolved in 5 mL CH$_2$Cl$_2$, when the solution was cool to 0 ^{o}C,

3.0 mmol TiCl$_4$ was added in, this mixture was stirred for about 15 min and then the

crude silyl enol ether solution was added in by dropwise at -78 ^{o}C, and this mixture was

warmed to -38 ^{o}C, and kept stirring for 1 hr, and added about 3 mmol water, the mixture

was stirred in 0 ^{o}C for 8 hr. The reaction was quenched by adding the Na$_2$CO$_3$ solution,

the oil lay was extracted with ethyl ether (20 mL), and the water lay was washed by ethyl

ether (3 x 20 mL). The solution was dried by MgSO$_4$, and the crude product was isolated

by a column chromatograph on silica gel (hexane/dichloromethane).

6.6.3 Typical Procedure of the Fluorination Reaction

When the catalytic reaction of ketone with vinylsilane was done, the toluene was evacuated, and the crude product (2.0 mmol) was dissolved in 2 mL CH_3CN, and the solution was cooled to 0 ^{o}C. Selectfluor (0.708 g, 2.0 mmol) was added in several portions to the solution. After the addition of Selectfluor, the cold bath was removed and the reaction mixture was allowed to warm to room temperature over several hours. After the completion of the fluorination, the solvent was evaporated. Water (10 mL) was added to the residue, and the product was extracted with ethyl ether (3 x 20 mL). The combined organic layers were washed with brine and dried over anhydrous Na_2SO_4, and the solvent was evaporated. The pure product was isolated as a colorless liquid by flash chromatography using EtOAc/*n*-hexane.

6.6.4 Typical Procedure of the Diketone Reactions

When the catalytic reaction of ketone with vinylsilane was done, the toluene was evacuated, and the crude product (2.0 mmol) was dissolved in 2 mL CH_2Cl_2. Acetyl chloride (2.5 mmol) was dissolved in 5 mL CH_2Cl_2, and the solution was cooled to 0 ^{o}C, 3 mmol $TiCl_4$ was added in. This mixture was stirred for about 15 min and then the crude

silyl enol ether solution was added dropwise at -78 $^{\circ}$C, and this mixture was warmed to

-38 $^{\circ}$C, and kept stirring for 1 hr. The reaction was quenched by adding the NH$_4$Cl

solution, the oil lay was extracted with ethyl ether (20 mL), and the water lay was washed

by ethyl ether (3 x 20 mL). The solution was dried by MgSO$_4$, and the crude product was

isolated by a column chromatograph on silica gel (*n*-hexane/ dichloromethane).

6.6.5 Typical Procedure of Aminomethylation Reaction

The experiment was performed by following a reported procedure. To a mixture

of *N,N*-dimethylanilines (1.5 mmol), CuBr (4 mg, 0.025 mmol), crude product **2** (0.5

mmol) and CH$_3$CN (5 mL), *t*-BuOOH (0.10 mL, 5.0 M in decane) was added dropwise at

room temperature. The resulting mixture was stirred at 50 °C for 12 h. After the reaction,

the mixture was filtered through a pad of celite, and the solvent was removed under

reduced pressure. The residue was purified on a silica gel column to afford the desired

product.

6.6.6 Hammett Study

In the glove box, $(PCy_3)_2(CO)RuHCl$ (0.5 mol %), *para*-substituted

acetophenones (0.2 mmol), vinyltrimethylsilane (0.4 mmol) and hexamethylbenzene (26

mg as the internal standard) were dissolved in 0.5 mL toluene-d_8 solution in a Wilmad

J-Young NMR tube with a Teflon screw cap. The tube was taken out and was heated in

an oil bath at 120 ^{o}C. The reaction was monitored every 30 min by ^{1}H NMR spectroscopy

at room temperature. The rate was measured by monitor the ^{1}H integration of the product

peak vinyl protons signal, and these were normalized vinyl protons against the internal

standard. The k_{obs} was estimated from a first–order plot of ln[product] vs. reaction time.

6.7 Characterization Data of Organic Products

For **67a**: ^{1}H NMR (400 MHz, CDCl$_3$) δ 7.82 (s, 2H), 7.52-7.32 (m, 10H), 2.93 (t,

J = 6.1 Hz, 4H), 1.78 (t, J = 6.1 Hz, 2H); ^{13}C{^{1}H} NMR (75 MHz, CDCl$_3$) δ 190.3,

137.0, 136.2, 136.0, 130.4 ,128.4, 128.6, 28.5, 23.0; GC-MS *m/z* = 274 (M$^+$).

For **67b**: ^{1}H NMR (400 MHz, CDCl$_3$) δ 7.60-7.36 (m, 12H), 3.09 (s, 1H);

^{13}C{^{1}H} NMR (100 MHz, CDCl$_3$) δ 196.5, 137.5, 135.9, 134.0, 130.9 128.9, 129.6, 26.7;

GC-MS *m/z* = 260 (M$^+$).

For **67c**: ^{1}H NMR (300 MHz, CDCl$_3$) δ 7.82 (s, 2H), 7.52-7.32 (m, 10H), 3.15 (d,

J = 15.6 Hz, 2H), 2.45 (t, J = 13.8 Hz, 2H), 1.48 (m, 1H), 0.96 (s, 9H); ^{13}C{^{1}H} NMR

(75 MHz, CDCl$_3$) δ 190.9, 137.0, 136.4, 136.2, 130.6, 128.8, 128.7, 44.6, 32.8, 29.8 and

27.5; GC-MS *m/z* = 330 (M$^+$).

For **67d**: ^{1}H NMR (300 MHz, CDCl$_3$) δ 8.16 (d, 2H, *J* = 8.9 Hz), 7.50 (d, 2H, *J* =

8.9 Hz,), 5.26 (s, 1H), 3.73 (s, 1H), 2.435 (m, *J* = 13.8 Hz, 1H), 2.60-2.40 and 1.80-1.20

(m,10H); ^{13}C{^{1}H} NMR (75 MHz, CDCl$_3$) δ 217.7, 149.8, 147.2, 126.9, 123.6   72.6,

57.4, 44.0, 29.2, 128.7, 44.6, 29.3, 29.2, 24.0, 23.7.

For **67e** *(syn)*: ^{1}H NMR (300 MHz, CDCl$_3$) δ 8.10 (d, 2H, *J* = 8.9 Hz), 7.32 (d,

2H, *J* = 8.9 Hz), 5.26 (s,1H), 4.00 (s, 1H), 3.26-1.68 (m, 8H) and 1.37 (s, 3H); ^{13}C{^{1}H}

NMR (75 MHz, CDCl$_3$) δ 214.4, 148.1, 146.8, 130.1, 123.9, 77.7, 47.9, 42.9, 35.7, 34.7,

25.3 and 22.5.

For **67e** (*anti*): ^{1}H NMR (300 MHz, CDCl$_3$) δ 8.13 (d, 2H, *J* = 8.9 Hz), 7.47(d,

2H, *J* = 8.9 Hz), 5.03 (s, 1H), 4.25 (s, 1H), 3.26-1.68 (m, 8H), 1.14 (s, 3H); ^{13}C{^{1}H}

NMR (75 MHz, CDCl$_3$) δ 219.0, 147.6, 146.8, 129.3, 123.0, 76.9, 52.7, 39.2, 37.1, 27.5,

20.7, 16.1.

For **67f** (*syn*): ^{1}H NMR (300 MHz, CDCl$_3$) δ 8.04 (d, *J* = 8.9 Hz, 2H), 7.41 (d, *J* =

8.9 Hz, 2H), 5.17 (s, 1H), 3.97 (s, 1H), 2.81 (m, 1H), 2.02 (s, 3H), 1.44 (m, 2H), 1.09 (m,

4H), 0.69 (t, *J* = 6.6 Hz, 3H) ppm. ^{13}C{^{1}H} NMR (75 MHz, CDCl$_3$) δ 211.1, 150.6,

147.2, 126.5, 123.6, 69.0, 50.6, 43.6, 31.2, 23.1, 22.4, 13.9 ppm. GC-MS *m/z* = 265 (M$^+$).

The ^{1}H and ^{13}C NMR spectral data are in good agreement with the literature data.

For **67f** (*anti*): ^{1}H NMR (300 MHz, CDCl$_3$) δ 8.04 (d, *J* = 8.9 Hz, 2H), 7.41 (d, *J* = 8.9 Hz, 2H), 4.94 (s, 1H), 3.74 (s, 1H), 2.81 (m, 1H), 2.02 (s, 3H), 1.44 (m, 2H), 1.09 (m, 4H), 0.69 (t, *J* = 6.6 Hz, 3H) ppm. ^{13}C{^{1}H} NMR (75 MHz, CDCl$_3$) δ 213.1, 149.8, 147.1, 127.1, 123.4, 72.9, 58.8, 31.5, 27.3, 23.4, 13.8 ppm. GC-MS *m/z* = 265 (M$^+$). The ^{1}H and ^{13}C NMR spectral data are in good agreement with the literature data.

For **67g**: ^{1}H NMR (400 MHz, CDCl$_3$) δ 8.16 (d, 2H, *J* = 8.9 Hz), 7.92 (d, 2H, *J* = 7.8 Hz), 7.50 (d, 2H, *J* = 8.9 Hz), 7.50-7.43 (3H), 5.44 (s, 1H), 3.99 (s, 1H), 3.35 (m, 2H); ^{13}C{^{1}H} NMR (75 MHz, CDCl$_3$) δ 199.6, 150.5, 147.4, 136.3, 134.2, 129.0, 126.7, 123.9, 69.3, 47.2.

For **67h**: ^{1}H NMR (300 MHz, CDCl$_3$) δ 8.16 (d, 2H, *J* = 8.9 Hz), 7.81 (d, 2H, *J* = 8.1 Hz,), 7.57 (d, 2H, *J* = 8.9 Hz), 7.23 (d, 2H, *J* = 8.1 Hz,), 5.44 (q, 1H, *J* = 4.0 Hz), 4.04 (s, 1H), 3.33 (m, 2H) and 2.39 (s, 3H); ^{13}C{^{1}H} NMR (100 MHz, CDCl$_3$) δ 199.1, 150.5, 147.2, 145.0, 133.7, 129.5, 128.3, 126.6, 123.7, 69.3, 46.8, 21.7.

For **67i**: ^{1}H NMR (300 MHz, CDCl$_3$) δ 8.16 (d, 2H, *J* = 8.9 Hz), 7.88 (d, 2H, *J* = 8.4 Hz,), 7.57 (d, 2H, *J* = 8.9 Hz), 6.90 (d, 2H, *J* = 8.4 Hz), 5.44 (m, 1H), 4.10 (s, 1H), 3.85 (s, 3H), 3.31(m, 2H); ^{13}C{^{1}H} NMR (75 MHz, CDCl$_3$) δ 198.2, 164.4, 150.7, 147.4, 130.8, 129.5, 126.8, 124.0, 114.2, 69.6, 55.8, 46.8.

For **67j**: ^{1}H NMR (300 MHz, CDCl$_3$) δ 8.16 (d, 2H, *J* = 8.9 Hz), 7.88 (d, 2H, *J* = 8.4 Hz,), 7.57 (d, 2H, *J* = 8.9 Hz), 6.90 (d, 2H, *J* = 8.4 Hz), 5.44 (m, 1H), 4.10 (s, 1H),

3.85 (s, 3H), 3.31(m, 2H); $^{13}C\{^{1}H\}$ NMR (75 MHz, CDCl$_3$) δ 198.2, 164.4, 150.7, 147.4, 130.8, 129.5, 126.8, 124.0, 114.2, 69.6, 47.3.

For **67k**: ^{1}H NMR (300 MHz, CDCl$_3$) δ 8.21 (d, 2H, J = 8.8 Hz), 7.88 (d, 2H, J = 8.6 Hz,), 7.60 (d, 2H, J = 8.8 Hz), 7.44 (d, 2H, J = 8.8 Hz), 5.45 (m, 1H), 3.77 (s, 1H) and 3.33 (m,2H); $^{13}C\{^{1}H\}$ NMR (75 MHz, CDCl$_3$) δ 198.4, 150.3, 147.6, 140.8, 134.7, 129.8, 129.4, 126.8, 124.1, 69.3, 47.3.

For **67l** (*syn*): ^{1}H NMR (400 MHz, CDCl$_3$) δ 8.16 (d, 2H, J = 8.8 Hz), 7.93 (d, 2H, J = 8.9 Hz), 7.62-7.44 (m, 5H), 5.34 (s, 1H), 4.08 (s, 1H), 3.79 (m, 1H) and 1.15 (d, 3H, J = 7.2 Hz); $^{13}C\{^{1}H\}$ NMR (75 MHz, CDCl$_3$) δ 205.3, 149.3, 147.1, 135.1, 134.0, 129.1, 128.7, 127.1, 123.7, 72.5, 46.8, 11.2.

For **67l** (*anti*): ^{1}H NMR (300 MHz, CDCl$_3$) δ 8.16 (d, 2H, J = 8.8 Hz), 7.93 (d, 2H, J = 8.9 Hz), 7.62-7.44 (m, 5H), 5.08 (d, J = 7.2 Hz), 4.08 (s, 1H), 3.82 (m, 1H) and 1.15 (d, 3H, J = 7.2 Hz); $^{13}C\{^{1}H\}$ NMR (75 MHz, CDCl$_3$) δ 204.4, 149.8, 147.6, 136.1, 133.8, 129.0, 128.6, 127.8, 123.8, 75.9, 47.8, 15.9.

For **67m** (*syn*): ^{1}H NMR (300 MHz, CDCl$_3$) δ 8.3-6.8 (m, 14H), 5.70 (d, J = 3.4 Hz 1H), 4.78 (d, J = 3.4 Hz, 1H), 3.90 (s, 1H) ppm. $^{13}C\{^{1}H\}$ NMR (75 MHz, CDCl$_3$) δ 202.1, 148.8, 147.6, 146.0, 138.1, 129.4, 133.4, 132.1, 130.4, 128.7, 128.3, 127.2, 124.1, 74.5, 60.0 ppm. GC-MS m/z = 347 (M$^+$). The ^{1}H and ^{13}C NMR spectral data are in good agreement with the literature data.

For **67m** (*anti*): ^{1}H NMR (300 MHz, CDCl$_3$) δ 8.10-6.85 (m, 14H), 5.55 (d, *J* = 8.9 Hz, 1H), 4.68 (d, *J* = 3.4 Hz, 1H), 3.50 (s, 1H) ppm. ^{13}C{^{1}H} NMR (75 MHz, CDCl$_3$) δ 198.1, 148.0, 147.0, 145.3, 137.9, 129.3, 133.5, 132.1, 130.4, 128.7, 128.4, 127.5, 124.3, 76.5, 62.3 ppm. GC-MS *m/z* = 347 (M$^+$). The ^{1}H and ^{13}C NMR spectral data are in good agreement with the literature data.

For **67n**: ^{1}H NMR (400 MHz, CDCl$_3$) δ 8.23-7.42 (m, 8H), 5.06 (s, 1H), 4.98 (d, 1H, *J* = 8.9 Hz), 3.00 (m, 1H), 2.73(m, 1H); ^{13}C{^{1}H} NMR (100 MHz, CDCl$_3$) δ 209.0, 153.6, 148.7, 148.0, 136.2, 136.1, 128.2, 128.0, 126.8, 124.5, 124.0, 75.0, 53.1, 29.7.

For **67o**: ^{1}H NMR (300 MHz, CDCl$_3$) δ 8.21 (d, 2H, *J* = 8.8 Hz), 8.05 (d, 1H, *J* = 8.0 Hz,), 7.58 (d, 2H, *J* = 8.8 Hz), 7.54-7.23 (m, 3H), 5.11 (d, 1H, *J* = 8.2 Hz), 5.02 (s, 1H), 2.89 (m, 2H), 2.75 (m, 1H), and 1.68 (m, 2H); ^{13}C{^{1}H} NMR (75 MHz, CDCl$_3$) δ 201.6, 148.7, 147.8, 144.4, 134.6, 132.2, 129.0, 128.3, 127.8, 127.2, 123.8, 74.8, 53.9, 28.9, 26.2.

For **67p**: ^{1}H NMR (300 MHz, CDCl$_3$) δ 8.44 (s, 1H), 8.22 (d, 2H, *J* = 8.8 Hz), 7.93 (m, 4H), 7.64 (d, 2H, *J* = 8.8 Hz), 7.61 (m, 3H), 5.51 (t, 1H, *J* = 4.0 Hz), 3.97 (s, 1H) and 3.51 (m, 2H); ^{13}C{^{1}H} NMR (75 MHz, CDCl$_3$) δ 201.6, 148.7, 147.8, 144.4, 134.6, 132.2, 129.0, 128.3, 127.8, 127.2, 123.8, 74.8, 53.9, 28.9, 26.2.

For **67q**: ^{1}H NMR (300 MHz, CDCl$_3$) δ 8.23 (d, 2H, *J* = 8.8 Hz), 7.61 (d, 2H, *J* = 8.8 Hz), 7.26 (m, 3H), 6.95 (m, 1H), 5.43 (m, 1H), 3.95 (s, 1H), 3.35 (m, 2H) and 3.00 (s,

6H); ^{13}C{^{1}H} NMR (75 MHz, CDCl$_3$) δ 200.7, 150.9, 150.6, 147.5, 137.1, 129.7, 126.8, 124.0, 118.0, 116.6, 111.0, 69.6, 47.2, 40.7.

For **67r**: ^{1}H NMR (300 MHz, CDCl$_3$) δ 7.8-7.2 (m, 5H), 5.55 (d, J_{HF} = 46.9 Hz, 2H); ^{13}C{^{1}H} NMR (75 MHz, CDCl$_3$) δ 193.1 (d, J_{CF} = 15.0 Hz), 145.4, 132.4, 130.4 127.6, 84.0 (d, J_{CF} = 188.9 Hz) ppm. GC-MS m/z = 138 (M$^+$).

For **67s:** ^{1}H NMR (300 MHz, CDCl$_3$) δ 7.70-7.30 (m, 4H), 5.14 (m, J_{HF} = 51.0 Hz, 1H), 3.35 (m, 1H), 3.08 (m, 1H) ppm. ^{13}C{^{1}H} NMR (75 MHz, CDCl$_3$) δ 199.9 (d, J_{CF} = 14.9 Hz), 149.7, 136.4, 133.7, 128.3, 126.9, 124.4, 91.7 (d, J_{CF} = 189.9 Hz), 33.2 (d, J_{CF} = 21.4 Hz) ppm. GC-MS *m/z* = 150 (M$^+$).

For **67t:** ^{1}H NMR (400 MHz, CDCl$_3$) δ 8.0-7.25 (m, 4H), 5.14 (ddd, J_{HF} = 46.9 Hz, J_{HH} = 12.8, 5.2 Hz, 1H), 3.12 (m, 2H), 2.56 (m, 1H), 2.34 (m, 1H) ppm. ^{13}C{^{1}H} NMR (100 MHz, CDCl$_3$) δ 193.6 (d, J_{CF} = 14.8 Hz), 143.2, 134.4, 131.4, 128.9, 128.0, 127.4, 91.2 (d, J_{CF} = 188.4 Hz), 30.4 (d, J_{CF} = 19.4 Hz), 27.1 (d, J_{CF} = 11.6 Hz) ppm. GC-MS *m/z* = 164 (M$^+$).

For **67u:** ^{1}H NMR (300 MHz, CDCl$_3$) δ 7.95-6.72 (m, 10H), 3.85 (t, *J* = 7.0 Hz, 2H), 3.24 (t, *J* = 7.0 Hz, 2H), 2.98 (s, 3H) ppm. ^{13}C{^{1}H} NMR (75 MHz, CDCl$_3$) δ 199.7, 148.8, 137.1, 133.4, 129.5, 128.8, 128.2, 116.7, 112.6, 48.1, 38.7, 35.3 ppm. GC-MS *m/z* = 239 (M$^+$).

For **67v:** ^{1}H NMR (300 MHz, CDCl$_3$) δ 7.26-6.75 (m, 5H), 3.89 (dd, *J* = 15.1, 4.5 Hz, 1H), 3.28 (dd, *J* = 15.1, 8.0 Hz, 1H), 2.96 (s, 3H), 2.53-2.45 (m, 1H), 2.37-1.63 (m,

6H) ppm. ^{13}C{^{1}H} NMR (75 MHz, CDCl$_3$) δ 220.2, 148.8, 129.3, 116.5, 112.3, 52.5, 48.4, 39.2, 38.1, 29.2, 20.8 ppm. GC-MS m/z = 203 (M$^+$).

For **67w:** ^{1}H NMR (300 MHz, CDCl$_3$) δ 7.30-6.70 (m, 5H), 3.89 (dd, J = 15.1, 5.6 Hz, 1H), 3.26 (dd, J = 15.3, 7.2 Hz, 1H), 3.02 (s, 3H), 2.78 (m, 1H), 2.50-1.42 (m, 8H) ppm. ^{13}C{^{1}H} NMR (75 MHz, CDCl$_3$) δ 212.5, 149.0, 129.2, 115.9, 111.7, 52.2, 49.2, 42.3, 39.6, 32.5, 27.9, 25.0 ppm. GC-MS m/z = 217 (M$^+$).

6.8 For Chapter 5

6.8.1 General Procedure of the Hydrosilylation of Alkynes

In a glove box, alkynes (1.0 mmol), triethylsilane (2.0 mmol) and the ruthenium catalyst **1** (7 mg, 1 mol %) were dissolved in 3 mL of CH$_2$Cl$_2$ in a 25 mL Schlenk tube equipped with a Teflon stopcock and a magnetic stirring bar. The reaction tube was brought out of the glove box, and was stirred at room temperature for 4-8 hours. The tube was opened to the air at room temperature, and the crude product mixture was analyzed by GC-MS. Analytically pure organic product was isolated by a column chromatography on silica gel (n-hexane/EtOAc).

6.8.2 General Procedure of the Hydrosilylation of Alkenes

In a glove box, alkenes (1.0 mmol), triethylsilane (2.0 mmol) and the ruthenium catalyst **1** (7 mg, 1 mol %) were dissolved in 3 mL of CH_2Cl_2 in a 25 mL Schlenk tube equipped with a Teflon stopcock and a magnetic stirring bar. The reaction tube was brought out of the glove box, and was stirred at 40 ^{o}C for 8 h. The tube was opened to the air at room temperature, and the crude product mixture was analyzed by GC-MS. Analytically pure organic product was isolated by a column chromatography on silica gel (*n*-hexane/EtOAc).

6.8.3 Hammett Study on the Hydrosilylation of Alkenes

In a glove box, a *para*-substituted styrene *p*-X-C_6H_4CCH (X = OMe, CH_3, Cl, Br) (0.20 mmol), triethylsilane (40 mg, 0.4 mmol), **1** (2 mg, 1 mol %) and C_6Me_6 (2 mg, internal standard) were dissolved in $CDCl_3$ (0.5 mL) solution in a J-Young NMR tube with a Teflon screw cap. The tube was brought out of the glove box and was heated in an oil bath set at 40 °C. The reaction was monitored in 10 min intervals by ^{1}H NMR. The k_{obs} was estimated from a first–order plot of *ln*[product] vs reaction time by measuring

the ^{1}H integration of the product peak ($=CH_2$, δ 5.81 ppm), which was normalized against the internal standard peak.

6.8.4 Isotope Labeling Study on the Hydrosilylation of Alkynes

In a glove box, triethylsilane (2.0 mmol) and DC≡CPh (102 mg, 1.0 mmol) were added via a syringe to a 25 mL Schlenk tube equipped with a magnetic stirring bar and Teflon stopcock. The catalyst **1** (7 mg, 1 mol %) and the solvent (3 mL) were added to the reaction tube. The reaction tubes were brought out of the box was stirred at room temperature for 4 h. The solvent was removed from a rotary evaporator, and the organic product was isolated by a column chromatography on silica gel (*n*-hexanes). The deuterium content of the product was measured by both ^{1}H NMR (CDCl$_3$ with 10 mg cyclohexane as the external standard) and ^{2}H NMR (CH$_2$Cl$_2$ with 50 μL CDCl$_3$).

6.8.5 Phosphine Inhibition Study on the Hydrosilylation of Alkynes

In a glove box, triethylsilane (0.20 mmol), phenylacetylene (0.1mmol), **1** (3 mg, 2 mol %) and C$_6$Me$_6$ (2 mg, internal standard) were dissolved in 0.5 mL of CDCl$_3$ solution in a J-Young NMR tube with a Teflon screw cap. A pre-dissolved PCy$_3$ in CDCl$_3$

solution (5 µL, 1.0 M) was added via syringe to the tube via syringe. The tube was

brought out of the glove box. The reaction was monitored by ^{1}H NMR in 30 min

intervals. The rate was measured by the ^{1}H integration of the product peak at δ 5.81

(=CHSi), and was normalized against the internal standard peak. The k_{obs} was estimated

from the first order plot of ln[product] vs reaction time.

6.8.6 Kinetic Studies on the Hydrosilylation of Alkenes

In the glove-box, the mixtures of styrene (0.006-0.2 M), triethyl silane (0.5 M), **1**

(2 mg, 1 mol %) and C_6Me_6 (2 mg, internal standard) were dissolved in 0.5 mL of $CDCl_3$

solution in a J-Young NMR tube with a Teflon screw cap. A pre-dissolved PCy_3 in

$CDCl_3$ solution (5 µL, 1.0 *M*) was added via syringe to the tube via syringe. The tube was

brought out of the glove box. The reaction was monitored by ^{1}H NMR in 10 min intervals

at 40 ^{o}C. The initial rate method was used to measure the rate of each reaction. The rate

was measured by the ^{1}H integration of the product peak at δ 5.81 ppm (=CHSi), and was

normalized against the internal standard peak. The k_{obs} was estimated from the first order

plot of ln[product] vs. reaction time.

6.8.7 Isotope Effect Study on the Hydrosilylation of Alkenes

In the glove-box, the mixtures of styrene (0.006-0.2 M), triethylsilane (0.5 M), **1** (2 mg, 1 mol %) and C_6Me_6 (2 mg, internal standard) were dissolved in 0.5 mL of $CDCl_3$ solution in a J-Young NMR tube with a Teflon screw cap. The tube was brought out of the glove box. The reaction was monitored by ^1H NMR in 10 min intervals at 40 ^{o}C. The initial rate method was used to measure the rate of each reaction. The rate was measured by the ^1H integration of the product peak at δ 5.81 ppm (=CHSi), and was normalized against the internal standard peak. The k_{obs} was estimated from the first order plot of *ln*[product] vs. reaction time. Under the similar reaction conditions, the reaction of deuterium styrene-d_8 (0.1 mmol) and triethylsilane (0.2 mmol) was monitored by ^1H NMR.

6.8.8 Carbon Isotope Effect Study on the Hydrosilylation of Alkenes

In the glove box, styrene (2.0 mmol), triethylsilane (3.0 mmol), **1** (14 mg, 1 mol %) were dissolved in 3 mL CH_2Cl_2 solution in two 25 mL Schlenk tubes equipped with a magnetic stirring bar. The tubes were brought out of the glove box. The reaction tube was heated in an oil bath at 40 °C for 10 min and was opened to air at room temperature, and the crude product mixture was analyzed by GC/MS (10 % conversion). The other reaction tube was heated in an oil bath at 40 °C for 8 h and was opened to the air at room

temperature. The crude product mixture was analyzed by GC/MS (98 % conversion). The

solvent was removed under a rotary aspirator, and the product *trans* vinylsilane was

isolated by a column chromatograph on silica gel (*n*-hexanes)

C#	98% conv.	18% conv.	18% conv./98% conv.	change (%)
1	2.9936 (3)	2.9925 (3)	0.9996 (3)	0.04 (3)
2	2.9827 (4)	2.9823 (4)	0.9998 (4)	0.02 (4)
3	0.9314 (5)	0.9208 (5)	0.9886 (5)	1.14 (5)
4	1.0084 (3)	1.0060 (3)	0.9976 (3)	0.24 (3)
5	0.9288 (4)	0.9272 (4)	0.9983 (4)	0.17 (4)
6	2.0000 (5)	2.0000 (5)	1.0000 (5)	0.00 (5)
7	1.9892 (3)	1.9884 (3)	0.9996 (5)	0.04 (5)
8	0.9938 (3)	0.9923 (3)	0.9985 (3)	0.15 (3)
C#	98% conv.	10% conv.	10% conv./98% conv.	change (%)
1	2.9936 (4)	2.9915 (4)	0.9993 (4)	0.07 (4)
2	2.9827 (4)	2.9813 (3)	0.9995 (3)	0.05 (3)
3	0.9314 (5)	0.9198 (5)	0.9875 (5)	1.25 (5)
4	1.0084 (3)	1.0074 (3)	0.9990 (3)	0.10 (3)
5	0.9288 (4)	0.9266(4)	0.9976 (4)	0.24 (4)
6	2.0000 (5)	2.0000 (5)	1.0000 (5)	0.00 (5)
7	1.9892 (3)	1.9879(3)	0.9993 (5)	0.07 (5)
8	0.9938 (3)	0.9953 (3)	1.0015 (3)	0.15 (3)

6.8.9 Synthesis of Carbonylchlorohydridotris(triphenyl-phosphine) Ruthenium (II)

A solution of 0.26 g (1.0 mmol) of hydrated ruthenium trichloride in 20 mL of 2-methoxyethanol and aqueous formaldehyde (20 ml, 40% w/v solution) are added rapidly and successively to a vigorously stirred, boiling solution of 1.58 g (6 mmol) of triphenylphosphine in 60 mL of 2-methoxyethanol. The mixture is heated under reflux for 10 min and allowed to cool. The precipitate which forms is separated and washed successively with ethanol, water, ethanol, and n-hexane and dried in vacuum.

6.8.10 Computational Study on Hydrosilylation of Alkynes

All calculations were carried out with Gaussian 09 program. First of all, all geometries of the reactants, transition structures and intermediates were fully optimized by B3LYP method. The 6-31G (d) basis set was used for H, C, O, P, Si and Cl atoms, while the Lanl2dz basis set and ECP were used for Ru atom. The Ru atom was augmented with f-polarization functions. The harmonic vibration frequency calculation was performed for each structure, from which the zero-point energy, thermal energy, entropy and free energy were derived. In order to minimize computation time,

RuH(PMe$_3$)$_2$Cl(CO) was chose to be the catalyst, with trimethylsilane and

phenylacetylene as the reacting silane and alkyne.

6.8.11 Characterization Data of Selected Organic Products of Hydrosilylation of Alkynes

For **69a**: ^{1}H NMR (400 MHz, CDCl$_3$) δ 7.50 (d, 1H, J = 15.6 Hz), 7.36-7.24 (m,

5H), 5.81 (d, 1H, J = 15.6 Hz), 0.91 (t, 9H), 0.59 (q, 6H); ^{13}C {^{1}H} NMR (75 MHz,

CDCl$_3$) δ 148.0, 140.8, 129.7, 128.1, 128.0, 127.6, 7.7, 5.0; GC-MS m/z = 218 (M$^+$).

For **69b**: ^{1}H NMR (400 MHz, CDCl$_3$) δ 7.46 (d, 1H, J = 15.6 Hz), 7.36-7.24 (m,

5H), 5.81 (d, 1H, J = 15.6 Hz), 0.91 (t, 6H), 0.59 (q, 4H), 0.01 (s, 3H); ^{13}C {^{1}H} NMR

(75 MHz, CDCl$_3$) δ 147.7, 140.6, 130.7, 128.2, 128.1, 127.6, 7.69, 6.8, -4.1; GC-MS m/z

= 204 (M$^+$).

For **69c**: ^{1}H NMR (300 MHz, CDCl$_3$) δ 7.82 (d, 1H, J = 15.6 Hz), 7.70-6.94 (m,

20H), 6.44 (d, 1H, J = 15.6Hz); ^{13}C {^{1}H} NMR (75 MHz, CDCl$_3$) δ 150.6, 138.2, 135.2,

129.6, 128.9, 128.0, 127.9, 1125.5, 127.7; GC-MS m/z = 376 (M$^+$).

For **69d**: ^{1}H NMR (300 MHz, CDCl$_3$) δ 7.46 (d, 1H, J = 15.6 Hz), 7.18 (m, 4H),

5.74 (d, 1H, J = 15.6 Hz), 2.38 (s, 3H), 0.94 (t, 9H), 0.62 (q, 6H); ^{13}C {^{1}H} NMR (75

MHz, CDCl$_3$) δ 147.9, 137.8, 137.3, 128.8, 128.0, 128.6, 21.5, 7.8, 5.0; GC-MS m/z =

232 (M$^+$).

For **69e**: ^{1}H NMR (300 MHz, CDCl$_3$) δ 7.42 (d, 1H, *J* = 15.6 Hz), 7.25 -6.86 (m, 4H), 5.67 (d, 1H, *J* = 15.6 Hz), 3.83 (s, 3H), 0.92 (t, 9H), 0.60 (q, 6H); ^{13}C {^{1}H} NMR (75M Hz, CDCl$_3$) δ 147.9, 159.3, 133.3, 129.3, 113.5, 127.5, 55.4, 7.8, 5.0; GC-MS *m/z* = 248 (M$^+$).

For **69f**: ^{1}H NMR (300 MHz, CDCl$_3$) δ 7.40 (d, 1H, *J* = 15.6 Hz), 7.25 - 7.00 (m, 4H), 5.68 (d, 1H, *J* = 15.6 Hz), 0.88 (t, 9H), 0.58 (q, 6H); ^{13}C {^{1}H} NMR (75 MHz, CDCl$_3$) δ 163.7, 161.3, 146.7, 136.8, 129.9, 129.7, 129.6, 115.1, 114.9, 7.7, 4.9; GC-MS *m/z* = 238 (M$^+$).

For **69g**: ^{1}H NMR (300 MHz, CDCl$_3$) δ 7.58-7.39 (d, 4H, *J* = 8.5 Hz), 7.46 (d, 1H, *J* = 15.4 Hz), 5.93 (d, 1H, *J* = 15.4 Hz), 0.89 (t, 9H), 0.57 (q, 6H); ^{13}C {^{1}H} NMR (75 MHz, CDCl$_3$) δ 146.1, 144.0, 132.2, 129.3, 128.1, 124.9, 126.5, 125.6, 122.8, 120.2, 7.4, 4.6; GC-MS *m/z* = 288 (M$^+$).

6.8.12 Characterization Data of Selected Organic Products of Hydrosilylation of Alkenes

For **70a**: ^{1}H NMR (400 MHz, CDCl$_3$) δ 7.52-7.24 (m, 5H), 6.96 (d, 1H, *J* = 19.4 Hz), 6.48 (d, 1H, *J* = 19.4 Hz), 1.06 (t, 9H), 0.73 (q, 6H); ^{13}C {^{1}H} NMR (75 MHz, CDCl$_3$) δ 145.1, 138.8, 128.7, 128.1, 126.0, 126.6, 7.7, 3.8; GC-MS *m/z* = 218 (M$^+$).

For **70b**: ^{1}H NMR (300 MHz, CDCl$_3$) δ 7.55-7.24 (m, 5H), 6.99 (d, 1H, J = 19.4 Hz,), 6.54 (d, 1H, J = 19.4 Hz), 1.08 (t, 9H), 0.73 (q, 6H), 0.22 (s, 3H); ^{13}C {^{1}H} NMR (75 MHz, CDCl$_3$) δ 145.1, 138.7, 128.8, 128.2, 127.4, 126.6, 7.7, 5.8, 5.3; GC-MS m/z = 218 (M$^+$).

For **70c**: ^{1}H NMR (300 MHz, CDCl$_3$) δ7.70-6.94 (m, 20H), 7.02 (d, 1H, J = 19.3 Hz,), 6.54 (d, 1H, J = 19.3 Hz); ^{13}C {^{1}H} NMR (75 MHz, CDCl$_3$) δ 146.3, 138.1, 135.4, 129.5, 128.9, 128.0, 127.9, 1125.5, 126.2; GC-MS m/z = 376 (M$^+$).

For **70d**: ^{1}H NMR (400 MHz, CDCl$_3$) δ 7.38 (d, J = 8.3 Hz, 2H), 7.17 (d, J = 8.3 Hz, 2H,), 6.91 (d, 1H, J = 19.3 Hz), 6.40 (d, 1H, J = 19.3 Hz), 2.38 (s, 3H), 1.04 (t, 9H), 0.70 (q, 6H); ^{13}C {^{1}H} NMR (75 MHz, CDCl$_3$) δ 145.0, 137.9, 136.2, 129.1, 124.6, 126.5, 21.1, 7.7, 3.8; GC-MS m/z = 232 (M$^+$).

For **70e**: ^{1}H NMR (300 MHz, CDCl$_3$) δ 7.45 (d, J = 8.8 Hz, 2H), 6.92 (d, 2H, J = 8.8 Hz), 6.92 (d, 1H, J = 19.4 Hz), 6.33 (d, 1H, J = 19.4 Hz), 3.85 (s, 3H), 1.07 (t, 9H), 0.74 (q, 6H); ^{13}C {^{1}H} NMR (75 MHz, CDCl$_3$) δ 144.5, 159.8, 131.8, 127.7, 114.1, 123.1, 55.5, 7.7, 3.8; GC-MS m/z = 248 (M$^+$).

For **70f**: ^{1}H NMR (400 MHz, CDCl$_3$) δ 7.46 (d, J = 8.5 Hz, 2H), 7.31 (d, J = 8.5 Hz, 2H), 6.83 (d, 1H, J = 19.4 Hz), 6.43 (d, 1H, J = 19.4 Hz), 1.00 (t, 9H), 0.67 (q, 6H); ^{13}C {^{1}H} NMR (75 MHz, CDCl$_3$) δ 143.7, 137.6, 131.8, 128.0, 121.9, 127.3, 7.7, 3.6; GC-MS m/z = 311 (M$^+$).

For **70g**: ^{1}H NMR (400 MHz, CDCl$_3$) δ 7.39 and 7.31 (m, 4H, Ar), 6.87 (d, 1H, *J* = 19.4 Hz,), 6.44 (d, 1H, *J* = 19.4 Hz), 1.02 (t, 9H), 0.69 (q, 6H); ^{13}C {^{1}H} NMR (75 MHz, CDCl$_3$) δ 143.7, 137.2, 133.7, 128.9, 127.7, 127.1, 7.7, 3.7; GC-MS *m/z* = 266 (M$^+$).

For **70h**: ^{1}H NMR (400 MHz, CDCl$_3$) δ 7.75 and 7.18 (m, 5H, Ar), 7.10 (d, 1H, *J* = 19.4 Hz, C*H*=CHSi), 6.55 (d, 1H, *J* = 19.4 Hz), 3.94 (OC*H$_3$*), 1.09 (t, 9H), 0.76 (q, 6H,); ^{13}C {^{1}H} NMR (75 MHz, CDCl$_3$) δ 145.1, 158.0, 134.7, 134.2, 126..06, 125.2, 124.1, 119.2, 106, 127.2, 55.5, 7.7, 3.8. GC-MS *m/z* = 298 (M$^+$).

For **70i**: ^{1}H NMR (300 MHz, CDCl$_3$) δ 7.64-7.32 (m, 9H), 6.98 (d, 1H, *J* = 19.5 Hz), 6.52 (d, 1H, *J* = 19.5 Hz), 1.06 (t, 9H), 0.73 (q, 6H); ^{13}C {^{1}H} NMR (75 MHz, CDCl$_3$) δ 144.6, 137.8, 129.0, 128.9, 128.5, 127.5, 127.3, 127.2, 126.4, 7.7, 3.8. GC-MS *m/z* = 294 (M$^+$).

References

(1) Fischer, B. J.; Eisenberg, R. *Organometallics* **1983**, *2*, 764.

(2) Sasaki, K.; Wada, K.; Tanaka, M. *Chem. Lett.* **1987**, *249*.

(3) Sasaki, K.; Wada, K.; Tanaka, M. *J. Am. Chem. Soc.* **1990**, *112*, 7221.

(4) Kunin, A. J.; Eisenberg, R. *Organometallics* **1988**, *7*, 2124.

(5) Liu, F.; Pak, E. B.; Sigh, B.; Jensen, C.M. Goldman, A. S. *J. Am. Chem. Soc.* **1999**, 121, 4086.

(6) Jia, C.; Piao, D.; Oyamada, J.; Lu, W.; Fijiwara, Y. *Science*. **2000**, *287*.

(7) Murai, S.; Kakiuchi, F.; Sekine, S.; Tanaka, Y.; Kamatani, A.; Sonoda, M.; Charani, N. *Nature* **1993**, *366*, 529.

(8) Lenges, C. P.; Brookhart, M. *J. Am. Chem. Soc.* **1999**, *121*, 6616.

(9) Hani, A.; Mohammad, J. C.; Klaus, E.; Mack, G.; Speiser, B.; Novak, F.; Kaska,W.; Mayer, H. *Activation and Functionalization of C-H Bonds,* **2004**, 234, Chapter 14.

(10) Filippini, M.; Rodriguez, J. *Org. Chem.* **1997**, *62*, 3034.

(11) Lenges, C. P.; Brookhart, M. *J. Am. Chem. Soc.* **1999**, *121*, 6616.

(12) Oi, S.; Ogino, Y.; Fukita.; Inoue, Y. *Org. Lett*. **2002**, *4*, 1783.

(13) Wang, X.; Lane, B. S.; Sames, D. *J. Am. Chem. Soc.* **2005**, *127*, 4996.

(14) (a) Stuart, D. R.; Villemure, E.; Fagnou, K. *J. Am. Chem. Soc*. **2007**, *129*, 12072.
      (b) Maehara, A.; Tsurugi, H.; Satoh, T.; Miura, M. *Org. Lett*. **2008**, *10*, 1159.

(15) Beck, E. M.; Grimster, N. P.; Hatley, R.; Gaunt, M. J. *J. Am. Chem. Soc.* **2006**, *128*, 2528.

(16) Lu, W.; Jia, C.; Kitamura, T.; Fujiwara, Y. *Org. Lett*. **2000**, *2*, 2927.

(17) Yang, Y.; Cheng, K.; Zhang, Y. *Org. Lett*. **2009**, *11*, 5606.

(18) Zhuang, W.; Gathergood, N.; Hazel, R. G.; Jørgensen, K. A. *J. Org. Chem.* **2001,** *66,* 1009.

(19) Palomo, C.; Oiarbide, M.; Kardak, B. G.; Garcfa, J. M.; Linden, A. *J. Am. Chem. Soc.* **2005**, *127*, 4154.

(20) Trost, B. M.; Muller, C. *J. Am. Chem. Soc.* **2008**, *130*, 2438.

(21) Breno, K. L.; Pluth, M. D.; Tyler, D. R. *Oranometallics* **2003**, *22*, 1203.

(22) Gruber, S.; Zaitsev, A.; Worle, M.; Pregosin, P. S. *Organometallics* **2008,** *27,* 3796.

(23) Hermatschweiler, R.; Fernandez, I.; Pregosin, P. S.; Watson, E. J.; Albinati, A.; Rizzato, S.; Veiros, L. F. *Organometallics* **2005**, *24,* 1809.

(24) Grigg, R.; Savic, V. *Tetrahedron Lett*. **1997**, *38*, 5737.

(25) Wang, X.; Lane, B. S.; Sames, D. J. *J. Am. Chem. Soc.* **2005**,*127*, 4996.

(26) (a) Marrero, A.; Cueto, M.; Dcroz, L.; Darias, J. *Org. Lett.* **2008**, *10*, 3057
      (b) Grundl, M.; Kennedy-Smith, J.; Trauner, D. *Organometallics* **2005**, *24*, 2831.

(27) Yi, C. S.; Zhang, J. *Chem. Commun.* **2008**, 2349.

(28) Li, Z.; Li, C. *Org. Lett*. **2004**, *6*, 4997.

(29) Sezen, B.; Franz, R.; Sames, D. *J. Am. Chem. Soc.* **2002**, *124*, 13372.

(30) Yanakawa, M.; Ito, H.; Noyoyi, R. *J. Am. Chem. Soc.* **2000**, *122*, 1466.

(31) Lane, B. S.; Sames, D. *Org. Lett.* **2004**, *6*, 2897.

(32) Murakami, M.; Hori, S. *J. Am. Chem. Soc.* **2003**, *125*, 4720.

(33) (a) Li, W. J.; Nelson, D. P.; Jensen, M. S.; Hoerrner, R. S.; Javadi, G. J.; Cai, D.; Larsen, R. D. *Org. Lett*. **2003**, *5*, 4835. (b) Mori, A.; Sekiguchi, A.; Masui, K.; Shimada, T.; Horie, M.; Osakada, K.; Kawamoto, M.; Ikeda,T. *J. Am. Chem. Soc*. **2003**, *125*, 1700.

(34) (a) Chaicharoenwimolkul, L.; Munmai, A.; Chairam, S.; Tewasekson,U.; Sapudom, S.; Lakliang, Y.; Somsook, E. *Tetrahedron Lett.* **2008**, *49*, 7299. (b) Sakurai, H.; Tsunoyama, H.; Tsukuda, T. *J. Organomet. Chem.* **2007**, *692*, 368.

(35) Campeau, L. C.; Rousseaux, S.; Faugnou, K. Ahrendt, K. A.; Borths, C. J.; MacMillan, D. W. C. *J. Am. Chem. Soc.* **2005**, *127*, 18020.

(36) Nakao, Y.; Kanyiva, K. S.; Hiyama, T. Ahrendt, K. A.; Borths, C. J.; MacMillan, D. W. C. *J. Am. Chem. Soc.* **2008**, *130*, 2448.

(37) (a) Ireland, R. E.; Mueller, R. H.; Willard, A. K. *J. Am. Chem.Soc.* **1976**, *98*, 2868. (b) Rasmuseen, J. K. *Synthesis* **1977**, 91. (c) Colvin, E. W. *Chem. Soc. Rev.* **1978**, *7*, 15. (d) Heathcock, C. H.; Buse, C. T.; Kleschick, W. A.; Pirrung, M. C., Sohn, J. E.; Lampe, J. *J. Org. Chem.***1980**, *45*, 1066. (e) Petrzilka, M.; Grayson, J. I. *Synthesis* **1981**, 753. (f) Brownbridge, P. *Synthesis* **1983**, 1 (g) Corey, E. J.; Gross, A. W. *Tetrahedron Lett.* **1984**, *25*, 495. (h) Cazeau, P.; Dubondin, F.; Moulines, F.; Babot, O.; Dunogues, J. *Tetrahedron* **1987**, *43*, 2075 and 2089. (i) Fleming, I.; Barbero, A.; Walter, D. *Chem. Rev.* **1997**, *97*, 2063.

(38) Hall, P. L.; Glchrist, J. H.; Collum, D. B. *J. Am. Chem. Soc.* **1991**, *113*, 9571.

(39) Tanable, Y.; Misaki, T.; Kurihara, M.; Iida, A.; Nishii, Y. *Chem.Commm.* **2002**, 1628.

(40) (a) Colquhoun, H. M.; Holton, J.; Thompson, D. J.; Twigg, M. V.*New Pathways for Organic Synthesis-Practical Applications of Transition Metals*; Plenum Press: London, 1984, 173. (b) McQuillin, F. J.; Parker, D. G.; Stephenson, G. R. *Transition Metal Organometallics for Organic Synthesis*; Cambridge University Press: New York, 1991, 27. (c) Otsuka, S.; Tani, K. *Synthesis* **1991**, 665.

(41) (a) Boeckel, C. A. A.; Boom, J. M. *Tetrahedron Lett.* **1979**, 3561. (k) Carless, H. A. J.; Haywood, D. J. *Chem. Commun.* **1980**, 980. (b) Oltvoort, J. J.; Van Bockel, C. A. A.; De Koning, J. H.; van Boom, J. H. *Synthesis* **1981**, 305. (c) Sodeoka, M.; Yamada, H.; Shibasaki, M. *J. Am. Chem. Soc.* **1990**, *112*, 4906. (d) Takahashi, M.; Suzuki, H.; Moro-oka, Y.; Ikawa, T. *Chem. Lett.* **1981**, 1435. (e) Takahashi, M.; Suzuki, H.; Moro-oka, Y.; Ikawa, T. *J. Org. Chem.* **1991**, *56*, 4569. (f) Mitchell, T.

N.; Gieselmann, F. *Synlett* **1996**, 475. (g) Wille, A.; Tomm, S.; Frauenrath, H. *Synthesis* **1998**, 305.

(42) Chatani, N.; Yamaguchi, S.; Fukumoto, Y.; Murai, S. *J. Am. Chem. Soc.* **1992**, *114*, 9710.

(43) Ohmura, T.; Yamamoto, Y.; Miyaura, N. *Organometallics* **1999**, *18*, 431.

(44) Trost, B.; Surivet, J. P.; Toste, D. *J. Am. Chem. Soc.* **2001**, *123*, 2897.

(45) Kownacki, I.; Marciniec, B.; Szubert, K.; Kubicki, M. *Organometallics* **2005**, *24*, 6179.

(46) (a) Urabe, H.; Suzuki, D.; Sasaki, M.; Sato, F. *J. Am. Chem. Soc.* **2003**, *125*, 4036. (b) Hara, H.; Hirano, M.; Tanaka, K. *Org. Lett.* **2008**, *10*, 2537. (c) Nair, V.; Deepthi, A. *Chem. Rev.* **2007**, *107*, 1862.

(47) (a) Brown, J. M. In *Comprehensive Asymmetric Catalysis*; Jacobsen, E. N., Pfalts, A., Yamamoto, H., Eds.; Springer: Berlin, Germany, 1999. (b) Ohkuma, T.; Kitamura, M.; Noyori, R. In *Catalytic Asymmetric Synthesis*; Ojima. I., Ed.; Wiley-VCH: Weinheim, Germany, 2000. (c) Tang, W.; Zhang, X. *Chem. Rev.* **2003**, *103*, 3029.

(48) Trost, B. M.; Toste, F. D.; Pinkerton, A. B. *Chem. Rev.* **2001**, *101*, 2067. (a) House, H. O. *Modern Synthetic Reactions*, 2nd Ed.; Benjamin/Cummings: Menlo Park, CA, 1972. (b) Smith, M. B.; March, M. *March's Advanced Organic Chemistry*, 5th Ed.; Wiley: New York, 2001.

(49) (a) Isambert, N.; Cruz, M.; Arévalo, M. J.; Gómez, E.; Lavilla, R. *Org. Lett.* **2007**, *9*, 4199. (a) Isambert, N.; Cruz, M.; Arévalo, M. J.; Gómez, E.; Lavilla, R. *Org. Lett.* **2007**, *9*, 4199. (b) Yanagisawa, A.; Matusumoto, Y.; Asakawa, K.; Yamamoto, H. *J. Am. Chem. Soc.* **1999**, *121*, 892. (c) Karlsson, S.; Hogberg, H. E. *Tetradron Asymmetry* **2001**, *12*, 1977. (d) Isam bert, N.; Cruz, M.; Arevalo, M. J.; Gomez, E.; Lavilla, R. *Org. Lett.* **2007**, *9*, 4199. (e) Clarke, P. A.; Zaytsev, A. V.; Morgan, T. W.; Whitwood, A. C.; Wilson, C. *Org. Lett.* **2008**, *10*, 2877.

(50) (a) House, H. O. *Modern Synthetic Reactions*, 2nd Ed.; Benjamin Cummings: Menlo Park, CA, 1972. (b) Smith, M. B.; March, M. *March's Advanced Organic Chemistry*, 5th Ed.; Wiley: New York, **2001**.

(51) (a) Wang, S.; Zhang, L. *J. Am. Chem. Soc.* **2006**, *128*, 8414. (b) Wang, S.; Zhang, L. *Org. Lett.* **2006**, *8*, 4585. (c) De Brabander, J. K.; Liu, B.; Qian, M. *Org. Lett.* **2008**, *10*, 2533. (d) Peng, Y.; Cui, L.; Zhang, G.; Zhang, L. *J. Am. Chem. Soc.* **2009**, *131*, 5062.

(52) (a) Wang, S.; Zhang, L. *J. Am. Chem. Soc.* **2006**, *128*, 8414. (b) Wang, S.; Zhang, L. *Org. Lett.* **2006**, *8*, 4585. (c) De Brabander, J. K.; Liu, B.; Qian, M. *Org. Lett.* **2008**, *10*, 2533. (d) Peng, Y.; Cui, L.; Zhang, G.; Zhang, L. *J. Am. Chem. Soc.* **2009**, *131*, 5062.

(53) DeBergh, J. R.; Spivey, K. M.; Ready, J. M. *J. Am. Chem. Soc.* **2008**, *130*, 7828.

(54) Reviews: (a) Bruneau, C.; Dixneuf, P. H. *Acc. Chem. Res.* **1999**, *32*, 311. (b) Drozdak, D.; Allaert, B.; Ledoux, N.; Dragutan, I.; Dragutan, V.; Verpoort, F. *Adv. Synth. Cat.* **2005**, *347*, 1721.

(55) Yoo, J. W.; Li, C. J. *J. Org. Chem.* **2006**, *71*, 6266.

(56) Schaefer, C.; Fu, G. C. *Angew. Chem., Int. Ed.* **2005**, *44*, 4606.

(57) Doucet, H.; Martin-Vaca, B.; Bruneau, C.; Dixneuf, P. H. *J. Org. Chem.* **1995**, *60*, 7247.

(58) Mitsudo, T.; Hori, Y.; Yamakawa, Y. *J. Org. Chem.* **1987**, *52*, 2230.

(59) Le Paih, J.; Monnier, F.; Dérien, S.; Dixneuf, P. H.; Clot, E.; Eisenstein, O. *J. Am. Chem. Soc.* **2003**, *125*, 11964.

(60) Drozdak, D.; Allaert, B.; Ledoux, N.; Dragutan, I.; Dragutan, V.; Verpoort, F. *Adv. Synth. Cat.* **2005**, *347*, 1721.

(61) (a) Bianchini, C.; Meli, A.; Peruzzini, M.; Zanobini, F.; Bruneau, C.; Dixneuf, P. H. *Organometallics* **1990**, *9*, 1155. (b) Doucet, H.; Höfer, J.; Bruneau. C.; Dixneuf, P. H. *Chem. Commun.* **1993**, 850. (c) Melis, K.; Opstal, T.; Verpoort, F. *Eur. J. Org. Chem.* **2002**, 3779. (d) Nakagawa, H.; Okimoto, Y.; Sakaguchi, S.; Ishii, Y. *Tetrahedron Lett.* **2003**, *44*, 103. (e) Hua, R.; Tian, X. *J. Org. Chem.* **2004**, *69*, 5782. (f) Doherty, S.; Knight, J. G.; Rath, R. K.; Clegg, W.; Harrington, R. W.; Newman, C. R.; Campbell, R.; Amin, H. *Organometallics* **2005**, *24*, 2633.

(62) Cherry, K.; Parrain, J.-L.; Thibonnet, J.; Duchêne, A.; Abarbri, M. *J. Org. Chem.* **2005**, *70*, 6669.

(63) Mitsudo, T.; Hori, Y.; Yamakawa, Y.; Watanabe, Y. *J. Org. Chem.* **1987**, *52*, 2230.

(64) (a) Ho, J. H. H.; Black, D. S. Messerle, B. A.; Clegg, J. K.; Turner, P. *Organometallics* **2006**, *25*, 5800. (b) Mitsudo, T.; Hori, Y.; Yamakawa, Y. *J. Org. Chem.* **1987**, *52*, 2230.

(65) Doucet, H.; Martin-Vaca, B.; Bruneau, C.; Dixneuf, P. H. *J. Org. Chem.* **1995**, *60*, 7247.

(66) Le Paih, J.; Monnier, F.; Dérien, S.; Dixneuf, P. H.; Clot, E.; Eisenstein, O. *J. Am. Chem. Soc.* **2003**, *125*, 11964.

(67) (a) Ueura, K.; Satoh, T.; Miura, M. *Org. Lett.* **2007**, *9*, 1407. (b) Kim, H.; Goble, S. D.; Lee, C. *J. Am. Chem. Soc.* **2007**, *129*, 1030.

(68) Wang, Y.; Burton, D. J. *J. Org. Chem.* **2006**, *71*, 3859.

(69) Ojima, I.; Li, Z.; Zhu, J. *In The Chemistry of Organosilicon Compounds;* Rappoport, S.; Apeloig, Y., Eds.; Wiley: New York, 1998: Laugkopf, E.; Schinzer, D. *Chem. Rev.* **1995**, *95*, 1375.

(70) (a) Hatanaka, Y.; Hiyama, T. *Synlett* **1991**, 845. Hiyama, T.Organosilicon Compounds in Cross-Coupling reactions. In Metal-catalyzed Cross-Coupling reactions; (b) Diederich, F.; Stang, P. wiley-VCH: Weiheim, 1998. (c) Mowery, M. E.; DeShong, P. *Org. Lett.* **1999**, *1*, 2137; (d) Denmark, S. E.; Neuville, L., *Org. Lett.* **2000**, *2*, 3221.

(71) Bunlaksananusorn, T.; Rodriguez, A. L.; Knochel, P. *Chem. Commun*. **2001**, 745.

(72) Tamao, K.; Kumada, M.; Maeda, K. *Tetrahedron Lett*. **1984**, *25*, 321.

(73) Blumenkopf, T. A.; Overman, L. E. *Chem. Rev*. **1986**, *86*, 857.

(74) (a) Murai, S.; Sonoda, N. *Angew. Chem. Int. Ed. Engl*. **1979**, *18*, 837. (b) Seki, Y.; Murai, S.; Hidaka, A.; Sonoda, N. *Angew. Chem. Int. Ed. Engl*. **1977**, *16*, 881. (c) Seki, Y.; Hidaka, A.; Makino, S; Murai, S.; Sonoda, N. *J. Organomet. Chem*. **1977**, *140*, 361.

(75) (a) Ikeda, S.; Chatani, N.; Kajikawa, Y.; Ohe, K.; Murai, S. *J. Org. Chem*. **1992**, *57*, 2. (b) Seki, Y.; Kawamoto, K.; Chatani, N.; Hidaka, A.; Sonoda, N.; Ohe, K.; Kawasaki, Y.; Muri, S. *J. orgomet. Chem*. **1991**, *403*, 73.

(76) (a) Matsuda, I.; Ogiso, A.; Sata, S.; Izumi, Y. *J. Am. Chem. Soc*. **1989**, *111*, 2332. (b) Ojallima, I.; Ingallina, P.; Donovan, R.J. Clos, N. *Organomettallics* **1991**, *10*, 38.

(77) Trost, B. M.; Ball, Z. T. *J. Am. Chem. Soc*. **2003**, *125*, 30.

(78) (a) Benkeser, R. A.; Burrous, M. L.; Nelson, L. E.; Swisher, J. V. *J. Am. Chem. Soc*. **1966**, *83*, 4385. (b) Amrein, S.; Timmermann, A.; Studer, A. *Org. Lett*. **2001**, *3*, 2357. (c) Asao, N.; Sudo, T.; Yamamoto, Y. *J. Org. Chem*. **1996**, *61*, 7654. (d) Sudo, T.; Asao, N.; Gevorgyan, V.; Yamamoto, Y. *J. Org. Chem*. **1999**, *64*, 2494.

(79) Hamze, A.; Provot, O.; Alami, M.; Brion, J., D. *Org. Lett.* **2005**, *7,* 5625.

(80) Gelloz, G. B.; Schumers, J. M.; Bo, G.; Marko, I. E. *J. Org. Chem*. **2008**, *73*,4190.

(81) Blug, M.; Goff, X.; Mezailles, N.; Floch, P. *Organomettallics* **2009**, *28*, 2360.

(82) Seki, Y.; Takeshita, K.; kawamoto, K.; Murai, S. *J. Org. Chem*. **1986**, *51*, 3890.

(83) Na, Y.; Chang, S. *Org. Lett.* **2000**, *2,* 1887.

(84) Trost, B.; Ball, Z. *J. Am. Chem. Soc*. **2003**, *125*, 30.

(85) Kawanami, Y.; Sonoda, Y.; Mori, T.; Yamamoto, K. *Org. Lett*. **2002**, *4,* 2825.

(86) Dichers, H. M.; Haszeldine, R. N.; Mather, A. P.; Parish, R. V. *J. orgomet. Chem*. **1978**, *161*, 91.

(87) Brady, K. A.; Nile, T. A. *J. organomet. Chem*. **1981**, *206*, 299.

(88) Ojima, I.; Clos, N.; Donovan, R. *Organomettallics* **1990**, *9*, 3127.

(89) (a) Trofimov, B. A.; Sobenina, L. N.; Demenev, A. P.; Mikhaleva, A. I. *Chem. Rev*. **2004**, *104*, 2481. (b) Cacchi, S.; Fabrizi, G. *Chem. Rev*. **2005**, *105*, 2873.

(90) (a) Murakami, M.; Horo, S. *J. Am. Chem. Soc.*, **2003**, *125*, 4720. (b) Zaitsev, A. B.; Gruber, S.; Plss, P. A.; Pregosin, P. S.; Veiros, L. F.; Wrle*,* M. *J. Am. Chem. Soc*. **2008**, *130*, 11604.

(91) (a) Stuart, D. R.; Villemure, E.; Keith Fagnou, K. *J. Am. Chem. Soc*. **2007**, *129*, 12072. (b) Maehara, A.; Tsurugi, H.; Satoh, T.; Miura, M. *Org. Lett.* **2008**, *10*, 1159.

(92) Gao, R.; Yi, S. C. *J. Org. Chem.* **2010**, *75*, 3144.

(93) Isaccs, M. *Phys. Org. Chem.* **1981**, 13, 4851.

(94) (a) Singleton, D. A.; Thomas, A. A. *J. Am. Chem. Soc.* **1995**, *117*, 9357. (b) Frantz, D. E.; Singleton, D. A. *J. Am. Chem. Soc.* **1997**, *119,* 3383.

(95) (a) Urabe, H.; Suzuki, D.; Sasaki, M.; Sato, F. *J. Am. Chem. Soc.* **2003**, *125*, 4036. (b) Hara, H.; Hirano, M.; Tanaka, K. *Org. Lett.* **2008**, *10*, 2537.

(96) (a) Brown, J. M. In *Comprehensive Asymmetric Catalysis*; Jacobsen, E. N., Pfalts, A., Yamamoto, H., Eds.; Springer: Berlin, Germany, **1999**. (b) Ohkuma, T.; Kitamura, M.; Noyori, R. In *Catalytic Asymmetric Synthesis*; Ojima. I., Ed.; Wiley-VCH: Weinheim, Germany, **2000**. (c) Tang, W.; Zhang, X. *Chem. Rev.* **2003**, *103*, 3029.

(97) Trost, B. M.; Toste, F. D.; Pinkerton, A. B. *Chem. Rev*. **2001**, *101*, 2067.

(98) Isambert, N.; Cruz, M.; Arévalo, M. J.; Gómez, E.; Lavilla, R. *Org. Lett.* **2007**, *9*, 4199.

(99) (a) House, H. O. *Modern Synthetic Reactions*, 2nd Ed.; Benjamin Cummings: Menlo Park, CA, 1972. (b) Smith, M. B.; March, M. *March's Advanced Organic Chemistry*, 5th Ed.; Wiley: New York, **2001**.

(100) Reviews: (a) Bruneau, C.; Dixneuf, P. H. *Acc. Chem. Res.* **1999**, *32*, 311. (b) Drozdak, D.; Allaert, B.; Ledoux, N.; Dragutan, I.; Dragutan, V.; Verpoort, F. *Adv. Synth. Cat.* **2005**, *347*, 1721.

(101) Doherty, S.; Knight, J. G.; Rath, R. K.; Clegg, W.; Harrington, R. W.; Newman, C. R.; Campbell, R.; Amin, H. *Organometallics* **2005**, *24*, 2633.

(102) Ho, J. H. H.; Black, D. S. Messerle, B. A.; Clegg, J. K.; Turner, P. *Organometallics* **2006**, *25*, 5800.

(103) Yi, S. C.; Gao, R. *Organometallics* **2009**, *28*, 6585.

(104) (a) Rybtchinski, B.; Milstein, D. *J. Am. Chem. Soc.* **1999**, *121*, 4528. (b) Feller, M.; Iron, M. A.; Shimon, L. J. W.; Diskin-Posner, Y.; Leitus, G.; Milstein, D. *J. Am. Chem. Soc.* **2008**, *130*, 14374.

(105) Swartz, B. D.; Reinartz, N. M.; Brennessel, W. W.; Garca, J. J.; Jones, W. D. *J. Am. Chem. Soc.* **2008**, *130*, 8548.

(106) (a) Grimster, N. P.; Gauntlett, C.; Godfrey, C. R. A.; Gaunt, M. J. *Angew. Chem., Int. Ed*. **2005**, *44*, 3125. (b) Ranu, B. C.; Chattopadhyay, K.; Adak, L. *Org. Lett.* **2007**, *9*, 4595. (c) Cheng, J.-S.; Wei, G.-F.; Huang, S.W.; Zhao, J.; Jiang, H. F. *J. Mol. Cat*. **2007**, *263*, 169. (d) Zott, A. D.; Prat, F. I.; Baratta, W.; Zangrando, E.; Rigo, P. *Inorg. Chim. Acta* **2009**, *362*, 97.

(107) (a) Bruce, M. I. *Chem. Rev.* **1991**, *91*, 197. (b) Tani, K.; Kataoka, Y. In *Catalytic Heterofunctionalization*, Togni, A., Grützmacher, H. Eds.; VCH-Wiley: Weinheim, 2001, 199. (c) Bruneau, C.; Dixneuf, P. H. *Angew. Chem., Int. Ed.* **2006**, *45*, 2176.

(108) (a) Grotjahn, D. B.; Incarvito, C. D.; Rheingold, A. L. *Angew. Chem., Int. Ed*. **2001**, *40*, 3884. (b) Tokunaga, M.; Suzuki, T.; Koga, N.; Fukushima, T.;

Horiuchi, A.; Wakatsuki, Y. *J. Am. Chem. Soc.* **2001**, *123*, 11917. (c) Grotjahn, D. B.; Lev, D. A. *J. Am. Chem. Soc.* **2004**, *126*, 12232. (d) Labonne, A.; Kribber, T.; Hintermann, L. *Org. Lett.* **2006**, *8*, 5853.

(109)   Recent reviews: (a) Trofimov, B. A.; Sobenina, L. N.; Demenev, A. P.; Mikhaleva, A. I. *Chem. Rev.* **2004**, *104*, 2481. (b) Cacchi, S.; Fabrizi, G. *Chem. Rev.* **2005**, *105*, 2873.

(110)   (a) Yi, C. S.; Yun, S. Y.; Guzei, I. A. *Organometallics* **2004**, *23*, 5392.

(111)   Saigo, K.; Osaki, M.; Mukaiyama, T. *Chem. Let.* **1976**, 163.

(112)   Guo, Y.; Tao, G.; Blumenfeld, A.; Shreeve, J. M. *Organometallics*, **2010**, *29*, 818.

(113)   (a) Bisswanger, H. *Enzyme Kinetics*; Wiley-VCH, Germany, 2002, 28. (b) Cornish-Bowden, A. Fundamentals of *Enzyme Kinetics* 3rd Ed.; Portland Press, London, 2000, 72. (c) Segel, I. H. *Enzyme Kinetics;* Wiley-VCH: New York, NY, 1975.